

**UCLA**

**UCLA Electronic Theses and Dissertations**

**Title**

Development of Potent, Small Molecule Inhibitors of Ghrelin O-acyltransferase (GOAT)

**Permalink**

<https://escholarship.org/uc/item/9fq6b1r5>

**Author**

Murzinski, Emily Suzanne

**Publication Date**

2020

Peer reviewed|Thesis/dissertation

UNIVERSITY OF CALIFORNIA

Los Angeles

Development of Potent, Small Molecule Inhibitors  
of Ghrelin O-acyltransferase (GOAT)

A dissertation submitted in partial satisfaction of the  
requirements for the degree Doctor of Philosophy in Chemistry

by

Emily Suzanne Murzinski

2020

© Copyright by  
Emily Suzanne Murzinski  
2020

## ABSTRACT OF THE DISSERTATION

### Development of Potent, Small Molecule Inhibitors of Ghrelin *O*-acyltransferase (GOAT)

by

Emily Suzanne Murzinski

Doctor of Philosophy in Chemistry

University of California, 2020

Professor Patrick G. Harran, Chair

Ghrelin *O*-acyltransferase (GOAT) is a membrane bound *O*-acyltransferase (MBOAT) that was recently discovered in 2008. GOAT functions to catalyze the octanoylation of ghrelin, a 28-residue peptide hormone with implications in various metabolic pathways. In its active form, ghrelin plays a role in processes such as glucose homeostasis, insulin secretion and feeding behavior. The ghrelin/GOAT system is unique in that ghrelin is the only known octanoylated hormone and GOAT is the only enzyme known to perform this octanoylation. Thus, the ghrelin/GOAT pathway has high selectivity and specificity. For years, as described in Chapter 1, the MBOAT family of enzymes have been targeted for various therapeutic treatments. We have envisioned that targeting GOAT to disrupt the ghrelin signaling pathway could offer a treatment pathway for metabolic diseases such as obesity and type II diabetes resultant from obesity.

Additionally, it is thought that targeting of GOAT could have beneficial implications in treatment of Prader-Willi syndrome, a condition that often leads to the inability for patients to suppress hunger.

Chapter 2 discusses the discovery of ghrelin and GOAT. In addition to the specificity afforded by the ghrelin/GOAT system, ghrelin and GOAT are both primarily produced in the stomach and thus inhibitors of GOAT would not need to penetrate the blood brain barrier and could thus mitigate potential toxicities associated with action of the CNS.

Chapter 3 describes our efforts toward the development of small molecule peptidomimetic inhibitors of GOAT. Starting from a pyrrolidine-containing lead inhibitor described and developed by former lab member Dr. Ryan Hollibaugh, we detail the efforts toward development of a compound displaying superior *in vitro*, cellular, and *in vivo* activity. Compound development led to the discovery of the most potent inhibitor *in vitro*, the discovery of compounds displaying superior cellular activity, and the first known macrocyclic inhibitor of GOAT.

In Chapter 4, the development of a small molecule heterocyclic GOAT inhibitor is described. Inspired by several pharmaceutical companies that began working on GOAT, we developed a small molecule heterocyclic inhibitor that is more “drug-like”. This work led to the discovery of an inhibitor displaying excellent *in vitro*, cellular, and *in vivo* efficacy. Compounds of this class provide a foundation for further medicinal chemistry efforts to fine tune the properties for the therapeutic potential of GOAT inhibition.

The dissertation of Emily Suzanne Murzinski is approved.

Neil Kamal Garg

Ohyun Kwon

Peter John Tontonoz

Patrick Harran, Committee Chair

University of California, Los Angeles

2020

*This dissertation is dedicated to my parents, Amy and Frank,  
and my sister, Alicia, who have always supported me.*

## TABLE OF CONTENTS

ABSTRACT OF THE DISSERTATION.....	ii
COMMITTEE PAGE.....	iv
DEDICATION PAGE.....	v
TABLE OF CONTENTS.....	vi
LIST OF FIGURES.....	ix
LIST OF SCHEMES.....	xiii
ACKNOWLEDGEMENTS .....	xv
VITA.....	xvii
<b>1 Membrane Bound O-Acyltransferases and Their Role in Drug Development.....</b>	<b>1</b>
1.1 Introduction.....	1
1.2 MBOATs Involved in Neutral Lipid Biosynthesis.....	2
1.3 MBOATs Involved in Phospholipid Remodeling.....	4
1.4 MBOATs Involved in Protein/Peptide Acylation.....	5
1.5 Conclusion.....	6
1.6 References.....	7
<b>2 Ghrelin and the Discovery of Ghrelin O-acyltransferase (GOAT).....</b>	<b>10</b>
2.1 Introduction.....	10
2.2 Discovery of Ghrelin and Its Role in Regulatory Metabolism.....	11
2.3 Discovery of Ghrelin O-Acyltransferase (GOAT).....	15
2.4 Targeting GOAT for Therapeutic Intervention.....	18
2.5 Conclusions.....	20
2.6 References.....	20
<b>3 Hypothesis Driven Design and Synthesis of Lipopeptidomimetic Inhibitors of GOAT.....</b>	<b>26</b>
3.1 Introduction.....	26
3.2 Pyrrolidine-Containing Inhibitors.....	30
3.2.1 Synthesis and Evaluation of Modifications of the P2 Residue.....	34
3.2.1.1 Synthesis of P2 Modifications.....	34
3.2.1.2 Evaluation of P2 Modifications.....	39



3.2.2 Evaluation of Covalent Modifiers.....	40
3.2.3 Synthesis and Evaluation of Side Chain Modifications.....	41
3.2.3.1 Synthesis of Side Chains.....	41
3.2.3.2 Evaluation of Side Chain Modifications.....	42
3.2.4 Discussion.....	43
3.3 Linear Peptidomimetic Inhibitors of GOAT.....	44
3.3.1 Development and Evaluation of <i>In Vitro</i> Linear Peptidomimetic Inhibitors of GOAT.....	45
3.3.1.1 Side Chain Modifications to Identify Desirable Binding Interactions.....	46
3.3.1.2 Evaluation of P4 Residue Modifications in the Generation of Potent Tetrapeptides.....	49
3.3.2 Development of an INS-1 Stable Cell Line for a Cell-Based GOAT Assay.....	53
3.3.2.1 Evaluation of Linear Peptidomimetics in a Cellular Assay.....	56
3.3.2.2 Optimizing the Cellular Activity of Tetrapeptide <b>59</b> .....	57
3.3.3 <i>In Vivo</i> Evaluation of Lead Compound <b>128</b> .....	62
3.3.4 Discussion.....	65
3.4 Macrocyclic Peptidomimetic Inhibitors of GOAT.....	65
3.4.1 Design and Development of Macrocycles.....	66
3.4.1.1 Design and Synthesis of Macrocyclic Aryl Ethers.....	67
3.4.1.2 Design, Synthesis, and Evaluation of Alkenyl Macrocyclic Inhibitors.....	69
3.4.1.3 Evaluation of Side Chain Modifications of Macrocyclic Inhibitors.....	77
3.5 Conclusion.....	78
3.6 References.....	79
<b>4 Design and Development of Small Molecule Heterocyclic Inhibitors of GOAT....</b>	<b>83</b>
4.1 Introduction.....	83

4.2 Hypothesis Driven Design and Development of Small Molecule Heterocyclic Inhibitors.....	86
4.2.1 Synthesis and Evaluation of Our First Small Molecule Heterocyclic Hybrid Inhibitor.....	86
4.2.2 Design and Evaluation of Derivatives of <b>22</b> to Improve Activity.....	90
4.3 Scale Up and Evaluation of Small Molecule Heterocyclic Inhibitors.....	92
4.3.1 Evaluation of Small Molecule Heterocyclic Inhibitors <b>6</b> and <b>7</b> .....	97
4.4 Current State of Small Molecule Heterocyclic Inhibitors.....	99
4.5 Conclusions.....	100
4.6 References.....	101
<b>5 Experimental Appendices.....</b>	<b>103</b>
<b>Experimental Procedures Supporting Chapter 3.....</b>	<b>104</b>
A. Materials and Methods.....	104
B. General Procedures (GP).....	104
C. Experimental Procedures and Characterization.....	107
D. References.....	163
<b>Experimental Procedures Supporting Chapter 4.....</b>	<b>163</b>
A. Materials and Methods.....	163
B. Reported GOAT Inhibitors.....	164
C. Preparation of Small-Molecule Heterocyclic Inhibitors.....	165
D. References.....	175
<b>6 Compiled <i>In Vitro</i> and Cellular Inhibition Assay Results.....</b>	<b>176</b>
<b><i>In Vitro</i> Inhibition Data.....</b>	<b>176</b>
A. Methods.....	176
B. <i>In Vitro</i> Assay Results.....	178
<b>INS-1 Cellular Inhibition Data.....</b>	<b>277</b>
A. Methods.....	277
B. Cellular Assay Results.....	280

## List of Figures

<b>Figure 1.1.</b> Sequence alignments of MBOATs.....	1
<b>Figure 1.2.</b> Compounds arising from medicinal chemistry campaigns targeting MBOATs for therapeutic potential.....	3
<b>Figure 1.3.</b> Inhibitors of GOAT designed to decrease the production of acyl-ghrelin (14).....	6
<b>Figure 2.1.</b> Physiology of Ghrelin.....	10
<b>Figure 2.2.</b> Agonists of GHS-r, Ghrelin (1), GHRP-6 (2), and Ibutamoren (MK-0677) (3).....	11
<b>Figure 2.3.</b> Discovery of MBOAT4/GOAT as the enzyme responsible for octanoylation.....	15
<b>Figure 2.4.</b> Predicted transmembrane topology of hGOAT.....	16
<b>Figure 2.5.</b> Structural model of the GOAT active site.....	17
<b>Figure 3.1.</b> Representative structures of the three major classes of GOAT inhibitors that have been disclosed.....	26
<b>Figure 3.2.</b> Reported peptidomimetic inhibitors of GOAT.....	27
<b>Figure 3.3.</b> <i>In vivo</i> pharmacology of GO-CoA-Tat.....	28
<b>Figure 3.4.</b> SAR exploration of pentapeptide 5 to produce peptidomimetic 9 with the key transformations identified.....	30
<b>Figure 3.5.</b> Evaluation of structural features deemed necessary for favorable binding (left) and sites where modification can be made to improve efficacy (right).....	32
<b>Figure 3.6.</b> Evaluation of <i>in vitro</i> efficacies of modified P2 inhibitor derivatives.....	39
<b>Figure 3.7.</b> Evaluation of <i>in vitro</i> potency of modified pyrrolidine derivatives.....	40

<b>Figure 3.8.</b> Incorporation and evaluation of sidechain modifications.....	42
<b>Figure 3.9.</b> Evaluation of <i>in vivo</i> properties.....	44
<b>Figure 3.10.</b> Development of linear peptidomimetic inhibitors.....	45
<b>Figure 3.11.</b> Evaluation of tetrapeptide sidechain modifications.....	48
<b>Figure 3.12.</b> Identification of aspects important for GOAT inhibition.....	49
<b>Figure 3.13.</b> Aromatic screening and evaluation of the P4 residue.....	50
<b>Figure 3.14.</b> Most probable charged states of tyrosine (left) and histidine (right) contributing to loss of activity.....	51
<b>Figure 3.15.</b> Evaluation of substituents on the phenyl ring of the P4 position.....	52
<b>Figure 3.16.</b> Western blot analysis of peptide extract of INS-1 cells.....	54
<b>Figure 3.17.</b> Optimization of a cellular assay for GOAT activity.....	55
<b>Figure 3.18.</b> Cellular analysis of minimally modified ghrelin truncation peptides ( <b>65–69</b> ).....	56
<b>Figure 3.19.</b> Evaluation of alterations to the C-terminal carboxamide to reduce tPSA and improve cellular activity.....	58
<b>Figure 3.20.</b> Cellular assay of C-terminus modified tetrapeptides.....	60
<b>Figure 3.21.</b> Implementation of C-terminus modification showing improvements in tetrapeptide scaffold.....	61
<b>Figure 3.22.</b> Cellular assay evaluation of C-terminus modified pentapeptides.....	61
<b>Figure 3.23.</b> Dietary and pharmacological effects on plasma acyl-ghrelin in wild type C57/BL6J male mice.....	62
<b>Figure 3.24.</b> Evaluation of pharmacokinetic properties of <b>128</b> .....	63

<b>Figure 3.25.</b> Regulation of mouse plasma ghrelin by food (Panel A) and through pharmacological inhibition of GOAT enzyme (Panels B and C).....	64
<b>Figure 3.26.</b> Macrocycles derived from pyrrolidine-containing inhibitors <b>9</b> .....	66
<b>Figure 3.27.</b> Aryl etherification using an iridium photocatalyst to generate macrocycles and macrocycle precursors.....	68
<b>Figure 3.28.</b> Ring closing metathesis precursor <b>142</b> developed from allyl-serine residue <b>143</b> and allyl-phenylalaninol residue <b>144</b> for generation of macrocyclic peptidomimetic GOAT inhibitors.....	69
<b>Figure 3.29.</b> Macrocycle compound <i>E-151</i> is a substrate competitive inhibitor of GOAT.....	71
<b>Figure 3.30.</b> Caco-2 permeability of <i>E-151</i> .....	72
<b>Figure 3.31.</b> Modifying macrocyclic inhibitors to improve <i>in vitro</i> and cellular activity.....	76
<b>Figure 3.32.</b> Evaluation of modification to the sidechain of macrocyclic GOAT inhibitors.....	77
<b>Figure 4.1.</b> Reported small molecule heterocyclic GOAT inhibitors reported by pharmaceutical companies and structure of Coenzyme A.....	83
<b>Figure 4.2.</b> Benzothiophene GOAT inhibitor developed by Takeda.....	84
<b>Figure 4.3.</b> Small molecule heterocyclic GOAT inhibitors designed to be a hybrid of <b>1</b> and <b>2</b> with incorporation of a pseudo-octanoyl tail for generation of <b>7</b> .....	86
<b>Figure 4.4.</b> Evaluation of derivative of <b>22</b> for improved activity.....	90
<b>Figure 4.5.</b> Evaluation of sidechain modifications.....	92
<b>Figure 4.6.</b> Pharmacological effect of <b>7</b> on plasma acyl-ghrelin in wild type C57BL male mice.....	98

**Figure 4.7.** GLWL-01, a compound currently undergoing clinical trials for various indications.....99

## List of Schemes

<b>Scheme 1.1.</b> Outcomes of MBOAT processing on cholesterol ( <b>1</b> ) and diacylglycerol ( <b>3</b> ).....	2
<b>Scheme 1.2.</b> LPAT processing of lysophospholipids into phospholipids.....	4
<b>Scheme 1.3.</b> MBOATs involved in protein/peptide acylation.....	5
<b>Scheme 2.1.</b> Mechanism of GOAT's action on ghrelin utilizing octanoyl CoA as the octanoyl source.....	16
<b>Scheme 3.1.</b> Synthesis of $\beta^3$ - <i>tert</i> -leucine residue <b>12</b> for the generation of modified inhibitor <b>20</b> .....	35
<b>Scheme 3.2.</b> Synthesis of $\beta^2$ - <i>tert</i> -leucine residue <b>26</b> for synthesis of <b>27</b> .....	36
<b>Scheme 3.3.</b> Synthesis of modified P2 residues.....	37
<b>Scheme 3.4.</b> Representative synthesis of cyclobutene-containing sidechains for development of inhibitors <b>51–54</b> .....	41
<b>Scheme 3.5.</b> Synthesis of 6-methyl octanoic acid <b>49</b> .....	41
<b>Scheme 3.6.</b> Probing the effects of mono-oxygenation along the sidechain.....	46
<b>Scheme 3.7.</b> Probing the effects of altering the amide/ester linkage of the octanoyl sidechain at the P3 position.....	47
<b>Scheme 3.8.</b> Synthesis of modified C-terminal residues.....	59
<b>Scheme 3.9.</b> Synthesis of macrocyclic GOAT inhibitor <b>150</b> .....	70
<b>Scheme 3.10.</b> Synthesis of alkenyl macrocyclic GOAT inhibitors utilizing an Fmoc-protected glycine residue to allow for deprotection without reduction of the olefin.....	71
<b>Scheme 3.11.</b> Synthesis of geminal di-methyl allyl ether <b>157</b> to mimic the P2 <i>tert</i> -leucine residue.....	73

<b>Scheme 3.12.</b> Synthesis of alkenyl residues for incorporation into macrocycles.....	74
<b>Scheme 4.1.</b> Partial syntheses of compound <b>1</b> (A) and <b>2</b> (B) for design of the synthetic route to <b>6</b> and <b>7</b> .....	87
<b>Scheme 4.2.</b> Stitching together key fragments <b>12</b> and <b>9</b> to afford desired hybrid inhibitors.....	88
<b>Scheme 4.3.</b> Synthesis of alkenyl hybrid inhibitor <b>22</b> .....	89
<b>Scheme 4.4.</b> Alternative annulation strategy employed by BI for the synthesis of compounds of type <b>34</b> .....	94
<b>Scheme 4.5.</b> Synthesis of key intermediate <b>35</b> .....	95
<b>Scheme 4.6.</b> Synthesis of compound <b>43</b> <i>via</i> utilization of alternative annulation strategy.....	96
<b>Scheme 4.7.</b> Synthesis of true hybrid compound <b>6</b> and its regioisomer <b>48</b> .....	96



## ACKNOWLEDGEMENTS

During my time as a student both at UCLA and prior to graduate school, there have been many who have helped me along the way. I am grateful for everyone who has stood by me and who have guided me throughout my career. I would not be the scientist I am today without the help of those surrounding me.

I want to thank my scientific advisors both past and present. First, I want to thank my advisor, Professor Patrick Harran for his guidance and support over the past five years. Thank you for challenging me scientifically and seeing in me what I could not see myself and encouraging me to tackle new challenges. I also want to thank Dr. Peter Pyun at Gilead Sciences for mentoring me as an intern eager to understand medicinal chemistry. A lot of my technical skills were learned and developed under your guidance and with your support and I am forever grateful for the opportunities provided during my time at Gilead. Thank you to Dr. Megan Bolitho at USF for allowing me to conduct undergraduate research and sparking my interest in organic chemistry. Finally, I want to thank my high school chemistry teacher, Susan Salb, for making chemistry so engaging and fun and inspiring me to pursue a career in chemistry!

Next, I want to thank those who were instrumental in the work described within. None of this would be possible without the work of Dr. David Strugatsky. He has been the lead biochemist on the project and has not only run all of the assays but also developed a reliable cellular assay that was instrumental in guiding our inhibitor developments. I have gotten the opportunity to mentor several graduate students and undergraduate students during my time on this project and I am thankful for their aid. Thank you to Luke Sisto who not only came in ready to help however necessary but who has also become

a great friend in my time here and someone who is always available to bounce ideas off of. To my undergraduates, Dyana Kenanova, Cole Meyer, and Melinda Cheng, thank you for the time you spent helping me as well as putting up with me when I was stressed out. Finally, I owe a huge amount of gratitude to Dr. Hui Ding. Not only was Hui an instrumental part of this project, but he is also a person I could go to for anything and everything. Thank you for always answering my questions and for tolerating my sometimes questionable music choices in lab. I will miss our conversations and math problem sessions. Funding support was provided by the NIH by the NIDDK (1R01DK100627), the NSF (CHE-1048804), and the SG fellowship.

I also want to thank the Harran lab members past, present, and adopted. Dr. Brice Curtin and Dr. Tyler Allred were tremendous supports during my first years of graduate school and are people I still go to for advice. Thank you to the current lab members, Rupert, Sal, Evan, Ishika, Anton, and Morris for their advice and support throughout the years. Finally, thank you to former adopted lab member Dr. Yolanda Li (Rubin lab) for helping me make it through our last five years together and allowing me to just walk in whenever I needed advice.

Last but not least, I want to thank my family for their continued support. Thank you to my parents, Amy and Frank, for always encouraging me to go after my dreams and believing in me even when I didn't believe in myself. Thank you to my sister, Alicia, for always being there for me no matter what. To my niece, Layla, thank you for being the crazy, goofy self you are and always putting a smile on my face even after the toughest days. Though you may not remember these years, I will forever cherish them.

To everyone I have encountered in these last five years, THANK YOU!

## VITA

### **FORMAL EDUCATION**

*University of California, Los Angeles, Los Angeles, CA*

Doctor of Philosophy in Chemistry

Expected: December 2020

Master of Science in Chemistry

June 2017

*University of San Francisco, San Francisco, CA*

Bachelor of Science in Chemistry, Cum Laude

December 2014

### **PUBLICATIONS**

**Emily Murzinski**, Hui Ding, Ishika Saha David Strugatsky, Peter Tontonoz, and Patrick G. Harran. Development of small molecule inhibitors of ghrelin O-acyltransferase. *Manuscript in preparation.*

**Emily Murzinski** and Patrick Harran. (2020) Compositions and Methods for Treating Obesity. Provisional Patent Application 62/979,915. *Filed Feb. 21, 2020.*

Patrick G. Harran, Peter Tontonoz, David Strugatsky, Hui Ding, and **Emily Murzinski**. (2017). Inhibitors of Ghrelin O-Acyl Transferase. Provisional Patent Application 62/608,238. Filed Dec. 20, 2017.

Kreuger, T.D.; **Murzinski, E.S.**; Rodriguez, K.E.; Li, J.J. Lorcaserin (Belviq): serotonin 2C receptor agonist for the treatment of obesity. In *Innovative Drug Synthesis*. 2016: 243–254.

### **PRESENTATIONS**

**Murzinski, E.S.\***; Ding, H.; Sisto, L.; Kenanova, D.; Strugatsky, D.; Harran, P.G. “Development of Potent, Small Molecule Inhibitors of Ghrelin O-Acyl Transferase (GOAT).” Seaborg Symposium 2016, UCLA, Los Angeles, CA, November 12, 2016. (**poster presentation**)

Cudia, D.L.\*; **Murzinski, E.S.\***; Corcoran, B.; Showell-Rouse, E.; Bolitho, M.E. “An Alternate Synthesis of S-D-Ribosyl-L-homocysteine (SRH) and Analogs.” 248<sup>th</sup> ACS National Meeting & Exposition, San Francisco, CA, August 10-14, 2014. (**poster presentation**)

Cudia, D.L.\*; **Murzinski, E.S.\***; Corcoran, B.; Showell-Rouse, E.; Bolitho, M.E. “An Alternate Approach for the Synthesis of S-Ribosylhomocysteine (SRH).” 26<sup>th</sup> Annual American Chemical Society Northern California Undergraduate Research Symposium, San Francisco, CA, May 3, 2014. (**poster presentation**)

Cudia, D.L.\*; **Murzinski, E.S.\***; Corcoran, B.; Showell-Rouse, E.; Bolitho, M.E. “An Alternate Approach for the Synthesis of S-Ribosylhomocysteine (SRH).” USF CARD Poster Session, San Francisco, CA, April 25, 2014. (**poster presentation**)

Showell-Rouse, E.\*; Corcoran, B.; **Murzinski, E.S.**; Cudia, D.L.; Bolitho, M.E. “Probing the scope of the chemical synthesis of S-ribosyl-L-homocysteine (SRH) from various homocysteine and ribose moieties.” 44<sup>th</sup> Western Regional Meeting of the American Chemical Society, Santa Clara, CA, October 3-6, 2013. (**poster presentation**)

### **HONORS – AWARDS**

2020 Michael E. Jung Excellence in Teaching Award

2019 UCLA Technology Development Group Innovation Fund Finalist

2019 SG Fellowship

2011–2014 University Scholar (USF)

2011–2014 USF Dean’s List

2013 USF Undergraduate Research Summer Fellowship

# 1. Chapter One – Membrane Bound O-Acyltransferases and Their Role in Drug Development

## 1.1 Introduction

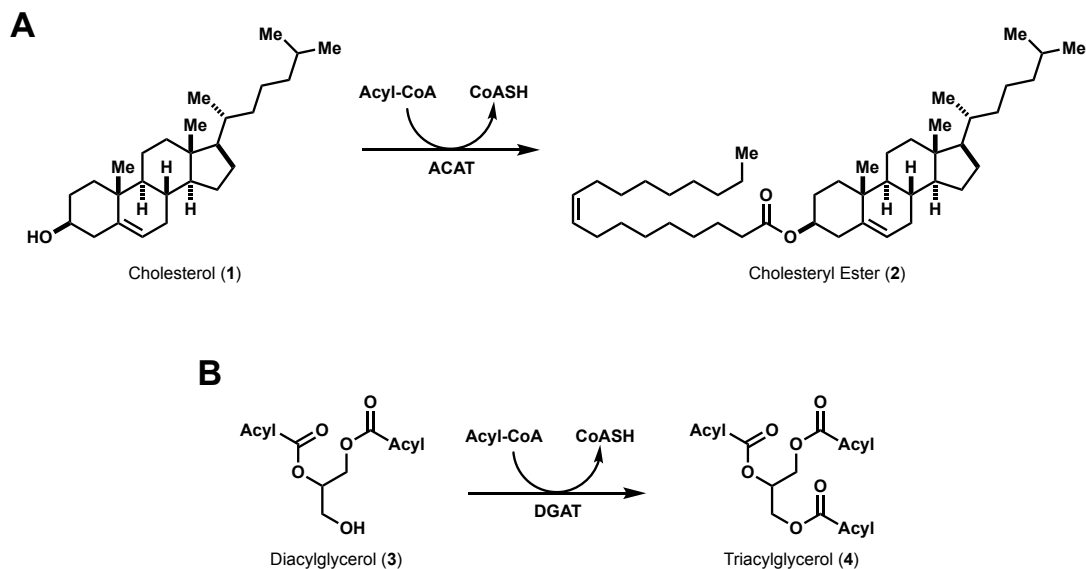
The membrane-bound O-acyltransferases (MBOATs) are a family of acyltransferase enzymes discovered two decades ago by Hofmann.<sup>1</sup> Hofmann identified the MBOAT family of enzymes through sequence homology amongst known acyltransferases. Consistent amongst the MBOAT enzymes are their transmembrane structure as well as two conserved active site residues, histidine and asparagine, which are highlighted in Figure 1.1. As the name implies, the MBOATs are a family of enzymes that are embedded in the membrane and are responsible for the transfer of organic fatty acids – most commonly onto a hydroxyl group within target substrates. MBOATs participate in several different biological functions which include neutral lipid biosynthesis, protein and peptide acylation, and phospholipid remodeling. Numerous MBOATs have become the subject of drug discovery efforts, targeting diseases such as atherosclerosis, obesity, Alzheimer’s, and viral infections.<sup>2</sup>

```

MBOAT1 347 ENWN IQTAT W LKVCYQ-----RVPWY-----PTVLT F I L S A L W H G 382 LPEAT1
MBOAT2 339 DNWN IQTAL W LKRVCYE-----RTSFS-----PTIQT F I L S A I W H G 374 LPCAT4
MBOAT3 337 THFDRGIND W LCKYVYN----HIGGEHSA VIPELAATVAT F A I T T L W L G 381 HHATL
MBOAT4 304 RKWNQSTAR W LRRLLVFQ-----HSRAW-----PLLQT F A F S A W W H G 339 GOAT
MBOAT5 335 A S F N I N T N A W V A R Y I F K - R L K F L G N K E L S Q ----- G L S L L F L - - A L W H G 375 LPCAT3
MBOAT7 318 R Y W N M T V Q W W L A Q Y I Y K S A ---- P A R S Y V L ----- R S A W T M L L S A Y W H G 357 LPIAT1

```

**Figure 1.1.** Sequence alignments of well-studied MBOATs showing the highly conserved N and H residues in red and moderately conserved residues in green (residues that are conserved in >50% of MBOAT sequences)



**Scheme 1.1.** Outcomes of MBOAT processing on cholesterol (1) and diacylglycerol (3). (A) Action of ACAT on cholesterol (1) to generate cholesteryl esters (2). (B) Action of DGAT on diacylglycerol (3) to generate triacylglycerols (4)

## 1.2 MBOATs Involved in Neutral Lipid Biosynthesis

The first class of MBOATs are those involved in neutral lipid biosynthesis, which includes the acyl-coenzyme A:cholesterol acyltransferases (ACATs) and diacylglycerol O-acyltransferase (DGAT). ACATs are a family of enzymes that are responsible for the acylation of the hydroxyl group of cholesterol with a long-chain fatty acid. Through the conversion of cholesterol to cholesteryl ester, ACATs prevent excess cholesterol from accumulating in the membranes of the endoplasmic reticulum and have thus garnered attention as drug targets.<sup>2</sup> Both ACAT1 and ACAT2 have been targeted for the treatment of atherosclerosis, a condition marked by the hardening of the arteries caused by the buildup of fats and cholesterol on artery walls and thereby reducing blood flow.<sup>3</sup> By inhibiting ACAT, the production of cholesteryl esters is reduced, which promotes the excretion of unacylated cholesterol in the bile. In the early 2000s, Pfizer reported on an ACAT inhibitor, Avasimibe (5), which was capable of reducing cholesterol levels while

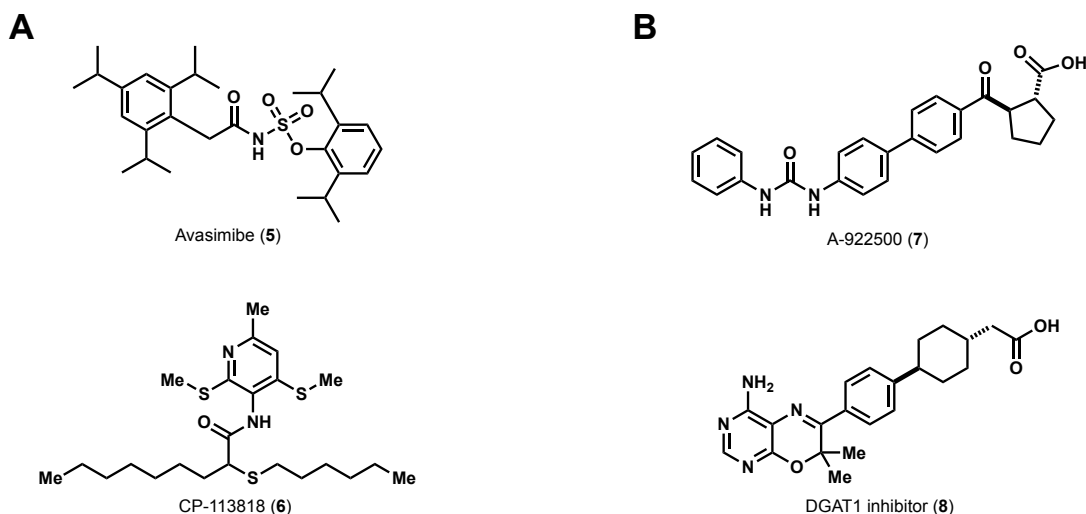


**Figure 1.2.** Compounds arising from medicinal chemistry campaigns targeting MBOATs for therapeutic potential. (A) ACAT inhibitors (B) DGAT1 inhibitors.

also reducing the incidence of atherosclerosis.<sup>4</sup> In 2003, clinical trials were ultimately halted for Avasimibe due to the difficulty of quantifying the prevention of plaque buildup in addition to the drug being shown to weaken effects of other drugs present in the body. ACAT1 has been further studied for its involvement in targeting Alzheimer's disease.<sup>5</sup> In a 2004 study by Hutter-Paier and coworkers, they demonstrated that when a mouse model for Alzheimer's disease was treated with CP-113818 (6), amyloid plaque density was significantly diminished.<sup>6</sup>

DGAT enzymes function to transfer long-chain fatty acids to hydroxyl groups of diacylglycerol and are multifunctional.<sup>7,8</sup> Studies on DGAT1 have demonstrated the DGAT1 knockout mice are resistant to diet-induced obesity and also display greater insulin sensitivity in comparison to wild-type mice.<sup>9</sup> Thus, DGAT1 inhibition has been targeted for its role in treatment regimens focused on obesity and type II diabetes. This focus has led to the discovery of DGAT1 inhibitors 7 and 8, which were key in studying therapeutic relevance of modulating DGAT1 activity.<sup>10,11</sup> Furthermore, recent studies

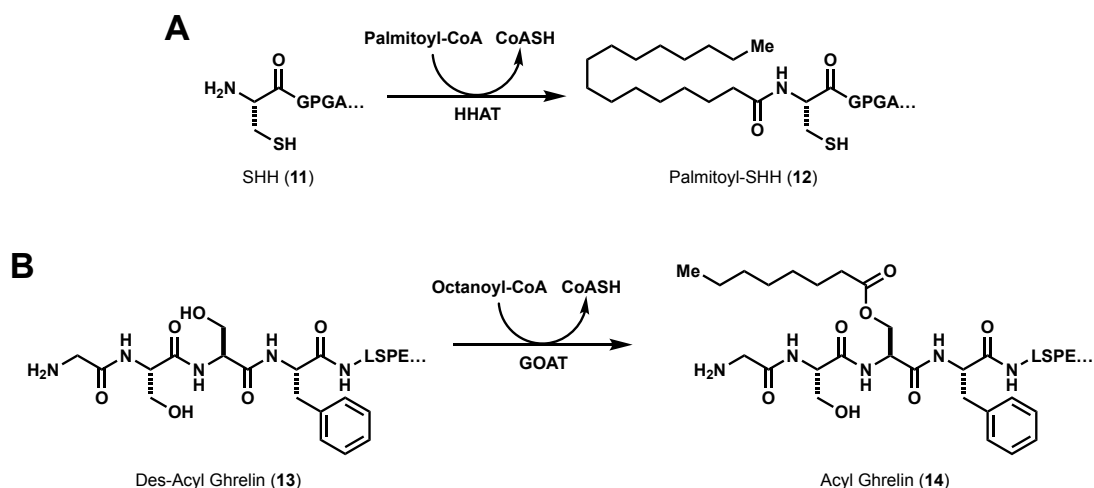




## 1.4 MBOATs Involved in Protein/Peptide Acylation

Certain MBOATs function to acylate nucleophiles in specific protein and peptide targets. These enzymes include Porcupine (PORCN), Hedgehog acyltransferases (HHAT), ghrelin O-acyltransferase (GOAT), and Hedgehog acyltransferase-like (HHATL). Porcupine played a crucial role in Hofmann's discovery of the MBOATs through recognition of the sequence homology between PORCN and the ACAT and DGAT enzymes.<sup>1</sup> PORCN acts to catalyze the acylation of serine and cysteine residues in the protein Wingless. This process underpins Wnt signaling, which plays a vital role in embryogenesis, normal physiological processes, and carcinogenesis.<sup>17-19</sup> HHAT enzymes are responsible for the palmitoylation of sonic hedgehog, which is a protein known for its important roles in the developmental processes.

GOAT was identified in 2008 as the enzyme responsible for the octanoylation of the serine-3 residue of ghrelin<sup>20</sup>, utilizing octanoyl CoA as its substrate.<sup>21,22</sup> Due to ghrelin's involvement in stimulated release of growth hormone from pituitary cells, both



**Scheme 1.3.** MBOATs involved in protein/peptide acylation. (A) HHAT processing of SHH (11) to palmitoylate the N-terminus. (B) GOAT processing of des-acyl ghrelin (13) to octanoylate the serine-3 residue.

ghrelin and GOAT have become drug targets for obesity.<sup>23</sup> Inhibitor development largely revolves around ghrelin mimetics following the discovery by Brown & Goldstein<sup>24</sup> that GOAT could be partially inhibited by its reaction product, acyl ghrelin (**14**), and furthermore by its pentapeptide mimic **15**. Studies into the role of GOAT inhibition in therapeutic regimens is still an ongoing and active field.



**Figure 1.3.** Inhibitors of GOAT designed to decrease the production of acyl-ghrelin (**14**). *Left:* acyl-ghrelin (**14**) (the product of enzymatic processing of des-acyl ghrelin by GOAT) was shown to partially inhibit the GOAT enzyme. *Right:* first five residues of the ghrelin sequence bearing an octanamide at the third position has been shown to be a potent inhibitor of GOAT.

## 1.5 Conclusion

MBOATs play myriad roles in signaling regulation and several members of the family have been validated as targets for drug discovery. Targeting these enzymes has the potential to reveal groundbreaking treatments for serious diseases that affect a large population of patients, but there are limitations to be overcome due to the unknown structural complexity of these enzymes. Additionally, further studies into the implications of chronically inhibiting these enzymes *in vivo* need to be conducted to validate treatment pathways. Thus, we have set forth to gain a better understanding of MBOAT4 specifically, and its role in ghrelin signaling as it relates to therapeutics.

## 1.6 References

- (1) Hofmann, K. A Superfamily of Membrane-Bound O-Acyltransferases with Implications for Wnt Signaling. *Trends Biochem. Sci.* **2000**, 25 (3), 111–112.
- (2) Chang, C. C. Y.; Sun, J.; Chang, T.-Y. Membrane-Bound O-Acyltransferases (MBOATs). *Front. Biol. (Beijing)*. **2011**, 6 (3), 177–182.
- (3) Chang, T.-Y.; Li, B.-L.; Y Chang, C. C.; Urano, Y. A:Cholesterol Acyltransferases. *Am J Physiol Endocrinol Metab* **2009**, 297, 1–9.
- (4) Delsing, D. J. M.; Offerman, E. H.; van Duyvenvoorde, W.; van der Boom, H.; de Wit, E. C. M.; Gijbels, M. J. J.; van der Laarse, A.; Jukema, J. W.; Havekes, L. M.; Princen, H. M. G. Acyl-CoA:Cholesterol Acyltransferase Inhibitor Avasimibe Reduces Atherosclerosis in Addition to Its Cholesterol-Lowering Effect in ApoE\*3-Leiden Mice. *Circulation* **2001**, 103 (13), 1778–1786.
- (5) Bryleva, E. Y.; Rogers, M. A.; Chang, C. C. Y.; Buen, F.; Harris, B. T.; Rousselet, E.; Seidah, N. G.; Oddo, S.; Laferla, F. M.; Spencer, T. A.; Hickey, W. F.; Chang, T. Y. ACAT1 Gene Ablation Increases 24(S)-Hydroxycholesterol Content in the Brain and Ameliorates Amyloid Pathology in Mice with AD. *Proc. Natl. Acad. Sci. U. S. A.* **2010**, 107 (7), 3081–3086.
- (6) Hutter-Paier, B.; Huttunen, H. J.; Puglielli, L.; Eckman, C. B.; Kim, D. Y.; Hofmeister, A.; Moir, R. D.; Domnitz, S. B.; Frosch, M. P.; Windisch, M.; Kovacs, D. M. The ACAT Inhibitor CP-113,818 Markedly Reduces Amyloid Pathology in a Mouse Model of Alzheimer's Disease. *Neuron* **2004**, 44 (2), 227–238.
- (7) Yen, C. L. E.; Stone, S. J.; Koliwad, S.; Harris, C.; Farese, R. V. DGAT Enzymes and Triacylglycerol Biosynthesis. *Journal of Lipid Research*. 2008, pp 2283–2301.
- (8) Turkish, A. R.; Sturley, S. L. The Genetics of Neutral Lipid Biosynthesis: An Evolutionary Perspective. *American Journal of Physiology - Endocrinology and Metabolism*. July 2009, pp E19–E27.
- (9) Lee, B.; Fast, A. M.; Zhu, J.; Cheng, J. X.; Buhman, K. K. Intestine-Specific Expression of Acyl CoA:Diacylglycerol Acyltransferase 1 Reverses Resistance to Diet-Induced Hepatic Steatosis and Obesity in Dgat1 *-/-* Mice. *J. Lipid Res.* **2010**, 51 (7), 1770–1780.
- (10) Harris, C. A.; Haas, J. T.; Streeper, R. S.; Stone, S. J.; Kumari, M.; Yang, K.; Han, X.; Brownell, N.; Gross, R. W.; Zechner, R.; Farese, R. V. DGAT Enzymes Are Required for Triacylglycerol Synthesis and Lipid Droplets in Adipocytes. *J. Lipid Res.* **2011**, 52 (4), 657–667.
- (11) A. M. Birch, L. K. B. A. V. T. DGAT1 Inhibitors as Anti-Obesity and Anti-Diabetic

Agents. *Curr Opin Drug Discov Devel* **2010**, *13* (4), 489–496.

- (12) Herker, E.; Harris, C.; Hernandez, C.; Carpentier, A.; Kaehlcke, K.; Rosenberg, A. R.; Farese, R. V.; Ott, M. Efficient Hepatitis C Virus Particle Formation Requires Diacylglycerol Acyltransferase-1. *Nat. Med.* **2010**, *16* (11), 1295–1298. h
- (13) Hishikawa, D.; Shindou, H.; Kobayashi, S.; Nakanishi, H.; Taguchi, R.; Shimizu, T. Discovery of a Lysophospholipid Acyltransferase Family Essential for Membrane Asymmetry and Diversity. *Proc. Natl. Acad. Sci. U. S. A.* **2008**, *105* (8), 2830–2835.
- (14) Zhao, Y.; Chen, Y. Q.; Bonacci, T. M.; Bredt, D. S.; Li, S.; Bensch, W. R.; Moller, D. E.; Kowala, M.; Konrad, R. J.; Cao, G. Identification and Characterization of a Major Liver Lysophosphatidylcholine Acyltransferase. *J. Biol. Chem.* **2008**, *283* (13), 8258–8265.
- (15) Ariyama, H.; Kono, N.; Matsuda, S.; Inoue, T.; Arai, H. Decrease in Membrane Phospholipid Unsaturation Induces Unfolded Protein Response. *J. Biol. Chem.* **2010**, *285* (29), 22027–22035.
- (16) Demeure, O.; Lecerf, F.; Duby, C.; Desert, C.; Ducheix, S.; Guillou, H.; Lagarrigue, S. Regulation of LPCAT3 by LXR. *Gene* **2011**, *470* (1–2), 7–11.
- (17) Logan, C. Y.; Nusse, R. The Wnt Signaling Pathway in Development and Disease. *Annual Review of Cell and Developmental Biology*. 2004, pp 781–810.
- (18) Moon, R. T.; Kohn, A. D.; Ferrari, G. V. De; Kaykas, A. WNT and  $\beta$ -Catenin Signalling: Diseases and Therapies. *Nat. Rev. Genet.* **2004**, *5* (9), 691–701.
- (19) Reya, T.; Clevers, H. Wnt Signalling in Stem Cells and Cancer. *Nature* **2005**, *434* (7035), 843–850.
- (20) Kojima, M.; Hosoda, H.; Date, Y.; Nakazato, M.; Matsuo, H.; Kangawa, K. Ghrelin Is a Growth-Hormone-Releasing Acylated Peptide from Stomach. *Nature* **1999**, *402* (6762), 656–660.
- (21) Gutierrez, J. A.; Solenberg, P. J.; Perkins, D. R.; Willency, J. A.; Knierman, M. D.; Jin, Z.; Witcher, D. R.; Luo, S.; Onyia, J. E.; Hale, J. E. Ghrelin Octanoylation Mediated by an Orphan Lipid Transferase. *Proc. Natl. Acad. Sci. U. S. A.* **2008**, *105* (17), 6320–6325.
- (22) Yang, J.; Brown, M. S.; Liang, G.; Grishin, N. V.; Goldstein, J. L. Identification of the Acyltransferase That Octanoylates Ghrelin, an Appetite-Stimulating Peptide Hormone. *Cell* **2008**, *132* (3), 387–396.
- (23) Lim, C. T.; Kola, B.; Korbonits, M. The Ghrelin/GOAT/GHS-R System and Energy Metabolism. *Rev. Endocr. Metab. Disord.* **2011**, *12* (3), 173–186.

- (24) Yang, J.; Zhao, T. J.; Goldstein, J. L.; Brown, M. S. Inhibition of Ghrelin O-Acyltransferase (GOAT) by Octanoylated Pentapeptides. *Proc. Natl. Acad. Sci. U. S. A.* **2008**, *105* (31), 10750–10755.

## 2. Chapter Two – Ghrelin and the Discovery of Ghrelin O-acyltransferase (GOAT)

### 2.1 Introduction

Ghrelin (1) is a 28 amino acid peptide hormone primarily produced in the stomach that regulates metabolic pathways controlling insulin secretion, feeding behavior and glucose homeostasis in calorie-restricted settings.<sup>1</sup> Modulating levels of circulating ghrelin has the potential to treat disorders in which elevated ghrelin levels are observed, such as type II diabetes and Prader-Willi syndrome. The biologically active form of ghrelin is acyl-ghrelin, in which the serine-3 position of ghrelin is octanoylated. This atypical lipidation is catalyzed by the enzyme ghrelin O-acyltransferase (GOAT). GOAT is a member of the MBOAT family of proteins, yet is the only enzyme known to catalyze octanoylation of its substrate. Moreover, ghrelin is the only known octanoylated hormone. The observed specificity of the system makes GOAT an attractive target for the development of human drug candidates.

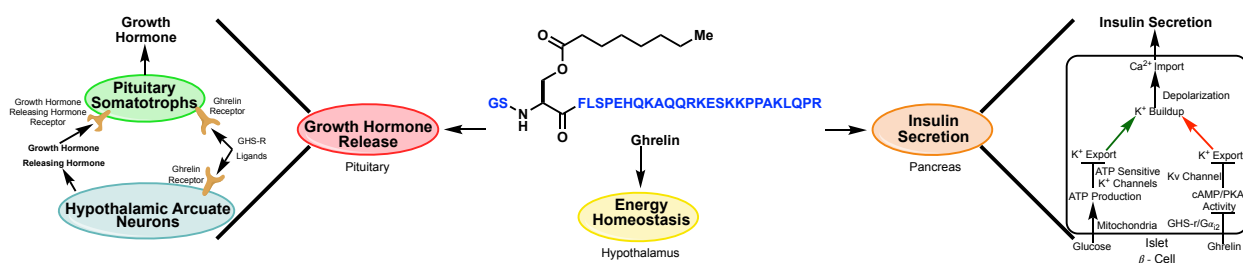


**Figure 2.1.** Physiology of Ghrelin. In the pituitary gland, GHS-r regulates the production of growth hormone through production of GHRH. In the pancreas, GHS-r is coupled to a different G-protein in which activation prevents accumulation of intracellular calcium which can suppress insulin release in response to glucose. In a context dependent manner, ghrelin also affects hunger, feeding behavior, and energy homeostasis.

## 2.2 Discovery of Ghrelin and Its Role in Regulatory Metabolism

The endogenous receptor for ghrelin was known prior to ghrelin itself, and it was identified using small molecule growth hormone secretagogues.<sup>2</sup> In 1996, researchers at Merck reported on small molecule growth hormone (GH) secretagogues, such as hexapeptide GHRP (**2**) and heterocyclic mimics of that peptide such as MK-0677 (**3**). Both of these substrates promoted the release of growth hormone from the pituitary.<sup>2,3</sup> During their experiments, they made the observation that these small molecules were acting with a different mechanism than that known to be associated with the GH release by growth hormone releasing hormones (GHRHs). Through competition studies with GHRH and **3** (as well as its derivatives), researchers noticed that cells that were treated with **2** and **3** still responded to treatment with GHRH. This led to the hypothesis that there existed a new receptor that was being targeted by these novel growth hormone secretagogues (GHSs). To explore their hypothesis, the researchers synthesized a <sup>35</sup>S-labeled variant of **3** as a detector for the specific binding site for the GHSs.<sup>2</sup> Through the study of <sup>35</sup>S-**3** in competition experiments, they uncovered that <sup>35</sup>S-**3** activity was inhibited by GHRP-6 (**2**) and that saturation with <sup>35</sup>S-**3** could displace GHRP-6 (**2**), thus fortifying the idea that these GHSs are competitively acting at the same binding site. Furthermore, when membranes were incubated with GHRH, <sup>35</sup>S-**3** activity was not inhibited, demonstrating

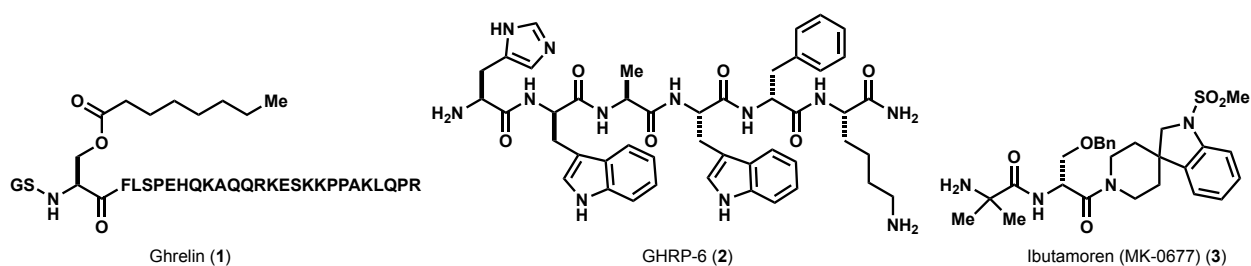


**Figure 2.2.** Agonists of GHS-r, Ghrelin (**1**), GHRP-6 (**2**), and Ibutamoren (MK-0677) (**3**).

the GHRH was not binding at the same receptor. GHSs have not only been linked to action at the GHS-R ligands that enable growth hormone release but they also effect activity of potassium channels that play a role in insulin secretion. The discovery of small molecules that could act independently of GHRH to promote growth hormone release garnered considerable attention from pharmaceutical firms as they sought to evaluate their utility in treatment of patients with GH deficiencies. MK-0677 and other GHS-R agonists entered clinical development without their receptor and its endogenous ligand being known<sup>3</sup>

In 1999, as small molecule GHSs and GHS-R agonists garnered more attention, Kojima and coworkers made a groundbreaking discovery in identification of the endogenous ligand for the GHS-R.<sup>1</sup> They constructed a stable CHO cell line expressing rat GHS-R, and after finding the highest activity in the stomach, purified stomach extracts to afford 16 micrograms of a lipidated 28 amino acid peptide, which they termed ghrelin, from 40g of rat stomach tissue. Initial sequencing of the peptide was unable to identify its third residue, but analysis of rat ghrelin suggested that position 3 would likely be serine, and that modification of that residue in the human hormone might be responsible for ambiguity in sequence data. Further analysis indicated that a hydrogen atom of the Ser3 residue was replaced with a C<sub>7</sub>H<sub>15</sub>CO moiety, a modification necessary for endocrine activity. Ghrelin was the first octanoylated peptide identified and remains the only known hormone bearing this modification.<sup>4</sup> Ghrelin can be found in circulation in both the acyl- and des-acyl forms.<sup>5</sup> However, at the time of its discovery, the mechanism by which octanoate was appended remained unknown but research elucidated the necessity of the octanoate for ghrelin activity.



The primary known function of ghrelin is to stimulate growth hormone release as discussed previously, but ghrelin has often been referred to as the “hunger hormone” due to its impact on feeding behavior and food intake. Analysis of ghrelin levels, first in rodents, and subsequently in humans, showed that ghrelin is secreted in a pulsatory manner. It was observed that ghrelin levels typically rise before a meal, or during a fasting period, and decrease following a meal.<sup>6,7</sup> This observation led to the hypothesis that ghrelin was acting as a hunger signal, signaling to the brain that it is time to eat. Support for this hypothesis arose when studies in the early 2000s showed that intravenous and subcutaneous administration of ghrelin increased food intake and furthermore that peripherally injected ghrelin stimulated hypothalamic neurons and food intake.<sup>8-10</sup> However, in a 2014 study, Zhao and co-workers made conflicting observations.<sup>11</sup> They determined that the amount of ghrelin required to induce a change in feeding behavior in mice far exceeded the level of circulating ghrelin observed under normal physiological conditions, even in fasted mice. Furthermore, in separate studies, several groups noted that ablation of ghrelin did not alter responses to food intake.<sup>11,12</sup>

Ghrelin’s role in hunger and feeding behavior is complex and not fully understood, however its role in glucose homeostasis has been well-studied and is better characterized.<sup>13,14</sup> Although ghrelin is primarily produced and stored in the stomach, ghrelin-producing cells as well as GHS-R can also be found in pancreatic islets, providing ghrelin an ability to play a crucial role in the modulation of insulin and glucagon release.<sup>15</sup> In a study conducted by Ghigo and coworkers, ghrelin was shown to increase plasma glucose levels and decrease insulin levels when it was injected in humans.<sup>16</sup> As shown in Figure 2.1, ghrelin acts on its receptor in pancreatic islets to suppress insulin secretion,

which has been supported by showing that blockage of endogenous ghrelin causes an increase in insulin secretion. This effect has consistently been observed not only in pancreatic islets<sup>17</sup>, but also in whole organism models.<sup>15</sup> Further studies on ghrelin's role in glucose homeostasis have been highly consistent and have demonstrated that administration of exogenous ghrelin reduces the response to glucose.<sup>18</sup> Infusion of ghrelin resulted in elevated blood glucose levels and decreased insulin levels, effects that could be reversed *via* introduction of a ghrelin antagonist. Moreover, when ghrelin knockout mice were subjected to a glucose tolerance test (GTT), they showed improved insulin secretion and glucose attenuation, readily clearing exogenous glucose.<sup>14</sup>

The key roles ghrelin plays in insulin regulation and glucose homeostasis exemplify the tractability of modification of ghrelin signaling as a therapeutic mechanism in conditions such as obesity and T2D resultant from obesity.<sup>19</sup> However, ghrelin signaling has been linked to various other disease processes and has the potential to be modulated for treatment of additional diseases. In addition to T2D and obesity, studies have indicated that ghrelin signaling can play either a positive or negative role in conditions involving heart failure, osteoporosis, aging, and even HIV.<sup>20-22</sup> Current treatments targeting the GHS-R such as **2** and **3**, rely on action at the receptor in the brain. However, because ghrelin is primarily produced in the stomach, if a compound was designed and developed to affect ghrelin production rather than targeting GHS-R specifically, it would obviate the necessity for a brain-penetrable compound and could offer significant advantages over compounds specifically targeting GHS-R.

### 2.3 Discovery of Ghrelin O-Acyltransferase (GOAT)

When ghrelin was identified in 1999, it was noted that the post-translational octanoylation of the serine-3 residue was necessary for its activity, but the enzyme or process responsible for its lipidation was not yet known. It was not until 2008 that two groups concurrently identified ghrelin O-acyltransferase (GOAT) as the enzyme responsible for octanoylation. As discussed in Chapter 1, the MBOATs are a family of membrane-bound enzymes that catalyze the transfer of medium and long chain fatty acids to peptidyl nucleophiles, mainly hydroxyl groups. Recognizing that this post-translational modification was likely the result of processing by an acyltransferase, Yang and co-workers screened all sixteen MBOATs encoded by the mouse genome and tested their ability to acylate des-acyl ghrelin.<sup>23</sup> Each MBOAT was expressed using a rat insulinoma (INS-1) cell line alongside des-acyl ghrelin. Octanoic acid was then added to the culture medium and the medium was analyzed for the presence of octanoyl ghrelin.

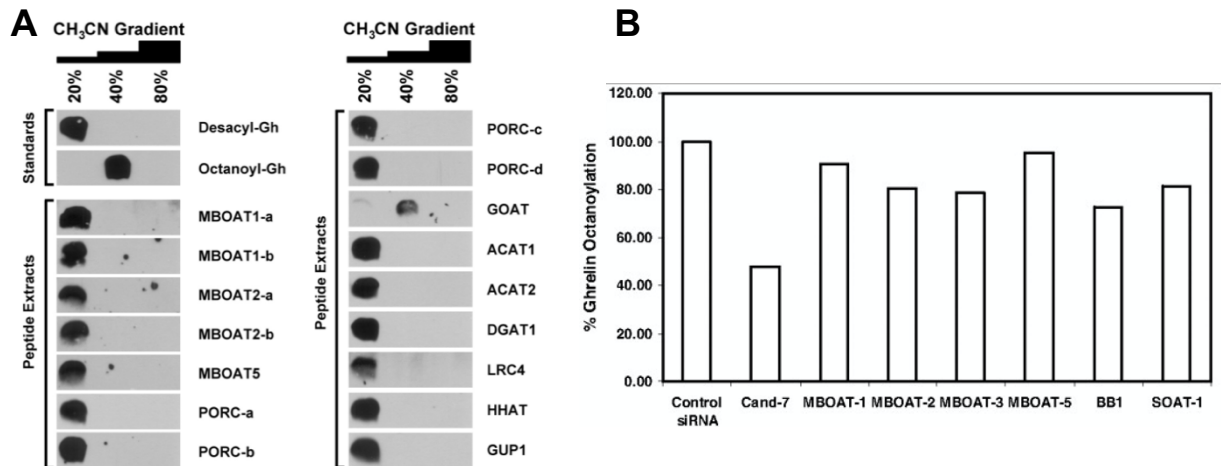
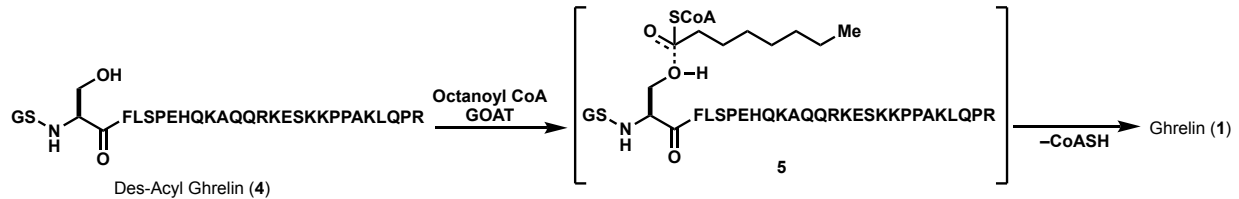


**Figure 2.3.** Discovery of MBOAT4/GOAT as the enzyme responsible for octanoylation. (A) Experiment by Yang and co-workers where MBOATs were cloned and analyzed for their ability to produce acyl-ghrelin. (B) Gene silencing experiment by Gutierrez and co-workers to identify enzymes required for octanoylation. Figures reprinted from Yang et al. *Cell* **2008**, 132, 387–396 and Gutierrez et al. *Proc. Natl. Acad. Sci. USA* **2008**, 105, 6320–6325.



**Scheme 2.1.** Mechanism of GOAT's action on ghrelin utilizing octanoyl CoA as the octanoyl source.

As shown in Figure 2.3A, octanoyl ghrelin could only be detected when ghrelin was processed by MBOAT4 – which was subsequently termed GOAT. Independently, Gutierrez and co-workers were also working to identify the ghrelin acyltransferase.<sup>24</sup> Their discovery was made through gene-silencing experiments. Short interfering RNAs (siRNAs) were produced and the effects of silencing individual MBOAT genes was observed. As shown in Figure 2.3B, when the candidate 7 gene (MBOAT4) was knocked down, ghrelin octanoylation was significantly diminished while octanoylation was minimally effected by silencing other MBOATs. Thus, they concluded that octanoylation was likely the result of processing by MBOAT4. Moreover, GOAT homozygous null mice have been shown to produce no acylated ghrelin.<sup>25</sup> Subsequently, octanoyl CoA was

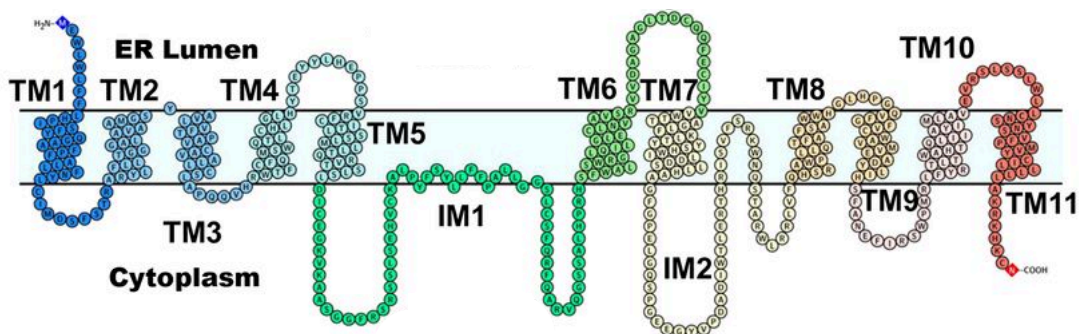


**Figure 2.4.** Predicted transmembrane topology of hGOAT. hGOAT contains eleven transmembrane (TM) domains and two intramembrane (IM) domains. It is thought that lipidation occurs at the IM1 domain. Figure reprinted from Houghland et al. bioRxiv 556233; doi: <https://doi.org/10.1101/556233>.

identified as the acyl donor, wherein the acylation occurs via the mechanism shown in Scheme 2.1.

Because GOAT resides in membranes of the endoplasmic reticulum, identifying GOAT constructs that would be amenable to X-ray crystallography or Cryo-EM analyses has thus far not been successful. Recently, a computational structure of human GOAT and a crystal structure of the bacterial MBOAT DltB have been reported.<sup>26</sup> Given the sequence homology of MBOAT enzymes, the crystal structure of DltB can provide useful information regarding potential organization of the GOAT active site, which may be useful for medicinal chemistry campaigns. That said, to date drug discovery efforts aimed at GOAT have been largely empirical, relying upon high throughput screens (see Chapter 4) or incremental manipulation of substrate analogs designed to be off-rate based

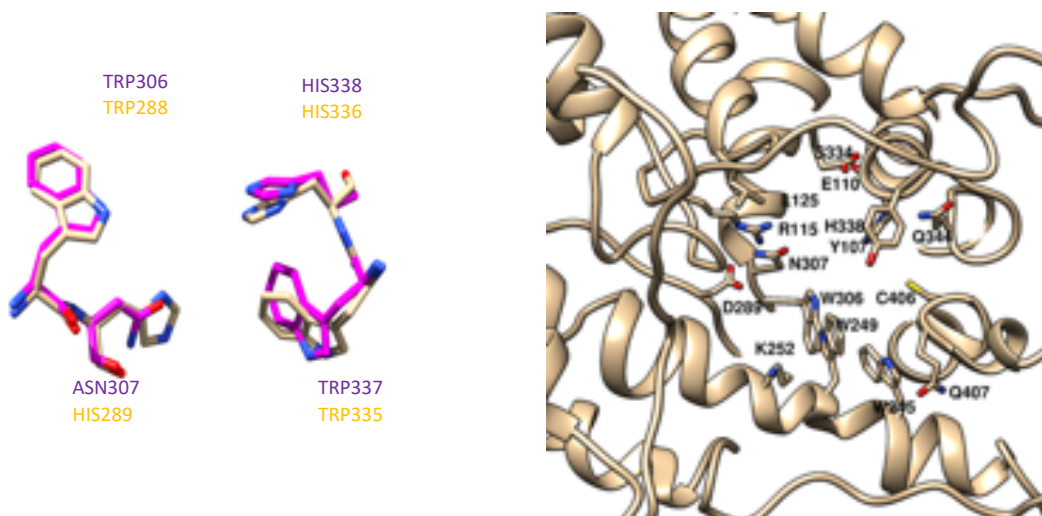


**Figure 2.5.** Structural model of the GOAT active site. First, a multiple sequence alignment was constructed with the T-coffee tool using the following MBOAT ortholog sequences: mouse GOAT (ACD93144), bacterial DltB (AUF35689), human DGAT1 (NP\_036211), human GOAT (ACB05873), human HHAT (NP\_001164051), human Lpcat3 (Q6P1A1), human Porcupine (NP\_073736) and human ACAT1 (P35610). Second, the multiple sequence alignment and crystal structure of bacterial DltB (6bui) were used as a template for MODELLER to build a homology model for mouse GOAT. *Left:* Four highly conserved residues of MBOAT active site that show very good overlap between bacterial DltB (yellow) and mouse GOAT (magenta). *Right:* Active site of GOAT enzyme from the luminal side with labeling of residues that are highly conserved among mammalian GOATs. Some secondary structure was dimmed for clarity. The images were created with UCSF-Chimera software.

inhibitors. Using the known structure of DltB as a starting template, Dr. David Strugatsky (biochemist on our team) generated a homology model of mouse GOAT (Figure 2.5).<sup>27–29</sup> Two key catalytic residues, His338 and Asn307, of mouse GOAT perfectly aligned with their corresponding residues in the DltB structure, His336 and His289. The structural alignment observed suggests that the homology model generated is reasonable in the catalytic domain. Furthermore, residues that build the catalytic cavity of the GOAT protein are tightly conserved among all mammalian GOAT orthologs, suggesting these residues might play a role in substrate recognition and binding.

Since its discovery over a decade ago, no other substrate of GOAT has been identified nor has any other enzyme been identified capable of octanoylating ghrelin. This notion represents a mutual specificity for the ghrelin/GOAT system, making it an attractive target for small molecule medicinal chemistry.<sup>18,24,30</sup> Moreover, given the recent determination of the structure of DltB, medicinal chemistry campaigns can now operate with refined structural information and compounds can be tailored to interact with specific residues within the catalytic site.

## **2.4 Targeting GOAT for Therapeutic Intervention**

The specificity afforded by the ghrelin/GOAT system is a phenomenon that has attracted many to development of agents to modulate ghrelin signaling, primarily through inhibition of GOAT. Moreover, the localization to the stomach has made this method of ghrelin regulation more attractive. Where inhibition of GOAT displays the most promise is in conditions exacerbated by elevated levels of acylated ghrelin. As ghrelin has been termed the ‘hunger hormone’, the most obvious treatment role for ghrelin regulation is in

patients with obesity, a condition commonly caused by overeating.<sup>9,31</sup> Inhibition of ghrelin production, coupled with lifestyle changes, could afford a treatment regimen for such patients. Closely related to obesity, T2D has been recognized as a disease that can be improved by ghrelin modulation. T2D is a disease typically resultant from obesity that leads to a dysregulation of the insulin signaling system. As mentioned previously, ghrelin plays a crucial role in glucose regulation through effects on insulin signaling. Through inhibition of ghrelin octanoylation,  $\beta$ -cell function could potentially be improved, providing a treatment route for T2D.<sup>32</sup>

One disease that has gained attention recently for its ability to benefit from inhibition of ghrelin production is Prader-Willi Syndrome (PWS). PWS is a condition that presents itself with a variety of symptoms such as growth hormone deficiency, behavioral issues, and short stature. Those affected by PWS commonly also suffer from obesity and excessive weight gain due to hyperphagia (insatiable appetite) leading to excessive overeating.<sup>33,34</sup> Examination of ghrelin levels in patients presenting with hyperphagia showed elevated ghrelin levels in both adults and children.<sup>6,35,36</sup> Historically, modulation of ghrelin levels in PWS patients has been tested using somatostatin but reduction of symptoms has not been substantiated.<sup>37,38</sup> Currently, several GOAT inhibitors are undergoing preclinical and clinical studies to observe pharmacological effects on hyperphagia in PWS patients and the outcomes are highly anticipated.

Finally, several companies have begun to look at the effects of down-regulation of ghrelin signaling in patients with addiction. In a study of patients undergoing treatment for alcohol addiction, it was observed that these patients presented with elevated levels of ghrelin.<sup>39,40</sup> Moreover, further studies have discovered that ghrelin levels positively

correlated to alcohol cravings and increased acyl-ghrelin levels are associated with alcohol-induced brain response.<sup>41–46</sup> The ghrelin signaling pathway has also been shown to correlate with opioid addiction as well as other drug addictions, implying that regulation of ghrelin levels could curb addiction behaviors.<sup>47–51</sup>

## 2.5 Conclusions

Data indicates that GOAT and other MBOATs are prime targets for small molecule drug development. In the case of GOAT, specific inhibitors would be both development candidates and valuable probes of ghrelin endocrine signaling. Selectivity observed in the GOAT/ghrelin system was cause for optimism that off target effects could be minimized. Moreover, because GOAT is largely localized to the fundus region of the stomach, a successful inhibitor need not, and ideally would not, penetrate the central nervous system. Taken in total, there seemed good potential for developing a safe, orally efficacious drug substance.

## 2.6 References

- (1) Kojima, M.; Hosoda, H.; Date, Y.; Nakazato, M.; Matsuo, H.; Kangawa, K. Ghrelin Is a Growth-Hormone-Releasing Acylated Peptide from Stomach. *Nature* **1999**, *402* (6762), 656–660.
- (2) Pong, S. S.; Chaung, L. Y.; Dean, D. C.; Nargund, R. P.; Patchett, A. A.; Smith, R. G. Identification of a New G-Protein-Linked Receptor for Growth Hormone Secretagogues. *Mol. Endocrinol.* **1996**, *10* (1), 57–61.
- (3) Smith, R. G. Development of Growth Hormone Secretagogues. *Endocrine Reviews*. *Endocr Rev* May 2005, pp 346–360.
- (4) Romero, A.; Kirchner, H.; Heppner, K.; Pfluger, P. T.; Tschöp, M. H.; Nogueiras, R. GOAT: The Master Switch for the Ghrelin System? *Eur. J. Endocrinol.* **2010**, *163* (1), 1–8.



- (5) Hosoda, H.; Kojima, M.; Matsuo, H.; Kangawa, K. Ghrelin and Des-Acyl Ghrelin: Two Major Forms of Rat Ghrelin Peptide in Gastrointestinal Tissue. *Biochem. Biophys. Res. Commun.* **2000**, *279* (3), 909–913.
- (6) Cummings, D. E.; Purnell, J. Q.; Frayo, R. S.; Schmidova, K.; Wisse, B. E.; Weigle, D. S. A Preprandial Rise in Plasma Ghrelin Levels Suggests a Role in Meal Initiation in Humans. *Diabetes* **2001**, *50* (8), 1714–1719.
- (7) Tschöp, M.; Wawarta, R.; Riepl, R. L.; Friedrich, S.; Bidlingmaier, M.; Landgraf, R.; Folwaczny, C. Post-Prandial Decrease of Circulating Human Ghrelin Levels. *J. Endocrinol. Invest.* **2001**, *24* (6), RC19–RC21.
- (8) Nakazato, M.; Murakami, N.; Date, Y.; Kojima, M.; Matsuo, H.; Kangawa, K.; Matsukura, S. A Role for Ghrelin in the Central Regulation of Feeding. *Nature* **2001**, *409* (6817), 194–198.
- (9) Perez-Tilve, D.; Heppner, K.; Kirchner, H.; Lockie, S. H.; Woods, S. C.; Smiley, D. L.; Tschöp, M.; Pfluger, P. Ghrelin-induced Adiposity Is Independent of Orexigenic Effects. *FASEB J.* **2011**, *25* (8), 2814–2822.
- (10) Wren, A. M.; Seal, L. J.; Cohen, M. A.; Brynes, A. E.; Frost, G. S.; Murphy, K. G.; Dhillon, W. S.; Ghatei, M. A.; Bloom, S. R. Ghrelin Enhances Appetite and Increases Food Intake in Humans. *J. Clin. Endocrinol. Metab.* **2001**, *86* (12), 5992–5992.
- (11) McFarlane, M. R.; Brown, M. S.; Goldstein, J. L.; Zhao, T. J. Induced Ablation of Ghrelin Cells in Adult Mice Does Not Decrease Food Intake, Body Weight, or Response to High-Fat Diet. *Cell Metab.* **2014**, *20* (1), 54–60.
- (12) Sun, Y.; Asnicar, M.; Saha, P. K.; Chan, L.; Smith, R. G. Ablation of Ghrelin Improves the Diabetic but Not Obese Phenotype of Ob/Ob Mice. *Cell Metab.* **2006**, *3* (5), 379–386.
- (13) Kurashina, T.; Dezaki, K.; Yoshida, M.; Sukma Rita, R.; Ito, K.; Taguchi, M.; Miura, R.; Tominaga, M.; Ishibashi, S.; Kakei, M.; Yada, T. The  $\beta$ -Cell GHSR and Downstream CAMP/TRPM2 Signaling Account for Insulinostatic and Glycemic Effects of Ghrelin. *Sci. Rep.* **2015**, *5* (1), 14041.
- (14) Dezaki, K.; Sone, H.; Koizumi, M.; Nakata, M.; Kakei, M.; Nagai, H.; Hosoda, H.; Kangawa, K.; Yada, T. Blockade of Pancreatic Islet-Derived Ghrelin Enhances Insulin Secretion to Prevent High-Fat Diet-Induced Glucose Intolerance. *Diabetes* **2006**, *55* (12), 3486–3493.
- (15) Salehi, A.; De La Cour, C. D.; Håkanson, R.; Lundquist, I. Effects of Ghrelin on Insulin and Glucagon Secretion: A Study of Isolated Pancreatic Islets and Intact Mice. *Regul. Pept.* **2004**, *118* (3), 143–150.

- (16) Van Der Lely, A. J.; Tschöp, M.; Heiman, M. L.; Ghigo, E. Biological, Physiological, Pathophysiological, and Pharmacological Aspects of Ghrelin. *Endocrine Rev.* **2004**, *25* (3), 426–457.
- (17) Dezaki, K.; Hosoda, H.; Kakei, M.; Hashiguchi, S.; Watanabe, M.; Kangawa, K.; Yada, T. Endogenous Ghrelin in Pancreatic Islets Restricts Insulin Release by Attenuating Ca<sup>2+</sup> Signaling in  $\beta$ -Cells: Implication in the Glycemic Control in Rodents. *Diabetes* **2004**, *53* (12), 3142–3151.
- (18) Müller, T. D.; Nogueiras, R.; Andermann, M. L.; Andrews, Z. B.; Anker, S. D.; Argente, J.; Batterham, R. L.; Benoit, S. C.; Bowers, C. Y.; Broglio, F.; Casanueva, F. F.; D'Alessio, D.; Depoortere, I.; Geliebter, A.; Ghigo, E.; Cole, P. A.; Cowley, M.; Cummings, D. E.; Dagher, A.; Diano, S.; Dickson, S. L.; Diéguez, C.; Granata, R.; Grill, H. J.; Grove, K.; Habegger, K. M.; Heppner, K.; Heiman, M. L.; Holsen, L.; Holst, B.; Inui, A.; Jansson, J. O.; Kirchner, H.; Korbonits, M.; Laferrère, B.; LeRoux, C. W.; Lopez, M.; Morin, S.; Nakazato, M.; Nass, R.; Perez-Tilve, D.; Pfluger, P. T.; Schwartz, T. W.; Seeley, R. J.; Sleeman, M.; Sun, Y.; Sussel, L.; Tong, J.; Thorner, M. O.; van der Lely, A. J.; van der Ploeg, L. H. T.; Zigman, J. M.; Kojima, M.; Kangawa, K.; Smith, R. G.; Horvath, T.; Tschöp, M. H. Ghrelin. *Molecular Metabolism* **2015**, *4* (6), 437–460.
- (19) Alamri, B. N.; Shin, K.; Chappe, V.; Anini, Y. The Role of Ghrelin in the Regulation of Glucose Homeostasis. *Horm. Mol. Biol. Clin. Investig.* **2016**, *26* (1), 3–11.
- (20) Hanada, T.; Toshinai, K.; Kajimura, N.; Nara-Ashizawa, N.; Tsukada, T.; Hayashi, Y.; Osuye, K.; Kangawa, K.; Matsukura, S.; Nakazato, M. Anti-Cachectic Effect of Ghrelin in Nude Mice Bearing Human Melanoma Cells. *Biochem. Biophys. Res. Commun.* **2003**, *301* (2), 275–279.
- (21) Hanada, T.; Toshinai, K.; Date, Y.; Kajimura, N.; Tsukada, T.; Hayashi, Y.; Kangawa, K.; Nakazato, M. Upregulation of Ghrelin Expression in Cachectic Nude Mice Bearing Human Melanoma Cells. *Metabolism* **2004**, *53* (1), 84–88.
- (22) Neary, N. M.; Small, C. J.; Wren, A. M.; Lee, J. L.; Druce, M. R.; Palmieri, C.; Frost, G. S.; Ghatei, M. A.; Coombes, R. C.; Bloom, S. R. Ghrelin Increases Energy Intake in Cancer Patients with Impaired Appetite: Acute, Randomized, Placebo-Controlled Trial. *J. Clin. Endocrinol. Metab.* **2004**, *89*, 2832–2836.
- (23) Yang, J.; Brown, M. S.; Liang, G.; Grishin, N. V.; Goldstein, J. L. Identification of the Acyltransferase That Octanoylates Ghrelin, an Appetite-Stimulating Peptide Hormone. *Cell* **2008**, *132* (3), 387–396.
- (24) Gutierrez, J. A.; Solenberg, P. J.; Perkins, D. R.; Willency, J. A.; Knierman, M. D.; Jin, Z.; Witcher, D. R.; Luo, S.; Onyia, J. E.; Hale, J. E. Ghrelin Octanoylation Mediated by an Orphan Lipid Transferase. *Proc. Natl. Acad. Sci. U. S. A.* **2008**, *105*

- (17), 6320–6325.
- (25) Kirchner, H.; Gutierrez, J. A.; Solenberg, P. J.; Pfluger, P. T.; Czyzyk, T. A.; Willency, J. A.; Schürmann, A.; Joost, H. G.; Jandacek, R. J.; Hale, J. E.; Heiman, M. L.; Tschöp, M. H. GOAT Links Dietary Lipids with the Endocrine Control of Energy Balance. *Nat. Med.* **2009**, *15* (7), 741–745.
- (26) Ma, D.; Wang, Z.; Merrih, C. N.; Lang, K. S.; Lu, P.; Li, X.; Merrih, H.; Rao, Z.; Xu, W. Crystal Structure of a Membrane-Bound O-Acyltransferase. *Nature* **2018**, *562* (7726), 286–290.
- (27) Pettersen, E. F.; Goddard, T. D.; Huang, C. C.; Couch, G. S.; Greenblatt, D. M.; Meng, E. C.; Ferrin, T. E. UCSF Chimera - A Visualization System for Exploratory Research and Analysis. *J. Comput. Chem.* **2004**, *25* (13), 1605–1612.
- (28) Notredame, C.; Higgins, D. G.; Heringa, J. T-Coffee: A Novel Method for Fast and Accurate Multiple Sequence Alignment. *J. Mol. Biol.* **2000**, *302* (1), 205–217.
- (29) Šali, A.; Blundell, T. L. Comparative Protein Modelling by Satisfaction of Spatial Restraints. *J. Mol. Biol.* **1993**, *234* (3), 779–815.
- (30) Yang, J.; Zhao, T. J.; Goldstein, J. L.; Brown, M. S. Inhibition of Ghrelin O-Acyltransferase (GOAT) by Octanoylated Pentapeptides. *Proc. Natl. Acad. Sci. U. S. A.* **2008**, *105* (31), 10750–10755.
- (31) Hopkins, A. L.; Nelson, T. A. S.; Guschina, I. A.; Parsons, L. C.; Lewis, C. L.; Brown, R. C.; Christian, H. C.; Davies, J. S.; Wells, T. Unacylated Ghrelin Promotes Adipogenesis in Rodent Bone Marrow via Ghrelin O-Acyl Transferase and GHS-R1a Activity: Evidence for Target Cell-Induced Acylation. *Sci. Rep.* **2017**, *7*.
- (32) Tong, J.; Prigeon, R. L.; Davis, H. W.; Bidlingmaier, M.; Kahn, S. E.; Cummings, D. E.; Tschöp, M. H.; D'Alessio, D. Ghrelin Suppresses Glucose-Stimulated Insulin Secretion and Deteriorates Glucose Tolerance in Healthy Humans. *Diabetes* **2010**, *59* (9), 2145–2151.
- (33) Holm, V. A.; Cassidy, S. B.; Butler, M. G.; Hanchett, J. M.; Greenswag, L. R.; Whitman, B. Y.; Greenberg, F. Prader-Willi Syndrome: Consensus Diagnostic Criteria. *Pediatrics* **1993**, *91* (2), 398–402.
- (34) Lindgren, A. C.; Barkeling, B.; Hägg, A.; Ritzén, E. M.; Marcus, C.; Rössner, S. Eating Behavior in Prader-Willi Syndrome, Normal Weight, and Obese Control Groups. *J. Pediatr.* **2000**, *137* (1), 50–55.
- (35) Delparigi, A.; Tschöp, M.; Heiman, M. L.; Salbe, A. D.; Vozarova, B.; Sell, S. M.; Bunt, J. C.; Tataranni, P. A. High Circulating Ghrelin: A Potential Cause for Hyperphagia and Obesity in Prader-Willi Syndrome. *J. Clin. Endocrinol. Metab.*

**2002**, 87 (12), 5461–5464.

- (36) Haqq, A. M.; Sadaf Farooqi, I.; O’Rahilly, S.; Stadler, D. D.; Rosenfeld, R. G.; Pratt, K. L.; LaFranchi, S. H.; Purnell, J. Q. Serum Ghrelin Levels Are Inversely Correlated with Body Mass Index, Age, and Insulin Concentrations in Normal Children and Are Markedly Increased in Prader-Willi Syndrome. *J. Clin. Endocrinol. Metab.* **2003**, 88 (1), 174–178.
- (37) Haqq, A. M.; Stadler, D. D.; Rosenfeld, R. G.; Pratt, K. L.; Weigle, D. S.; Frayo, R. S.; Lafranchi, S. H.; Cummings, D. E.; Purnell, J. Q. Circulating Ghrelin Levels Are Suppressed by Meals and Octreotide Therapy in Children with Prader-Willi Syndrome. *J. Clin. Endocrinol. Metab.* **2003**, 88 (8), 3573–3576.
- (38) De Waele, K.; Ishkanian, S. L.; Bogarin, R.; Miranda, C. A.; Ghatei, M. A.; Bloom, S. R.; Pacaud, D.; Chanoine, J. P. Long-Acting Octreotide Treatment Causes a Sustained Decrease in Ghrelin Concentrations but Does Not Affect Weight, Behaviour and Appetite in Subjects with Prader-Willi Syndrome. *Eur. J. Endocrinol.* **2008**, 159 (4), 381–388.
- (39) Kraus, T.; Schanze, A.; Gröschl, M.; Bayerlein, K.; Hillemacher, T.; Reulbach, U.; Kornhuber, J.; Bleich, S. Ghrelin Levels Are Increased in Alcoholism. *Alcohol. Clin. Exp. Res.* **2005**, 29 (12), 2154–2157.
- (40) Kim, D. J.; Yoon, S. J.; Choi, B.; Kim, T. S.; Woo, Y. S.; Kim, W.; Myrick, H.; Peterson, B. S.; Choi, Y. Bin; Kim, Y. K.; Jeong, J. Increased Fasting Plasma Ghrelin Levels during Alcohol Abstinence. *Alcohol Alcohol.* **2005**, 40 (1), 76–79.
- (41) Addolorato, G.; Capristo, E.; Leggio, L.; Ferrulli, A.; Abenavoli, L.; Malandrino, N.; Farnetti, S.; Domenicali, M.; D’Angelo, C.; Vonghia, L.; Mirijello, A.; Cardone, S.; Gasbarrini, G. Relationship between Ghrelin Levels, Alcohol Craving, and Nutritional Status in Current Alcoholic Patients. *Alcohol. Clin. Exp. Res.* **2006**, 30 (11), 1933–1937.
- (42) Leggio, L.; Ferrulli, A.; Cardone, S.; Nesci, A.; Miceli, A.; Malandrino, N.; Capristo, E.; Canestrelli, B.; Monteleone, P.; Kenna, G. A.; Swift, R. M.; Addolorato, G. Ghrelin System in Alcohol-Dependent Subjects: Role of Plasma Ghrelin Levels in Alcohol Drinking and Craving. *Addict. Biol.* **2012**, 17 (2), 452–464.
- (43) Akkişi Kumsar, N.; Dilbaz, N. Relationship Between Craving and Ghrelin, Adiponectin, and Resistin Levels in Patients with Alcoholism. *Alcohol. Clin. Exp. Res.* **2015**, 39 (4), 702–709.
- (44) Hillemacher, T.; Kraus, T.; Rauh, J.; Weiß, J.; Schanze, A.; Frieling, H.; Wilhelm, J.; Heberlein, A.; Gröschl, M.; Sperling, W.; Kornhuber, J.; Bleich, S. Role of Appetite-Regulating Peptides in Alcohol Craving: An Analysis in Respect to Subtypes and Different Consumption Patterns in Alcoholism. *Alcohol. Clin. Exp.*

Res. **2007**, 31 (6), 950–954.

- (45) Koopmann, A.; Bach, P.; Schuster, R.; Bumb, J. M.; Vollstädt-Klein, S.; Reinhard, I.; Rietschel, M.; Witt, S. H.; Wiedemann, K.; Kiefer, F. Ghrelin Modulates Mesolimbic Reactivity to Alcohol Cues in Alcohol-Addicted Subjects: A Functional Imaging Study. *Addict. Biol.* **2019**, 24 (5), 1066–1076.
- (46) Bach, P.; Bumb, J. M.; Schuster, R.; Vollstädt-Klein, S.; Reinhard, I.; Rietschel, M.; Witt, S. H.; Wiedemann, K.; Kiefer, F.; Koopmann, A. Effects of Leptin and Ghrelin on Neural Cue-Reactivity in Alcohol Addiction: Two Streams Merge to One River? *Psychoneuroendocrinology* **2019**, 100, 1–9.
- (47) Jerlhag, E.; Engel, J. A. Ghrelin Receptor Antagonism Attenuates Nicotine-Induced Locomotor Stimulation, Accumbal Dopamine Release and Conditioned Place Preference in Mice. *Drug Alcohol Depend.* **2011**, 117 (2–3), 126–131.
- (48) Jerlhag, E.; Egecioglu, E.; Dickson, S. L.; Engel, J. A. Ghrelin Receptor Antagonism Attenuates Cocaine- and Amphetamine-Induced Locomotor Stimulation, Accumbal Dopamine Release, and Conditioned Place Preference. *Psychopharmacology (Berl)*. **2010**, 211 (4), 415–422.
- (49) Sustkova-Fiserova, M.; Jerabek, P.; Havlickova, T.; Syslova, K.; Kacer, P. Ghrelin and Endocannabinoids Participation in Morphine-Induced Effects in the Rat Nucleus Accumbens. *Psychopharmacology (Berl)*. **2016**, 233 (3), 469–484.
- (50) Sustkova-Fiserova, M.; Jerabek, P.; Havlickova, T.; Kacer, P.; Krsiak, M. Ghrelin Receptor Antagonism of Morphine-Induced Accumbens Dopamine Release and Behavioral Stimulation in Rats. *Psychopharmacology (Berl)*. **2014**, 231 (14), 2899–2908.
- (51) Havlickova, T.; Charalambous, C.; Lapka, M.; Puskina, N.; Jerabek, P.; Sustkova-Fiserova, M. Ghrelin Receptor Antagonism of Methamphetamine-Induced Conditioned Place Preference and Intravenous Self-Administration in Rats. *Int. J. Mol. Sci.* **2018**, 19 (10).

### 3. Chapter Three – Hypothesis Driven Design and Synthesis of Lipopeptidomimetic Inhibitors of GOAT

*Emily Murzinski, Hui Ding, Luke Sisto, Ryan Hollibaugh, David Strugatsky and Patrick  
Harran*

#### 3.1 Introduction

Since the discovery of GOAT as the enzyme responsible for octanoylation of ghrelin in 2008, a variety of inhibitors have been reported. These have included substrate peptidomimetics, steroid homologs and various heterocyclic small molecules (Figure 3.1). Our group, like several other laboratories, has largely focused on peptidomimetic inhibitors. This was driven by the fact that 1) structure based drug design was not a viable option in this case, and 2) Brown and Goldstein have shown that GOAT was product inhibited.<sup>1,2</sup> They demonstrated that pure octanoyl ghrelin (**1**) dose dependently inhibited GOAT activity in stabilized membrane fractions with an  $IC_{50} = 7 \mu M$ .<sup>3</sup> They further showed

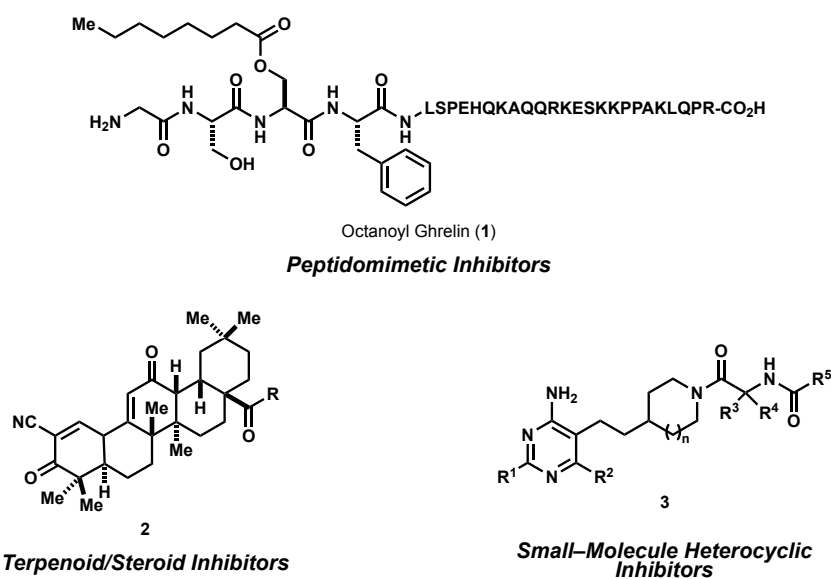


**Figure 3.1.** Representative structures of the three major classes of GOAT inhibitors that have been disclosed.

that removing a structural liability improved performance. Namely, replacement of the key serine–3 ester linkage with an amide bond (*i.e.* to afford **4**) markedly improved *in vitro* potency ( $IC_{50}$  of 0.2  $\mu$ M), likely by eliminating deactivation by esterase enzymes present in the assay media.

Brown and Goldstein’s robust GOAT assay and seminal discoveries regarding product inhibition sparked considerable research in both academia and the private sector. Numerous additional inhibitors of the enzyme were reported (Figure 3.2). During their initial studies on GOAT, Brown and Goldstein also found that a small segment of the ghrelin N-terminus was sufficient to inhibit the enzyme. Pentapeptide **5** blocked GOAT

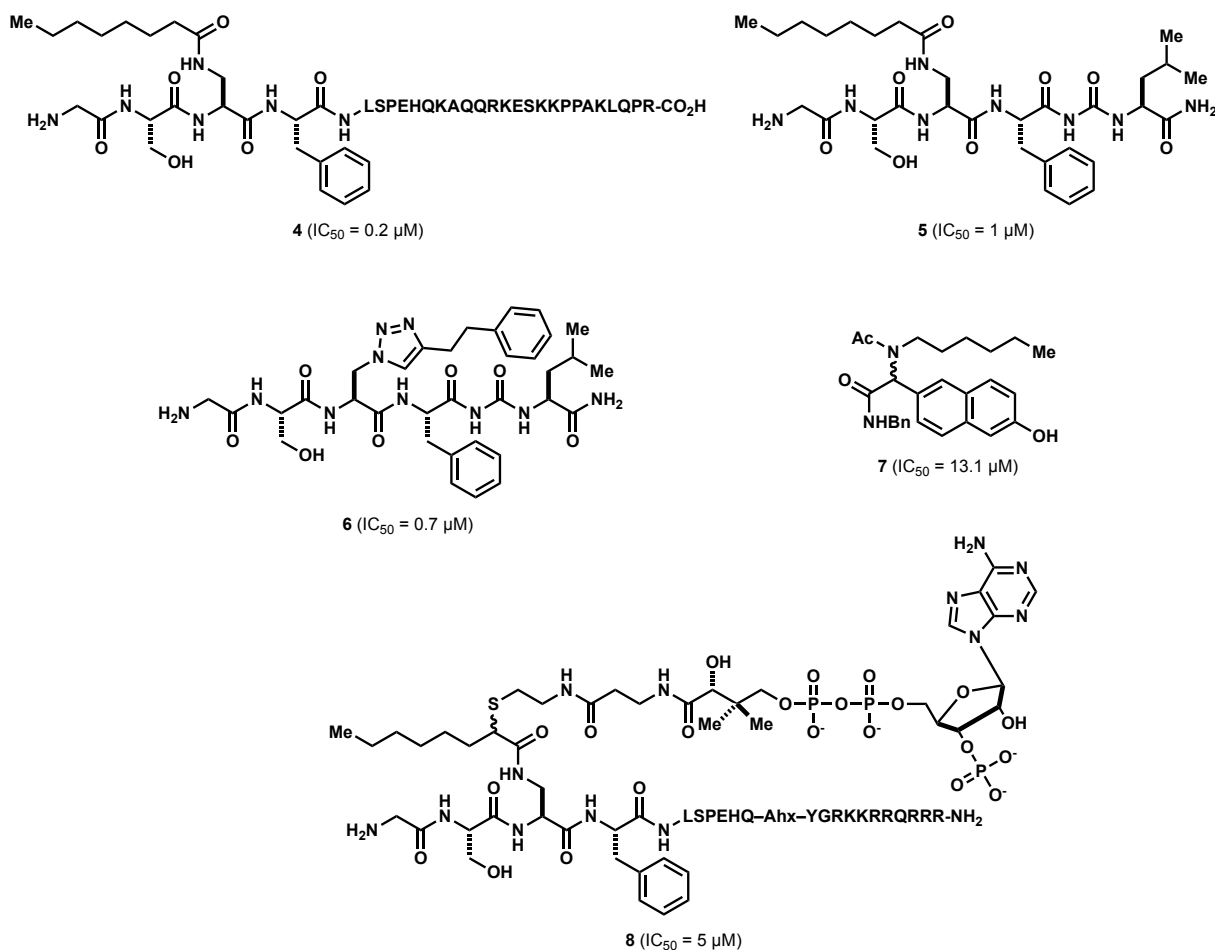


**Figure 3.2.** Reported peptidomimetic inhibitors of GOAT.

activity only five-fold less potently ( $IC_{50} = 1 \mu\text{M}$ ) than the corresponding full-length peptide **4**.<sup>3</sup> In 2015, Hougland and co-workers reported that peptidyl inhibitors need not harbor the octanamide side chain,<sup>4,5</sup> wherein compound **6** has a  $\beta$ -phenethylated triazole in place of the octanamide in **5**, yet **6** is slightly more potent as a GOAT inhibitor *in vitro*. This result demonstrated that GOAT recognition could be achieved with a core pentapeptide skeleton and a hydrophobic side chain. Through screening of a focused

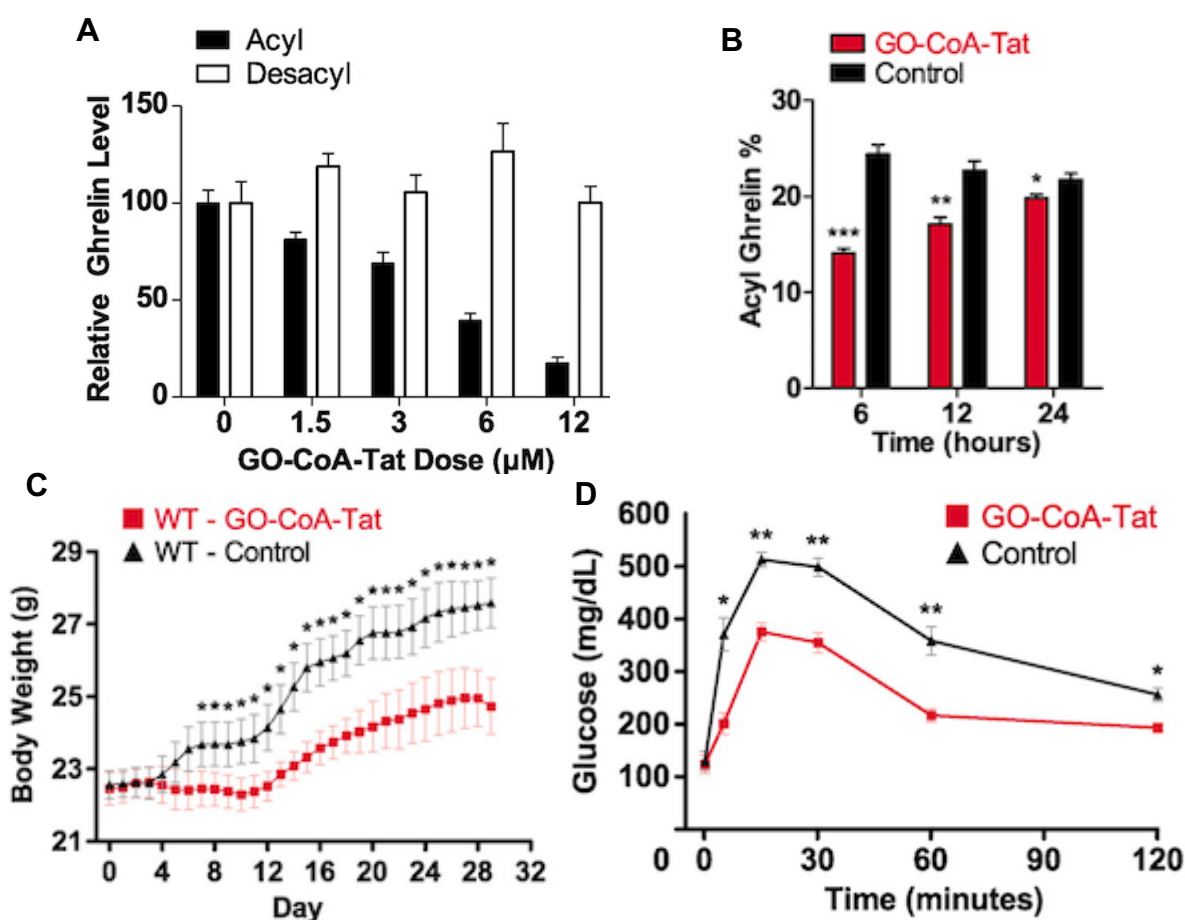


**Figure 3.3.** *In vivo* pharmacology of GO-CoA-Tat. (A) Dose-response reduction of acyl but not desacyl ghrelin levels by GO-CoA-Tat in GOAT/preproghrelin-transfected HeLa cells after 24 hours incubation. (B) In mice, GO-CoA-Tat reduces the fraction of acyl ghrelin; maximum observed effect after 6 hours, followed by slow recovery to the resting state. (C) Body weights in WT C57BL6 mice on a MCT diet treated with 11  $\mu\text{mol/kg}$  of **8** (red,  $n = 5$ ) or vehicle (black,  $n = 6$ ) for 1 month ( $*P < 0.05$ ). (D) Decrease in blood glucose as compared with control mice when **8** was administered 24 hours before ip glucose challenge (2.5 g/kg) ( $*P < 0.05$ ,  $**P < 0.01$ ). Figures reprinted from Barnett et al. *Science* **2010**, 330, 1689–1692.



library of non-natural peptides, Janda and Garner identified **7** as a weak GOAT inhibitor ( $IC_{50} = 13.1 \mu M$ ) wherein the branched hexylated acetamide was thought to be a surrogate for octanamide.<sup>6,7</sup> Interestingly, when tested in our *in vitro* assay format, **7** lacked GOAT inhibitory activity.

Perhaps one of the most studied peptidomimetic GOAT inhibitors is GO-CoA-Tat (**8**), which was reported in 2010 by Cole and co-workers.<sup>8,9</sup> GO-CoA-Tat was designed to act as a bi-substrate mimetic which could take advantage of both the ghrelin binding site as well as the adjacent CoA binding site in GOAT. In addition to the presence of the appended CoA, **8** features a Tat sequence that promotes endocytosis appended to the C-terminus of a ghrelin decapeptide *via* an aminohexanoate (Ahx) linker. Tat (transactivating transcriptional activator) is an arginine rich cell-penetrating peptide isolated from HIV-1 that can be efficiently taken up from surrounding media by numerous cell types in culture.<sup>10</sup> It promotes endocytosis and thereby allows the compound to remain active in cell-based assays. It has been utilized as a translocation vehicle for drug delivery and has been suggested as a tool for enhancing cell permeability of compounds not typically thought to possess such properties. The hallmarks of this discovery were that **8** could reduce circulating acyl-ghrelin levels *in vivo* and, with chronic administration, could decrease weight gain in mice fed a high fat diet (Figure 3.3). Moreover, **8** was able to improve response in a glucose tolerance test (GTT). While it remains to be seen whether GO-CoA-Tat can be utilized clinically, these findings demonstrate a promise for GOAT inhibition as a treatment modality.

Although the data surrounding GO-CoA-Tat is encouraging, it has its limitations. Given the conditions that GOAT inhibition are sought to impact, daily treatment regimens

will likely be necessary. With its high molecular weight and largely peptidyl character, **8** will likely need to be non-orally administered, potentially with repeated IP dosing, thereby limiting its utility. In an effort to discover an orally available, small molecule peptidomimetic with *in vivo* activity, our group introduced a series of pyrrolidine-containing compounds (**9**) that could potentially inhibit GOAT ( $IC_{50} = 1.1 \mu M$ ).<sup>11,12</sup> Additionally, preliminary studies demonstrated the ability of these compounds to decrease levels of octanoylated ghrelin *in vivo* for up to 3 hours. We later discovered that the *in vivo* effects that we observed were likely a result of toxicity which caused an immediate drop in acyl-ghrelin levels and adversely affected the mice. As such, the search for an orally available, small molecule inhibitor remains of paramount importance as it would allow for a suitable means for validating GOAT as a tractable target for treating such conditions as diabetes and Prader-Willi syndrome. Moreover, development of an orally available small molecule would bolster research in the field of diabetes and its connection to ghrelin signaling.

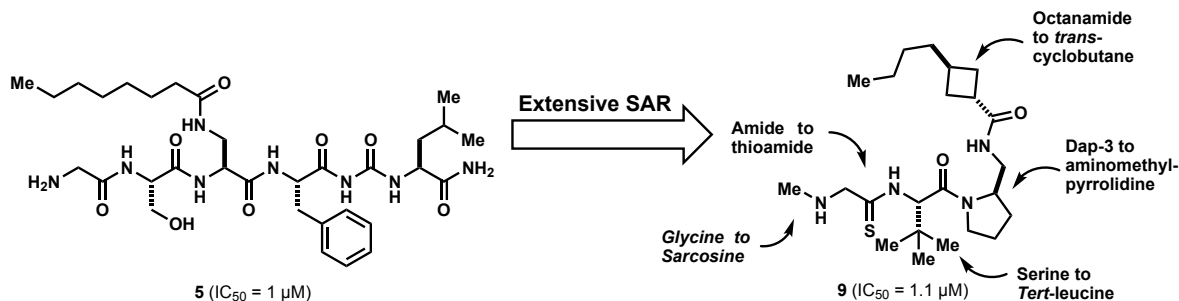


**Figure 3.4.** SAR summary of pentapeptide **5** to produce peptidomimetic **9** with the key transformations identified.

### 3.2 Pyrrolidine-Containing Inhibitors

Through years of work spearheaded by Drs. Haixia Liu and Ryan Hollibaugh, a library of peptidomimetic GOAT inhibitors were discovered.<sup>11,12</sup> These discoveries were

founded upon a strategy capitalizing on the understanding that GOAT could be inhibited by its pentapeptide **5** that carries an octanamide side chain. The goal of inhibitor development was to transform **5** into a small molecule that retained necessary binding properties but harbored various modifications designed to increase membrane permeability and metabolic stability.

Extensive SAR studies were performed to define a minimal pharmacophore present in **5**. These efforts led to the identification of pyrrolidine containing thioamide **9**. The experiments are detailed in the PhD thesis of Ryan Hollibaugh.<sup>12</sup> As shown in Figure 3.4, the key changes made to the parent structure are: methylation of the terminal glycine to slow cleavage by proteases; replacement of serine-2 with *tert*-leucine; replacement of Dap-3 with (*R*)-2-methylaminopyrrolidine; substitution of the octanoyl side chain with a *trans*-configured 3-butyl cyclobutanyl motif; and thionation of the N-terminal amide linkage. While the potency of **9** was comparable to **5** as a GOAT inhibitor, it was lower in mass, harbored less exposed polar surface area, had fewer H-bond donors and less translational degrees of freedom.

During the study of these pyrrolidine-containing inhibitors, we were initially encouraged by the observation of a rapid drop in circulating acyl ghrelin levels when **9** was dosed in mice. However, the effect was not sustained and its rapid onset seemed inconsistent with cellular performance data reported by Cole for GOAT-CoA-Tat. Further mouse studies showed IP dosage of **9** at 80 mg/kg caused severe loss of motor functions, occasionally resulting in death. Moreover, when negative control **10** was synthesized and tested in both wildtype (WT) and GOAT knockout (KO) mice, severe lethargy indistinguishable from that caused by **9** was observed. Since **10** is not a GOAT inhibitor

(as determined by *in vitro* assays) and identical observations were made in WT and KO mice, the toxicity observed could not result from GOAT inhibition. While the acute toxicity of **9** precluded its further development, the fact that it was not mechanism based allowed us to re-evaluate our lead series in an attempt to improve performance while eliminating liability.

Earlier SAR studies had established core elements in **9** needed to inhibit GOAT (Figure 3.5). When designing new inhibitors, we sought to make modifications which were previously unexplored. Modifications included: introduction of a methylene spacer in the second *tert*-leucine residue (P2); extension of the recognition sequence at the 3-position of the pyrrolidine; introduction of a moiety capable of covalent bonding at the 4-position of the pyrrolidine; and introduction of polar functionality in the side chain. We hypothesized that by making these modifications, we could not only identify which facet of the original structure (**9**) was causing overt toxicity, but also gain insight on the structure of the active site of GOAT by observing the tolerance of such modifications. Through previous research and observations, it was revealed that the first residue was necessary for recognition by the enzyme and thus remained untouched in further modifications.

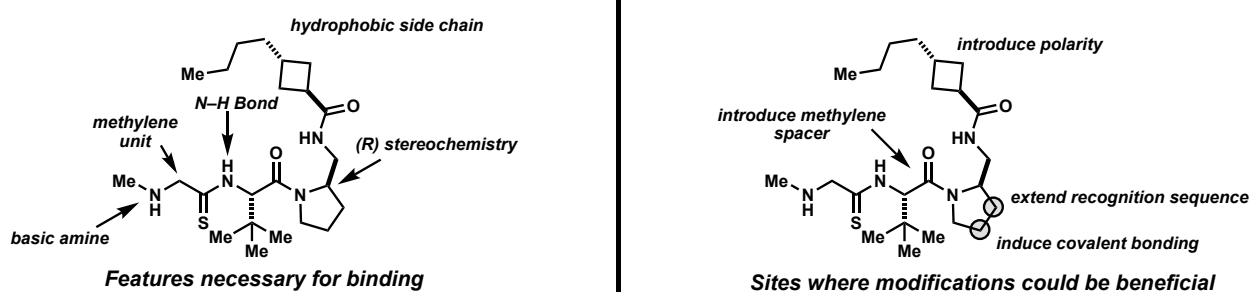


**Figure 3.5.** Evaluation of structural features necessary for GOAT inhibition (left) and sites where modifications were pursued to improve performance (right).

The first modifications we focused on were of the P2 *tert*-leucine residue. A main focus for modification was the second residue (P2 residue). P2 had already been modified from its parent serine residue to a *tert*-leucine residue, but we felt further modification could be beneficial. When designing effective drugs, it is important to scrutinize the structure of any promising molecule. In looking at **9**, the residues used are primary  $\alpha$ -amino acids, which are known to have low proteolytic stability *in vivo*. Since **9** primarily suffers *in vivo*, it is possible that the toxicity arises from proteolytic cleavage. One strategy for mitigating this instability is the introduction of  $\beta$ -amino acid residues.<sup>13</sup> Introduction of  $\beta$ -amino acids has been shown to effectively modulate peptide structure, conformational preference, and proteolytic susceptibility of native peptides.<sup>13–17</sup> Using this knowledge, we envisioned that introduction of a  $\beta^2$ - or  $\beta^3$ -*tert*-leucine residue at the P2 position of the peptide structure would eliminate or reduce proteolytic cleavage and bolster *in vivo* performance.

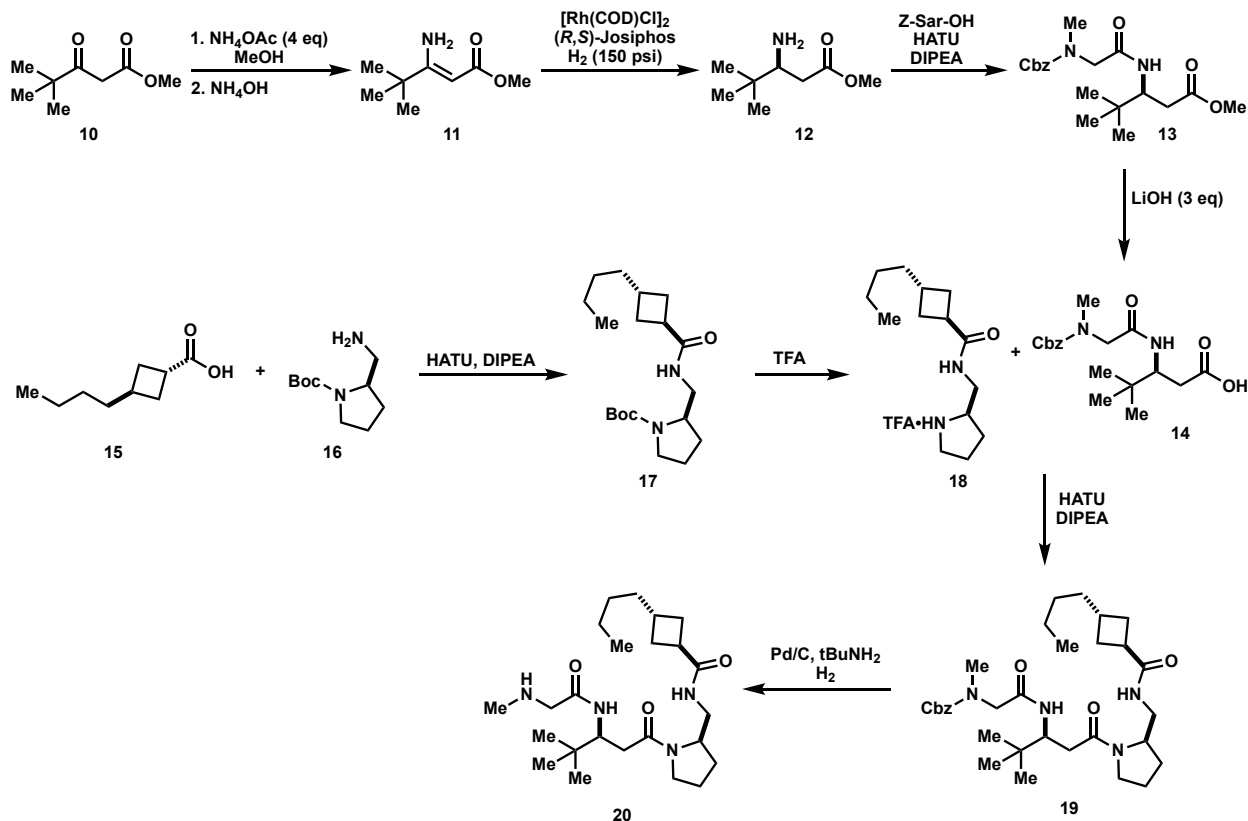
Next, we looked at modifying the pyrrolidine moiety. The MBOAT family of enzymes are characterized by conserved histidine and asparagine residues and it is believed that the conserved histidine residue lies in the active site of GOAT. We envisioned that incorporating functionalities capable of covalently bonding with the key histidine residue could greatly improve the overall performance of the inhibitors. Thus, we sought to generate inhibitors bearing an electrophilic moiety, such as a Michael acceptor or an epoxide, at the 4-position of the pyrrolidine in the efforts to generate covalent modifiers as suicide inhibitors.

Finally, we explored alterations to the side chain for enhancement of inhibitor activity. Although the octanoyl chain is crucial for binding GOAT, we desired to explore

modifications that could boost the potency of the inhibitors. Our first goal was to determine whether the side chain could benefit from the addition of hydrogen bond acceptors that could bind with residues within the binding site and thus we aimed to introduce more polar functionality into the side chain. In an effort to further probe the structure of the active site of GOAT, we then designed side chain modifications in which the octanoyl chain was methylated at varying positions to gauge the tolerance of branching. Finally, we sought to generate transition-state mimetics at the side chain position. During the production of acyl ghrelin, octanoyl-CoA transfers its octanoyl group to ghrelin. Through the mechanism of octanoylation, a tetrahedral intermediate is formed at which time ghrelin and octanoyl-CoA are temporarily bonded to each other and there exists a negatively charged oxygen atom that then collapses the tetrahedral intermediate to form the desired octanoyl ester. It is well-known that enzymes often bind their transition state products better than their substrate or product, so we desired to generate a tetrahedral N-oxide in the side chain to promote stronger binding of inhibitors to GOAT. With our proposed modifications in mind, we sought out synthetic routes to access the desired derivatives.

### **3.2.1 Synthesis and Evaluation of Modifications of the P2 Residue**

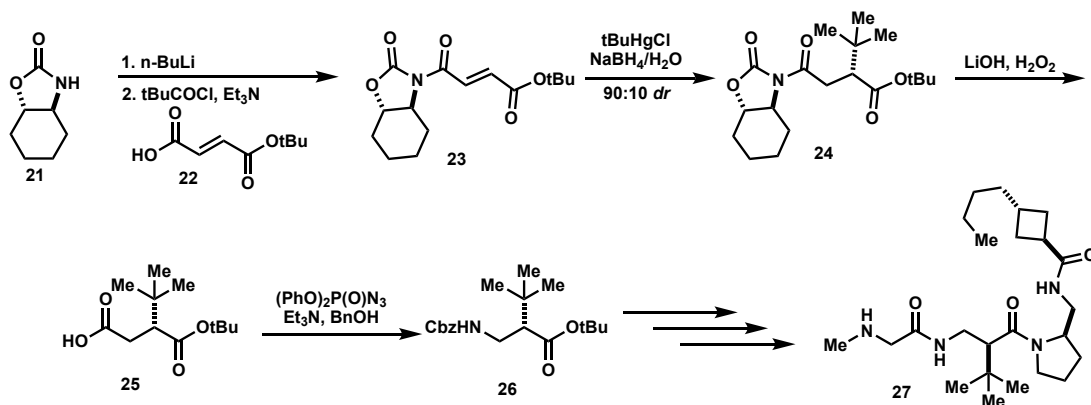
#### **3.2.1.1 Synthesis of P2 Modifications**



**Scheme 3.1.** Synthesis of  $\beta^3$ -*tert*-leucine residue **12** for the generation of modified inhibitor **20**.

Our approach to modifying **9** in effort to improve stability, and thus mitigate proteolytic cleavage, commenced with the generation of  $\beta^2$ - and  $\beta^3$ -*tert*-leucine amino acid residues. Generation of  $\beta^3$ -*tert*-leucine hinged on the synthesis of optically active methyl ester **12**. In 2004, researchers at Merck laboratories introduced a powerful method for the asymmetric catalytic hydrogenation of enamines utilizing rhodium based catalysts with ferrocenyl ligands to generate  $\beta$ -amino acids.<sup>18</sup> In 2005, Merck followed up on their methodology by showing that *in situ* protection of the amine using (Boc)<sub>2</sub>O could improve the efficiency of the reaction, which they applied directly to the synthesis of **12** *via* enamine **11**.<sup>19</sup> Utilizing Stork chemistry, enamine **11** could be obtained, which allowed for the facile formation of desired compound **12**. Since this methodology produces the free amine, **12** was first coupled to Cbz-protected sarcosine to afford peptide **13** before being

coupled to **18** following saponification of the methyl ester to the free acid (**14**). Following the HATU-mediated coupling of **14** and **18** to produce **19**, Cbz deprotection under catalytic hydrogenative conditions afforded desired inhibitor **20**.

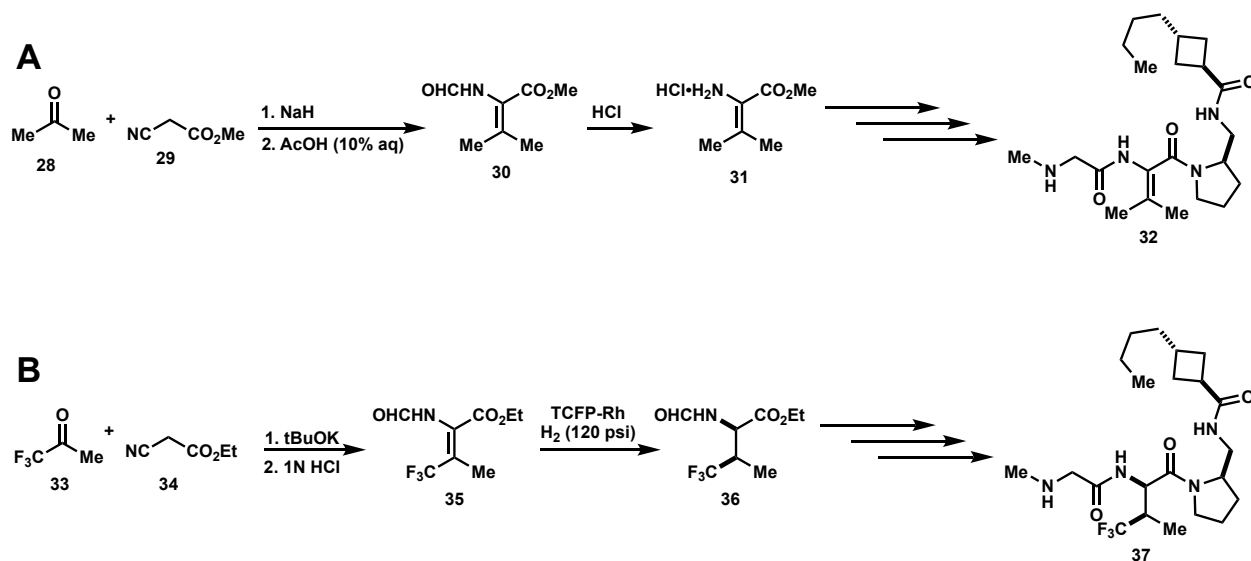


**Scheme 3.2.** Synthesis of  $\beta^2$ -*tert*-leucine residue **26** for synthesis of **27**.

Preparation of the  $\beta^2$ -*tert*-leucine was not as straightforward as the process utilized for the  $\beta^3$ -*tert*-leucine residue and required the use of a chiral auxiliary (**21**) to afford the desired regioisomer and enantiomer.<sup>20</sup> Chiral auxiliary **21** was deprotonated using *n*-BuLi and a solution of the mixed anhydride generated from the mixing of fumarate derivative **22** and pivaloyl chloride was added to afford the acylated imide derivative **23**. In a process governed by the chiral auxiliary, **23** could undergo a radical alkylation using *tert*-butyl mercuric chloride which installed the desired *tert*-butyl group at the alpha position of the ester with a *dr* of 90:10. Following the Evans' protocol<sup>21</sup>, the chiral auxiliary could be removed cleanly to afford the free acid **25**. Generation of the acyl azide using DPPA promoted a Curtius rearrangement in which the intermediate isocyanate was trapped with benzyl alcohol to provide the Cbz-protected  $\beta^2$  amino ester **26**. Following standard peptide coupling protocols, **26** could be elaborated into desired compound **27**.



Next, we turned our attention toward investigating the necessity of stereochemistry at the P2  $\alpha$ -carbon. The field of peptide chemistry as it relates to drug discovery is ever evolving. In the late 70's and early 80's, Stammer and co-workers demonstrated that incorporation of dehydroamino acids helped to protect peptides from proteolysis.<sup>22–25</sup> Building on this concept, Castle and co-workers studied the roles of bulky dehydroamino acids containing tetra-substituted alkenes such as dehydrovaline in stabilizing peptides against proteolysis.<sup>26</sup> They hypothesized that the stabilization would arise due to the elevated levels of  $A_{1,3}$ -strain that restricts flexibility in addition to being less reactive Michael acceptors than dehydroamino acid residues bearing di- and tri-substituted alkenes. Through their studies, they were pleased to find that incorporation of bulky dehydroamino acids, namely dehydrovaline, did not perturb secondary structure, enhanced proteolytic stability, and could be combined with D-amino acid residues to synergistically improve a peptide's resistance to proteolysis. With this in mind, we sought to incorporate a dehydrovaline residue at the P2 position of our inhibitors to analyze its



**Scheme 3.3.** Synthesis of modified P2 residues. (A) Synthesis of dehydrovaline residue **31** for elaboration to inhibitor derivative **32**. (B) Synthesis of chiral trifluoromethyl valine residue **36** toward the development of **37**.

effects on potency and further on its ability to diminish toxicity if it proved to be a suitable inhibitor. Synthesis of the dehydrovaline residue could easily be carried out utilizing the Schöllkopf-formylamino-methylenation protocol. Following this protocol, acetone was reacted with isocyanide **29** to afford the fully protected dehydrovaline residue **30**. After deprotection of the formyl group, **31** was then poised to be incorporated and elaborated to the desired inhibitor **27**.

Finally, we explored the idea of replacing the *tert*-leucine residue with a valine residue in which one of the methyl groups of the valine side chain was replaced with a trifluoromethyl group.<sup>27</sup> The trifluoromethyl group has often been utilized in medicinal chemistry as an isosteric replacement of various moieties from simple chloride substituents to methyl groups to nitro groups. While the introduction of the trifluoromethyl group can serve a variety of functions, it is notable for its ability to increase steric bulk and its ability to increase stability of compounds by decreasing sites of metabolism at the location in which it is introduced. The synthesis of the desired trifluoromethyl containing residue began in a similar fashion used to synthesize dehydrovaline derivative **31**. Again, utilizing the Schöllkopf-formylamino-methylenation protocol, trifluoroacetone (**33**) is reacted with ethyl isocyanomalonate (**34**) to afford the dehydro derivative **35** as exclusively the *Z*-isomer. We were not concerned with the specific stereochemistry at the  $\beta$  position, so we simply sought out methodology to generate the desired *R* stereochemistry at the  $\alpha$ -carbon. To accomplish this, **35** underwent an asymmetric hydrogenation using (*R*)-TCFP-Rh which allowed for *syn* addition of hydrogen from the  $\alpha$ -face to generate desired compound **36** which could then be elaborated further into inhibitor derivative **37**.

### 3.2.1.2 Evaluation of P2 Modifications

Although our main focus was on improving the toxicity associated with **9** and its derivatives, we needed to ensure that the compounds were inhibitors of GOAT. Upon synthesis of the desired inhibitor derivatives, they could be tested in our *in vitro* assay (details outlined in the experimental) to evaluate potency and ability to act as GOAT inhibitors. Unfortunately, each modification made to the second residue (P2) of the inhibitor structures led to a complete depletion of inhibitory activity. This demonstrated several aspects of the second residue that were important for activity: 1) defined stereochemistry in the natural *R* configuration is necessary at the alpha position and 2) introduction of methylene spacer units caused a distortion in secondary structure that was not suitable to binding in the GOAT active site. Thus, we turned our attention toward other points of modification around structure **9**.

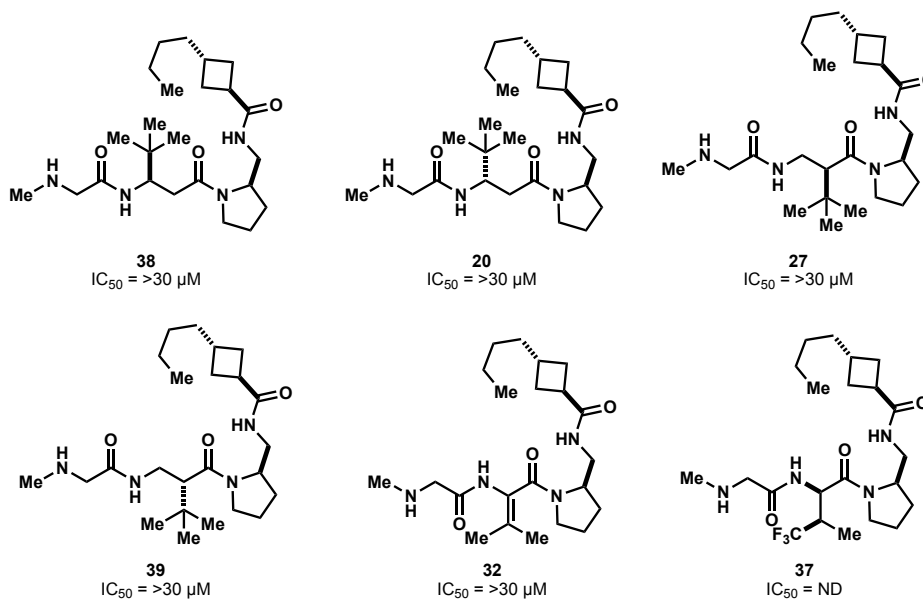


**Figure 3.6.** Evaluation of *in vitro* efficacies of modified P2 inhibitor derivatives.

### 3.2.2 Evaluation of Covalent Modifiers

Due to the presence of a conserved histidine residue amongst the MBOAT family which is thought to be located in the active site of the enzyme, we sought to generate modifications to the pyrrolidine ring that might engage the imidazole of the histidine residue. Our studies largely focused on the incorporation of electrophilic moieties onto the pyrrolidine ring that might undergo reaction with the imidazole as covalent modifiers. To study our hypothesis, we generated acrylate **40**, acrylamide **41** and epoxide **42** which all could readily undergo reaction with histidine. Unfortunately, the acrylate and acrylamide derivatives were unable to inhibit GOAT and **42** was ultimately not tested. While not a covalent modifier, we sought to generate pyrrole containing derivative **43** that could harness the potential to undergo pi-stacking with the imidazole of histidine, or other aromatics that may be present in the active site. Additionally, introduction of the pyrrole could reduce flexibility with increased planarity. We were pleased to see that incorporation of the pyrrole did not deplete all inhibitory activity but likely suffered from diminished potency due to elimination of the stereocenter at the alpha center which had been shown to be crucial in prior experiments.

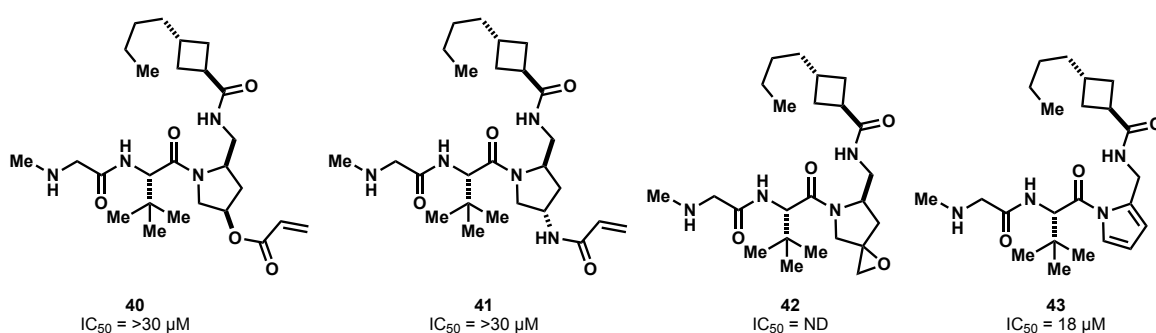
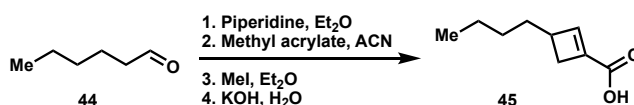


**Figure 3.7.** Evaluation of *in vitro* potency of modified pyrrolidine derivatives.

### 3.2.3 Synthesis and Evaluation of Side Chain Modifications

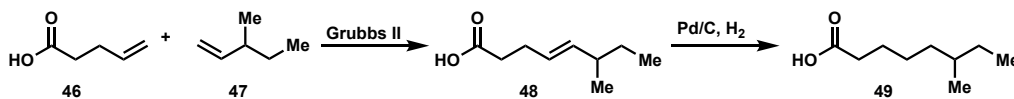
#### 3.2.3.1 Synthesis of Side Chains

The side chain modifications we sought after looked to explore the importance of chain length on inhibitory activity, effects on introducing hydrophobicity, and effects on increasing polarity in the side chain. To explore chain length requirements, we synthesized cyclobutene derivatives in which the chain extending from the cyclobutene was iteratively shortened by a single methylene unit. A representative synthesis of the cyclobutene side chains as described in the thesis of Dr. Ryan Hollibaugh<sup>12</sup> is shown in Scheme 3.4 in which the chain lengths could be altered based upon the aldehyde used.



**Scheme 3.4.** Representative synthesis of cyclobutene-containing side chains for development of inhibitors **51–54**.

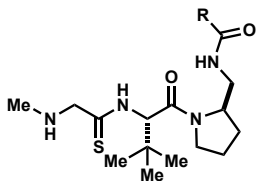
We next looked at developing methylated octanoyl chain derivatives with the hope that the methyl substituent would harness the potential to fit into an unknown hydrophobic pocket in the binding site and afford a better binding affinity. Most of the desired methylated derivatives were commercially available as the carboxylic acids and could easily be incorporated into the final inhibitor. The side chain for **56** was not readily available but could easily be synthesized *via* a metathesis process between pentenoic acid **46** and methylated pentene derivative **47** as depicted in Scheme 3.5. Catalytic hydrogenation could then afford desired acid **49**.



**Scheme 3.5.** Synthesis of 6-methyl octanoic acid **49**.

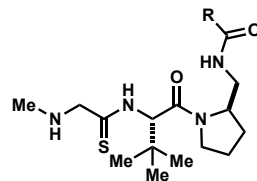
### 3.2.3.2 Evaluation of Side Chain Modifications

**A**



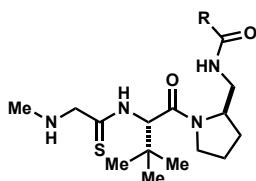
#	R	IC <sub>50</sub> (μM)
50		1
51		3
52		7
53		13
54		17

**B**



#	R	IC <sub>50</sub> (μM)
55		3
56		15
57		4
58		ND
59		ND

**C**



#	R	IC <sub>50</sub> (μM)
60		7
61		> 30
62		1.8

**Figure 3.8.** Incorporation and evaluation of side chain modifications.

Upon synthesis of inhibitors bearing modified side chains, we then moved forward with evaluation of the new inhibitors *in vitro*. We began by screening the cyclobutene-containing derivatives and were interested, though not surprised, to see that as the chain

length decreased, as did the *in vitro* efficacy. This demonstrated that binding to GOAT shows a preference for the native octanoyl chain which much better mimics acylated ghrelin. Next, we looked at the inhibitory effects on adding the methyl substituents along the octanoyl chain. Examining the data presented in Figure 3.8, we observed that while methylation along the side chain does not deplete inhibitory activity, it does not afford us the substantial increase in potency that we thought would be afforded by binding in an additional hydrophobic pocket. Finally, we studied the effects of adding polarity along the side chain in the form of mono- and di-oxygenation of the chain. From this data, we observed that the bis-oxygenated side chain led to a complete loss of inhibitory activity. Thus, for further inhibitor derivatives where modifications of the side chain were not being conducted, we retained the native octanoyl chain due to ease of incorporation and availability.

### 3.2.4 Discussion

Although various modifications of **9** were achieved, none proved substantively more potent than the optimized lead *in vitro*. SAR appeared to be very tight around the lead and we were unable to achieve a desirable sub-micromolar efficacy *in vitro*. Moreover, compounds that were able to retain the potency of **9** were unable to alter the *in vivo* results. In most cases, the compounds displayed the same kinetics as **9** (Figure 3.9A) of ghrelin decrease in mice and the observed toxicity was the same or worse. We also observed that acetamide **63**, which lacks the hydrophobic side chain and is thus not a GOAT inhibitor *in vitro*, caused the same rapid decrease in circulating ghrelin levels when tested at comparable doses. Furthermore, we discovered that pyrrolidine-

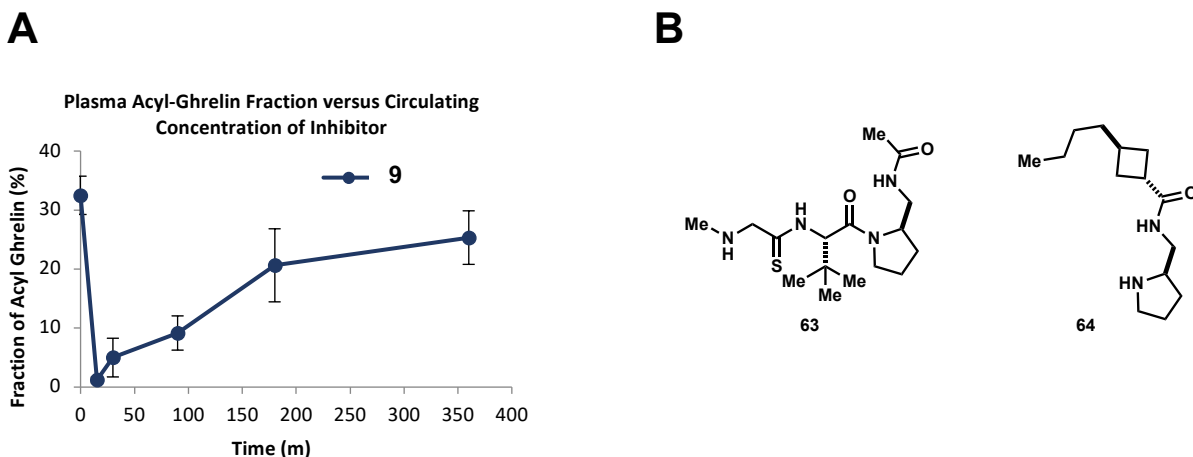


**Figure 3.9.** Evaluation of *in vivo* properties. (A) Preliminary *in vivo* effect of **9** on circulating ghrelin. (B) Negative controls synthesized to observe pharmacological effects for insight on the mechanism of toxicity.

containing fragment **64**, which can be derived from **9** *in vivo* by proteolysis or self-immolation (*via* its N-terminal amine attacking the P2 carbonyl) was the most toxic compound we had evaluated to date. This data demonstrated to us that these series of compounds had intrinsic, off-target limitations and thus we needed to pursue a new avenue of inhibitor development.

### 3.3 Linear Peptidomimetic Inhibitors of GOAT

Prior to arriving at lead compound **9**, hundreds of compounds had been synthesized as documented in the thesis of Dr. Ryan Hollibaugh.<sup>12</sup> Along the route to discovery, it was recognized that inhibition of GOAT required an N-terminal glycine residue but N-methylation was also tolerated. Additionally, it was realized that an adjacent *tert*-leucine residue (P2 residue) was more favorable than the native serine. With this information in hand, we sought to re-screen truncated ghrelin peptides bearing these modifications in addition to the inclusion of an acylated DAP residue at the P3 position which had been identified by Brown and Goldstein<sup>3</sup> for proteolytic stability. The results



obtained were striking (Figure 3.10A). While we had optimized the pyrrolidine-containing inhibitors down to what was in essence a tripeptide mimetic, and Brown and Goldstein had identified the pentapeptide as the minimally required recognition sequence, our data suggested that the apparent optimum for *in vitro* inhibition was the tetrapeptide. This newly recognized tetrapeptide not only showed a 50-fold increase in potency, but also the pentapeptide bearing our modifications of the first three residues was 20-fold better than the pentapeptide identified by Brown and Goldstein in their seminal reports. We quickly sought to generate derivatives of **65** to identify congeners capable of improved binding affinity.

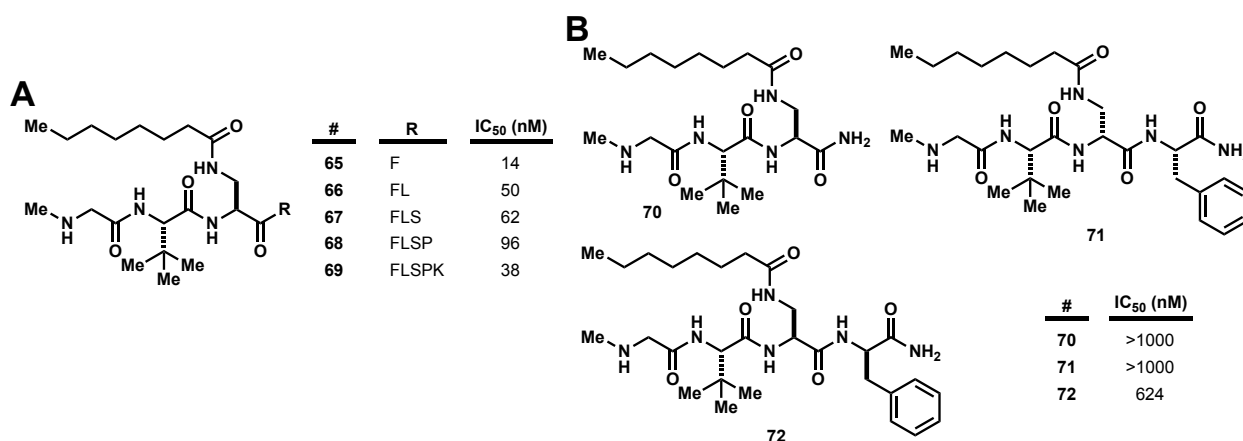


**Figure 3.10.** Development of linear peptidomimetic inhibitors. (A) Evaluation of minimally modified acyl ghrelin truncation peptides. (B) Evaluation of necessary requirements for potency.

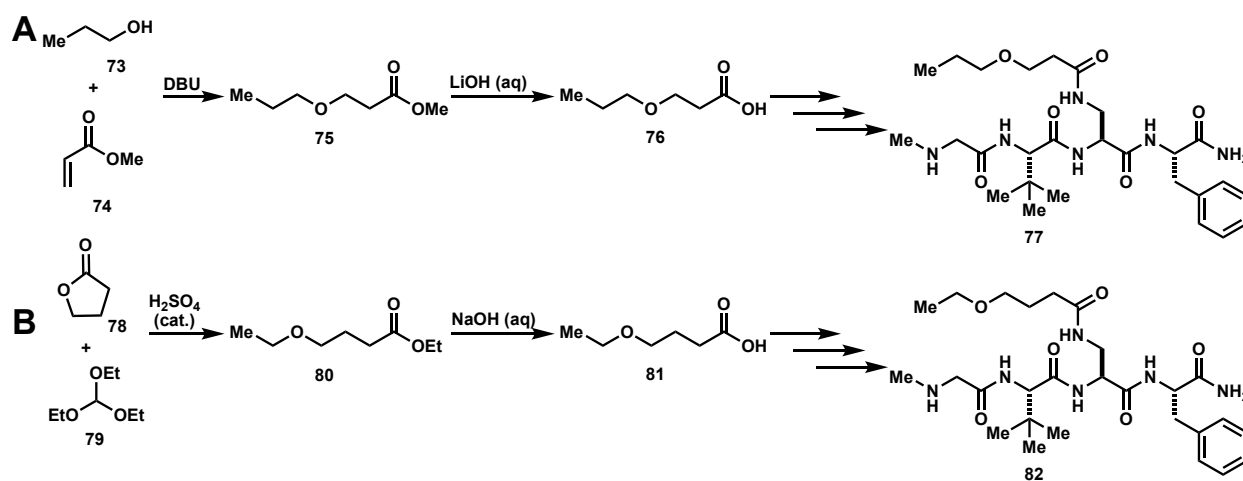
### 3.3.1 Development and Evaluation of *In Vitro* Linear Peptidomimetic Inhibitors of GOAT

Prior to fully delving into modifications of **65**, we set forth to identify key functionalities responsible for GOAT recognition (Figure 3.10B). To accomplish this, we synthesized tripeptide **70** and were not surprised to find that it was inactive in the nanomolar range and appeared to have an *in vitro* IC<sub>50</sub> slightly above 1  $\mu$ M, consistent

with the values observed in the pyrrolidine-containing inhibitors which were mimicking the tripeptide. Furthermore, as expected, the stereochemistry at the P3 DAP residue was crucial. As seen, when the *S* enantiomer of DAP is utilized in this position (**71**), the compound is rendered inactive. Lastly, we replaced the P4-Phe residue with its antipode (**72**). Although this substitution impacts the potency immensely, because it does not eliminate activity in its entirety and we thus hypothesized that modifications at the P4 residue could be suitably tolerated. With this information, and the data observed with the prior series of inhibitors, we identified that favorable modifications were likely only tolerable at the side chain position and the P4 position and thus commenced identification of modifications that could improve the activity.

### 3.3.1.1 Side Chain Modifications to Identify Desirable Binding Interactions

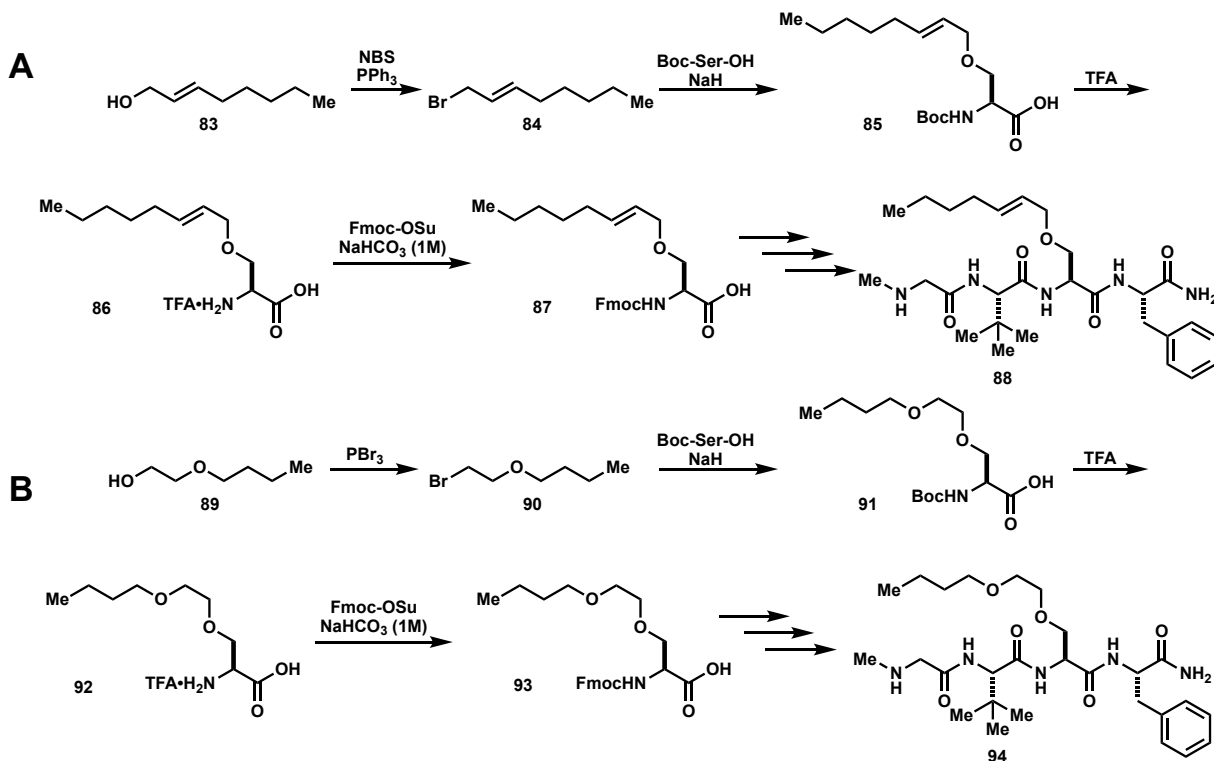
As seen in the generation of **60** in the previous series of compounds, mono-oxygenation of the side chain is well-tolerated. In an effort to determine the most desirable position of oxygenation, we performed a scan of mono-oxygenated side chains *via* the



**Scheme 3.6.** Probing the effects of mono-oxygenation along the side chain. (A) Synthesis of **76** for elaboration to **77**. (B) Synthesis of acid **81** for elaboration to **82**.

generation of acids **76** and **81**.<sup>28,29</sup> Acid **76** arises from the Michael addition of propanol (**73**) to methyl acrylate (**74**) to afford methyl ester **75**, which then undergoes saponification using aqueous lithium hydroxide to afford acid **76**. Further elaboration and incorporation of the new side chain led to the generation of compound **77**. Following the same general Scheme, acid **81** could be generated *via* the opening of  $\gamma$ -butyrolactone (**78**) with triethylorthoformate (**79**) in the presence of catalytic sulfuric acid using ethanol as the solvent. The resultant ethyl ester (**80**) could then be saponified under aqueous basic conditions to afford the desired acid **81** and further elaborated to compound **82**.

To further evaluate the importance of the interactions of the side chain in binding, we studied the role and necessity of the ester/amide linkage of the side chain to the peptide backbone. To study this, we circled back to having the native serine residue at



**Scheme 3.7.** Probing the effects of altering the amide/ester linkage of the octanoyl side chain at the P3 position. (A) Generation of ether derivative **88** *via* etherification of serine. (B) Synthesis of ether derivative **94** utilizing oxygenated side chain **90**.

the third position, but instead of generating an ester linkage to the side chain, we focused on forming ether linkages *via* the generation of bromides **84** and **90**. Generation of the bromides could allow for Williamson ether synthesis with serine to afford our desired residues. Generation of ether-containing inhibitor derivative **87** commences with an Appel reaction of allyl alcohol **83** using NBS and triphenylphosphine to generate the key allyl bromide **84**. Etherification of Boc-protected serine with **84** afforded **85** which then underwent a protecting group swap to generate Fmoc-protected **87** that was poised for solid phase peptide synthesis (SPPS) for incorporation and elaboration to tetrapeptide **88**. Similarly, alcohol **89** could be transformed to bromide **90** using phosphorus tribromide. Etherification of Boc-protected serine followed by protecting group exchange afforded Fmoc-protected **93** that was then utilized in SPPS to generate derivative **94**.

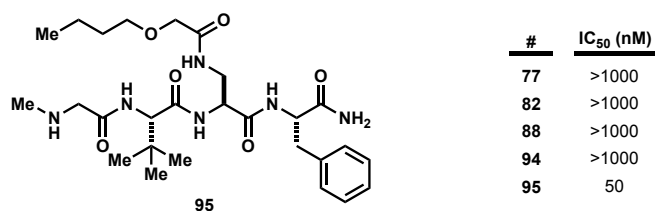


**Figure 3.11.** Evaluation of tetrapeptide side chain modifications.

Upon evaluation of the side chain modifications that were made (Figure 3.11), we observed complete loss of inhibitory activity for all modifications except for **95**, which contained the same side chain that retained activity in the pyrrolidine-containing series as seen in compound **60**. Although the loss of activity is undesirable, this information was still useful as it provided us with key details about necessary requirements for GOAT binding. Through the generation of derivatives **77** and **82**, we could see that oxygenation is only tolerated at the 3-position of the side chain and introduction of polar functionality

elsewhere was not tolerated. Additionally, we could deduce that rigidity afforded by having the ester/amide linkage was important. Derivative **94** was thought to mimic the butoxyacetic acid side chain of **60** by incorporation of the additional oxygen in the same position, but it appears that the amide linkage is key in governing binding affinity. As no side chain modification afforded a significant increase in potency, we moved forward with derivative generation utilizing primarily the native octanoyl side chain.

### 3.3.1.2 Evaluation of P4 Residue Modifications in the Generation of Potent Tetrapeptides

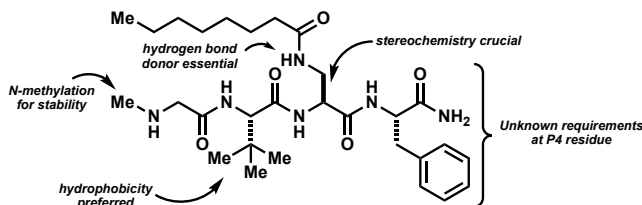


**Figure 3.12.** Identification of aspects important for GOAT inhibition.

From the data acquired through evaluation of the pyrrolidine-containing series in addition to the primary modifications made on the linear tetrapeptide, we generated key ideas on functionality necessary for inhibitory activity which are presented in Figure 3.12. In summary, it appeared that the first three residues were critical for activity with minor modifications tolerated. However, we still did not have clear information on the important features of the fourth phenylalanine residue that was seemingly responsible for achieving low double digit nanomolar potency. Thus, we set forth to synthesize derivatives of the phenylalanine residue with the desire to improve inhibitory activity while also mitigating sites of oxidation on the phenyl ring.

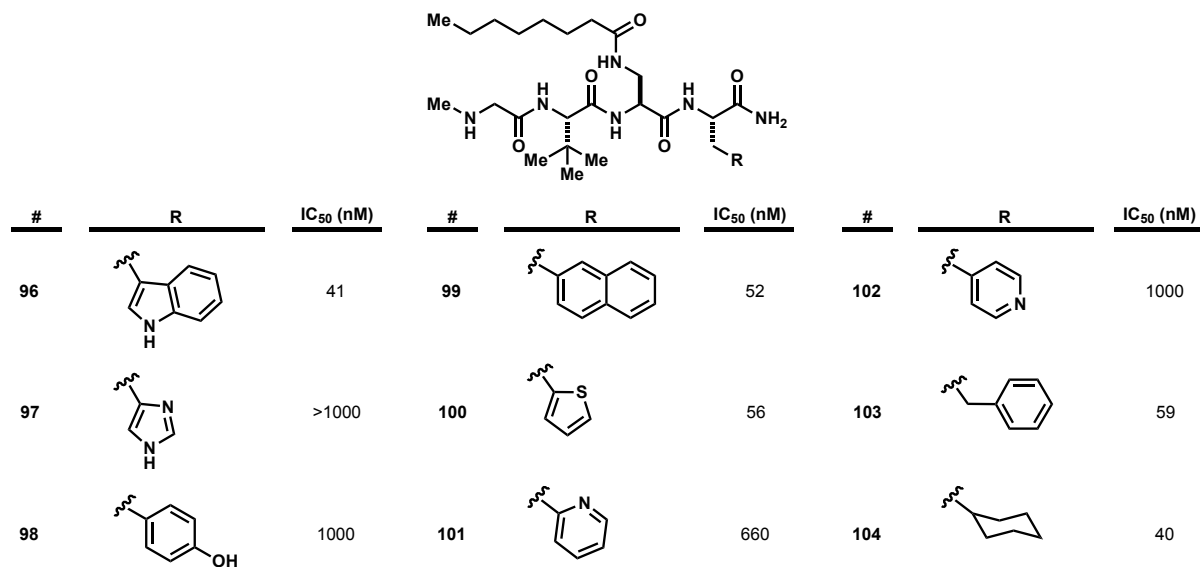


**Figure 3.13.** Aromatic screening and evaluation of the P4 residue.

We began our exploration of the fourth residue by conducting an aromatic screen utilizing a combination of natural amino acid residues and non-natural amino acid residues bearing aromatic substituents as shown in Figure 3.13. Screening commenced with the replacement of phenylalanine with natural amino acids bearing aromatic side chains. To this end, we synthesized tetrapeptides containing tryptophan (**96**), histidine (**97**), and tyrosine (**98**) as the C-terminal residue. Surprisingly, only tryptophan replacement retained potency *in vitro* while histidine was completely inactive, and tyrosine resulted in a significant decrease in potency. We hypothesized that the reason for the substantive impact in activity for tyrosine and histidine likely arises from the ability of both

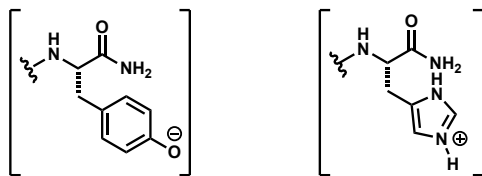


**Figure 3.14.** Most probable charged states of tyrosine (left) and histidine (right) contributing to loss of activity.

tyrosine and histidine to exist in a charged state readily. Our hypothesis was further solidified when the generation of the anisole derivate **110** was able to restore potency.

Following screening of natural amino acid residues bearing aromatic side chains, we evaluated non-natural, aromatic ring bearing residues. We were pleased to find that the aromatic system could extend beyond just a phenyl ring as evidenced by the retention of potency when naphthalene derivative **99** was incorporated. Furthermore, heteroaromatic rings could be incorporated, but inclusion of a pyridine side chain (**101** and **102**) caused a significant decrease in potency. The most surprising substitution was the incorporation of the non-aromatic cyclohexane-containing residue to generate inhibitor derivate **104**. We were under the impression that the significant increase in potency afforded by the tetrapeptide over the tripeptide was primarily due to the phenyl ring likely engaging in pi interactions such as pi-stacking or cation-pi interactions with another aromatic residue in the active site. However, when **104** was synthesized and evaluated, we observed only a minimal decrease in activity, suggesting that the affinity at this fourth residue does not arise from pi interactions but rather interactions with a hydrophobic pocket.

With the aromatic screening completed, we turned to evaluating substituted phenyl rings. It is well known in medicinal chemistry campaigns that phenyl rings harness the

potential to be oxidized readily in the body primarily by P450 enzymes. Since we observed a complete loss of inhibitory activity when tyrosine was incorporated in this fourth position, we knew that the sites of oxidation should be protected to preserve the activity of these compounds downstream. Derivatization commenced with the incorporation of halogen substituents as demonstrated by bromo-derivatives **105** and **106** and fluoro-derivatives **107**, **108**, and **109**, which all retained potency and could have more favorable pharmacokinetic properties *in vivo*. As previously mentioned, when anisole derivative **110** was introduced to cap the phenol and prevent deprotonation of the phenolic hydrogen, potency was diminished, but was greatly improved over the parent tyrosine derivative. We continued our screening with mono- and di-methyl substituted derivatives **111** and **112** which were able to retain potency as well. This data showed us that substitution of the phenyl ring was highly tolerated with the only derivative to lead to a complete loss of activity was the para phenyl derivative **113** which was likely too large to fit into the binding pocket occupied by this fourth residue.

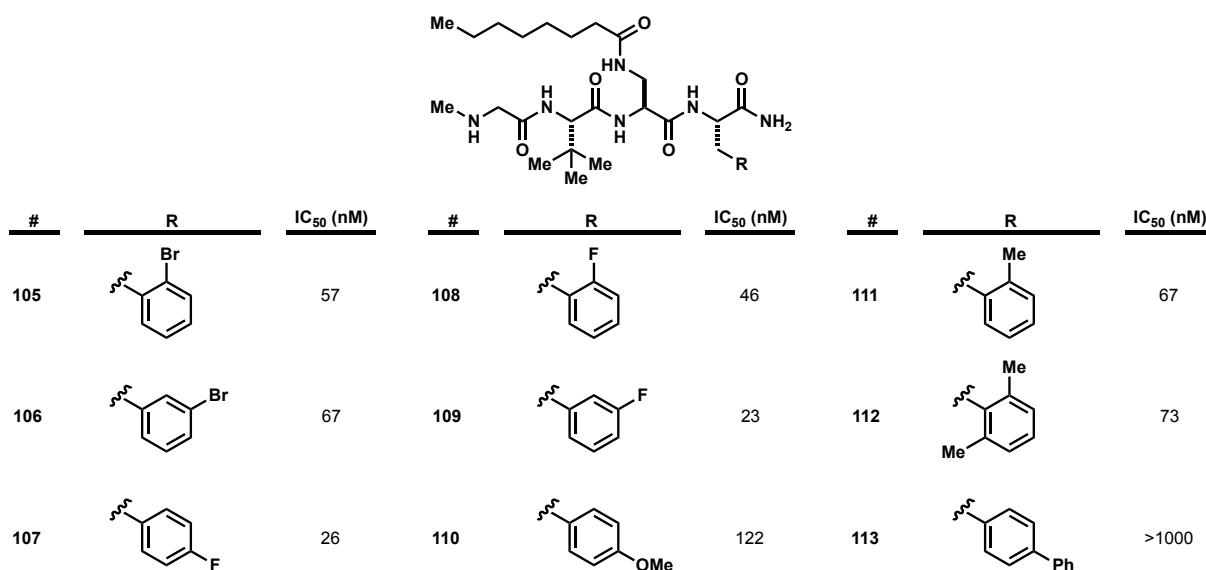


**Figure 3.15.** Evaluation of substituents on the phenyl ring of the P4 position.



Evaluation of our compounds using a well-established *in vitro* GOAT assay provided us with a critical first layer of selection for compound efficacy. While our IC<sub>50</sub> evaluations allow us to narrow down the number of candidates, it still leaves us with a large pool of potentially good inhibitors whose complete characterization *in vivo* is not feasible. To increase our chances of unveiling a strong biologically active GOAT inhibitor amongst our vast pool of enzymatically active compounds, we invested considerable time and effort in developing a cell-based assay as an additional screening step.

### **3.3.2 Development of an INS-1 Stable Cell Line for a Cell-Based GOAT Assay**

In 2008, Brown and Goldstein<sup>2</sup> showed that upon transient transfection of insulinoma INS-1 cells with plasmid bearing the preproghrelin gene, both proghrelin (aa 1-94) and mature ghrelin (aa 1-28) could be detected in the cellular peptide extract. Furthermore, when the INS-1 cells were co-transfected with preproghrelin and GOAT plasmids and maintained in a growth media supplemented with octanoyl-BSA, acylated ghrelin could be detected. Dr. David Strugatsky, our resident biochemistry co-worker, sought to adapt this cell line for our drug discovery program.

Initial observations on studies with the INS-1 cells showed a large variability in the amount of hormone expression between experiments, but we were eventually able to arrive at the development of INS-1 cells that could stably express GOAT and preproghrelin genes. To achieve stable incorporation into the INS-1 genome, we constructed a retrovirus for the GOAT gene and a lentivirus for the preproghrelin gene. This resulted in 3 cell lines: INS/GOAT which expresses GOAT; INS/GOAT/GHRL which expresses GOAT plus proghrelin; and INS/GHRL which expresses just preproghrelin.

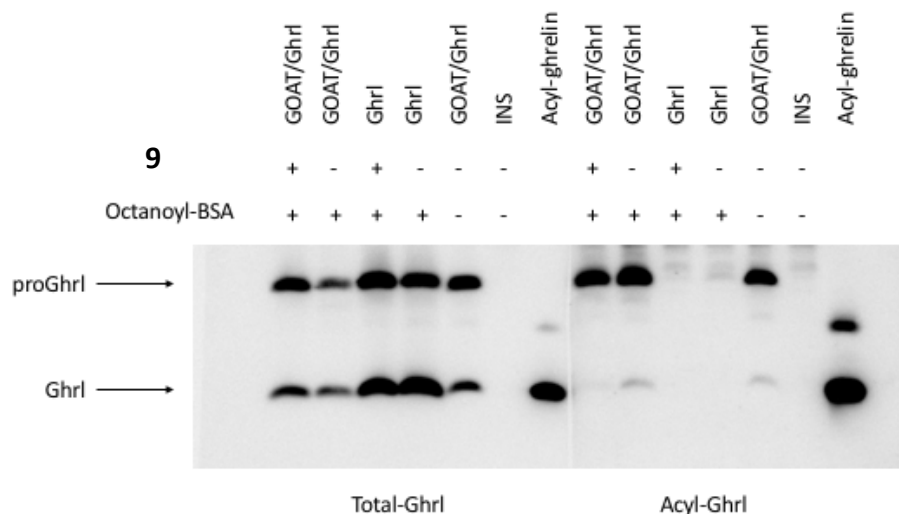


**Figure 3.16.** Western blot analysis of peptide extract of INS-1 cells. INS-1 cell lines stably expressing GOAT enzyme and preproghrelin genes were produced via infection with retrovirus and lentivirus respectively. Cells were plated in 6-well plates to achieve near full confluency. Octanoyl-BSA and 10  $\mu$ M of compound **9** were added to indicated wells and cells were incubated for 24 hours. Cells were collected and subjected to peptide extract. Each sample was separated on 16% Tricine polyacrylamide gel. Gel blots were immunostained with anti-Total and anti-acyl ghrelin antibodies. For quantification of protein bands, gel images were analyzed with ImageJ software (NIH). Percent of inhibition by compound **9** was calculated from band intensities as  $(Acyl/Total)^9 / (Acyl/Total)^{control}$  and found to be 46% for proghrelin (upper band) and 87% for mature ghrelin (lower band). Lanes: COAT/Ghrl-INS-1 cell lines expressing both GOAT and preproghrelin; Ghrl-INS-1 cell lines expressing only preproghrelin; INS-control uninfected cells; Acyl-ghrelin – synthetic acyl ghrelin peptide.

Previous lead compound **9** was used to preliminarily observe the cellular assay in action, the results of which are displayed in Figure 3.16. Compound **9** was added to the growth medium of the INS/GOAT/GHRL cell culture at a concentration of 10  $\mu$ M, which caused a decrease in the levels of proghrelin and mature ghrelin by 46% and 87% respectively.

The development of this cellular assay not only allowed us to add another layer of screening to our inhibitor selection process, but also gave us some further insight on the mechanism by which ghrelin acylation occurs. The western blot of the peptide extract from INS/GOAT/GHRL clearly showed that proghrelin was the predominant form that was octanoylated while only a small fraction of the mature ghrelin was acylated. It is known that the *in vivo* substrate for GOAT is proghrelin, so it was unclear to us why most of the

acylated proghrelin was unprocessed. One would expect that half of the acyl proghrelin would be processed to its mature form, as shown in the western blot, in which total ghrelin is reflective of both the acyl and des-acyl species. Moreover, we discovered that INS/GOAT/GHRL cells were able to secrete des-acyl ghrelin but not acyl ghrelin by measuring both species in the growth medium utilizing ghrelin specific ELISAs. Thus, we concluded that the maturation process of des-acyl and acyl proghrelin species are independent of each other and that acylation is linked to the secretion process that is likely specific to ghrelin producing cells that do not exist in INS-1 cells. Further studies provided strong evidence that acylation of proghrelin occurs co-translationally.

Optimization of the cellular assay continued by using a derivative of **3** (**3a**) which was developed by Eli Lilly<sup>30</sup> and was shown to possess desirable *in vitro* activity (lit. IC<sub>50</sub> = 57 nM) and *in vivo* activity when utilized in a feeding experiment in mice. Compound **3a** was administered *via* oral gavage and showed a favorable decrease in feeding behavior which suggested that the compound was able to permeate cells and find its desired target

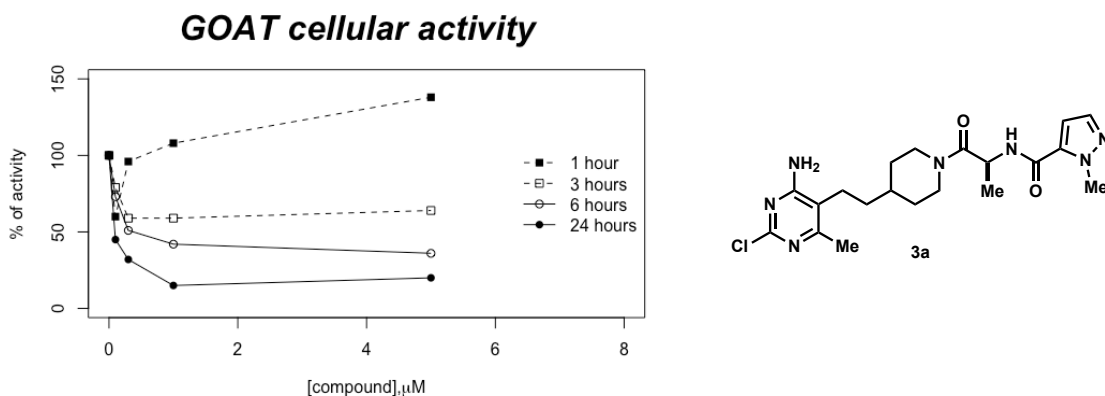


**Figure 3.17.** Optimization of a cellular assay for GOAT activity. Compound **3a** was used as a positive control for optimization. INS/GOAT/GHRL cells were seeded in 96-well plate at 90% confluency. On the next day, media was removed, cells were washed with 100  $\mu$ L of fresh media. Different concentration of compound **3a** were prepared in vehicle composed of growth media and 2.5% DMSO. After adding compound to the cells, plate was placed in incubator and 20  $\mu$ L of media was removed at different time points and stored at -80  $^{\circ}$ C for further analysis of secreted acyl-ghrelin. Acyl-ghrelin concentration was normalized to vehicle control and expressed as percent of activity of the compound.

(GOAT) and thus would be a reliable control for improving and optimizing our cellular assay. The results of the optimization experiments are shown in Figure 3.17. From this data, it is apparent that inhibition of acyl-ghrelin secretion is time dependent. This likely reflects an intracellular store of acyl-ghrelin present in the secretory vesicles that is insensitive to acute GOAT inhibition. Based on this data, we chose to use the longest incubation time for compounds in order to maximize the chances of observing a pharmacological effect.

### 3.3.2.1 Evaluation of Linear Peptidomimetics in a Cellular Assay

With the cellular assay established, we were poised to screen compounds that showed favorable *in vitro* potency. Before delving into a full cellular screen of all of our highly active *in vitro* inhibitors, we began by screening the minimally modified ghrelin truncation peptides (**65–69**) previously discussed, the results of which are shown in Figure 3.18. We were shocked by the outcome of this experiment. Given the low

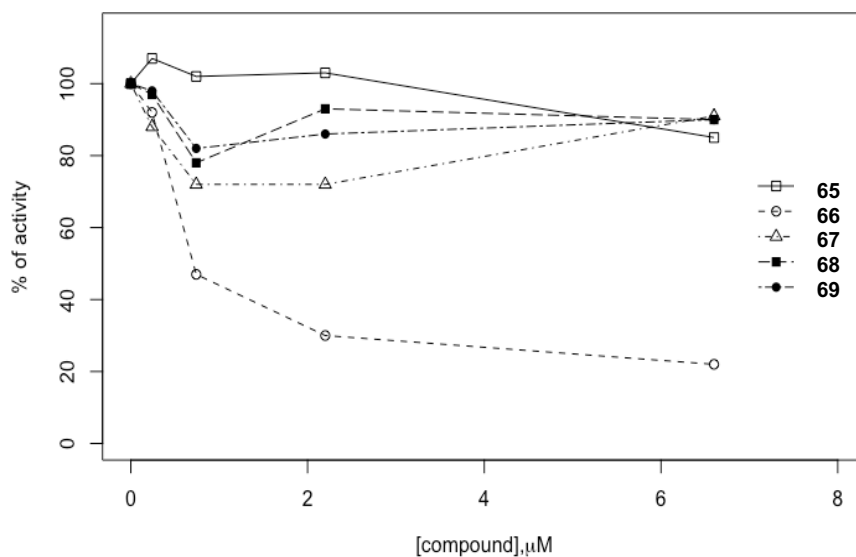
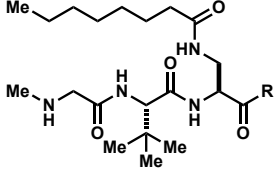


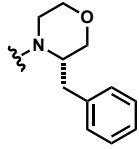
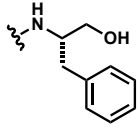
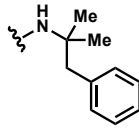
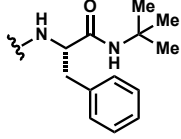
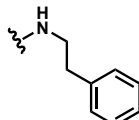
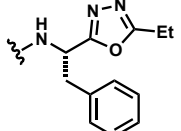
**Figure 3.18.** Cellular analysis of minimally modified ghrelin truncation peptides (**65 – 69**).

nanomolar efficacies of the minimally modified tetrapeptide (**65**) and its various derivatives, we were highly optimistic that the cellular assay would follow suit. However, as shown clearly from the data, the only minimally modified peptide that displayed any significant activity in cells was pentapeptide **66**. While this data was discouraging given the excitement around **65** and its derivatives, we remained optimistic that we could further modify **65** in a manner that would enable cellular activity. We recognized, however, that there existed the possibility that the 3.5 times less potent pentapeptide derivative **66** could still be a viable candidate option.

### **3.3.2.2 Optimizing the Cellular Activity of Tetrapeptide 59**

From separate work on templated macrocyclization of peptides in the Harran laboratory, we learned valuable cellular permeability information. During the course of that work, PAMPA assays were utilized to observe permeability profiles of the vast library of peptidyl macrocycles. One observation made by researchers on this project which was critical to our understanding of how best to modify our cellularly inactive peptide structures was that when a free carboxamide was present in the molecule, cellular permeability was adversely affected. We hypothesized that this negative effect on permeability was due to the innate polarity associated with the carboxamide. Typically, compounds with a total polar surface area (tPSA) greater than 140 angstroms have difficulty permeating cells. With a tPSA value of around 172, it is less surprising that **65** does not possess desirable cellular activity. With this information in hand, we set out to generate derivatives of **65** that lacked the C-terminus carboxamide and diminished the overall polar character at this position.

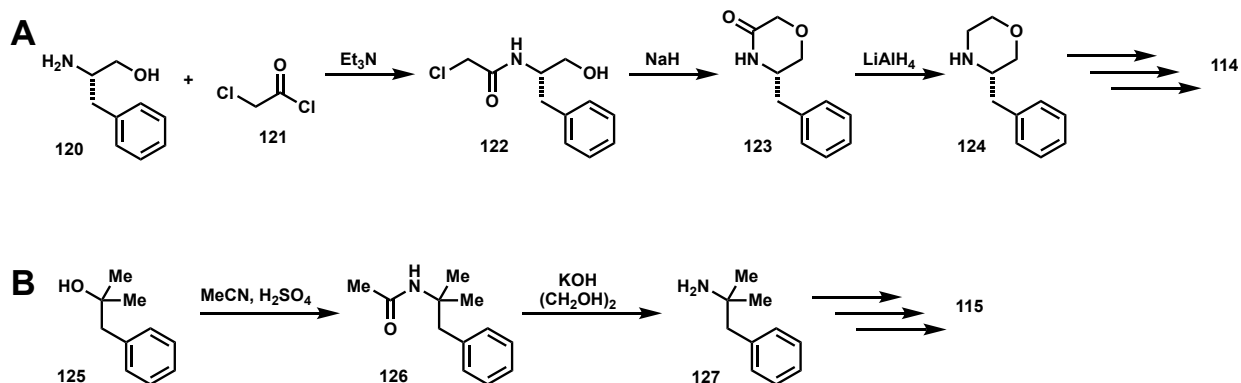


#	R	tPSA (Å)	IC <sub>50</sub> (nM)	#	R	tPSA (Å)	IC <sub>50</sub> (nM)
114		128.87	307	117		148.66	29
115		128.43	>1000	118		151.53	125
116		128.43	43	119		162.38	74

**Figure 3.19.** Evaluation of alterations to the C-terminal carboxamide to reduce total polar surface area (tPSA) and improve cellular activity.

Modification commenced with the synthesis of morpholine-containing tetrapeptide **114** which arises *via* the elaboration of **124**. The synthesis of **124** is pretty straightforward<sup>31</sup> as shown in Scheme 3.8 and begins with the N-acylation of phenylalaninol (**120**) with chloroacetyl chloride (**121**) to afford amide derivative **122**. In the presence of sodium hydride, **122** can undergo an intramolecular cyclization with loss of HCl to afford morpholinone **123**. Finally, reduction of the amide using lithium aluminum hydride provided desired morpholine residue **124**. Through standard liquid phase peptide chemistry, **124** can be incorporated into the peptide sequence and elaborated to desired derivative **114**. We were grateful to see that though the terminal carboxamide was not present, **114** still possessed moderate *in vitro* activity, though we desired a compound with sub-100 nanomolar efficacy.

Continuing our pursuit of eliminating superfluous polarity, we designed and synthesized phenethylamine derivatives **115** and **116**, which completely eliminate the



**Scheme 3.8.** Synthesis of modified C-terminal residues. (A) Synthesis of morpholine-containing residue **124** for elaboration to tetrapeptide **114**. (B) Synthesis of benzylamine derivative **127** for elaboration to tetrapeptide **115**.

terminal carboxamide in addition to any added hydrogen bond acceptors, such as the oxygen still present in **114**. Compound **116** could be easily synthesized *via* the incorporation of commercially available phenethylamine whereas compound **115** relied on the successful synthesis of the geminal-di-methyl phenethylamine derivative **127**.<sup>32</sup> To accomplish this, first, tertiary alcohol **125** undergoes a Ritter reaction with acetonitrile in the presence of sulfuric acid followed by acetic acid to afford acetamide **126**. Then, in refluxing, basic conditions, the amine can be deprotected to afford the desired compound **127**. Similarly, for the synthesis of **114**, **127** can be incorporated into the peptide sequence utilizing standard liquid phase peptide synthesis. Unfortunately, upon testing of these two derivatives (**115** and **116**), it was found that compound **115** was completely inactive in our *in vitro* assay. However, simpler phenethylamine derivative **116** was significantly improved over morpholine-containing **114**.

To further probe the effects of modifying the terminal carboxamide, derivatives **117** – **119** were synthesized, each addressing a separate feature of the carboxamide. Derivative **117** was the most potent of the derivatives, displaying only a 2-fold decrease in potency relative to the parent molecule **65**. While the free alcohol of **117** is still relatively

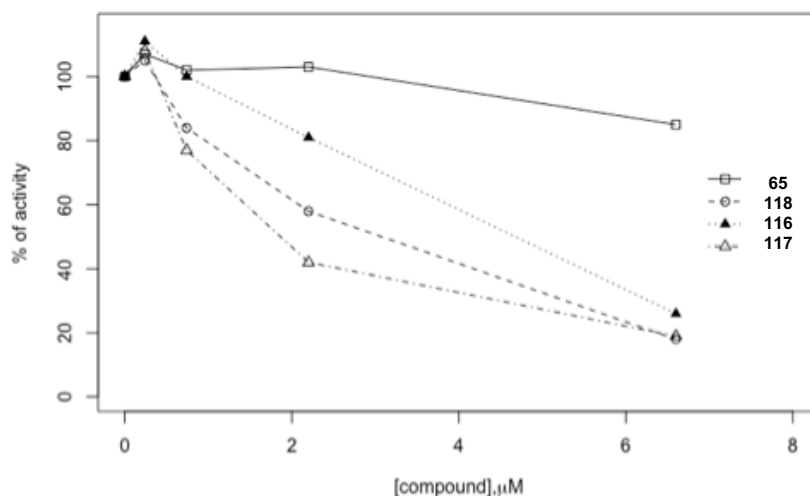


**Figure 3.20.** Cellular assay of C-terminus modified tetrapeptides.

polar, this minor change results in a 23 angstrom decrease in tPSA. While derivatives **118** and **119** did not have as significant of a decrease in tPSA, we were hopeful that masking of the carboxamide would be beneficial to cellular activity.

While most of the synthesized derivatives still retained activity *in vitro*, the true test of these compounds was in their performances in the cellular assay. Upon testing, we were pleased to find that the modifications made were successful in affording cellular permeability to the tetrapeptide scaffold (Figure 3.20). Given this significant positive impact on cellular activity, we sought to incorporate these modifications into to the pentapeptide with the hope that it would further improve the cellular activity of the pentapeptide scaffold, which already displayed favorable cellular activity. The results of this derivatization experiment are presented in Figure 3.21 and were very encouraging. During our first pass evaluation *in vitro*, these compounds were shown to be on par with the parent pentapeptide with compound **130** being the worst compound *in vitro* with only a 4-fold decrease in potency. The true test of improvement, however, was in the evaluation of the cellular efficacy. If our hypothesis that reduction of tPSA from the parent



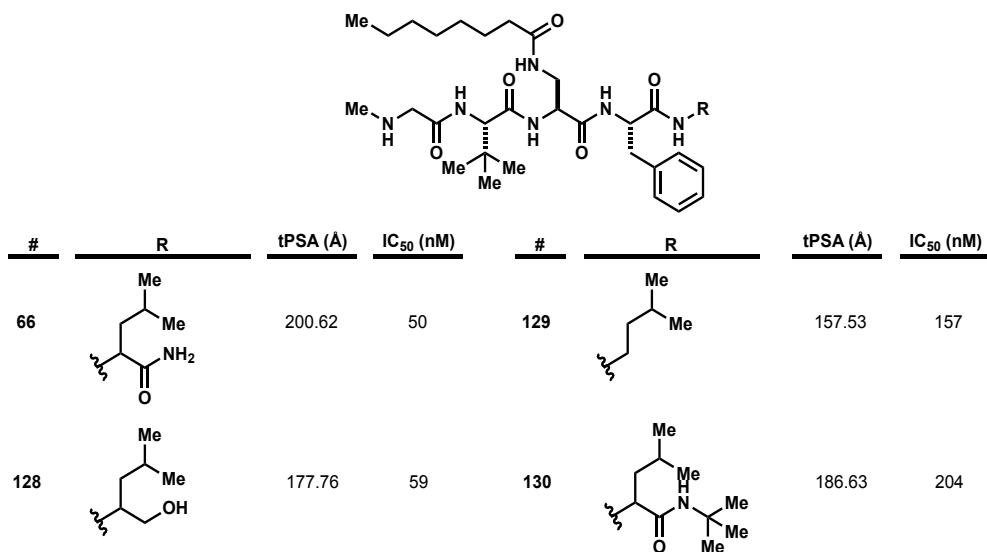


**Figure 3.21.** Implementation of C-terminus modifications showing improvements in tetrapeptide scaffold.

carboxamide leads to an improvement in cellular efficacy is true, then we should expect to see a substantial improvement in cellular efficacy over **66**. As shown in Figure 3.22, when **128** and **129** were dosed at varying concentrations in the INS-1 cells, we observed a substantial improvement in cellular potency over **66**. Reduction of tPSA not only improved the cellular efficacy but did so in a manner that brought the efficacy well under 1  $\mu$ M and much closer to the efficacies observed *in vitro*. Moreover, these modifications

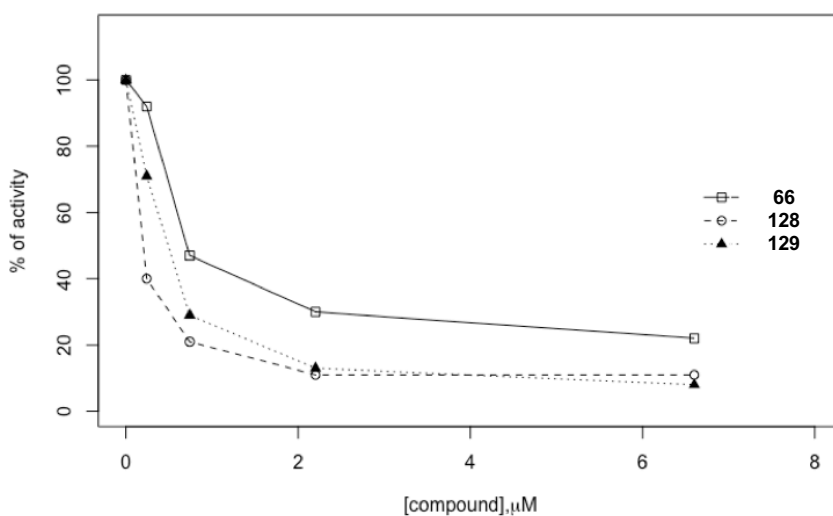


**Figure 3.22.** Cellular assay evaluation of C-terminus modified pentapeptides.

afforded us our most potent compound in cells to date in compound **128** ( $EC_{50} \sim 200$  nM) and was even shown to be more potent than the inhibitor from Eli Lilly (**3a**,  $EC_{50} \sim 1000$  nM). With an *in vitro*  $IC_{50}$  of 59 nM and a cellular  $EC_{50}$  of  $\sim 200$  nM, we felt confident in designating **128** as our lead compound and thus moved forward to study its properties and activity in preliminary mouse studies.

### 3.3.3 In Vivo Evaluation of Lead Compound 128

Among the first *in vivo* experiments conducted for **128** was an evaluation of the pharmacological inhibitory effects on plasma ghrelin levels as described in Figure 3.23. This experiment was run as a side by side evaluation with **3a** using the same conditions

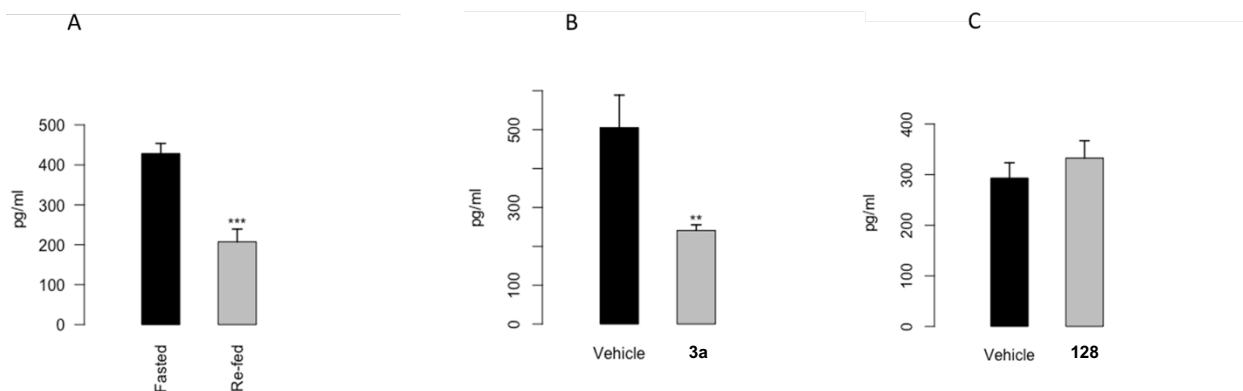


**Figure 3.23.** Dietary and pharmacological effects on plasma acyl-ghrelin in wild type C57/BL6J male mice. (A) Fast/Re-fed experiment. Sixteen 10-week old mice were fasted overnight. The next morning, mice were divided into two groups (8 mice per group). The animals from the “fast” group were anesthetized and blood was collected with capillary tubing accessing retro-orbital cavity. Collected blood was immediately mixed with anti-coagulant, EDTA, and protease inhibitor aprotinin. After short spin, plasma was saved, acidified by adding 100 mM HCl and frozen by placing on dry ice. 20  $\mu$ L of the plasma was used to measure acyl-ghrelin with commercial ELISA. The second “re-fed” group was given access to standard chow food for two hours and blood was collected and processed as above. (B) Pharmacological effect of **3a** on plasma acyl-ghrelin. Vehicle animals (7 per group) and treated animals (8 per group) were orally gavaged with vehicle solution (1% hydroxyethylcellulose, 0.25% Tween 80, 0.05% antifoam) or with compound **3a** in vehicle solution at 10 mg/kg dose. Animals received 5 doses in total given twice a day (morning and evening) over three days. After last dose in the morning of the third day, animals were fasted for 5 hours and blood was collected and processed as above. (C) Pharmacological effect of compound **128** on plasma acyl-ghrelin. Vehicle animals (9 per group) and treated animals (10 per group) were administered through i.p. injections vehicle solution (1% Tween 80 in PBS) or with compound **128** in vehicle solution at 9 mg/mL per dose. The length of experiment and sample preparation were as in (B). The data was analyzed with unpaired t-test and following p values considered significant:  $p < 0.05$  (\*),  $p < 0.01$  (\*\*),  $p < 0.001$  (\*\*\*).

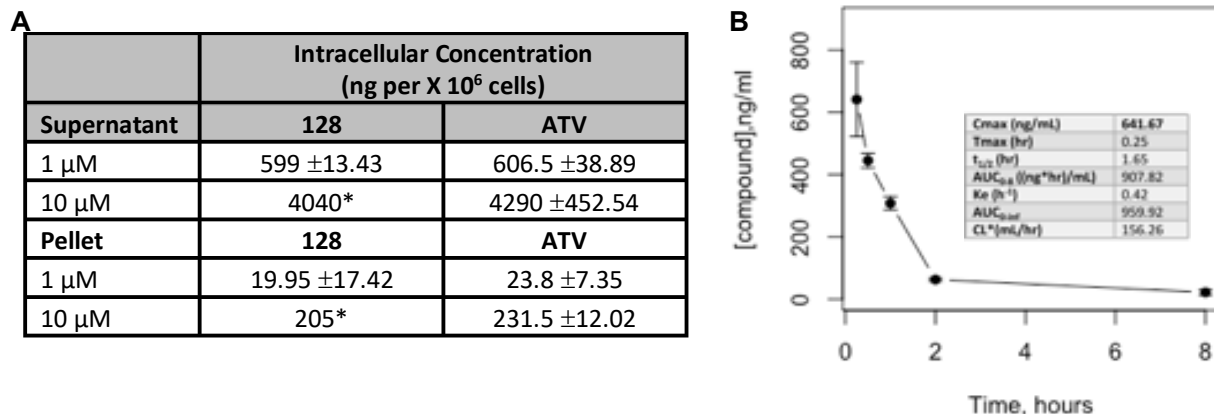


**Figure 3.24.** Evaluation of pharmacokinetic properties of **128**. Intracellular concentration of **128** and ATV (atazanavir, HIV protease inhibitor) in cytoplasm and membrane fraction in 1 X 10<sup>6</sup> CEM cells. (human lymphoblastic leukemia cell line). Data provided by Prof. Louie (USC).

outlined by Eli Lilly in their disclosure patent.<sup>30</sup> Furthermore, we looked at how pharmacological inhibition by GOAT inhibitors compared to simply re-feeding the mice. Through fast/re-fed studies that have been conducted, it has been demonstrated that acyl ghrelin levels are highest right before feeding and rapidly drop once the animal is re-fed. Unfortunately, the results of this experiment were not encouraging. When tested, we observed that administration of **3a** was on par with the pharmacological effects provided when the animals were re-fed, but administration of **128** had no effect on plasma ghrelin levels and actually showed an increase in plasma ghrelin levels compared to the vehicle control group.

While these results were discouraging, we were hopeful that we could gain *in vivo* efficacy through optimization of administration route or formulation of **128**. However, as a primarily organic chemistry team in academia, we are not experts in formulation mediums and thus sought out advice and collaboration with Professor Stan Louie at USC. Prof. Louie used **128** in a variety of experiments and compared the results to atazanavir (ATV) which is a peptidyl HIV protease inhibitor that is pharmacologically active. The results of

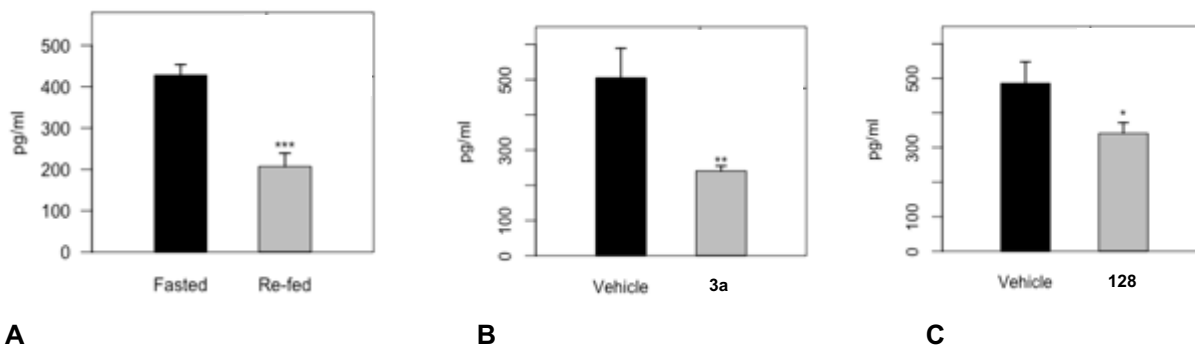


**Figure 3.25.** Regulation of mouse plasma ghrelin by food (Panel A) and through pharmacological inhibition of GOAT enzyme (Panels B and C). Panel A: Wild-type, C57BL6 male mice (20 total) were fasted overnight and in the morning, animals were divided into two groups (n=10/group). Group “Fasted” continued without food access and group “Re-fed” received regular chow diet. After 2 hours, blood was collected from retro-orbital cavity, preserved with protease inhibitors and spun down to isolate plasma. Plasma was acidified with 100 mM HCl final concentration in order to stabilize acyl-ghrelin. The levels of acyl-ghrelin were measured with commercial ELISA. Panel B: Effect of Lilly on plasma acyl-ghrelin. Male, C57BL6 mice (n=10 per group) were treated with Lilly compound prepared in vehicle solution consists of 1% hydroxyethylcellulose, 0.25% Tween 80 and 0.05% antifoam by oral gavage at 10 mg/kg per dose twice a day. After total 5 doses, animals were fasted for 5 hours to induce ghrelin secretion and blood was collected for ELISA assay of acyl-ghrelin as in panel A. Panel C: Effect of linear peptidomimetic, HD8-122 (**8**), compound on plasma acyl-ghrelin. Male, C57BL6 mice (n=10 per group) were treated with **8** prepared in vehicle solution consists of 50% propylene glycol and 30% PEG400 via s.c. injection at 60 mg/kg twice a day. After total 8 doses, animals were fasted for 5 hours and acyl-ghrelin levels were measured as in experiment in Panel A.

these studies are shown in Figure 3.24A and demonstrated that **128** had comparable cellular concentrations in both soluble and pellet fractions of CEM cells to ATV. Therefore, we decided to advance the compound further into *in vivo* studies and began with studying its plasma pharmacokinetics. As seen in Figure 3.24B, the data suggested that **128** has a systemic exposure of about 2-5 times the cellular  $EC_{50}$  (400–1000 nM or 250–650 ng/mL) in the first hour upon injection.

Using the information gained from the experimentation conducted by Prof. Louie, we re-evaluated the regulation of mouse plasma ghrelin by food, **3a**, and **128** similar to the experiment conducted previously (see Figure 3.23). For this experiment, however, we adjusted the vehicle solution used for **128**, which was derived from advice provided by Prof. Louie. Furthermore, we opted for a subcutaneous route of injection as opposed to

the intraperitoneal injection route used previously. The results of this experiment, as shown in Figure 3.25, were more encouraging. Utilizing a different formulation in addition to a different route of administration allowed us to finally observe a pharmacological effect of our compound in mice!

### 3.3.4 Discussion

The discovery of tetrapeptide **65** catalyzed an immense discovery of highly active inhibitors of GOAT. During this discovery, we not only realized the most potent compound known to date *in vitro* but also unveiled linear peptidomimetics capable of exhibiting cellular permeability in the nanomolar range. Moreover, while not as substantial as **3a**, we were able to display a favorable pharmacological effect in the reduction of plasma ghrelin levels when we administered **128** to mice *in vivo* which led to us licensing this compound to Enspire BioPharma so that further testing and development could be conducted that may one day catapult this compound onto the market.

## 3.4 Macrocyclic Peptidomimetic Inhibitors of GOAT

Despite the spectacular data afforded by **128** and having licensed it to Enspire, we continued our pursuit in generating peptidomimetic inhibitors of GOAT. Our motivation arose from the concern that **128** was primarily a straightforward peptide that could still be a liability metabolically, namely through proteolysis. The Harran laboratory has long been interested in the macrocyclization of peptides largely due to the ability of macrocyclization to overcome some of the inherent problems associated with peptides in a therapeutic context. The overarching goal that macrocyclization aims to achieve is to alter the peptidyl structure to improve pharmacokinetic properties without hampering its ability to bind its

target. In the last decade or so, peptide therapeutics have become increasingly popular. Cyclic peptides and peptidomimetics have been shown to often have improved stability and pharmacokinetic properties relative to their linear counterparts. This is due to restricted conformational freedom and protection from exo-peptidase activities. This surge toward peptide therapeutics is motivated by various factors, but the main push for peptide therapeutics is that peptides (as well as proteins) bind with exceptional specificity for their targets, which results in spectacular binding affinities with limited off-target effects. The most substantive drawback to peptide therapeutics, however, is that they suffer from various disadvantageous pharmacokinetic properties which has resulted in injection as the viable, most preferred method of delivery. Some of these limiting properties include poor metabolic stability, limited membrane permeability, poor oral bioavailability, and rapid clearance. With the goal of improving cellular activity and performance of our linear peptidomimetic compounds, we set out to generate macrocyclic peptidomimetics.

### 3.4.1. Design and Development of Macrocycles

Previously, our team had explored the potential of macrocycles back when we were working on structures derived from pyrrolidine-containing inhibitor **9**. The details of

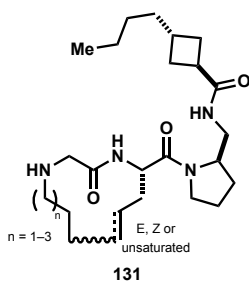


**Figure 3.26.** Macrocycles derived from pyrrolidine-containing inhibitors **9**.

this work are extensively described in the thesis of Dr. Tyler Allred.<sup>33</sup> To summarize, Dr. Allred explored the possibility of generating macrocycles *via* the stitching of an allyl glycine residue at the second position to an alkenyl fragment derived from the N-terminal amine to afford macrolactams of type **131**. These macrolactams, however, were severely impaired as GOAT inhibitors. We hypothesized that the impairment was due to the necessity for the N-terminal to be unrestricted as it is the key residue necessary for recognition by the target, GOAT. However, addition of a fourth residue (namely in **65**) provided options for alternative cyclization modes.

#### **3.4.1.1 Design and Synthesis of Macrocylic Aryl Ethers**

Incorporation of a phenyl substituent opens the door to an array of methodology that could be exploited for macrocyclization. One such methodology we sought to pursue was a photochemical reaction published by the MacMillan group of Princeton University in which they demonstrated that through the utilization of an aryl bromide, they could undergo photochemical aryl etherification using an aliphatic alcohol.<sup>34</sup> Moreover, MacMillan and co-workers demonstrated that this reaction could be applied to a protected serine derivative as shown in Figure 3.27A, demonstrating its compatibility with peptide residues.

Applying this methodology to our peptides, we began by generating aryl bromide containing hexapeptide **135** *via* SPPS. Then, employing the conditions set forth by the MacMillan group, we irradiated our compound using blue LEDs and then monitored the reaction over a period of 24 hours. Over the course of the reaction, it was apparent that there was no reaction taking place which likely arose from the overall strain energy

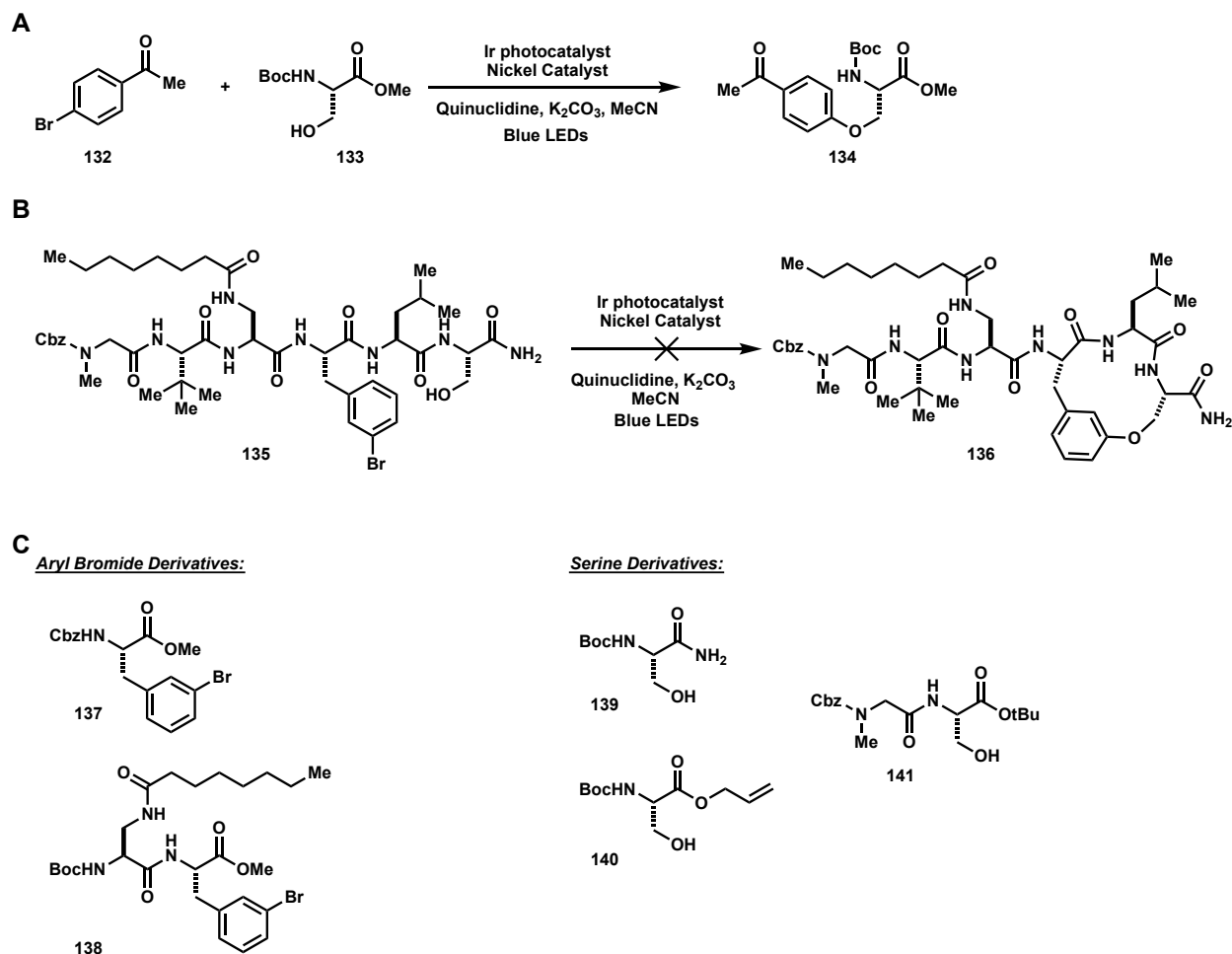


**Figure 3.27.** Aryl etherification using an iridium photocatalyst to generate macrocycles and macrocycle precursors. (A) Aryl etherification reported by MacMillan and co-workers demonstrating compatibility with amino acid residues. (B) Attempted aryl etherification using hexapeptide **135** to generate macrocycle **136**. (C) Aryl bromide (left) and serine (right) derivatives synthesized for attempted bimolecular aryl etherification.

necessary to overcome to generate the desired 13-membered macrocycle **136**. Next, we looked at performing the photoetherification intermolecularly using protected and derivatized bromo-phenylalanine residues **137** and **138** and protected and derivatized serine residues **139**, **140**, and **141** to afford aryl ethers. Unfortunately, even in the bimolecular reactions, we were not able to observe desired reactivity and obtained near complete recovery of starting materials (namely, the aryl bromides). Thus, we moved forward toward exploration of an alternative form of macrocyclic connectivity.



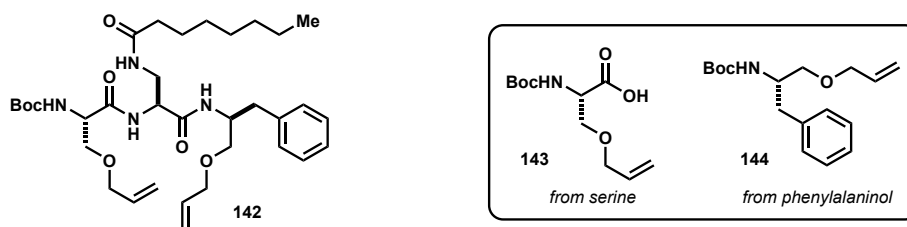
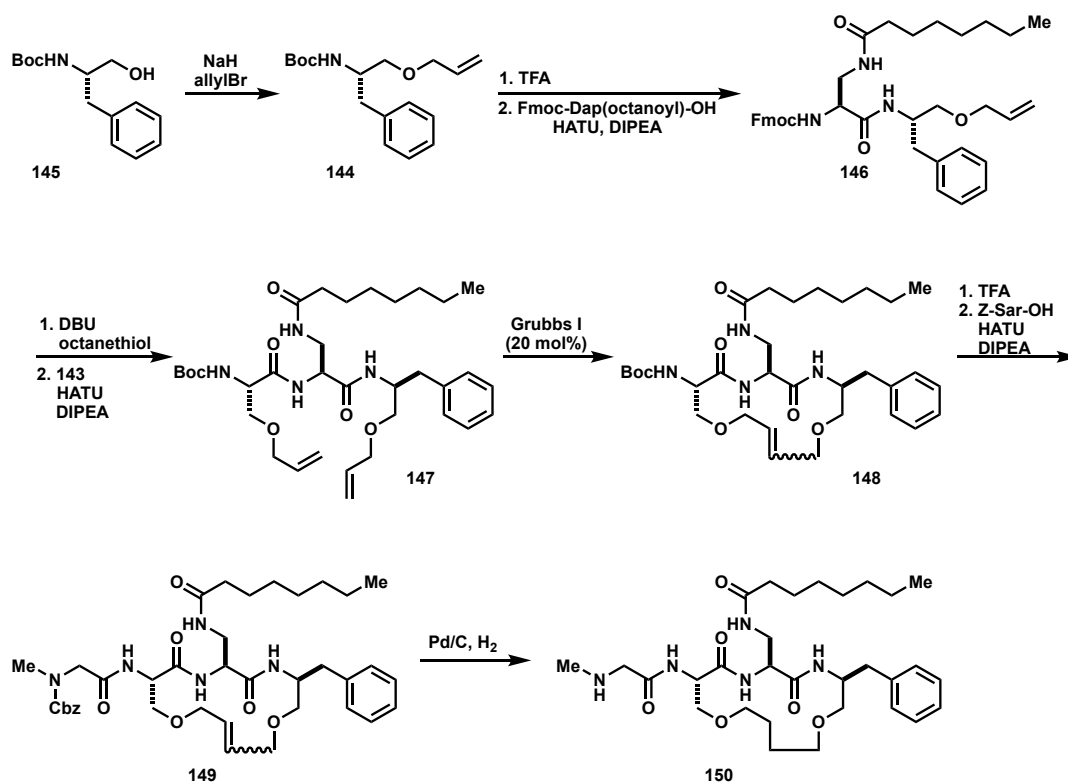


**Figure 3.28.** Ring closing metathesis precursor **142** developed from allyl-serine residue **143** and allyl-phenylalaninol residue **144** for generation of macrocyclic peptidomimetic GOAT inhibitors.

### 3.4.1.2 Design, Synthesis, and Evaluation of Alkenyl Macrocyclic Inhibitors

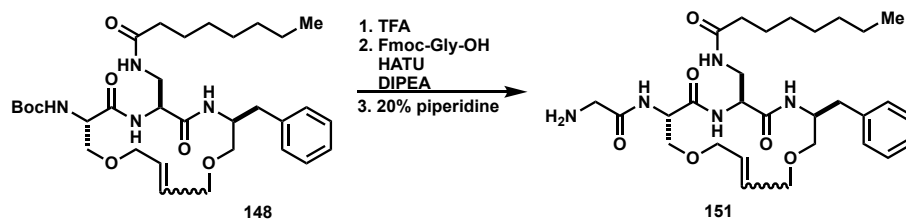
Due to the difficulty experienced trying to derivatize the phenyl substituent of phenylalanine for macrocyclization, we sought to explore alternative methods of macrocyclization. Moreover, based on the positive data obtained when the terminal carboxamide was modified or eliminated, we sought to explore possibilities around tethering the C-terminus of the linear peptides to the second residue. The most straightforward method of accomplishing these types of derivatives to allow for rapid evaluation of our hypothesis was *via* a ring closing metathesis (RCM) strategy. We envisioned that bis-allyl ether derivative **142** could undergo RCM to afford a desired macrocyclic derivative. Furthermore, we hypothesized that the ether linkages could afford cellular potency by masking polarity as they harness the potential to form transannular hydrogen bonds with the amide backbone.

Arrival at **142** required the synthesis of allyl ether derivatives **143** and **144** which could be derived from serine and phenylalaninol, respectively. Starting with Boc-phenylalaninol (**145**), the allyl ether can be formed *via* allylation using sodium hydride and allyl bromide. Following allylation, **144** can be deprotected using trifluoroacetic acid to afford the TFA salt which is then immediately subjected to a peptide coupling with an



**Scheme 3.9.** Synthesis of macrocyclic GOAT inhibitor **150**.

Fmoc-protected octanoylated Dap residue to afford peptide **146**. Removal of the Fmoc group using DBU followed by coupling with allyl-serine residue **143** afforded RCM precursor **147**. RCM using Grubbs first generation catalyst forged the desired macrocyclic linkage as a mixture of *E* and *Z* isomers which were carried forward as a mixture. The Boc group was removed under acidic conditions and then coupled with a Cbz-protected sarcosine residue to afford macrocycle **149**. Lastly, **149** undergoes Cbz deprotection under catalytic hydrogenative conditions which resulted in concurrent reduction of the alkene to afford desired macrocycle **150**. Excitingly, evaluation of **150** *in vitro* revealed that macrocyclization did not preclude the compound's ability to act as a GOAT inhibitor although the potency was no longer sub 100 nanomolar ( $IC_{50} = 253$  nM).



**Scheme 3.10.** Synthesis of alkenyl macrocyclic GOAT inhibitors utilizing an Fmoc-protected glycine residue to allow for deprotection without reduction of the olefin.

Having made the discovery that macrocyclization was seemingly well tolerated, we set out to explore additional macrocyclic derivatives capable of inhibiting GOAT with the goal of discovering an inhibitor that afforded inhibition at potencies closer in value to the linear counterparts. First, we looked at the effects of rigidifying the macrocyclic linkage by keeping the alkenyl linker intact following RCM. To do this, we simply adjusted the protecting group of the sarcosine residue utilized for the final coupling reaction. We opted to utilize an Fmoc-glycine residue for the final coupling to allow for final deprotection of the macrocycle that would not affect the alkene as shown in Scheme 3.10. Upon synthesis and evaluation of these rigidified macrocycles, we were excited to see that both the *E*- and *Z*-**151** macrocycles could inhibit GOAT with sub 100 nanomolar potencies ( $IC_{50} = 48$  and 62 nM, respectively).

Anxious to pursue these macrocycles further, we immediately began additional testing of these inhibitors and chose *E*-**151** due to its superior *in vitro* activity. Primarily

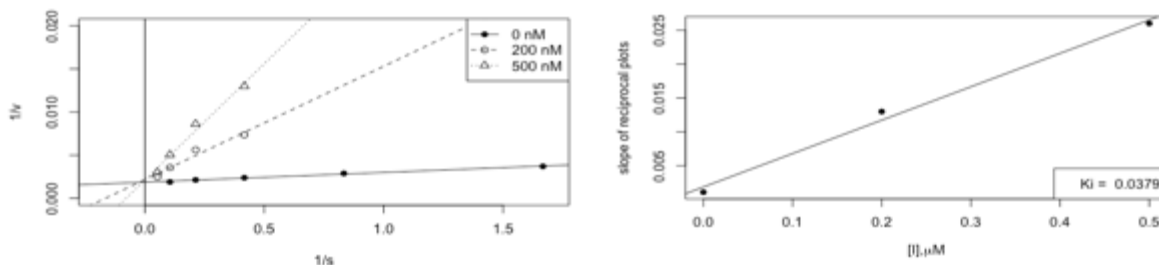


**Figure 3.29.** Macrocycle compound *E*-**151** is a substrate competitive inhibitor of GOAT. Left panel: Double reciprocal plot of GOAT enzymatic activity in presence of fixed (0, 200, and 500 nM) concentrations of *E*-**151**. Right panel: Replot of slopes from the left plot to estimate  $K_i$  (38 nM).

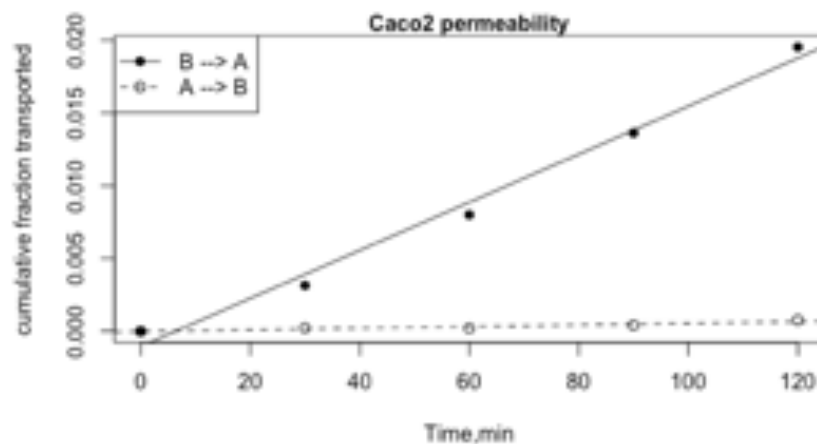
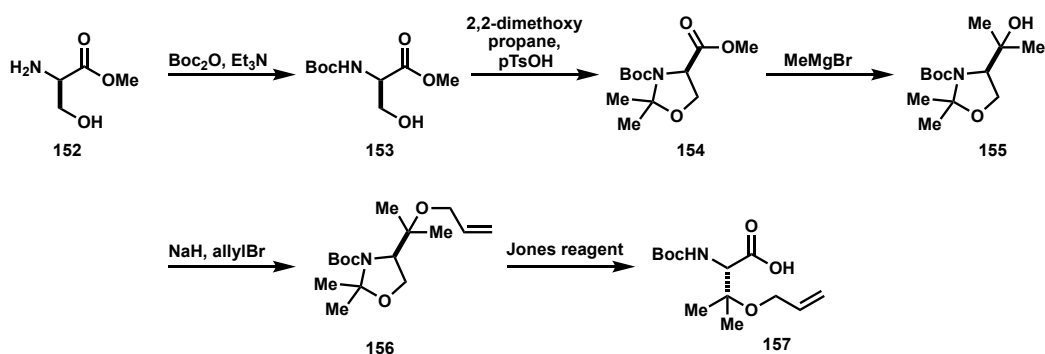


**Figure 3.30.** Caco-2 permeability of *E-151*.  $A \rightarrow B$  is passive transport across apical membrane.  $B \rightarrow A$  is a combination of passive and active transport across basolateral membrane.

due to the additional conformational complexity and bulk afforded by the macrocyclic linkage, we wanted to verify the mode of inhibition of these compounds. With the assumption that these compounds are mimicking acylated ghrelin – the product of the enzymatic reaction – these compounds might share a similar binding site with the substrate ghrelin. Based on this assumption, the  $K_m$  for substrate ghrelin was measured in the presence of fixed concentrations of *E-151* (see figure 3.29). The data fit well to a competitive mode of inhibition, showing that these compounds elicit their inhibitory effect through interaction with the ghrelin binding site either directly, or through stabilization of a conformation that prevents substrate binding in the enzyme.

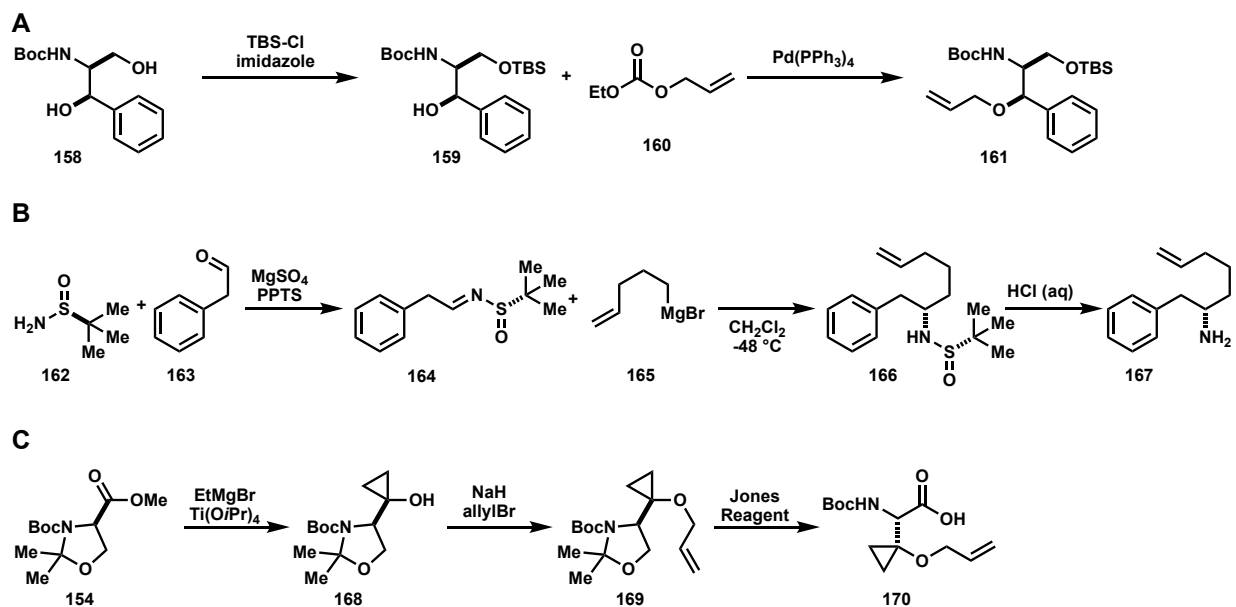
Next, we sought to evaluate the cellular efficacy of the macrocyclic inhibitors and were discouraged to see that *E-151* lacked any cellular activity. To better understand the cellular activity of these macrocycles, we worked with our long-time collaborator Dr. Noelle Williams from UTSW to study uptake and efflux of *E-151*. Notably, she discovered that *E-151* appears to be a substrate for active efflux in Caco-2 cells as seen in Figure 3.30. This is an important finding as it suggests cellular activity can be refined *via*



**Scheme 3.11.** Synthesis of geminal di-methyl allyl ether **157** to mimic P2 *tert*-leucine residue.

minimizing interactions with drug transporters (a common but routinely surmounted issue in pharma) while retaining a core pharmacophore for GOAT inhibition. Thus, we sought to generate macrocyclic inhibitors designed to optimize both parameters by varying exposed polar surface area and hydrogen bonding capabilities of the macrocyclic linkage while also displaying its peptidomimetic functionality in favorable conformations.

The first modification we sought to make was based upon findings discovered in the previous inhibitor series in which it was realized that *tert*-leucine replacement of the second serine residue afforded better stability and potency. We first looked at generation of a *tert*-leucine mimic bearing a terminal olefin poised for RCM. We turned our efforts toward generating **157** to act as a *tert*-leucine mimic. Compound **157** is unknown in the literature, but the des-allyl tertiary alcohol is<sup>35</sup>, so we generated a synthesis of **157** which is presented in Scheme 3.11. Synthesis commences with the Boc-protection of D-Ser-OMe (**152**) to afford **153**. Next, cyclization with 2,2-dimethoxypropane using catalytic pTsOH afforded oxazolidinone **154**. Compound **154** can then undergo a double Grignard addition using methyl Grignard to afford known tertiary alcohol **155**. The tertiary alcohol can then undergo allylation using allyl bromide and sodium hydride to afford our desired allyl ether derivative **156**. Finally, reaction with Jones reagent disassembles the



**Scheme 3.12.** Synthesis of alkenyl residues for incorporation into macrocycles. (A) Synthesis of allyl ether **161** that would incorporate a free hydroxymethyl moiety. (B) Synthesis of all-carbon pentenyl derivative **167** to observe effects of removing oxygenation. (C) Synthesis of cyclopropyl allyl ether **170** from common intermediate **154**.

oxazolidine and oxidizes the resultant alcohol to the carboxylic acid to afford key residue **157**. Residue **157** could then be incorporated in the general synthetic route utilized for the macrocyclic inhibitors, replacing the allyl-serine residue (**143**) in the synthetic Scheme and afford inhibitor **171** as a mixture of *E* and *Z* isomers that could be separated during final purification. We were elated to discover that installation of the *tert*-leucine mimicking residue was able to afford cellular potency to our macrocycles (Figure 3.31B)!

In addition to the *tert*-leucine mimicking macrocycles, we investigated additional derivatives sought to further improve cellular efficacy, which are shown in Scheme 3.12. As seen in the cellular data for **117** and **128**, presence of the terminal hydroxymethyl moiety afforded a substantial improvement in cellular activity over those bearing the terminal carboxamide. In an effort to achieve the best of both worlds and observe synergistic effects, we sought to generate a macrocyclic derivative that could bare the

terminal hydroxymethyl. Synthesis of this derivative was thought to arise from the successful synthesis of allyl ether **161**. Boc-protected diol **158** could undergo TBS protection at the more sterically accessible primary alcohol to afford the mono-TBS-protected alcohol **159**. Then, utilizing a Tsuji-Trost allylation, the secondary alcohol could be allylated to generate key compound **161** which could easily be elaborated to inhibitor derivative **173**. Unfortunately, compound **173** was only mildly active in our *in vitro* assay ( $IC_{50} > 500$  nM) and thus we did not pursue the compounds further for testing in our cellular assay. To further study this compound, we looked at generation of the same macrocycle lacking the hydroxymethyl moiety (**174**) and were surprised to find that potency could be restored, though still inferior to **171** and its relatives.

Next, given the difficulty synthesizing an all-carbon variant of **157**, we sought instead to synthesize an all-carbon variant of **144**. Utilizing Ellmann's auxiliary, we could rapidly generate desired alkene **167**. Phenylacetaldehyde (**163**) could undergo condensation with auxiliary **162** to generate sulfinyl imine **164**. Addition of pentenyl Grignard resulted in the generation of sulfinamide **166**. Finally, under acidic conditions, the chiral auxiliary could be released to afford amine **167** which was ready for incorporation into macrocycle synthesis to forge macrocycle **175**. While still able to act as a GOAT inhibitor ( $IC_{50} = 432$  nM), macrocycle **175** was not pursued further as it did not prove superior to previous macrocycles.

We then looked at replacement of the gem-dimethyl moiety of **171** with a cyclopropyl group which could be generated from intermediate **154** and was utilized toward the synthesis of **170**. Ester **154** could undergo a Kulinkovich reaction to afford cyclopropanol **168**. Then, using standard allylation conditions, the tertiary alcohol could

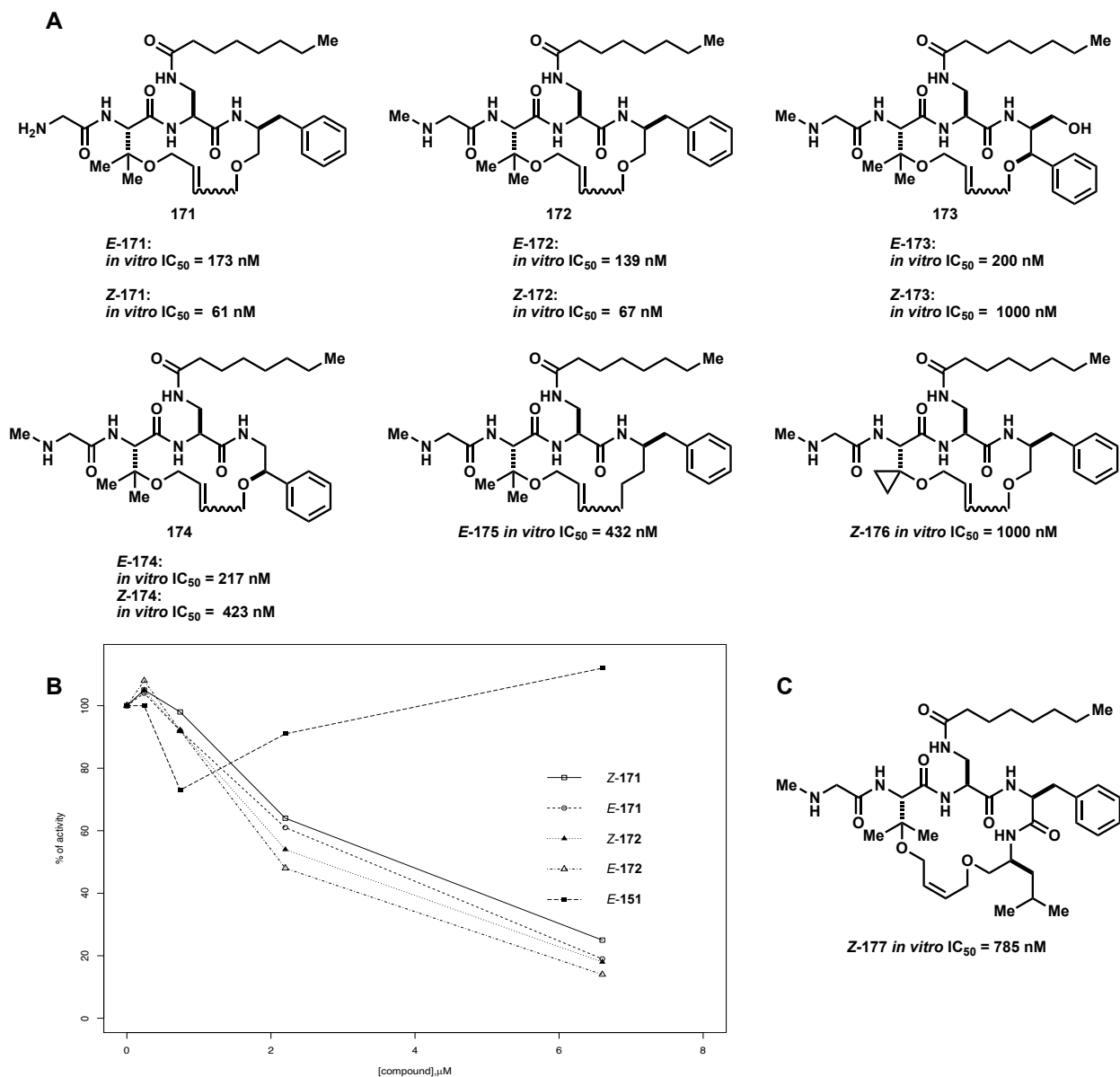


**Figure 3.31.** Modifying macrocyclic inhibitors to improve *in vitro* and cellular activity. (A) Tetrapeptidyl macrocycles varying the P2 and P4 residues. (B) Cellular activity data for compounds **171**, **172**, and *E*-151. (C) Macrocycle derived from **128**.

be allylated to afford allyl ether **169**. Finally, reaction with Jones reagent afforded the desired Boc-protected amino acid **170** that could be incorporated into macrocycle synthesis to afford **176**. Surprisingly, given the similarity of **171** and **176**, installation of the cyclopropane ring rendered the derived macrocycle inactive *in vitro*, and so we sought to examine alternate strategies for macrocycle derivatives.



Finally, we looked to capitalize on the significant cellular potency afforded by **128** and explored the generation of a macrocycle *via* linkage of an allyl ether derivative of leucinol to the allyl ether on the second residue. Similarly to the synthesis of macrocycle **171**, compound **177** could be synthesized readily following the standard macrocycle synthetic Scheme described previously. Although we were hopeful that **177** would afford a compound displaying superb *in vitro* and cellular efficacies, when it was tested *in vitro*, there was a substantial decrease in activity, resulting in an IC<sub>50</sub> of 785 nM.

### 3.4.1.3 Evaluation of Side Chain Modifications of Macrocylic Inhibitors

Modification of the macrocycle pharmacophore did not appear to provide significant improvements over **171** and thus we turned to exploration of side chain modifications. A summary of the side chain derivatives tested is shown in Figure 3.32. Most of the side chain modifications we made were based upon side chain modifications utilized in previous peptidomimetic series. Given the likely changed conformation of the macrocycles from their linear counterparts, we envisioned that the side chain could be binding in a slightly different manner and thus modifications in the side chain would

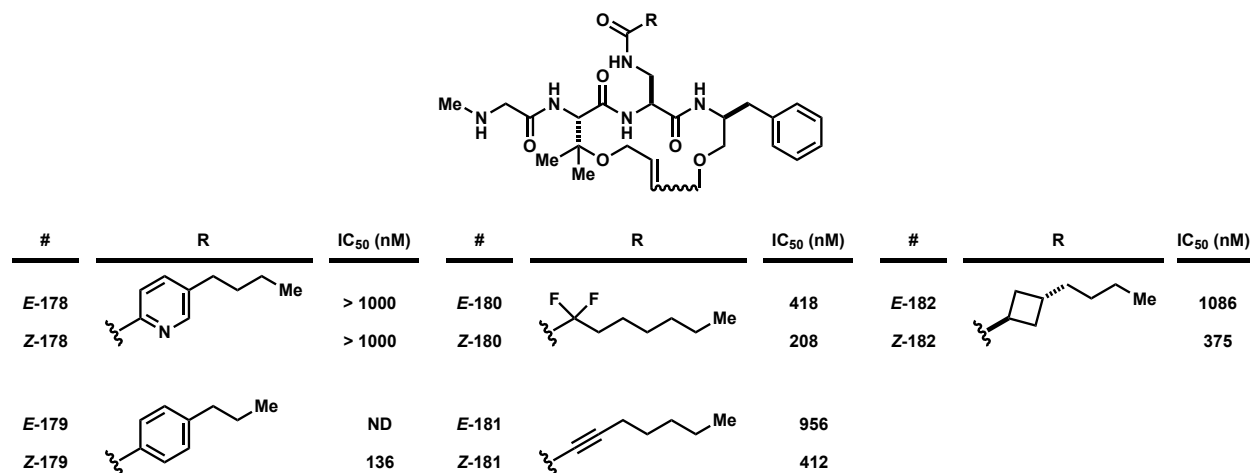


**Figure 3.32.** Evaluation of modifications to the side chain of macrocyclic GOAT inhibitors.

harness the potential to interact more effectively. As the data shows, modifications of the side chain were tolerated with the Z isomer consistently displaying better efficacy. We then looked at what effects the side chain modifications had on the cellular activity of the macrocycles and found that modifications appeared to significantly diminish cellular activity with most macrocycles failing to reach an EC<sub>50</sub> even at concentrations of 6.6 μM.

### 3.5 Conclusion

The development of peptidomimetic inhibitors provides an exciting pathway for the selective inhibition of GOAT ideal for studying the ghrelin pathway in greater detail. Through various SAR campaigns, pentapeptide **5** had been transformed to pyrrolidine-containing small molecule lead **9** and through further optimizations and modifications, **5** has been converted to a modified variant **128** and further into macrocyclic inhibitor **171**, which both display favorable *in vitro* activity and excellent to moderate cellular activity. However, as was a concern with **5**, these structures remain largely peptidyl in nature, which means that they are still highly polar compounds that can suffer immensely from chemical and physical instabilities. While **171** is thought to possess less metabolic liability, the lack of desirable pharmacokinetic properties has led us to halt progress on this class of inhibitors. This does not indicate an execution or extinction of peptidomimetic inhibitors as there are technologies that can be further pursued that would enable these compounds to come to fruition as therapeutics. Furthermore, peptidomimetics are paramount to the study of the role of the ghrelin pathway and will remain of utmost importance for biochemical studies of this nature. Until such time when the limitations associated with

these peptidomimetic inhibitors can be overcome, investigations and developments of other inhibitor classes as therapeutics will remain at the forefront of research efforts.

### 3.6 References

- (1) Darling, J. E.; Zhao, F.; Loftus, R. J.; Patton, L. M.; Gibbs, R. A.; Hougland, J. L. Structure-Activity Analysis of Human Ghrelin O-Acyltransferase Reveals Chemical Determinants of Ghrelin Selectivity and Acyl Group Recognition. *Biochemistry* **2015**, *54* (4), 1100–1110.
- (2) Yang, J.; Brown, M. S.; Liang, G.; Grishin, N. V.; Goldstein, J. L. Identification of the Acyltransferase That Octanoylates Ghrelin, an Appetite-Stimulating Peptide Hormone. *Cell* **2008**, *132* (3), 387–396.
- (3) Yang, J.; Zhao, T. J.; Goldstein, J. L.; Brown, M. S. Inhibition of Ghrelin O-Acyltransferase (GOAT) by Octanoylated Pentapeptides. *Proc. Natl. Acad. Sci. U. S. A.* **2008**, *105* (31), 10750–10755.
- (4) Zhao, F.; Darling, J. E.; Gibbs, R. A.; Hougland, J. L. A New Class of Ghrelin O-Acyltransferase Inhibitors Incorporating Triazole-Linked Lipid Mimetic Groups. *Bioorganic Med. Chem. Lett.* **2015**, *25* (14), 2800–2803.
- (5) Hougland, J. L. Inhibitors targeting human ghrelin O-acyltransferase. US 20150018520 A1. 2015 May 17.
- (6) Garner, A. L.; Janda, K. D. Cat-ELCCA: A Robust Method to Monitor the Fatty Acid Acyltransferase Activity of Ghrelin O-Acyltransferase (GOAT). *Angew. Chemie - Int. Ed.* **2010**, *49* (50), 9630–9634.
- (7) Garner, A. L.; Janda, K. D. A Small Molecule Antagonist of Ghrelin O-Acyltransferase (GOAT). *Chem. Commun.* **2011**, *47* (26), 7512–7514.
- (8) Cole, P. A.; Barnett, B. P.; Hwang, Y.; Boeke, J. D. Methods for Synthesis and Uses of Inhibitors of Ghrelin O-Acyltransferase as Potential Therapeutic Agents for Obesity and Diabetes. US 8772229B2. 8 April 2010.
- (9) Barnett, B. P.; Hwang, Y.; Taylor, M. S.; Kirchner, H.; Pfluger, P. T.; Bernard, V.; Lin, Y. Y.; Bowers, E. M.; Mukherjee, C.; Song, W. J.; Longo, P. A.; Leahy, D. J.; Hussain, M. A.; Tschöp, M. H.; Boeke, J. D.; Cole, P. A. Glucose and Weight Control in Mice with a Designed Ghrelin O-Acyltransferase Inhibitor. *Science (80-. )*. **2010**, *330* (6011), 1689–1692.
- (10) Frankel, A. D.; Pabo, C. O. Cellular Uptake of the Tat Protein from Human Immunodeficiency Virus. *Cell* **1988**, *55* (6), 1189–1193.

- (11) HARRAN, P. G. .; HOLLIBAUGH, R. A. .; LIU, H. Small lipopeptidomimetic inhibitors of ghrelin O-acyl transferase. WO 2016044467 A1. 2016 Mar 24.
- (12) Hollibaugh, R. A. Defining a Minimal Pharmacophore to Selectively Inhibit MBOAT4 (Ghrelin O-Acyl Transferase) - ProQuest, University of California, Los Angeles, Los Angeles, 2016.
- (13) Cabrele, C.; Martinek, T. A.; Reiser, O.; Berlicki, Ł. Peptides Containing  $\beta$ -Amino Acid Patterns: Challenges and Successes in Medicinal Chemistry. *J. Med. Chem.* **2014**, pp 9718–9739.
- (14) Horne, W. S. Peptide and Peptoid Foldamers in Medicinal Chemistry. *Expert Opin Drug Discov.* **2011**, pp 1247–1262.
- (15) Koyack, M. J.; Cheng, R. P. Design and Synthesis of Beta-Peptides with Biological Activity. *Methods Mol Biol* **2006**, pp 95–109.
- (16) Goodman, C. M.; Choi, S.; Shandler, S.; DeGrado, W. F. Foldamers as Versatile Frameworks for the Design and Evolution of Function. *Nature Chem. Biol.* **2007**, pp 252–262.
- (17) Cheng, R. P.; Gellman, S. H.; DeGrado, W. F.  $\beta$ -Peptides: From Structure to Function. *Chem. Rev.* **2001**, pp 3219–3232.
- (18) Hsiao, Y.; Rivera, N. R.; Rosner, T.; Krska, S. W.; Njolito, E.; Wang, F.; Sun, Y.; Armstrong, J. D.; Grabowski, E. J. J.; Tillyer, R. D.; Spindler, F.; Malan, C. Highly Efficient Synthesis of  $\beta$ -Amino Acid Derivatives via Asymmetric Hydrogenation of Unprotected Enamines. *J. Am. Chem. Soc.* **2004**, 126 (32), 9918–9919.
- (19) Hansen, K. B.; Rosner, T.; Kubryk, M.; Dormer, P. G.; Armstrong, J. D. Detection and Elimination of Product Inhibition from the Asymmetric Catalytic Hydrogenation of Enamines. *Org. Lett.* **2005**, 7 (22), 4935–4938.
- (20) Escudero-Casao, M.; Juaristi, E. Asymmetric Synthesis of  $\beta^2$ -Homo- *Tert*-Leucine via Radical Addition to Enantiopure *N*-Fumaroylhexahydrobenzooxazolidin-2-One. *Helv. Chim. Acta* **2012**, 95 (10), 1714–1722.
- (21) Evans, D. A.; Britton, T. C.; Ellman, J. A.; Dorow, R. L. The Asymmetric Synthesis of  $\alpha$ -Amino Acids. Electrophilic Azidation of Chiral Imide Enolates, a Practical Approach to the Synthesis of (r)- and (s')- $\alpha$ -Azido Carboxylic Acids. *J. Am. Chem. Soc.* **1990**, 112 (10), 4011–4030.
- (22) English, M. L.; Stammer, C. H. D-Ala<sup>2</sup>,  $\Delta$ zPhe<sup>4</sup>-Methionine Enkephalin Amide, a Dehydropeptide Hormone. *Biochem. Biophys. Res. Commun.* **1978**, 85 (2), 780–782.

- (23) Shimohigashi, Y.; Stammer, C. H. Dehydro-Enkephalins. Part 7. A Potent Dehydroleucine-Enkephalin Resistant to Carboxypeptidase. *J. Chem. Soc. Perkin Trans. 1* **1983**, 803–808.
- (24) Shimohigashi, Y.; Chen, H. C.; Stammer, C. H. The Enzyme Stability of Dehydro-Enkephalins. *Peptides* **1982**, 3 (6), 985–987.
- (25) English, M. L.; Stammer, C. H. The Enzyme Stability of Dehydropeptides. *Biochem. Biophys. Res. Commun.* **1978**, 83 (4), 1464–1467.
- (26) Jalan, A.; Kastner, D. W.; Webber, K. G. I.; Smith, M. S.; Price, J. L.; Castle, S. L. Bulky Dehydroamino Acids Enhance Proteolytic Stability and Folding in  $\beta$ -Hairpin Peptides. *Org. Lett.* **2017**, 19 (19), 5190–5193.
- (27) Enders, D.; Chen, Z. X.; Raabe, G. Stereoselective Synthesis of 3-Substituted Ethyl (Z)-4,4,4-Trifluoro-2-Formylamino-2-Butenoates. *Synthesis*. **2005**, 2005 (2), 306–310.
- (28) Chenard, B.; Gallaschun, R. Substituted Xanthenes and Methods of Use Thereof. WO2014143799A4. 14 Mar 2014.
- (29) King, S. A. Orthoester-Dependent Alcoholysis of Lactones. Facile Preparation of 4-Alkoxybutanoates and 5-Alkoxy-pentanoates. *J. Org. Chem* **1994**, pp 2253–2256.
- (30) GALKA, C. S.; HEMBRE, E. J.; HONIGSCHMIDT, N. A.; KEDING, S. J.; MARTINEZ-GRAU, M. A.; PLAZA, G. R.; RUBIO, A.; SMITH, D. L. Ghrelin O-Acyl Transferase Inhibitors. WO2016168225 A1. 2016 Oct 20.
- (31) Alexander, R.; Balasundaram, A.; Batchelor, M.; Brookings, D.; Crépy, K.; Crabbe, T.; Deltent, M. F.; Driessens, F.; Gill, A.; Harris, S.; Hutchinson, G.; Kulisa, C.; Merriman, M.; Mistry, P.; Parton, T.; Turner, J.; Whitcombe, I.; Wright, S. 4-(1,3-Thiazol-2-Yl)Morpholine Derivatives as Inhibitors of Phosphoinositide 3-Kinase. *Bioorganic Med. Chem. Lett.* **2008**, 18 (15), 4316–4320.
- (32) Hoenke, C.; Bouyssou, T.; Tautermann, C. S.; Rudolf, K.; Schnapp, A.; Konetzki, I. Use of 5-Hydroxy-4H-Benzo[1,4]Oxazin-3-Ones as B2-Adrenoceptor Agonists. *Bioorganic Med. Chem. Lett.* **2009**, 19 (23), 6640–6644.
- (33) Allred, T. K. Synthetic Studies on the Marineosins and Other Related Complex Prodiginines, University of California, Los Angeles, California, 2018.
- (34) Terrett, J. A.; Cuthbertson, J. D.; Shurtleff, V. W.; MacMillan, D. W. C. Switching on Elusive Organometallic Mechanisms with Photoredox Catalysis. *Nature* **2015**, 524 (7565), 330–334.
- (35) Avenozza, A.; Busto, J. H.; Cativiela, C.; Peregrina, J. M.; Sucunza, D.; Zurbano, M.

M. Synthesis of Enantiopure (AMe)Dip and Other  $\alpha$ -Methylated  $\beta$ -Branched Amino Acid Derivatives. *Tetrahedron Asymmetry* **2003**, 14 (3), 399–405.

## 4. Chapter Four – Design and Development of Small Molecule Heterocyclic Inhibitors of GOAT

*Emily Murzinski, Hui Ding, and Patrick Harran*

### 4.1 Introduction

Prior to 2016, it was known the pharmaceutical sector was pursuing GOAT inhibitors, but the results of these efforts remained largely unpublished. Academic research on inhibitors focused largely on peptidomimetics and their utility in elucidating aspects of GOAT enzymology. In time, however, GOAT inhibitors discovered *via* high throughput screening in industry began appearing in patent applications. These compounds were not substrate inspired peptidyl species, but rather more conventional drug-like heterocyclic substances. These better conform to the traditional parameters of drug discovery – namely conforming to Lipinski's<sup>1</sup> rule of five used to anticipate oral bioavailability.

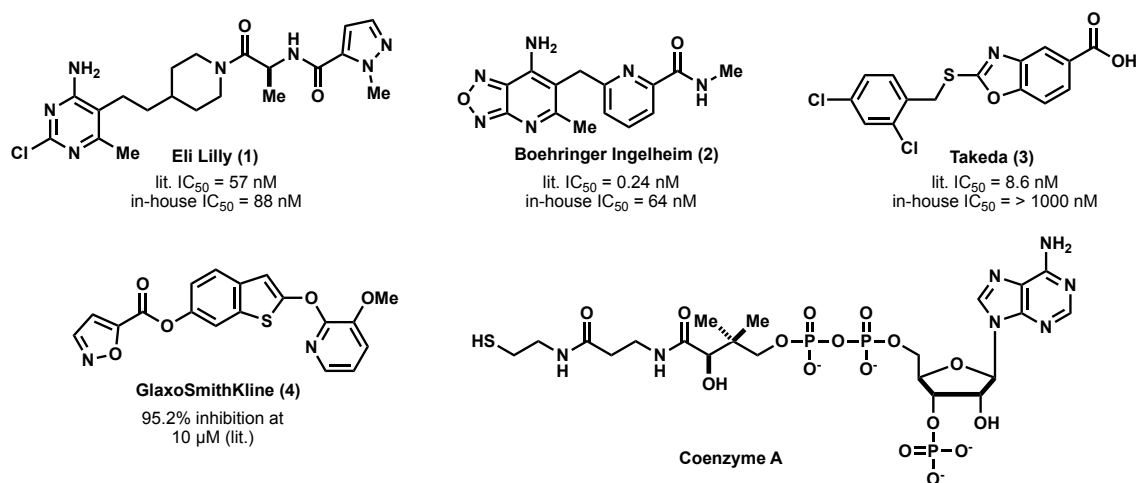


**Figure 4.1.** Reported small molecule heterocyclic GOAT inhibitors reported by pharmaceutical companies and structure of Coenzyme A.

Given that these new structures were markedly different from the native ghrelin sequence, we began to question the mode of action of these compounds. Through competition experiments with the representative Eli Lilly<sup>2</sup> compound (1), we found that this compound was not directly competitive to ghrelin, and thus is likely acting as a noncompetitive inhibitor. As GOAT has two binding sites within its active site – the ghrelin binding site and the coenzyme A binding (CoA) site – we hypothesized that these inhibitors were likely primarily acting at the CoA site. This binding modality is likely arising *via* mimicry of the adenine base within CoA. Furthermore, in 2018 Takeda Pharmaceuticals published on a series of GOAT inhibitors in which they were able to demonstrate experimentally that their compounds were competitive to coenzyme A.<sup>3</sup> Due to this alternative mechanism of inhibition, compounds of structures similar to those presented in Figure 4.1 could be problematic as about 4% of cellular enzymes utilize CoA as a substrate, imparting the ability of these compounds to suffer from potential off-target effects.

Despite the concern for off-target activity of this class of compounds, we remained highly interested in their properties and activities. Inhibitors developed by Boehringer Ingelheim<sup>4</sup> (represented by compound 2) were reported to have picomolar efficacies in cellular assays and researchers at Eli Lilly were able to demonstrate promising data in mouse with their compounds. Eli Lilly demonstrated that their compounds (represented

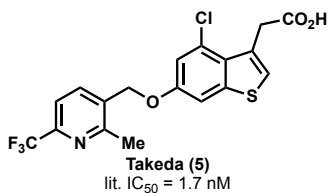


**Figure 4.2.** Benzothiophene GOAT inhibitor developed by Takeda.



by compound **1**) not only possessed the ability to reduce acyl ghrelin levels in mice but also reduce food intake in mice when compared to control.<sup>2</sup> Furthermore, Takeda showed that benzothiophene **5** could reduce circulating acyl-ghrelin levels without affecting the amount of circulating ghrelin.<sup>3</sup> Interestingly, when related compound **3** (also developed by Takeda) was tested in our *in vitro* and cellular assays, we observed no inhibitory activity. With structures similar to **5**, GlaxoSmithKline (GSK) disclosed series of GOAT inhibitors bearing the same benzothiophene acetic acid core but with an incorporated functionalized bicyclic pyridocyclopentyl ether demonstrated by compound **4**.<sup>5</sup> The modifications made by GSK appear to offer inhibitory improvement over the compounds generated by Takeda, with most of their compounds demonstrating *in vitro* efficacies below 50 nM. Moreover, GSK was able to demonstrate *in vivo* effects with their compounds, demonstrating effect in mice, rats, and cynomolgus monkeys at doses of 10 mg/kg.

The results that are actively being disclosed by pharmaceutical companies are very encouraging and exciting to us. Having not yet obtained desirable *in vivo* results for compounds represented in our various peptidomimetic series (see chapter 3), we envisioned development of a small molecule heterocyclic GOAT inhibitor bearing resemblance to those presented by the pharmaceutical industries. Our hypothesis was that hybridization of compounds presented in Figure 4.1 could afford the *in vivo* efficacy we were searching for while retaining the spectacular *in vitro* and cellular activities.

## **4.2 Hypothesis Driven Design and Development of Small Molecule Heterocyclic Inhibitors**

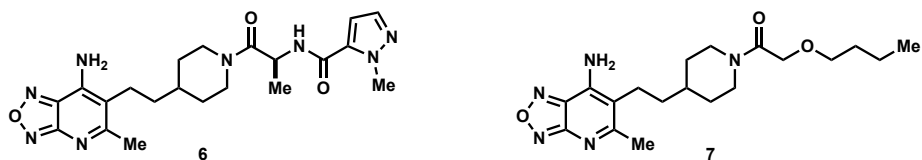
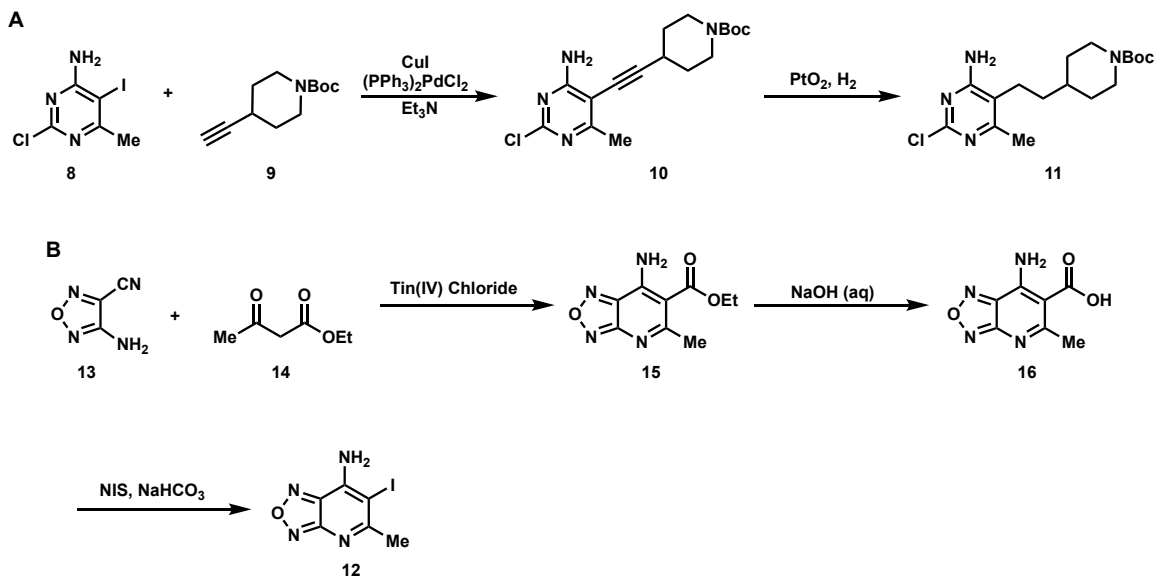


**Figure 4.3.** Small molecule heterocyclic GOAT inhibitor designed to be a hybrid of **1** and **2** with incorporation of a pseudo-octanoyl tail for generation of **7**.

During the course of our research into inhibitors, we had synthesized and tested compounds **1** (Eli Lilly) and **2** (Boehringer Ingelheim) most extensively. Given their favorable *in vitro* and cellular activities (INS-1  $IC_{50}$  = 670 nM and 540 nM for **1** and **2**, respectively), we sought to develop a compound that merged these two structures. Our hope was that this new compound would possess the same desirable inhibitory effects *in vitro* and *in cellulo* and furthermore, *in vivo*. Thus, we designed compounds **6** and **7** which incorporate the oxadiazolopyridine of **2** as the adenine mimic that would engage the CoA binding site. The oxadiazolopyridine portion would then be tethered to the piperidinyll moiety of **1** utilizing an ethylene linkage. For compound **6**, alanine and methyl-pyrazole could be incorporated to represent a true hybrid of **1** and **2**. To accomplish **7**, the piperidine moiety would then be coupled to an octanoyl chain mimetic that was heavily utilized in our peptidomimetic inhibitors.

#### 4.2.1 Synthesis and Evaluation of Our First Small Molecule Heterocyclic Hybrid Inhibitor

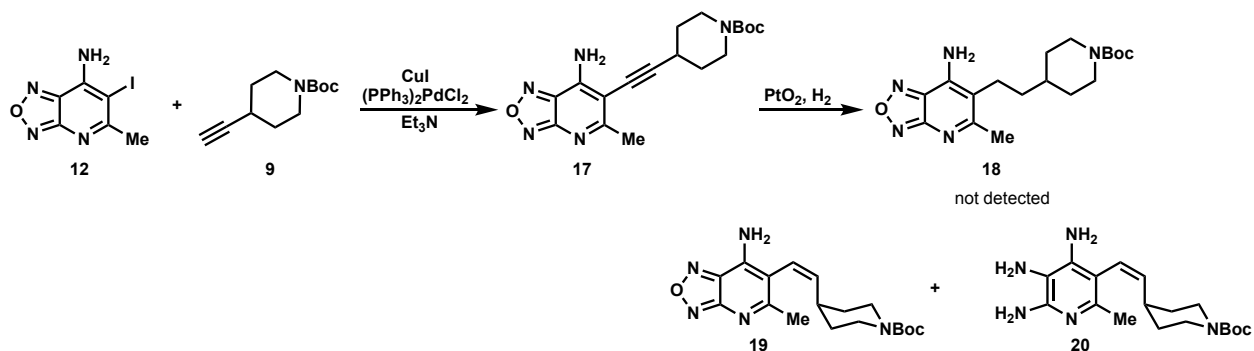
To synthesize compounds of this nature, we sought to simply merge the two synthetic routes utilized to synthesize **1** and **2**, focusing on generating the linkage of the oxadiazolopyridine moiety to the piperidine ring. During analysis of the two synthetic routes for accessing **1** and **2**, we were able to realize a key connection point. As shown



**Scheme 4.1.** Partial syntheses of compound **1** (A) and **2** (B) for design of the synthetic route to **6** and **7**.

in Scheme 4.1, the linkage of the pyrimidine ring of **1** to the desired piperidine ring could be forged *via* a Sonogashira coupling of aryl iodide **8** and alkynyl piperidine **9**. Subsequent catalytic hydrogenation using Adams catalyst ( $\text{PtO}_2$ ) could fully reduce the alkyne (**10**) to the alkane to afford the desired compound **11**. In the synthesis of compounds structurally related to **2**, aryl iodide **12** could be readily generated. As reported by BI, synthesis of **12** could be carried out in a relatively simplistic manner starting with oxadiazole **13**. Annulation of **13** with ethyl acetoacetate (**14**) could afford the aryl ester **15**. Then, the ester could be saponified to afford free acid **16** which could undergo a modified Hunsdiecker reaction to afford our desired aryl iodide **12**.

Employing this reactivity, we synthesized aryl iodide **12** which then underwent a Sonogashira coupling with alkynyl piperidine **9** to generate **17** utilizing the same reaction conditions carried out in the synthesis of **10**. We were pleased to see that the cross-coupling could be effectively carried out even with the more elaborate aryl iodide **12**. Next, we needed to reduce the alkyne to the alkane and proceeded to do so *via* catalytic

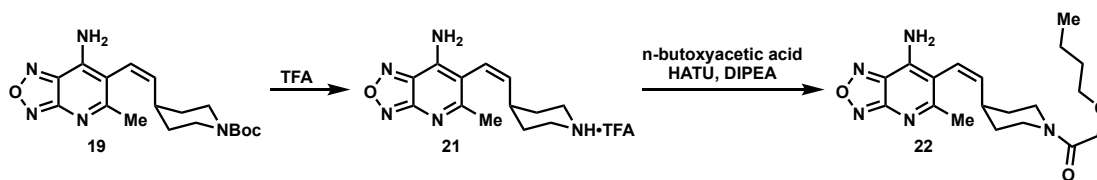


**Scheme 4.2.** Stitching together key fragments **12** and **9** to afford desired hybrid inhibitors.

hydrogenation with Adams catalyst. Expecting to see the same desired reactivity as before, we were surprised when we obtained no desired alkane product **18**, nor could we detect it *via* mass analysis of the reaction mixture. Instead, what we were observing was primarily partial reduction of the alkyne to *cis*-alkene **19** as well as a compound with a mass consistent with oxadiazole N–O bond reduction represented by structure **20**.

In our attempts to saturate the alkyne, we consistently saw conversion of starting material, but most reactions halted at the *cis*-alkene and, if pushed further, cleaved the N–O bonds of the oxadiazole. This setback allowed for the opportunity to explore other methods of saturating the bond. The first variation we made was to employ a different catalyst system in the hydrogenation reaction. We tested Lindlar's catalyst, Raney nickel, and Wilkinson's catalyst and largely saw N–O reduction products. We then turned to investigating various palladium catalysts and the only hint of success arose from a combination approach wherein we first performed the hydrogenation with Pearlmann's catalyst and then resubjected the material to hydrogenation using palladium on carbon. However, this result was not reliably reproducible and attempts to observe the same reactivity were met with primarily production of **19**. Upon observing that catalytic hydrogenation methods were not able to provide the desired material, the next approach

aimed to observe the effects of stoichiometric methods. We chose to use diimide which is known to reduce alkynes to alkanes.<sup>6</sup> However, this method was unsuccessful and did not afford any reduction product. Finally, we attempted to carry out a Suzuki-Miyaura cross-coupling by generating an alkyl boron derivative of **9** using 9-BBN that could be coupled with **12** but no desired product could be detected from these reaction attempts either.



**Scheme 4.3.** Synthesis of alkenyl hybrid inhibitor **22**.

Through examination of various methods for reducing the alkyne, it became apparent to us that the oxadiazolopyridine moiety was too labile and would continue to hinder our efforts. Thus, we decided to move forward with the synthesis and carry forth the *cis* alkene through the remainder of the synthesis as shown in Scheme 4.3. To this end, alkene **19** was deprotected to afford **21** as the TFA salt which was then coupled to n-butoxyacetic acid utilizing standard coupling methods to afford final compound **22**. Although we were concerned with the metabolic liabilities that often times are attributed to the presence of *cis*-alkenes in drug development, we were eager to test our hypothesis of generating these hybrid molecules.

Evaluation of **22** commenced with observation of its *in vitro* activity. Upon *in vitro* testing, we were pleased to see that these hybrid inhibitors still retained GOAT inhibitory activity, affording an IC<sub>50</sub> value of 303 nM. Although the potency was 3–5 times less potent than **1** and **2**, we were still excited because we hypothesized that we could refine and

modify the structure more to improve the *in vitro* efficacy. After evaluation *in vitro*, we turned to cellular evaluation of **22** and found that this compound was amongst one of the most potent cellular compounds to date with an INS-1 cellular IC<sub>50</sub> of 600 nM! In all evaluations of cellular activity, **22** outperformed **1** and was on par with the activity of **2**. However, if we wanted to compete with **2**, we needed to find a way to improve the *in vitro* activity of the compounds, which could additionally afford improved cellular activities.

#### 4.2.2 Design and Evaluation of Derivatives of **22** to Improve Activity

Toward improvement of the *in vitro* activity of compound **22**, we looked primarily at the role of the alkene in addition to the role of the oxadiazolopyridine moiety. Shown in Figure 4.4 is a summary of the various derivatives we synthesized and evaluated for determination of where improvements could be introduced. The first modification we looked at was the transformation of the *cis*-alkene to the *trans*-alkene (**23**), which could be accomplished *via* photoisomerization. Excitingly, this transformation resulted in an

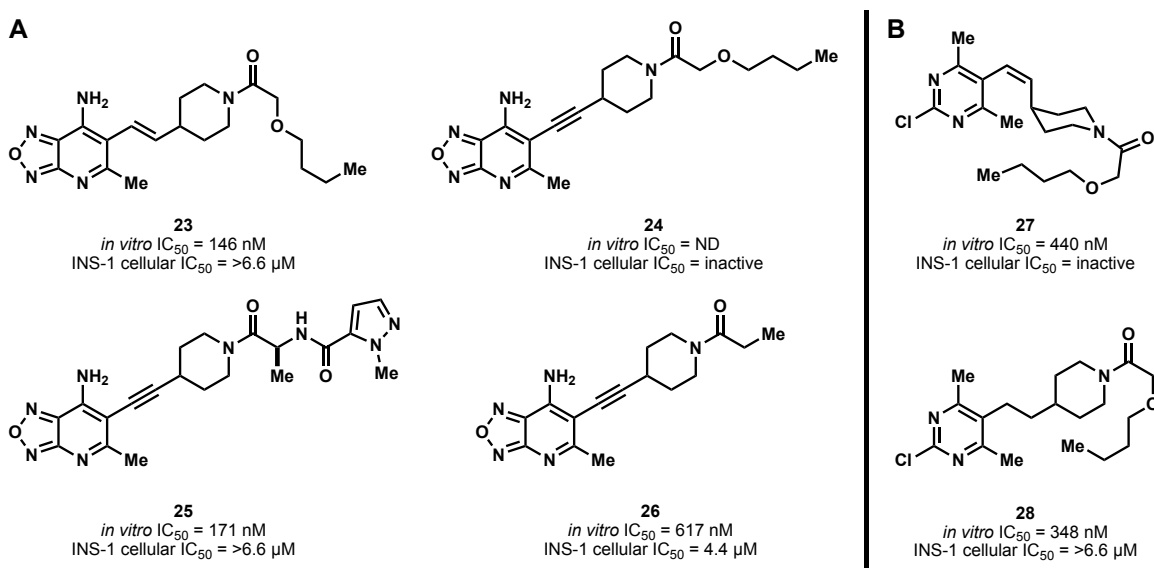


**Figure 4.4.** Evaluation of derivatives of **22** for improved activity. (A) Modifications to the alkene and the side chain. (B) Substitution of the oxadiazolopyridine with the pyrimidine of **1**.

inhibitor with two times better *in vitro* potency ( $IC_{50} = 146 \text{ nM}$ )! However, when we moved forward with cellular evaluation of **23**, we found that had a cellular efficacy greater than  $6.6 \mu\text{M}$  which was not desirable for further inhibitor progression.

Next, given the difficulties surrounding the reduction of the alkyne, we looked at the effect of leaving the alkyne intact in addition to modifying the side chain. Simply leaving the alkyne intact, as shown for compound **24**, afforded no benefit to activity, rendering the compound completely inactive in our cellular assay. However, if we modified the side chain to either be the corresponding propylamide (**26**) or the fully expanded hybrid *via* incorporation of the alanine and pyrazole moieties from **1** to generate **25**, we could restore some cellular activity. Additionally, **25** and **26** displayed respectable *in vitro* activities with **25** outperforming **22**.

Finally, we looked at the results of replacing the oxadiazolopyridine moiety of **2** with the pyrimidine moiety of **1** while still incorporating the butoxyacetamide side chain. To this end, we developed alkenyl compound **27** and the fully saturated compound **28**. Interestingly, while the *in vitro* potencies were on par with **22**, the cellular activity suffered immensely. The closely related derivative **27** was completely inactive in the cellular assay while the fully saturated **28** displayed an efficacy slightly above  $6.6 \mu\text{M}$ .

Consistent with our peptidomimetic series of inhibitors, we were interested in evaluating the effects of modifying the side chain of **22**. Given that these compounds were likely now binding in a different space within the active site, alteration of the side chain could harness the potential to impart a significant change in binding and activity. Unlike the values discovered from modifying the heterocycles and linker, modifications to the side chain were very well tolerated. The first substitution we made was to replace the

#	R	<i>in vitro</i> IC <sub>50</sub> (nM)	INS-1 cellular IC <sub>50</sub> (nM)
22		303	600
29		652	220
30		ND	750
31		ND	1520
32		ND	750

**Figure 4.5.** Evaluation of side chain modifications.

butoxyacetamide with the native octanoyl chain (**29**) and experienced a two times loss in *in vitro* potency but gained a substantial (nearly 3x) increase in cellular efficacy! While we did not evaluate the *in vitro* potencies of the further side chain modified derivatives, we evaluated their cellular potencies and were pleased to find that they largely retained the cellular efficacy of the parent compound **22**. Pleased with the results we obtained for both **22** and **29**, we sought to scale up the syntheses of these two compounds in order to supply material for further testing.

### 4.3 Scale Up and Evaluation of Small Molecule Heterocyclic Inhibitors

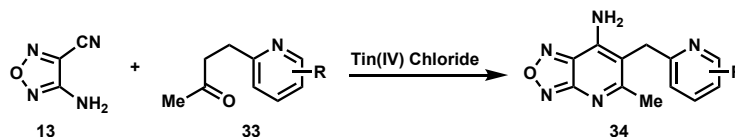
In order to carry forward with evaluation of **22** and **29**, we had to scale up the synthesis of key intermediate **19**. Throughout our studies of methods to reduce the alkyne, we settled upon utilizing 20 mol% Pearlmann's catalyst under a hydrogen



atmosphere to afford the desired alkene **19** which afforded only minimal production of **20** when short reaction times were used. Upon scale up of this transformation, while monitoring the reaction *via* LCMS, an additional small peak was observed in the UV trace that corresponded to the mass of **19** + 2 m/z. This peak had not been observed previously, though we speculated that it could be our desired alkane **18** that we consistently struggled to obtain. At this stage of the synthesis, the two compounds were not easily separable. Therefore, we carried the mixture of **19** and what we presumed to be **18** through the final two synthetic steps (Boc deprotection and final coupling). Through HPLC purification, we were able to isolate both **22** and the M + 2 peak and analyze them separately *via* NMR. Upon evaluation of the NMR of this secondary peak, we were able to ascertain that the M + 2 peak did indeed correspond to our previously desired alkane product **7**!

Eager to evaluate the inhibitory properties of **7**, we immediately set out to test it in both our *in vitro* and cellular assays. When tested *in vitro*, we were elated to discover that its potency had a nearly five-time improvement in activity over **22** with an *in vitro* IC<sub>50</sub> of just 63 nM! Not only was this compound significantly improved over **22** but also was superior to **1** and on par with the activity of **2**. Previously, such as with compound **23**, we could gain potency *in vitro* but had struggled to improve the cellular potency as well, so we set out to evaluate its potency in our INS-1 cellular assay. Gratefully, we observed that when tested in cells, **7** could exhibit a potency of just 240 nM, which was significantly better than either **1**, **2**, and **22**!

With this newly found data, we decided to pursue **7** as a lead inhibitor and desired to test it further. However, in its current form, the synthesis was not conducive to providing significant amounts of material necessary for further testing. Furthermore, when we tried

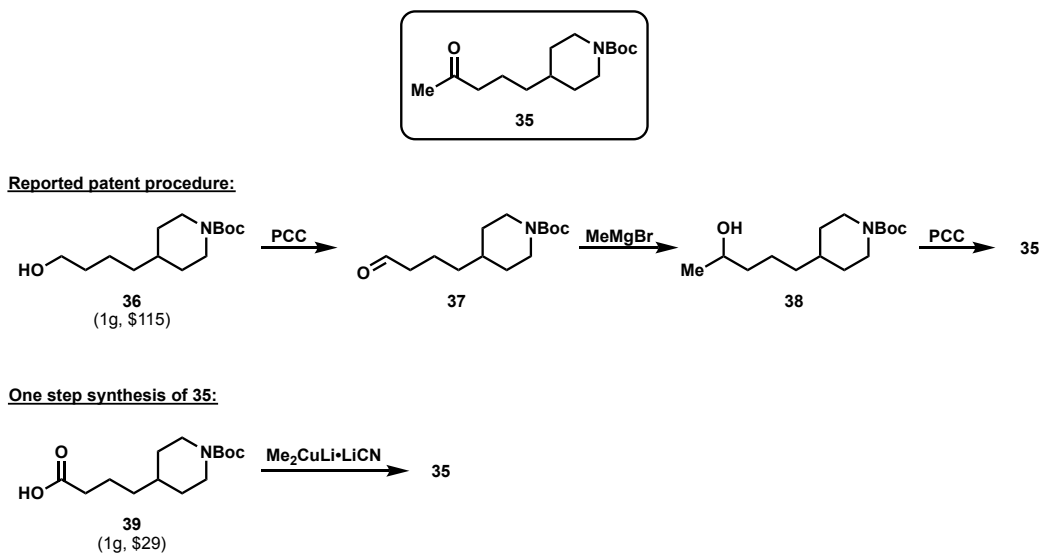


**Scheme 4.4.** Alternative annulation strategy employed by BI for the synthesis of compounds of type **34**.

to scale up the hydrogenation further in order to increase the amount of isolable **7**, we got inconsistent production results. It was clear to us that we needed to determine a more effective synthetic route to enable production of **7** in the quantities necessary.

In evaluating the patent literature disclosed by Boehringer Ingelheim<sup>4</sup> in their disclosure of compounds of type **2**, they presented an alternate strategy for forging the linkage to the substituted pyridine rings. In this alternate approach, aryl iodide **12** was not employed. As shown in Scheme 4.4, the annulation of oxadiazole **13** proceeded *via* reaction with a methyl ketone tethered to the pyridine ring (compound **33**) instead of with ethyl acetoacetate to afford derivatives of **34**. We envisioned that generation of a piperidine motif with a tethered methyl ketone of type **35** could allow us to employ this reactivity and synthesize **7**, and potentially **6**, in a more efficient manner.

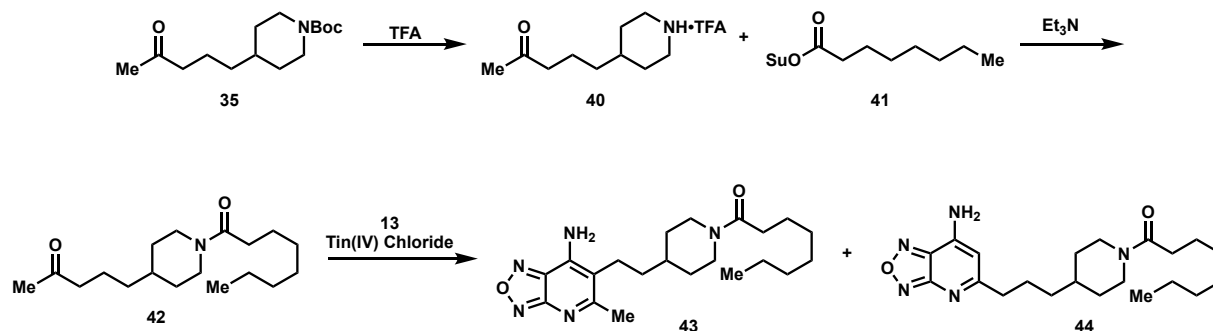
As we began to envision methods of generating **35**, we discovered that its synthesis had only been reported a single time in a 2018 patent from Merck.<sup>7</sup> As seen in Scheme 4.5, the synthesis is fairly straightforward but requires multiple steps, largely manipulating oxidation states. Moreover, the starting material utilized (**36**) is relatively expensive, costing \$115 for just 1 gram of material. Wanting to cut down on the number of steps required to access **35**, we sought out an alternative strategy to generate the desired methyl ketone. In 2011, Posner and Genna at The Johns Hopkins University reported on the direct conversion of carboxylic acids to ketones through the use of cyanocuprates.<sup>8</sup> In their discovery, they reported a broad variety of substrates and



**Scheme 4.5.** Synthesis of key intermediate **35**.

demonstrated its utility on both aromatic and aliphatic carboxylic acids with yields up to 99%. Employing this methodology in our system, we were pleased to find that we could transform carboxylic acid **39** into methyl ketone **35** in just a single step with high efficiency. Furthermore, the starting acid **39** is significantly cheaper than alcohol **36**, costing only \$29 for a single gram of material. With **35** now in hand, we could move forward in the synthesis to evaluate the alternate annulation strategy.

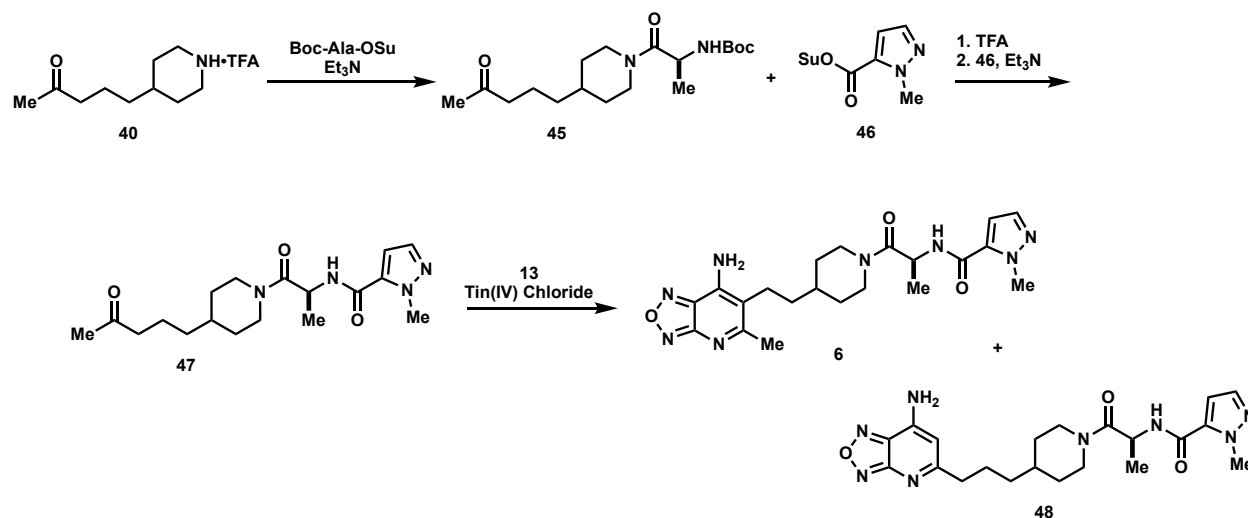
Concerned with the likelihood of the Boc-protecting group to be removed during the annulation process as it is conducted in highly acidic conditions, we elected to couple the side chain to the piperidine prior to annulation. Thus, as depicted in Scheme 4.6, compound **35** was deprotected using TFA at 0 °C to mitigate condensation of the newly formed amine with the methyl ketone. TFA salt **40** was then reacted with succinimidyl ester **41** to afford the coupled product **42**. Compound **42** was then poised to undergo annulation with oxadiazole **13**. Upon reaction of **13** with **42** in the presence of tin(IV) tetrachloride, the annulation proceeded as desired forging compound **43**. However, upon



**Scheme 4.6.** Synthesis of compound **43** via utilization of alternative annulation strategy.

HPLC-MS analysis of the crude product mixture, two peaks with the desired mass were discovered with a ratio of about 1.5:1. Upon purification, the two major compounds were isolated and analyzed. Using NMR analysis, it could be deduced that the secondary product formed was a regioisomer of **43** and bared the structure **44**. Despite the formation of the regioisomer, this alternative synthesis of **43** was much more efficient than the previous route which employed the alkyne.

With this new route in hand, we set forth to synthesize the true hybrid of **1** and **2** and commenced the synthesis of **6**. Starting with methyl TFA salt **40**, Boc-Ala-OSu could



**Scheme 4.7.** Synthesis of true hybrid compound **6** and its regioisomer **48**.

be introduced to afford the coupled product **45**. Subsequent deprotection and coupling with pyrazole derivative **46** could afford the annulation precursor **47**. We were pleased to see that the annulation reaction could still proceed smoothly given the added functionality present in **47** and were able to synthesize the true hybrid **6** as well as its regioisomer (**48**) in the similar 1.5:1 regiomer ratio in which **6** prevails.

#### 4.3.1 Evaluation of Small Molecule Heterocyclic Inhibitors **6** and **7**

Having successfully completed the syntheses of **6** and **7** (and its derivatives), we wanted to evaluate the compounds further. Evaluation commenced with observing the activity of compound **6** in both the *in vitro* and cellular assays. Additionally, we were curious to see whether the regioisomers obtained in the annulation reactions afforded any GOAT inhibitory activity. *In vitro* analysis of **6** and **43** demonstrated that potency could, in fact, be vastly improved by having the fully saturated linker, showing potencies of 84 nM and 98 nM, respectively. However, when the regioisomers **44** and **48** were tested *in vitro*, they lacked any activity as GOAT inhibitors, demonstrating that the interactions at the methyl position are key to binding. Next, we looked at the performance of these compounds in our INS-1 cellular assay and were pleased to find that **6** afforded a cellular IC<sub>50</sub> of just 160 nM while **43** was on par with the activity of **2** with a cellular IC<sub>50</sub> of 560 nM.

Pleased with these results, we then selected compound **7** for further evaluation. Up until this point, we seldom had success *in vivo* with any of our compounds. The only effects we ever observed were minimal and showed little significance compared to the control/vehicle groups. However, with the significant improvements that these current small molecule heterocyclic inhibitors were showing, we were eager to understand their potential in *in vivo* studies in mice. In an experiment conducted by Dr. David Strugatsky as outlined in Figure 4.6, compound **7** was dosed in mice at both 4 mg/kg and 20 mg/kg doses. Excitingly, upon evaluation of the compounds in mice, we were able to observe a significant decrease in plasma acyl-ghrelin levels at both doses! At just 4 mg/kg, we observe a decrease in the amount of circulating plasma acyl-ghrelin by half when compared to the vehicle control group. These results are significant as they highlight an

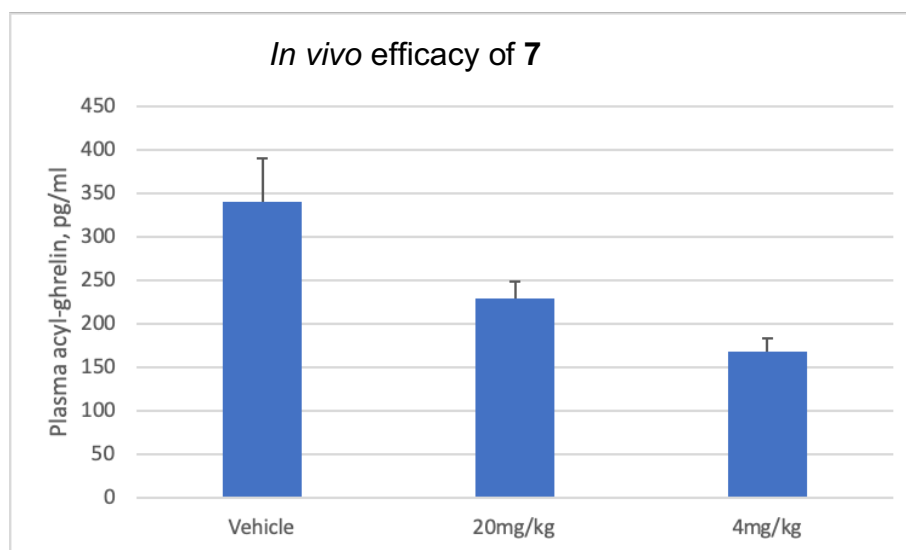


**Figure 4.6.** Pharmacological effect of **7** on plasma acyl-ghrelin in wild type C57BL male mice. Vehicle animals (8 per group) and treated animals (8 per group) were administered vehicle solution (50% propylene glycol, 30% PEG400, 20% DI H<sub>2</sub>O) or with compound **7** in vehicle solution at either 20 mg/kg or 4 mg/kg dose subcutaneously. Animals received 5 doses in total given twice a day (morning and evening) over three days. After last dose in the morning of the third day, animals were fasted for 5 hours and blood was collected and processed as described: collected blood was immediately mixed with anti-coagulant, EDTA, and protease inhibitor aprotinin; after short spin, plasma was saved, acidified by adding 100 mM HCl and frozen by placing on dry ice; 20  $\mu$ L of the plasma was used to measure acyl-ghrelin with commercial ELISA.

achievement of the first compound we have developed that displays favorable data in each aspect of testing: *in vitro*, *in cellulo*, and *in vivo*. Although these results are only preliminary, they are still exciting and provide a steppingstone to the vast array of further future tests that need to be conducted on these hybrid compounds.

#### 4.4 Current State of Small Molecule Heterocyclic Inhibitors

While we have not yet pursued further testing of our heterocyclic small molecules, many in the pharmaceutical sector have. Most notably, GLWL Research Inc. has engaged in numerous clinical trials with compound GLWL-01 (previously LY3073084) to demonstrate proof-of-concept in several indications such as T2D, PWS, appetite regulation, and alcohol use disorder.<sup>9-11</sup> GLWL-01 was first employed in a phase 1 clinical trial to evaluate its safety, tolerability, pharmacokinetics, and pharmacodynamics for the condition of Diabetes Mellitus, Type 2. This study was a three-part study that was ultimately terminated due to insufficient efficacy for the indicated condition. The study, however, was useful in assessing key details such as safety and pharmacodynamics. At doses of 150 mg or greater dosed BID, GLWL-01 could decrease plasma acyl-ghrelin levels by up to 117% in obese patients with T2D. Furthermore, this study demonstrated that the compound was safe and well tolerated up to 600 mg BID with the only AEs reported being mild and largely localized to the GI tract.

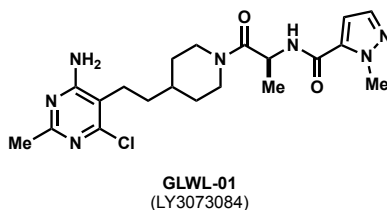


**Figure 4.7.** GLWL-01, a compound currently undergoing clinical trials for various indications.

More recently, GLWL-01 has entered into phase 2 clinical trials to study its role in patients with Prader-Willi syndrome.<sup>10</sup> The goal of this trial is to determine the effects on hyperphagia in patients dosed with compound at a dose of 450 mg BID. Over the course of the trial, patients are exposed to two treatment periods that include two, two-week placebo lead-in phases followed by a four-week treatment of either compound or placebo. During the trial, each patient is treated with the active compound either in treatment cycle 1 or treatment cycle 2. The results of this study are still being released, but thus far the results show no significant deviation from placebo.

In addition to GLWL-01, recently RM-853 (previously T-3525770, structure unknown) has begun progression into further evaluation. Developed by Takeda and licensed by Rhythm Pharmaceuticals, RM-853 is a GOAT inhibitor that is being investigated as a treatment for PWS.<sup>12</sup> It is currently in preclinical trials, but Rhythm Pharmaceuticals has plans to file an IND soon and progress into phase 1 clinical trials.

#### **4.5 Conclusions**

Though GOAT was only discovered about a decade ago, already tremendous progress has been made in development of inhibitors for the treatment of a variety of indications. Currently, there is an influx of research and data being produced that represents an exciting time for therapeutic development of GOAT inhibitors. In just a short time, we were able to not only generate our peptidomimetic inhibitors as discussed in Chapter 3, but also develop hybrid compounds such as **6** and **7** wherein the latter displays significant preliminary *in vivo* efficacy. Moreover, these small molecule heterocyclic compounds display fantastic *in vitro* and cellular potencies that are on par with those



reported in Figure 4.1 and can likely be further optimized. There is still work to be done, but current research efforts have enabled the possibility of understanding the role of circulating ghrelin on multiple disorders, which is an achievement that did not seem to be eminent just five short years ago.

#### 4.6 References

- (1) Lipinski, C. A.; Lombardo, F.; Dominy, B. W.; Feeney, P. J. Experimental and Computational Approaches to Estimate Solubility and Permeability in Drug Discovery and Development Settings. *Adv. Drug Deliv. Rev.* **2001**, *46* (1–3), 3–26.
- (2) Galka, C. S.; Hembre, E. J.; Honigschmidt, N. A.; Keding, S. J.; Martinez-Grau, M. A.; Plaza, G. R.; Rubio, A.; Smith, D. L. Ghrelin O-Acyl Transferase Inhibitors. WO2016168225A1. 13 April 2016.
- (3) Yoneyama-Hirozane, M.; Deguchi, K.; Hirakawa, T.; Ishii, T.; Odani, T.; Matsui, J.; Nakano, Y.; Imahashi, K.; Takakura, N.; Chisaki, I.; Takekawa, S.; Sakamoto, J. Identification and Characterization of a New Series of Ghrelin O-Acyl Transferase Inhibitors. *SLAS Discov.* **2018**, *23* (2), 154–163.
- (4) Godbout, C.; Trieselmann, T.; Vintonyak, V. Oxadiazolopyridine Derivatives for Use as Ghrelin O-Acyl Transferase (GOAT) Inhibitors. WO2018024653A1. 8 February 2018.
- (5) Bandyopadhyay, A.; Cheung, M.; Eidam, H. S.; Joshi, H.; Su, D.-S. Ghrelin O-Acyltransferase Inhibitors. WO2019149959A1. 8 August 2019.
- (6) Pasto, D. J.; Taylor, R. T. Reduction with Diimide. In *Organic Reactions*; John Wiley & Sons, Inc.: Hoboken, NJ, USA, 1991; pp 91–155.
- (7) Bennett, D. J.; Brnardic, E. J.; Han, Y.; Huang, C.; Liverton, N. J.; Meng, Z.; Rudd, M. T.; Stachel, S. J.; Tempest, P.; Wai, J.; Xu, X.; Zhu, B.; Zhu, J. Piperidine Derivatives as Liver X Receptor B Agonists, Compositions, and Their Use. WO2018071313. 19 April 2018.
- (8) Genna, D. T.; Posner, G. H. Cyanocuprates Convert Carboxylic Acids Directly into Ketones. *Org. Lett.* **2011**, *13* (19), 5358–5361.
- (9) Ghrelin Signaling Via GOAT Inhibition in Alcohol Use Disorder - Full Text View - ClinicalTrials.gov <https://clinicaltrials.gov/ct2/show/NCT03896516?term=GLWL-01&draw=2&rank=2>.

- (10) A Study of GLWL-01 in Patients With Prader-Willi Syndrome - Full Text View - ClinicalTrials.gov <https://clinicaltrials.gov/ct2/show/NCT03274856>.
- (11) A Study to Assess the Safety, Tolerability, Pharmacokinetics, and Pharmacodynamics of GLWL-01 - Full Text View - ClinicalTrials.gov <https://clinicaltrials.gov/ct2/show/NCT02377362>.
- (12) Prader-Willi Syndrome Investigational Therapy RM-853 Acquired by Rhythm <https://praderwillinews.com/2018/04/09/prader-willi-syndrome-investigational-therapy-rm-853-acquired-rhythm-pharmaceuticals/>.

## Experimental Appendices

## Experimental Procedures Supporting Chapter 3

### A. Materials and Methods

All reactions were carried out using oven- or flame-dried glassware and a magnetic stir bar under an atmosphere of argon (Ar) unless otherwise indicated. Methylene chloride ( $\text{CH}_2\text{Cl}_2$ ), tetrahydrofuran (THF), diethyl ether ( $\text{Et}_2\text{O}$ ), toluene, and acetonitrile (MeCN) were dried by passage through activate alumina using a GlassContour<sup>®</sup> solvent drying system. Commercial reagents and catalysts were used as received unless otherwise indicated.

NMR spectra were recorded on Bruker Advance spectrometers (300 MHz, 400 MHz, 500 MHz) and are reported as  $\delta$  values in ppm relative to  $\text{CDCl}_3$  (calibrated to 7.26 ppm in  $^1\text{H}$  NMR and 77.16 ppm in  $^{13}\text{C}$  NMR, unless otherwise indicated). Splitting patterns are abbreviated as follows: singlet (s), doublet (d), triplet (t), quartet (q), multiplet (m), broad (br), and combinations thereof. Column chromatography was conducted on silica gel 60 (240–400 mesh) purchased from Silicycle. Thin layer chromatography (TLC) was performed using pre-coated, glass-backed plates (silica gel 60 PF254, 0.25 mm) and visualized using a combination of UV and potassium permanganate staining. HPLC analyses were carried out using an Agilent 1200 HPLC system equipped with an Agilent Quadrupole 6130 ESI-MS detector. Mobile phase was prepared with 0.1% TFA.

### B. General Procedures (GP)

#### General Procedure 1 (Coupling using EDC/HOBt)

Carboxylic acid (1 equiv), amine (1.05 equiv), HOBt (1.05 equiv), and EDC·HCl (1.05 equiv) are suspended in DMF (0.4 M). To the suspension is added DIPEA (3.5 equiv) and the resultant solution is allowed to stir at room temperature until completion as determined by LCMS. Upon completion, the reaction mixture is diluted with EtOAc and washed with saturated aqueous  $\text{NaHCO}_3$  (x2) and brine (x2). Organics are dried ( $\text{MgSO}_4$ ), filtered, and concentrated under reduced pressure.

**General Procedure 2 (Coupling using HATU)**

Carboxylic acid (1 equiv), amine (1.1 equiv), and HATU (1.1 equiv) are suspended in DMF (0.3 M). To the suspension is added DIPEA (2.5 equiv) and the resulting solution is allowed to stir at room temperature until completion as determined by LCMS. Upon completion, the reaction mixture is diluted with EtOAc and washed with saturated aqueous  $\text{NH}_4\text{Cl}$  (x2), water (x3), saturated aqueous  $\text{NaHCO}_3$  (x1), and brine (x1). Organics are dried ( $\text{MgSO}_4$ ), filtered, and concentrated under reduced pressure.

**General Procedure 3 (Boc deprotection with HCl)**

To a solution of the Boc-protected amine (1 equiv) is added HCl (4 N in Dioxane, 5 equiv). Resulting solution is allowed to stir at room temperature until completion as determined by TLC or LCMS. Reaction mixture is concentrated under reduced pressure.

**General Procedure 4 (Boc deprotection with TFA)**

To a solution of the Boc-protected amine (1 equiv) in  $\text{CH}_2\text{Cl}_2$  (0.4 M) is added TFA (10% v/v). Resulting solution is allowed to stir at room temperature until completion as determined by TLC or LCMS. Reaction mixture is concentrated under reduced pressure.

**General Procedure 5 (Cbz deprotection)**

In a round-bottom flask under Ar atmosphere, Cbz-protected amine (1 equiv) and Pd/C (10 wt% Pd/C, 10 mol%) are suspended in MeOH (0.1 M). Resultant suspension is then placed under an  $\text{H}_2$  (balloon) atmosphere until full consumption of starting material as determined by TLC or LCMS. Upon completion, reaction mixture is filtered thru a pad of celite and rinsed with MeOH. Filtrate is concentrated under reduced pressure to afford the deprotected amine.

**General Procedure 6 (Alloc deprotection – solution phase)**

Alloc-protected material (1 equiv) and TPPTS (10 mol%) are dissolved in  $\text{H}_2\text{O}/\text{MeCN}/\text{Et}_2\text{NH}$  (0.1 M) and resultant solution is sparged with argon for 10 minutes before addition of  $\text{Pd}(\text{OAc})_2$  (20 mol%). Reaction is allowed to stir at room temperature until determined complete by TLC or LCMS. Upon completion, the mixture is diluted with

EtOAc and washed with saturated sodium bicarbonate (x1), water (x1), and brine (x1). Organics are dried ( $\text{MgSO}_4$ ), filtered, and concentrated under reduced pressure.

**General Procedure 7** (Alloc deprotection – solid phase)

Resin is suspended in  $\text{CH}_2\text{Cl}_2$  (8 mL) and sparged with argon for 10 minutes. Phenylsilane (10 equiv) and  $\text{Pd}(\text{PPh}_3)_4$  (0.23 equiv) were added and the resulting mixture was sparged with argon for 1 minute and then shaken for 2 hours.

**General Procedure 8** (Fmoc deprotection with DBU – solution phase)

To a solution of the Fmoc-protected amine (1 equiv) and octanethiol (10 equiv) in THF (0.1 M) was added DBU (1.1 equiv). Resultant solution was stirred at room temperature for 15 minutes and then concentrated under reduced pressure. Resultant residue is purified by column chromatography.

**General Procedure 9** (Fmoc deprotection with piperidine – solution phase)

Upon completion of coupling of Fmoc-protected residue, a 20% v/v piperidine in DMF (0.1 M) solution is added to the reaction mixture and the resultant solution is stirred for 15 minutes. Reaction mixture is used directly for HPLC purification.

**General Procedure 10** (RCM to forge macrocycles)

The diene (1 equiv) is dissolved in  $\text{CHCl}_3$  (0.01 M) and sparged with argon for 10 minutes and then a solution of Grubbs I (20 mol%) in  $\text{CHCl}_3$  (0.02 M) is added. Resultant solution is stirred under argon until completion as determined by TLC or LCMS.

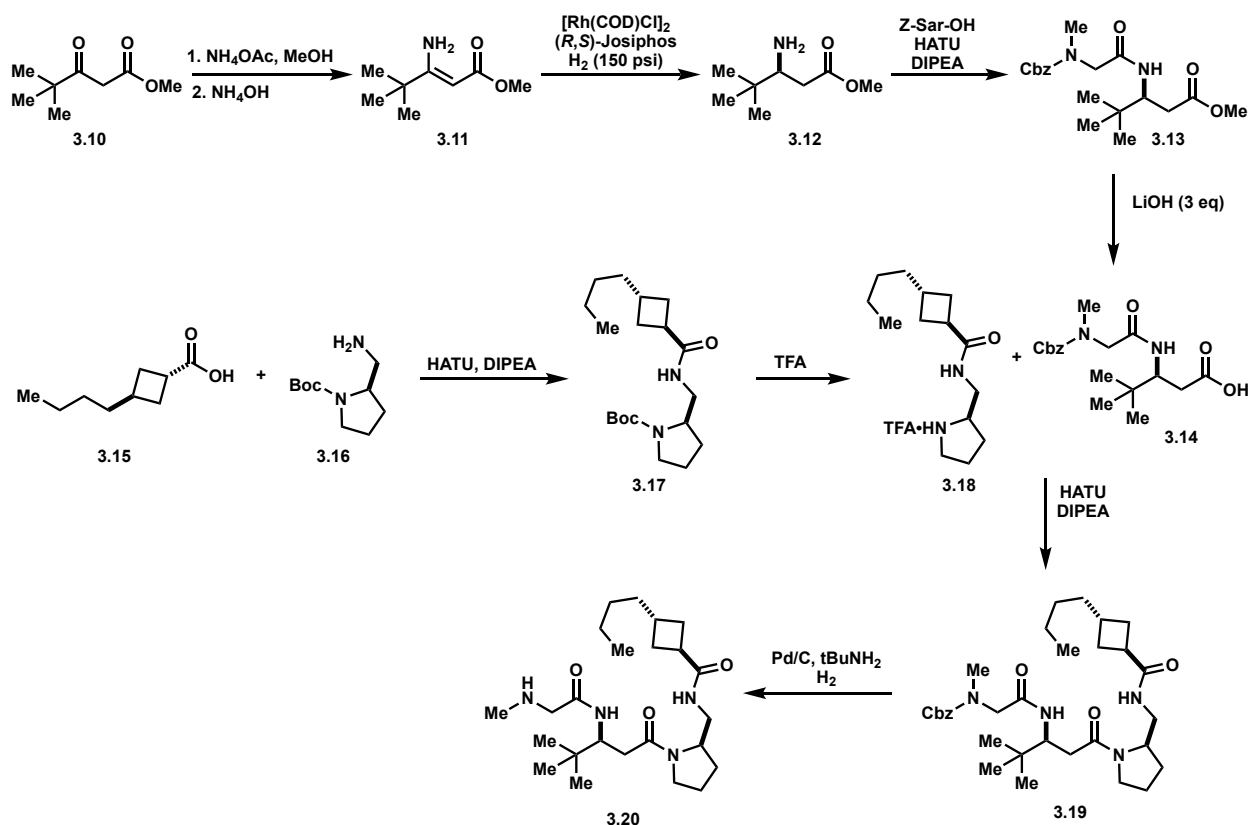
**General Procedure 11** (Solid phase peptide synthesis)

Peptides were synthesized *via* standard Fmoc solid phase peptide synthesis conditions using Rink Amide MBHA resin (polystyrene, 1% DVB, 0.7 mmol/g).<sup>1</sup>

## C. Experimental Procedures and Characterization

### C1. Pyrrolidine-Containing Inhibitors

#### Preparation of 3.20



#### Methyl (Z)-3-amino-4,4-dimethylpent-2-enoate (3.11):

To a solution of methyl pivaloylacetate (10 mL, 62.6 mmol) in MeOH (300 mL) was added  $\text{NH}_4\text{OAc}$  (20.5 g, 250.33 mmol) and warmed to 50 °C. Resulting mixture was stirred at 50 °C for 24 h and cooled to rt.  $\text{NH}_4\text{OH}$  (8.7 mL, 125.2 mmol) was added dropwise followed by water (30 mL). Volume was reduced to ~50 mL and placed in -20 °C freezer overnight. Mixture was filtered and solid was washed with 1:1 MeOH: $\text{H}_2\text{O}$  and dried in vacuo to produce crop 1. Filtrate was concentrated down to remove MeOH and placed in freezer overnight. Resulting was filtered and resulting filter cake was dried in vacuo to produce crop 2. Crop 1 and crop 2 were combined to obtain **13** (6.0g) in 61% yield as a white solid.  $^1\text{H}$  NMR (400MHz,  $\text{CDCl}_3$ )  $\delta$  4.66 (s, 1H), 3.64 (s, 3H), 1.17 (s, 9H).  $^{13}\text{C}$  NMR (126 MHz,  $\text{CDCl}_3$ )  $\delta$  172.0, 171.3, 79.8, 50.2, 35.8, 28.8.

**methyl (S)-3-amino-4,4-dimethylpentanoate (3.12):**

Part 1: [Rh(COD)Cl]<sub>2</sub> (9.4 mg, 0.019 mmol) and (*R,S*)-Josiphos (10.8 mg, 0.020 mmol) were suspended in TFE (2.5 mL) and allowed to stir under Ar for 40 minutes.

Part 2: **1** (1.0 g, 6.36 mmol) was dissolved in TFE (10 mL) in hydrogenation vessel. To this solution was added the catalyst mixture and resulting suspension was placed in the BOMB reactor and allowed to stir under H<sub>2</sub> atmosphere (~150 psi) at 50 °C for 68 hours at which time NMR analysis showed the desired product as the major component. The reaction mixture was cooled to room temperature and filtered to remove the catalyst. The filtrate was concentrated under reduced pressure and resultant residue was carried forward without further purification. (1.016 g, quant. crude yield). <sup>1</sup>H NMR (400 MHz, CDCl<sub>3</sub>) δ 3.68 (s, 3H), 2.95 (d, *J* = 9.2 Hz, 1H), 2.55 (t, *J* = 7.7 Hz, 1H), 2.17 (q, *J* = 8.7 Hz, 1H), 0.90 (s, 9H).

**methyl (S)-3-(2-(((benzyloxy)carbonyl)(methyl)amino)acetamido)-4,4-dimethyl-pentanoate (3.13):**

Following GP 2, **3.13** (1.2g, 52%) was obtained following purification *via* column chromatography using DCM:MeOH (100% DCM to 95:5 DCM:MeOH) as eluents. <sup>1</sup>H NMR (400 MHz, CDCl<sub>3</sub>) δ 7.35 (s, 5H), 5.16 (s, 2H), 4.18 (m, 1H), 3.62 (s, 2H), 3.02 (s, 3H), 2.80 (s, 3H), 2.54 (d, *J* = 11.6 Hz, 1H), 2.23 (q, *J* = 7.9 Hz, 1H), 0.85 (s, 9H). HPLC/MS MH<sup>+</sup> 365.2.

**(S)-3-(2-(((benzyloxy)carbonyl)(methyl)amino)acetamido)-4,4-dimethylpentanoic acid (3.14):**

**3.13** (1.2 g, 3.19 mmol) was dissolved in MeOH (5.3 mL) and THF (5.3 mL). To resulting solution was added LiOH•H<sub>2</sub>O (0.4 g, 9.58 mmol) and H<sub>2</sub>O (5.3 mL). The resultant reaction mixture was allowed to stir at room temperature for 15 minutes and then cooled to 0 °C and acidified to pH 4 using 1N HCl. Organics were extracted into EtOAc (x2), dried (MgSO<sub>4</sub>), filtered, and concentrated under reduced pressure to obtain **3.14** (725 mg, 65%) as an oil. <sup>1</sup>H NMR (400 MHz, MeOD) δ 7.31 (bs, 5H), 5.10 (s, 2H), 4.16 (t, *J* = 10.4 Hz,



1H), 2.95 (s, 2H), 2.79 (s, 3H), 2.47 (t,  $J = 11.0$  Hz, 1H), 2.15 (q,  $J = 11.8$  Hz, 1H), 0.89 (s, 9H). HPLC/MS  $MH^+$  351.2.

***tert*-butyl (*R*)-2-(((1*S*,3*R*)-3-butylcyclobutane-1-carboxamido)methyl)pyrrolidine-1-carboxylate (3.17):**

Following GP 1, coupled product **3.17** was produced as a yellow oil. (401 mg, 76.7%).  $^1H$  NMR (400 MHz,  $CDCl_3$ )  $\delta$  4.02 (s, 1H), 3.33 (m, 3H), 3.21 (s, 1H), 2.94 (m, 1H), 2.31 (m, 3H), 1.97 (m, 2H), 1.82 (m, 3H), 1.68 (s, 1H), 1.46 (s, 9H), 1.41 (m, 1H), 1.27 (m, 3H), 1.18 (m, 2H), 0.87 (t,  $J = 7.2$  Hz, 3H). HPLC/MS  $MH^+$  239.3 (-Boc).

**(1*S*,3*R*)-3-butyl-*N*-(((*R*)-pyrrolidin-2-yl)methyl)cyclobutane-1-carboxamide TFA salt (3.18):**

Following GP 4, **3.17** could be deprotected to afford **3.18** as the TFA salt which was used without purification.  $^1H$  NMR (400 MHz, MeOD)  $\delta$  3.65 (m, 1H), 3.44 (d,  $J = 5.8$  Hz, 2H), 3.25 (m, 1H), 3.05 (m, 1H), 2.30 (m, 3H), 2.11 (m, 1H), 2.01 (m, 2H), 1.85 (m, 2H), 1.74 (m, 1H), 1.46 (m, 2H), 1.29 (m, 3H), 1.21 (m, 2H), 0.88 (t,  $J = 7.2$  Hz, 3H). HPLC/MS  $MH^+$  239.2.

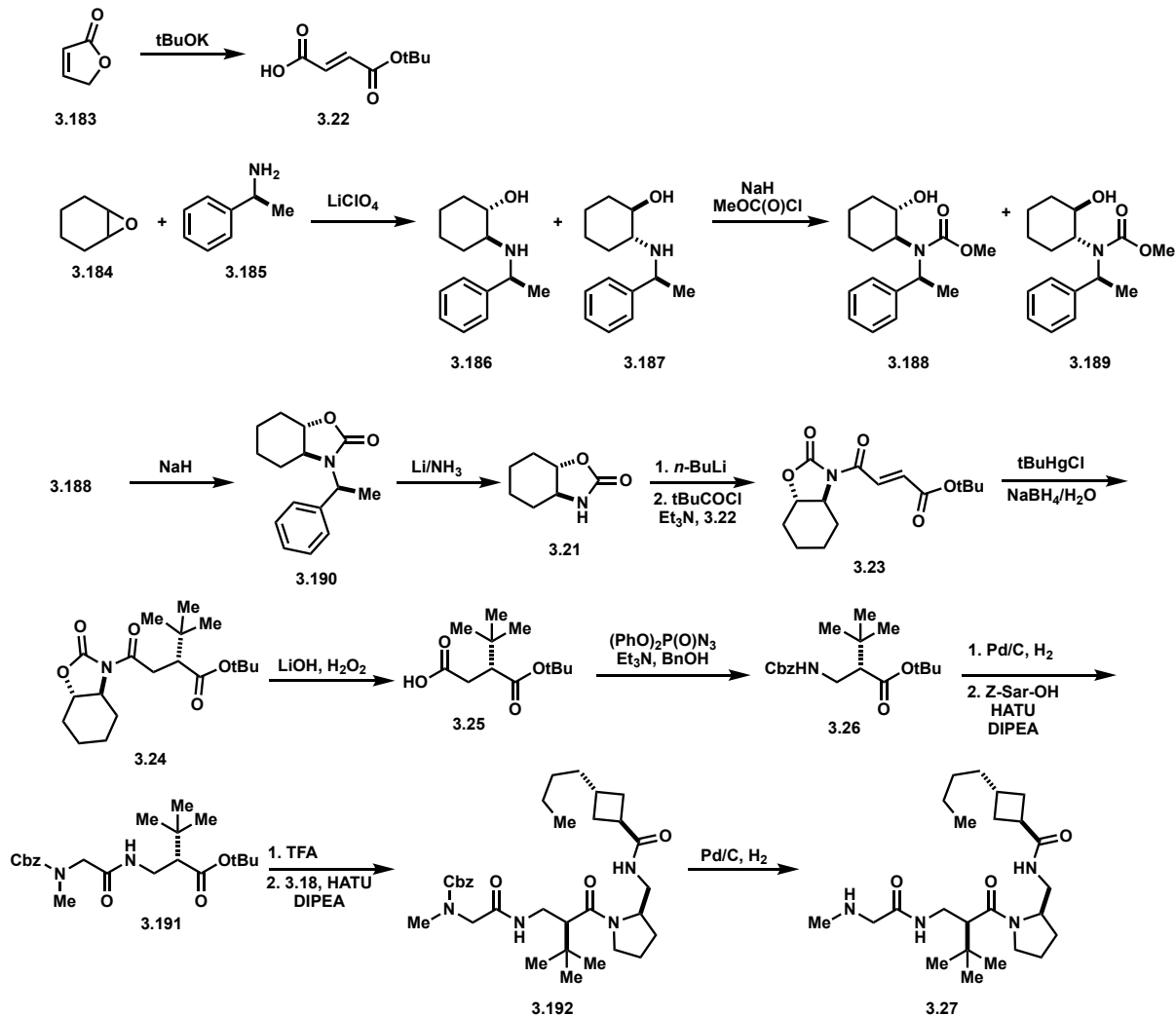
**benzyl (2-(((*S*)-1-((*R*)-2-(((1*S*,3*R*)-3-butylcyclobutane-1-carboxamido)methyl)pyrrolidin-1-yl)-4,4-dimethyl-1-oxopentan-3-yl)amino)-2-oxoethyl)(methyl)carbamate (3.19):**

Following GP 1, coupled product **3.19** could be obtained. (177 mg, 57%).  $^1H$  NMR (400 MHz, MeOD)  $\delta$  7.31 (bs, 5H), 5.10 (m, 2H), 4.28-3.79 (m, 5H), 3.54 (bs, 1H), 3.44-3.32 (m, 1H), 3.16-2.97 (m, 2H), 2.94 (s, 3H), 2.61-2.49 (m, 1H), 2.26 (bs, 3H), 2.07-1.69 (m, 5H), 1.50-1.38 (m, 2H), 1.37-1.13 (m, 5H), 0.94-0.86 (m, 12H). HPLC/MS  $MH^+$  571.4.

**(1*s*,3*R*)-3-butyl-*N*-(((*R*)-1-((*S*)-4,4-dimethyl-3-(2-(methylamino)acetamido)pentanoyl)pyrrolidin-2-yl)methyl)cyclobutane-1-carboxamide (3.20):**

Following GP 5, **3.20** was obtained and purified by preparative HPLC. <sup>1</sup>H NMR (400MHz, MeOD) δ 4.25-4.16 (d, *J*=10.6, 1H), 4.13-4.02 (m, 1H), 3.91-3.70 (m, 2H), 3.56-3.45 (m, 2H), 3.26-3.16 (m, 2H), 3.08-2.96 (m, 1H), 2.72 (s, 3H), 2.68-2.60 (m, 2H), 2.34-2.21 (m, 4H), 1.99-1.80 (m, 6H), 1.48-1.43 (m, 2H), 1.32- 1.27 (m, 2H), 1.22-1.18 (m, 2H), 0.93 (s, 9 H), 0.90-0.86 (t, *J*=7.1, 3H). HPLC/MS MH<sup>+</sup> 437.4.

**Preparation of 3.27**



**(E)-4-(tert-butoxy)-4-oxobut-2-enoic acid (3.22):**

To a solution of tBuOK (1.16 g, 10.3 mmol) in THF (20 mL) at 0 °C was added maleic anhydride (1 g, 10.2 mmol). Resulting mixture was stirred at 0 °C for 2.5 h and diluted with EtOAc and acidified to pH 2 with 1 M HCl. Organic phase was separated and aqueous was extracted with EtOAc (x 3). Combined organics were washed with brine (x 2), dried (MgSO<sub>4</sub>), filtered, and concentrated under reduced pressure. Residue was suspended in EtOAc and filtered through celite plug. Filtrate was concentrated down to obtain **3.22** (0.95 g, 54%) as a brown solid, which was used without further purification. <sup>1</sup>H NMR (300 MHz, CDCl<sub>3</sub>) δ 6.35 (dd, *J* = 12.8, 29.3 Hz, 2H), 1.57 (s, 9H). <sup>13</sup>C NMR (126 MHz, CDCl<sub>3</sub>) δ 169.6, 163.9, 137.2, 131.9, 82.3, 27.9.

**(1S,2S)-2-(((S)-1-phenylethyl)amino)cyclohexan-1-ol (3.186) and (1R,2R)-2-(((S)-1-phenylethyl)amino)cyclohexan-1-ol (3.187):**

Cyclohexene oxide (2.06 mL, 20.4 mmol) and LiClO<sub>4</sub> (2.17 g, 20.4 mmol) were dissolved in MeCN (20 mL) and cooled to 0 °C. (S)-(a)-methylbenzylamine (2.63 mL, 20.4 mmol) was added dropwise. Resulting mixture was heated to 85 °C and allowed to stir for 18 h before cooling to rt. To reaction mixture was added water and resulting was extracted with CH<sub>2</sub>Cl<sub>2</sub> (x 3). Combined organics were washed with brine, dried (MgSO<sub>4</sub>), filtered, and concentrated under reduced pressure to obtain a mixture of **3.186** and **3.187** (4.5g, 99%). <sup>1</sup>H NMR (400 MHz, CDCl<sub>3</sub>) δ 7.33 (m, 8H), 7.24 (m, 2H), 4.00 (q, *J* = 6.6 Hz, 1H), 3.92 (q, *J* = 6.5 Hz, 1H), 3.12 (m, 2H), 2.33 (m, 1H), 2.16 (m, 1H), 2.05 (m, 1H), 1.96 (m, 3H), 1.67 (m, 4H), 1.39 (d, *J* = 7.1 Hz, 1H) 1.35 (t, *J* = 6.7 Hz, 6H), 1.24 (m, 4H), 1.08 (m, 2H), 0.88 (m, 2H).

**methyl ((1S,2S)-2-hydroxycyclohexyl)((S)-1-phenylethyl)carbamate (3.188):**

**3.186** & **3.187** (4.5 g, 20.4 mmol) and NaH (60% dispersion in oil, 0.82 g, 20.4 mmol) were dissolved in THF (22 mL) at 0 °C. To solution was added methyl chloroformate (1.6 mL, 20.4 mL) dropwise. Resulting mixture was heated to 70 °C for 2.5 h and cooled to rt. Resulting white mixture was cooled to 0 °C and quenched with water. Reaction mixture

was extracted with CH<sub>2</sub>Cl<sub>2</sub> (x 3) and combined extracts were dried (MgSO<sub>4</sub>), filtered, and concentrated under reduced pressure. Purification via column chromatography using hexanes:EtOAc (5:1 to 3:1) as eluents afforded the desired isomer **3.188** (2.1 g, 36%) as a white solid. <sup>1</sup>H NMR (400 MHz, CDCl<sub>3</sub>) δ 7.44 (d, *J* = 7.5 Hz, 2H), 7.35 (t, *J* = 7.5 Hz, 1H), 7.29 (d, *J* = 7.5 Hz, 2H), 3.85 (br, 1H), 3.67 (s, 3H), 1.98 (d, *J* = 10 Hz, 1H), 1.73 – 1.79 (m, 2H), 1.61 – 1.63 (m, 6H), 1.24 – 1.27 (m, 3H). <sup>13</sup>C NMR (126 MHz, CDCl<sub>3</sub>) δ 158.9, 141.3, 129.0, 128.0, 127.8, 70.4, 62.4, 54.3, 52.7, 35.3, 30.6, 26.1, 24.8.

**(3a*S*,7a*S*)-3-((*S*)-1-phenylethyl)hexahydrobenzo[*d*]oxazol-2(3*H*)-one (3.190):**

To a solution of **22** (2 g, 7.2 mmol) in THF (60 mL) was added NaH (60% dispersion in oil, 343 mg, 8.6 mmol). Resulting mixture was heated to reflux for 2 h. Reaction mixture was cooled to 0 °C and quenched with H<sub>2</sub>O. Resulting mixture was extracted with CH<sub>2</sub>Cl<sub>2</sub> (x 3). Combined organics were dried (MgSO<sub>4</sub>), filtered, and concentrated under reduced pressure to afford **3.190** (1.8g, quant.) as a white solid. <sup>1</sup>H NMR (400 MHz, CDCl<sub>3</sub>) δ 7.35 (m, 5H), 5.29 (q, *J* = 7.3 Hz, 1H), 3.75 (dt, *J* = 3.6, 11.3 Hz, 1H), 2.73 (dt, *J* = 3.6, 11.3 Hz, 1H), 2.11 (m, 1H), 2.01 (m, 1H), 1.79 (m, 1H), 1.70 (m, 1H), 1.62 (d, *J* = 7.4 Hz, 3H), 1.45 (m, 3H), 1.33 (m, 2H), 1.09 (m, 1H), 0.85 (m, 1H). <sup>13</sup>C NMR (126 MHz, CDCl<sub>3</sub>) δ 159.2, 141.0, 128.0, 127.1, 126.7, 80.7, 61.2, 51.3, 28.6, 28.2, 23.4, 23.3, 15.2.

**(3a*S*,7a*S*)-hexahydrobenzo[*d*]oxazol-2(3*H*)-one (3.21):**

In a round-bottomed flask in an acetone/dry ice bath was collected ~30 mL or liquified ammonia. To vessel at -40 °C was added lithium shot (88 mg, 12.6 mmol). Reaction mixture turned dark blue and a solution of **3.190** (440 mg, 1.8 mmol) in THF (20 mL) was added. Resulting mixture was stirred at -40 °C for 1 h at which time TLC showed no presence of starting material. Reaction mixture was quenched with solid NH<sub>4</sub>Cl (660 mg, 12.6 mmol) and allowed to warm to room temperature overnight. To reaction mixture was added H<sub>2</sub>O (25 mL) and 1N HCl until pH=7. Mixture was extracted with CH<sub>2</sub>Cl<sub>2</sub> (x 3) and combined organics were dried (MgSO<sub>4</sub>), filtered, and concentrated under reduced pressure. Residue was purified via column chromatography using hexanes:EtOAc (4:1 to 1:1) as eluents to obtain **3.21** (128mg, 51%) as a white solid. <sup>1</sup>H NMR (400 MHz, CDCl<sub>3</sub>)

$\delta$  4.97 (br s, 1H), 3.89 (m, 1H), 3.31 (m, 1H), 2.19 (m, 1H), 2.04 (m, 1H), 1.92 (m, 1H), 1.82 (m, 1H), 1.65 (dq,  $J = 3.9, 11.8$  Hz, 4H), 1.42 (m, 3H).  $^{13}\text{C}$  NMR (126 MHz,  $\text{CDCl}_3$ )  $\delta$  160.5, 84.3, 61.4, 29.6, 29.0, 24.2, 24.0.

***tert*-butyl (E)-4-oxo-4-((3a*S*,7a*S*)-2-oxohexahydrobenzo[*d*]oxazol-3(2*H*)-yl)but-2-enoate (3.23):**

To a suspension of 19 (128 mg, 0.744 mmol) in THF (3 mL) at  $-30^\circ\text{C}$  was added Et<sub>3</sub>N (0.114 mL, 0.818 mmol) and pivaloyl chloride (0.092 mL, 0.744 mmol) dropwise. Resulting mixture was allowed to stir at  $-30^\circ\text{C}$  for 2h. Meanwhile, a solution of n-BuLi (2.5 M in hexanes, 0.298 mL, 0.744 mmol) was added to a suspension of **3.21** (105 mg, 0.744 mmol) in THF (3 mL) at  $0^\circ\text{C}$ . Resulting mixture was cooled to  $-30^\circ\text{C}$  and allowed to stir for 30 min. Resulting solution was added to the mixed anhydride solution and resulting mixture was allowed to warm to RT overnight. After 15 h, reaction mixture was quenched with saturated  $\text{NH}_4\text{Cl}$  and diluted with EtOAc. Organics were separated and washed with brine (x 2) and aqueous was extracted with EtOAc (x 2). Combined organics were dried ( $\text{MgSO}_4$ ), filtered, and concentrated in vacuo. Resulting residue was purified by column chromatography using 25 – 50% EtOAc in hexanes as eluents to obtain **3.23** (36 mg, 17%).  $^1\text{H}$  NMR (400 MHz,  $\text{CDCl}_3$ )  $\delta$  7.75 (d,  $J = 15.5$  Hz, 1H), 6.78 (d,  $J = 15.5$  Hz, 1H), 3.93 (td,  $J = 3.6, 11.2$  Hz, 1H), 3.60 (m, 1H), 2.79 (m, 1H), 2.23 (m, 1H), 1.95 (m, 1H), 1.85 (m, 1H).  $^{13}\text{C}$  NMR (126 MHz,  $\text{CDCl}_3$ )  $\delta$  165.93, 164.17, 154.43, 135.48, 132.81, 81.93, 63.16, 28.49, 28.47, 28.05, 23.73, 23.60.

***tert*-butyl (R)-2-(*tert*-butyl)-4-oxo-4-((3a*S*,7a*S*)-2-oxohexahydrobenzo[*d*]oxazol-3(2*H*)-yl)butanoate (3.24):**

**3.23** (190 mg, 0.64 mmol) was dissolved in  $\text{CH}_2\text{Cl}_2$  (3.2 mL) and cooled to  $0^\circ\text{C}$ . To solution was added tBuHgCl (280 mg, 0.96 mmol),  $\text{NaBH}_4$  (40 mg, 0.96 mmol), and  $\text{H}_2\text{O}$  (0.3 mL). Resulting mixture was allowed to stir at  $0^\circ\text{C}$  for 2 h and then diluted with  $\text{CH}_2\text{Cl}_2$ , dried ( $\text{MgSO}_4$ ), and concentrated in vacuo. Residue was purified by column chromatography using 25% EtOAc in hexanes to obtain **3.24** (82 mg, 36%).  $^1\text{H}$  NMR (400MHz,  $\text{CDCl}_3$ )  $\delta$  3.93 (td,  $J = 3.6, 11.6$  Hz, 1H), 3.49 (td,  $J = 3.3, 11$  Hz, 1H), 3.1 (m, 2H), 2.73 (m, 1H),

2.60 (dd,  $J = 4.1, 11.3$  Hz, 1H), 2.21 (m, 1H), 1.91 (m, 1H), 1.80 (m, 1H), 1.63 (m, 1H), 1.42 (s, 9H), 1.34 (m, 3H), 0.98 (s, 9H).  $^{13}\text{C}$  NMR (126 MHz,  $\text{CDCl}_3$ )  $\delta$  174.75, 173.52, 154.87, 81.57, 80.28, 63.13, 51.62, 35.64, 32.49, 28.63, 28.51, 28.18, 28.09, 23.76, 23.63. HPLC/MS  $\text{MH}^+$  280.2 (-OtBu).

**(R)-3-(*tert*-butoxycarbonyl)-4,4-dimethylpentanoic acid (3.25):**

Flask A: To a stirring solution of  $\text{LiOH}\cdot\text{H}_2\text{O}$  (20 mg, 0.47 mmol) in THF/ $\text{H}_2\text{O}$  (1:1, 3 mL) at  $0^\circ\text{C}$  was added  $\text{H}_2\text{O}_2$  (30% aq solution, 0.11 mL, 0.93 mmol).

Flask B: **27** (82 mg, 0.23 mmol) was dissolved in THF (3 mL) and placed in an ice bath. To resulting solution was added the mixture from flask A and allowed to stir in an ice bath for 30 min. To reaction mixture was added a solution of  $\text{Na}_2\text{SO}_3$  (118 mg, 0.93 mmol) in  $\text{H}_2\text{O}$  (3 mL) and resulting mixture was allowed to stir for 30 min at  $0^\circ\text{C}$ .  $\text{H}_2\text{O}$  (3 mL) was added and resulting mixture was extracted with EtOAc (x 2). Aqueous layer was acidified to pH 2 with 1N HCl at  $0^\circ\text{C}$ . Aqueous solution was extracted with EtOAc (x 3) and organics were combined, washed with brine, dried ( $\text{MgSO}_4$ ), filtered, and concentrated under reduced pressure to obtain **3.25** (46 mg, 85%) as a yellow oil which was used without further purification.  $^1\text{H}$  NMR (400 MHz,  $\text{CDCl}_3$ )  $\delta$  10.76 (s, 1H), 2.74 (q,  $J = 10.4$  Hz, 1H), 2.46 (m,  $J = 4.9$  Hz, 1H), 1.42 (s, 1H), 0.96 (s, 1H).  $^{13}\text{C}$  NMR (126 MHz,  $\text{CDCl}_3$ )  $\delta$  178.97, 172.98, 80.70, 51.94, 32.75, 32.59, 28.07, 27.96.

***tert*-butyl (S)-2-(((benzyloxy)carbonyl)amino)methyl)-3,3-dimethylbutanoate (3.26):**

To a solution of **3.25** (46 mg, 0.20 mmol) in toluene (1.7 mL) and  $\text{Et}_3\text{N}$  (0.06 mL, 0.40 mmol) was added  $(\text{PhO})_2\text{P}(\text{O})\text{N}_3$  (0.05 mL, 0.24 mmol) and BnOH (0.04 mL, 0.40 mmol). The resulting mixture was allowed to stir at room temperature for 1 hour and then heated at reflux for 3 hours. Toluene was evaporated under reduced pressure and resulting residue was dissolved in EtOAc (3.4 mL) and 2N HCl (1.7 mL). Organic phase was separated and washed with saturated aqueous  $\text{NaHCO}_3$ , dried ( $\text{MgSO}_4$ ), filtered, and concentrated under reduced pressure. Residue was purified via column chromatography

using 10% EtOAc in hexanes to afford **3.26** (38 mg, 58%). <sup>1</sup>H NMR (400 MHz, CD<sub>3</sub>OD) δ 7.31 (bs, 5H), 6.91 (bs, 1H), 3.40 (m, 1H), 3.25 (m, 1H), 2.37 (m, 1H), 1.39 (s, 9H), 0.97 (s, 9H). HPLC/MS MH<sup>+</sup> 301.3 (-OtBu).

**tert-butyl (S)-2-((2-(((benzyloxy)carbonyl)(methyl)amino)acetamido)methyl)-3,3-dimethylbutanoate (3.191):**

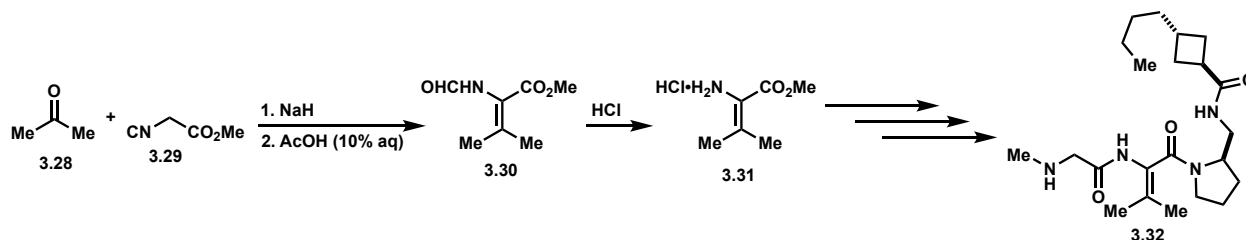
Following GP 5, the Cbz group could be removed to afford the free amine. The resultant residue was coupled to Z-Sar-OH following GP 2 to afford **3.191** (36 mg, 88%) as an oil which was used without further purification. <sup>1</sup>H NMR (400 MHz, CD<sub>3</sub>OD) δ 7.30 (bs, 5H), 5.11-5.07 (m, 2H), 3.93-3.88 (m, 2H), 2.97-2.93 (m, 4H), 2.40-2.33 (m, 1H), 1.45 (s, 9H), 0.97 (s, 9H). HPLC/MS MH<sup>+</sup> 351.3 (-OtBu).

**benzyl (2-(((S)-2-((R)-2-(((1s,3R)-3-butylcyclobutane-1-carboxamido)methyl)pyrrolidine-1-carbonyl)-3,3-dimethylbutyl)amino)-2-oxoethyl)(methyl)carbamate (3.192).**

Following the conditions outlined in GP 4, the tBu ester could be saponified. The residue was immediately subjected to coupling with **3.18** following GP 2 to afford **3.192** (18 mg, 35%) as a yellow oil. <sup>1</sup>H NMR (400 MHz, CDCl<sub>3</sub>) δ 7.34(m, 5H), 5.11 (m, 2H), 4.01-3.77 (m, 2H), 3.59-3.35 (m, 4H), 3.25-3.13 (m, 1H), 2.94 (s, 3H), 2.27 (bs, 4H), 1.97-1.69 (m, 6H), 1.50-1.38 (m, 2H), 1.37-1.24 (m, 4H), 1.24-1.14 (m, 2H), 0.99 (s, 9H), 0.91-0.83 (m, 3H). HPLC/MS MH<sup>+</sup> 571.5.

**(1s,3R)-3-butyl-N-(((R)-1-((S)-3,3-dimethyl-2-((2-(methylamino)acetamido)methyl)butanoyl)pyrrolidin-2-yl)methyl)cyclobutane-1-carboxamide (3.27).** Following GP 5, the Cbz group could be removed to afford **3.27** which was then purified by preparative HPLC. <sup>1</sup>H NMR (400MHz, CD<sub>3</sub>OD) δ 4.32 (bs, 1H), 4.03-3.91 (m, 1H), 3.89-3.78 (m, 1H), 3.75-3.54 (m, 3H), 3.52-3.39 (m, 2H), 3.07-2.88 (m, 3H), 2.78 (s, 3H), 2.34 (bs, 3H), 1.86-1.78 (m, 5H), 1.41-1.39 (m, 2H), 1.26-1.23 (m, 4H), 1.19-1.15 (m, 3H), 0.99 (s, 9H), 0.86-0.82 (t, *J*=14.4, 7.3, 3H). HPLC/MS MH<sup>+</sup> 437.4.

## Preparation of 3.32



### methyl 2-formamido-3-methylbut-2-enoate (3.30):

To a suspension of NaH (60% in mineral oil, 79 mg, 1.98 mmol) in THF (1.65 mL) was added a solution of acetone (0.121 mL, 1.65 mmol) and methyl isocyanoacetate (0.15 mL, 1.65 mmol) in THF (1.65 mL) dropwise. The resulting mixture was allowed to stir at room temperature for 2 hours and then cooled to 0 °C. A 10% aqueous solution of AcOH (1.65 mL) was added. The reaction mixture was concentrated in vacuo to remove THF. Residue was extracted with DCM (x3) and organics were dried (MgSO<sub>4</sub>), filtered, and concentrated under reduced pressure to afford **3.30** (56 mg, 21%). <sup>1</sup>H NMR (300 MHz, CDCl<sub>3</sub>) δ 8.46 (br, 1H), 8.14 (d, *J* = 1.1 Hz, 1H), 3.67 (s, 3H), 2.07 (s, 3H), 1.84 (s, 3H).

### methyl 2-amino-3-methylbut-2-enoate hydrochloride salt (3.31):

To a solution of **3.30** (56 mg, 0.35 mmol) in MeOH (1 mL) and ether (5 mL) was added a solution of HCl (1.4M in MeOH, 1 mL). Resulting mixture was allowed to stir at room temperature for 30 minutes. Reaction mixture was then concentrated under reduced pressure and then co-evaporated with MeOH to remove any remaining HCl. Resultant residue was used without further purification. <sup>1</sup>H NMR (400 MHz, D<sub>2</sub>O) δ 3.88 (s, 3H), 2.28 (s, 3H), 2.06 (s, 3H). <sup>13</sup>C NMR (126 MHz, CDCl<sub>3</sub>) δ 164.1, 152.8, 114.8, 53.0, 22.0, 21.6.

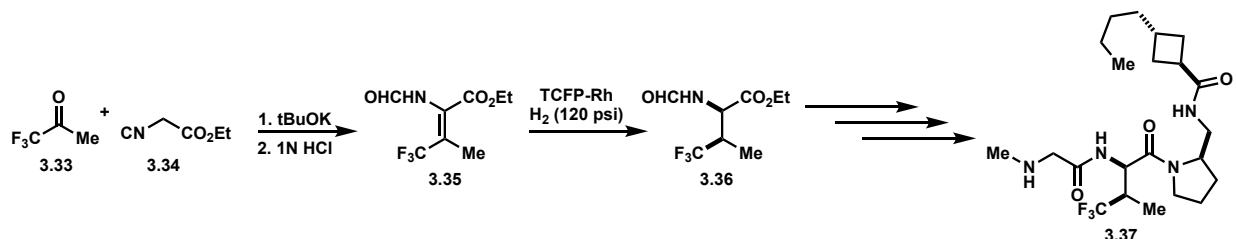
### (1*s*,3*R*)-3-butyl-*N*-(((*R*)-1-(3-methyl-2-(2-(methylamino)acetamido)but-2-enoyl)pyrrolidin-2-yl)methyl)cyclobutane-1-carboxamide (3.32):

Following standard peptide synthesis conditions outlined above, **3.31** could be elaborated to **3.32** which was purified *via* preparative HPLC. <sup>1</sup>H NMR (500 MHz, MeOD) δ 4.22 (m, 2H), 4.03 (d, *J* = 2.6 Hz, 1H), 3.88 (s, 1H), 3.67 (m, 3H), 3.43 (m, 4H), 3.01 (m, 3H), 2.93



(s, 2H), 2.72 (s, 2H), 1.47 (m, 3 H), 1.30 (m, 6H), 1.21 (m, 3H), 0.89 (t,  $J = 7.3$  Hz, 3H).  $^{13}\text{C}$  NMR (126 MHz, MeOD)  $\delta$  179.5, 171.5, 163.8, 143.9, 107.9, 100.7, 59.3, 57.8, 49.8, 49.4, 43.3, 42.5, 39.0, 34.8, 30.2, 28.3, 27.9, 19.9, 18.8, 17.6. HPLC/MS  $\text{MH}^+$  407.4.

### Preparation of 3.27



### ethyl (Z)-4,4,4-trifluoro-2-formamido-3-methylbut-2-enoate (3.35):

KOtBu (494 mg, 4.4 mmol) was dissolved in dry THF (2.6 mL) and cooled to  $-78$  °C. To the solution was added a solution of **3.34** (0.48 mL, 4.4 mmol) in dry THF (0.66 mL) dropwise over 5 minutes. Resulting mixture was allowed to stir at  $-78$  °C for 30 min and then a solution of **3.33** (0.39 mL, 4.4 mmol) in THF (0.66 mL) was added dropwise. The resulting solution was stirred at  $-78$  °C for an hour and then warmed to room temperature over 1 hour.  $1\text{N HCl}$  (4.4 mL) was added dropwise and the resulting mixture was allowed to stir at room temperature for 30 minutes. The THF layer was separated and the aqueous layer was extracted with DCM (x3). Organics were combined, dried ( $\text{MgSO}_4$ ), filtered, and concentrated under reduced pressure. Residue was purified via column chromatography using 1:1 hexanes:EtOAc as eluents to afford **3.35** (81 mg).  $^1\text{H}$  NMR (300 MHz,  $\text{CDCl}_3$ )  $\delta$  8.21 (s, 1H), 7.46 (s, 1H), 4.38 (q,  $J = 7.2$  Hz, 2H), 2.01 (s, 3H), 1.39 (t,  $J = 7.1$  Hz, 3H).  $^{19}\text{F}$  NMR (282 MHz,  $\text{CDCl}_3$ )  $\delta$  -62.05.

### ethyl (2R,3R)-4,4,4-trifluoro-2-formamido-3-methylbutanoate (3.36):

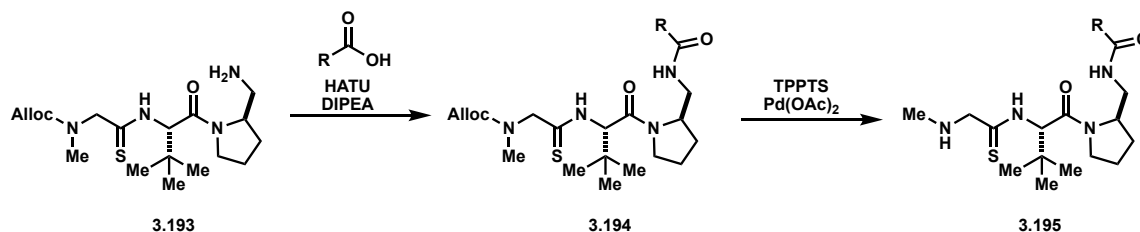
TCFP-Rh (1 mg, 0.0019 mmol) was suspended in dry MeOH (0.2 mL) and allowed to stir at room temperature under argon for 30 min. A solution of **3.35** (43 mg, 0.19 mmol) in dry MeOH (0.2 mL) was added and resulting mixture was placed under  $\text{H}_2$  atmosphere ( $\sim 120$  psi) and stirred at  $60$  °C overnight. Reaction mixture was filtered through a plug of celite and filtrate was concentrated under reduced pressure to afford **3.36** (33 mg).  $^1\text{H}$

NMR (300 MHz, CDCl<sub>3</sub>) δ 8.24 (s, 1H), 7.81 (br, 1H), 5.10 (q, *J* = 4.4 Hz, 1H), 4.23 (q, *J* = 7.1 Hz, 2H), 3.05 (m, 1H), 1.21 (d, *J* = 7.2 Hz, 3H). <sup>19</sup>F NMR (282 MHz, CDCl<sub>3</sub>) δ -71.47.

**(1*s*,3*R*)-3-butyl-*N*-(((*R*)-1-((2*R*,3*R*)-4,4,4-trifluoro-3-methyl-2-(2-(methylamino)acetamido)butanoyl)pyrrolidin-2-yl)methyl)cyclobutane-1-carboxamide (3.37):**

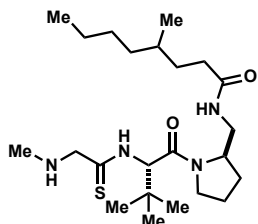
Following standard peptide synthesis conditions outlined above, **3.36** could be elaborated to **3.37** which was purified *via* preparative HPLC. <sup>1</sup>H NMR (300 MHz, CDCl<sub>3</sub>) δ 5.08 (t, *J* = 6.6 Hz, 1H), 4.13 (s, 1H), 3.70 (q, *J* = 6.4 Hz, 1H), 3.54 (t, *J* = 8.8 Hz, 1H), 3.41 (m, 2H), 3.22 (m, 1H), 2.99 (m, 2H), 2.39 (s, 2H), 2.31 (m, 2H), 2.00 (m, 2H), 1.86 (m, 4H), 1.49 (m, 2H), 1.32 (q, *J* = 6.6 Hz, 2H), 1.23 (m, 9H), 0.92 (t, *J* = 7.1 Hz, 3H). <sup>19</sup>F NMR (282 MHz, CDCl<sub>3</sub>) δ -72.55 (d, *J* = 8.9 Hz). HPLC/MS MH<sup>+</sup> 463.3.

**Preparation of Sidechain-Modified Inhibitors**



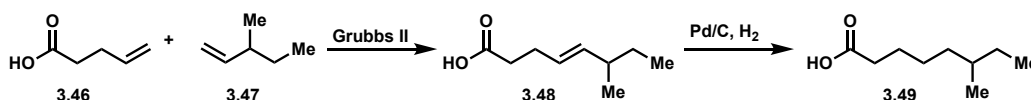
**General Procedure:** For sidechain modifications, the desired sidechain was coupled to **3.193** following GP 2 to afford **3.194**. Next, the Alloc protecting group could be removed following GP 6 to afford the final product derivative of **3.195**. Compounds were then purified by preparative HPLC.

***N*-(((*R*)-1-(((*S*)-3,3-dimethyl-2-(2-(methylamino)ethanethioamido)-butanoyl)pyrrolidin-2-yl)methyl)-4-methyloctanamide (3.55):**



$^1\text{H}$  NMR (500 MHz,  $\text{CD}_3\text{CN}$ )  $\delta$  6.76 (s, 1H), 5.26 (s, 1H), 4.19 (d,  $J = 14.6$  Hz, 1H), 4.07 (s, 1H), 4.01 (d,  $J = 14.9$  Hz, 1H), 3.84 (s, 1H), 3.61 (m, 1H), 3.29 (m, 1H), 3.16 (s, 1H), 2.72 (s, 3H), 2.11 (m, 2H), 1.88 (m, 2H), 1.80 (m, 1H), 1.57 (m, 1H), 1.35 (m, 1H), 1.26 (m, 8H), 1.11 (m, 1H), 1.05 (s, 9H), 0.89 (t,  $J = 6.7$  Hz, 3H), 0.86 (d,  $J = 6.3$  Hz, 3H).  $^{13}\text{C}$  NMR (126 MHz, Acetone)  $\delta$  194.57, 173.62, 175.0, 64.17, 57.46, 55.85, 47.92, 39.67, 36.34 (d,  $J = 3.3$  Hz, 1C), 35.72, 33.68, 32.85, 32.77, 32.74, 32.36, 32.31, 27.49, 26.13, 23.29, 22.76, 22.75, 18.85, 13.51. HPLC/MS  $\text{MH}^+$  441.4.

**Synthesis of 3.49**



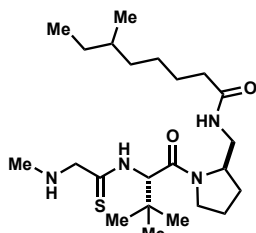
**(*E*)-6-methyloct-4-enoic acid (3.48):**

A solution of **3.46** (0.20 mL, 2 mmol) and **3.47** (1.26 mL, 10 mmol) in  $\text{CH}_2\text{Cl}_2$  (40 mL) was sparged with argon for 30 minutes before addition of Grubbs II (85 mg, 0.1 mmol). The resulting solution was sparged with argon for 10 minutes before heating to 40 °C. Reaction was allowed to stir at 40 °C until completion as determined by TLC. Reaction mixture was concentrated under reduced pressure and resultant residue was purified by column chromatography to afford **3.48** (230 mg, 75%).  $^1\text{H}$  NMR (400 MHz,  $\text{CDCl}_3$ )  $\delta$  11.38 (br, 1H), 5.35 (t,  $J = 5.4$  Hz, 2H), 2.42 (q, 3H), 2.32 (m, 2H), 1.97 (m, 1H), 1.27 (m, 3H), 0.94 (d,  $J = 6.7$  Hz, 3H), 0.82 (t,  $J = 7.4$  Hz, 3H).

**6-methyloctanoic acid (3.49):**

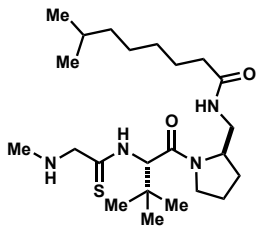
To a solution of **3.48** (215 mg, 1.38 mmol) in MeOH (20 mL) under argon was carefully added Pd/C (10 wt% Pd/C, 147 mg, 0.138 mmol). The argon was then replaced with an H<sub>2</sub> balloon and head space was filled, evacuated, and refilled (x3) and then resulting mixture was allowed to stir under an H<sub>2</sub> atmosphere until completion as determined by TLC. Upon completion, reaction was diluted with MeOH and filtered through a plug of celite to remove Pd. Filter cake was rinsed with additional MeOH and filtrate was concentrated under reduced pressure to afford **3.49** (188 mg) which was used without further purification. <sup>1</sup>H NMR (500 MHz, CDCl<sub>3</sub>) δ 10.58 (s, 1H), 2.35 (t, *J* = 7.5 Hz, 2H), 1.61 (m, *J* = 6.8 Hz, 2H), 1.32 (t, *J* = 5.8 Hz, 5H), 1.12 (m, *J* = 5.8 Hz, 2H), 0.85 (q, *J* = 5.1 Hz, 6H). <sup>13</sup>C NMR (126 MHz, CDCl<sub>3</sub>) δ 180.4, 38.7, 34.1, 29.3, 27.9, 27.0, 24.7, 22.2.

***N*-(((*R*)-1-(((*S*)-3,3-dimethyl-2-(2-(methylamino)ethanethiolamido)-butanoyl)pyrrolidin-2-yl)methyl)-6-methyloctanamide (3.56):**



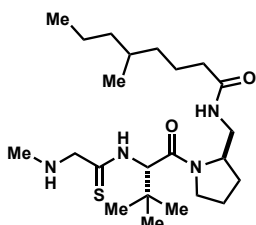
<sup>1</sup>H NMR (500 MHz, CD<sub>3</sub>CN) δ 9.36 (s, 1H), 6.79 (s, 1H), 5.26 (d, *J* = 7.8 Hz, 1H), 4.22 (d, *J* = 14.4 Hz, 1H), 4.10 (s, 1H), 4.00 (d, *J* = 14.5 Hz, 1H), 3.82 (t, *J* = 7.0 Hz, 1H), 3.62 (d, *J* = 8.8 Hz, 1H), 3.29 (s, 2H), 3.16 (s, 1H), 2.75 (s, 3H), 2.11 (t, *J* = 7.3 Hz, 2H), 1.88 (m, 3H), 1.79 (d, *J* = 8.7 Hz, 1H), 1.52 (s, 2H), 1.29 (m, 5H), 1.12 (m, 3H), 1.05 (s, 9H), 0.86 (m, 6H). <sup>13</sup>C NMR (126 MHz, CD<sub>3</sub>CN) δ 194.28, 64.30, 57.12, 55.84, 47.99, 39.83, 36.02, 35.70, 34.15, 33.22, 29.18, 27.38, 26.41, 25.93 (d, *J* = 4.0 Hz, 1C), 23.28, 18.52, 10.71. HPLC/MS MH<sup>+</sup> 441.3.

***N*-(((*R*)-1-(((*S*)-3,3-dimethyl-2-(2-(methylamino)ethanethioamido)-butanoyl)pyrrolidin-2-yl)methyl)-7-methyloctanamide (3.57):**



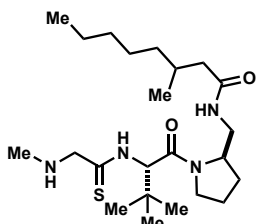
$^1\text{H}$  NMR (500 MHz,  $\text{CD}_3\text{CN}$ )  $\delta$  9.28 (s, 1H), 6.75 (s, 1H), 5.26 (s, 1H), 4.19 (d,  $J = 14.7$  Hz, 1H), 4.10 (s, 1H), 4.00 (d,  $J = 14.7$  Hz, 1H), 3.82 (d,  $J = 6.9$  Hz, 1H), 3.63 (t,  $J = 8.1$  Hz, 1H), 3.23 (s, 2H), 2.74 (s, 3H), 2.10 (t,  $J = 7.1$  Hz, 2H), 1.89 (m, 2H), 1.79 (m, 1H), 1.52 (m, 3H), 1.28 (m, 4H), 1.17 (q,  $J = 7.1$  Hz, 2H), 1.05 (s, 9H), 0.87 (d,  $J = 6.6$  Hz, 6H).  $^{13}\text{C}$  NMR (126 MHz, Acetone)  $\delta$  194.53, 64.19, 57.19, 55.89, 48.79, 47.97, 39.61, 38.77, 35.73, 33.10, 27.75, 27.33, 27.00, 26.10, 25.74, 23.29, 22.02. HPLC/MS  $\text{MH}^+$  441.3.

***N*-(((*R*)-1-(((*S*)-3,3-dimethyl-2-(2-(methylamino)ethanethioamido)-butanoyl)pyrrolidin-2-yl)methyl)-5-methyloctanamide (3.58):**



$^1\text{H}$  NMR (500 MHz,  $\text{CD}_3\text{CN}$ )  $\delta$  9.41 (s, 1H), 6.83 (s, 1H), 5.26 (d,  $J = 8.3$  Hz, 1H), 4.25 (d,  $J = 14.9$  Hz, 1H), 4.11 (s, 1H), 4.00 (d,  $J = 14.8$  Hz, 1H), 3.83 (q,  $J = 5.9$  Hz, 1H), 3.62 (q,  $J = 8.4$  Hz, 1H), 3.28 (s, 2H), 3.11 (s, 1H), 2.75 (s, 3H), 2.09 (t,  $J = 7.2$  Hz, 2H), 1.89 (m, 3H), 1.79 (d,  $J = 7.8$  Hz, 1H), 1.56 (q,  $J = 6.1$  Hz, 1H), 1.51 (q,  $J = 5.4$  Hz, 1H), 1.40 (m, 1H), 1.30 (m, 5H), 1.10 (m, 2H), 1.05 (s, 9H), 0.87 (m, 6H).  $^{13}\text{C}$  NMR (126 MHz,  $\text{CD}_3\text{CN}$ )  $\delta$  194.31, 167.78, 64.29, 57.06, 55.81, 54.62, 48.91, 48.01, 39.80, 39.01 (d,  $J = 4.1$  Hz, 1C), 36.26 (d,  $J = 12.3$  Hz, 1C), 35.72, 33.25, 32.08, 27.34, 25.92, 23.22 (d,  $J = 6.7$  Hz, 1C), 19.81 (d,  $J = 2.2$  Hz, 1C), 18.88 (d,  $J = 3.6$  Hz, 1C), 13.69. HPLC/MS  $\text{MH}^+$  441.3.

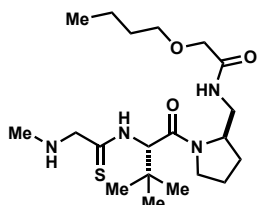
***N*-(((*R*)-1-(((*S*)-3,3-dimethyl-2-(2-(methylamino)ethanethioamido)butanoyl)-pyrrolidin-2-yl)methyl)-3-methyloctanamide (3.59):**



$^1\text{H}$  NMR (500 MHz,  $\text{CD}_3\text{CN}$ )  $\delta$  9.54 (s, 1H), 6.86 (s, 1H), 5.26 (d,  $J = 8.2$  Hz, 1H), 4.31 (d,  $J = 15.1$  Hz, 1H), 4.11 (s, 1H), 4.01 (d,  $J = 15.3$  Hz, 1H), 3.85 (t,  $J = 8.1$  Hz, 1H), 3.61 (q,  $J = 8.5$  Hz, 1H), 3.35 (d,  $J = 12.5$  Hz, 1H), 3.28 (s, 1H), 2.99 (m, 1H), 2.75 (s, 3H), 2.11

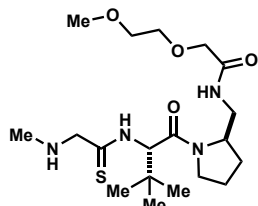
(m, 1H), 1.87 (m, 4H), 1.78 (m, 1H), 1.27 (m, 7H), 1.15 (q,  $J = 6.6$  Hz, 1H), 1.05 (s, 9H), 0.88 (m,  $J = 3.3$  Hz, 6H).  $^{13}\text{C}$  NMR (126 MHz,  $\text{CD}_3\text{CN}$ )  $\delta$  194.42, 64.34, 57.01, 55.70, 48.91, 47.99, 43.72, 39.68, 36.41 (d,  $J = 4.2$  Hz, 1C), 35.75, 33.22, 31.84, 31.81, 30.70, 30.63, 27.31, 26.35, 26.33, 25.94, 23.14, 22.39, 22.38, 19.01, 18.93, 13.39. HPLC/MS  $\text{MH}^+$  441.3.

**2-butoxy-*N*-(((*R*)-1-((*S*)-3,3-dimethyl-2-(2-(methylamino)ethanethioamido)-butanoyl)pyrrolidin-2-yl)methyl)acetamide (3.60):**



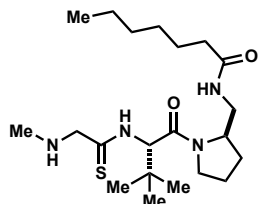
$^1\text{H}$  NMR (500 MHz, DMSO)  $\delta$  10.42 (s, 1H), 8.82 (s, 1H), 7.74 (t,  $J = 6.0$  Hz, 1H), 5.18 (s, 1H), 4.06 (t,  $J = 6.4$  Hz, 2H), 3.83 (d,  $J = 13.1$  Hz, 1H), 3.79 (s, 2H), 3.58 (q,  $J = 8.6$  Hz, 1H), 3.43 (t,  $J = 6.7$  Hz, 1H), 3.39 (t,  $J = 6.6$  Hz, 2H), 3.22 (t,  $J = 3.9$  Hz, 2H), 2.57 (s, 3H), 1.84 (m,  $J = 9.8$  Hz, 3H), 1.76 (m,  $J = 3.5$  Hz, 2H), 1.50 (m,  $J = 7.1$  Hz, 3H), 1.32 (m,  $J = 7.4$  Hz, 3H), 1.06 (s, 1H), 1.00 (s, 9H), 0.86 (t,  $J = 7.4$  Hz, 3H).  $^{13}\text{C}$  NMR (126 MHz, DMSO)  $\delta$  194.52, 169.94, 167.37, 70.99, 70.19, 64.05, 57.39, 48.10, 39.02, 35.93, 33.11, 31.48, 27.57, 27.29, 26.93, 23.64, 19.16. HPLC/MS  $\text{MH}^+$  415.3.

***N*-(((*R*)-1-((*S*)-3,3-dimethyl-2-(2-(methylamino)ethanethioamido)butanoyl)-pyrrolidin-2-yl)methyl)-2-(2-methoxyethoxy)acetamide (3.61):**



$^1\text{H}$  NMR (500 MHz, DMSO)  $\delta$  10.43 (s, 1H), 8.76 (s, 1H), 7.77 (t,  $J = 6.0$  Hz, 1H), 5.21 (s, 1H), 4.05 (d,  $J = 6.1$  Hz, 1H), 3.84 (s, 2H), 3.81 (t,  $J = 4.2$  Hz, 1H), 3.58 (d,  $J = 9.0$  Hz, 1H), 3.54 (q,  $J = 3.1$  Hz, 2H), 3.46 (q,  $J = 3.1$  Hz, 3H), 3.25 (s, 3H), 3.22 (t,  $J = 6.1$  Hz, 2H), 2.57 (s, 3H), 1.83 (m, 6H), 1.00 (s, 9H).  $^{13}\text{C}$  NMR (126 MHz, Acetone)  $\delta$  194.83, 170.27, 167.69, 71.47, 70.55, 70.10, 64.07, 58.05, 57.21, 48.74, 47.92, 39.78, 35.54, 27.68, 26.09, 23.53. HPLC/MS  $\text{MH}^+$  417.3.

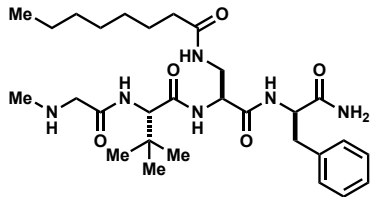
***N*-(((*R*)-1-(((*S*)-3,3-dimethyl-2-(2-(methylamino)ethanethioamido)-butanoyl)pyrrolidin-2-yl)methyl)heptanamide (3.62):**



$^1\text{H}$  NMR (500 MHz, Acetone)  $\delta$  7.06 (s, 1H), 5.26 (s, 1H), 4.11 (d,  $J$  = 2.2 Hz, 1H), 3.96 (m, 1H), 3.73 (m, 2H), 3.57 (m, 3H), 3.38 (q,  $J$  = 6.5 Hz, 1H), 3.29 (m, 1H), 2.45 (s, 3H), 2.09 (q,  $J$  = 6.2 Hz, 1H), 1.98 (m,  $J$  = 3.7 Hz, 1H), 1.88 (m,  $J$  = 5.7 Hz, 1H), 1.55 (t,  $J$  = 6.6 Hz, 1H), 1.28 (s, 1H), 1.08 (s, 9H), 0.86 (t,  $J$  = 4.5 Hz, 3H).  $^{13}\text{C}$  NMR (126 MHz, Acetone)  $\delta$  172.33, 168.25, 62.13, 57.65, 47.93, 40.32, 36.02, 35.44, 34.98, 31.74, 31.47, 27.91, 26.13, 25.52, 23.56, 22.34, 13.44. HPLC/MS  $\text{MH}^+$  413.3.

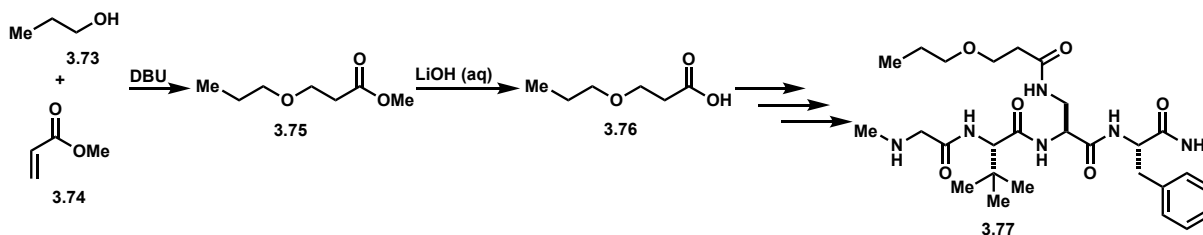
## C2. Linear Peptidomimetic Inhibitors

**Sar-Tle-Dap(Octanoyl)-D-Phe-NH<sub>2</sub> (3.72):**



Following GP 11, Fmoc-D-Phe-OH, Fmoc-Dap(Alloc)-OH, Fmoc-Tle-OH, and Fmoc-Sar-OH were coupled. Alloc was removed following GP 7 and then octanoic acid was coupled following GP 11 to afford compound **3.72**.  $^1\text{H}$  NMR (500 MHz, MeOD)  $\delta$  7.27 (d,  $J$  = 4.3 Hz, 4H), 7.19 (m, 1H), 4.63 (m, 1H), 4.33 (m, 1H), 4.07 (s, 1H), 3.97 (s, 2H), 3.35 (d,  $J$  = 5.0 Hz, 2H), 3.17 (dd,  $J$  = 5.1, 13.6 Hz, 1H), 2.95 (dd,  $J$  = 9.6, 13.8 Hz, 1H), 2.77 (s, 3H), 2.10 (t,  $J$  = 7.6 Hz, 2H), 1.55 (m, 2H), 1.29 (s, 8H), 1.05 (s, 9H), 0.89 (t,  $J$  = 6.9 Hz, 3H).  $^{13}\text{C}$  NMR (126 MHz,  $\text{CDCl}_3$ )  $\delta$  176.43, 174.86, 171.20, 170.00, 166.46, 137.12, 129.02, 128.08, 126.36, 63.40, 54.25, 49.39, 40.56, 37.74, 35.58, 35.52, 32.98, 32.32, 31.47, 28.93, 28.74, 25.87, 25.39, 22.27, 13.00. HPLC/MS  $\text{MH}^+$  561.4.

## Preparation of 3.77



### methyl 3-propoxypropanoate (3.75):

To a solution of methyl acrylate (2.63 mL, 29.0 mmol) in 1-propanol (7.89 mL, 105.5 mmol) was added DBU (0.22 mL, 1.45 mmol) dropwise. The resulting mixture was allowed to stir at room temperature overnight. The solution was diluted with EtOAc and washed with saturated aqueous NH<sub>4</sub>Cl (x2). Organics were dried (MgSO<sub>4</sub>), filtered, and concentrated under reduced pressure to afford **3.75** (1.26 g) in 30% yield which was used without further purification. <sup>1</sup>H NMR (500 MHz, CDCl<sub>3</sub>) δ 4.05 (m, 2H), 3.69 (m, 5H), 3.39 (t, *J* = 6.7 Hz, 2H), 2.57 (t, *J* = 6.4 Hz, 2H), 1.57 (quint., *J* = 7.1 Hz, 2H), 0.89 (t, *J* = 7.4 Hz, 3H).

### 3-propoxypropanoic acid (3.76):

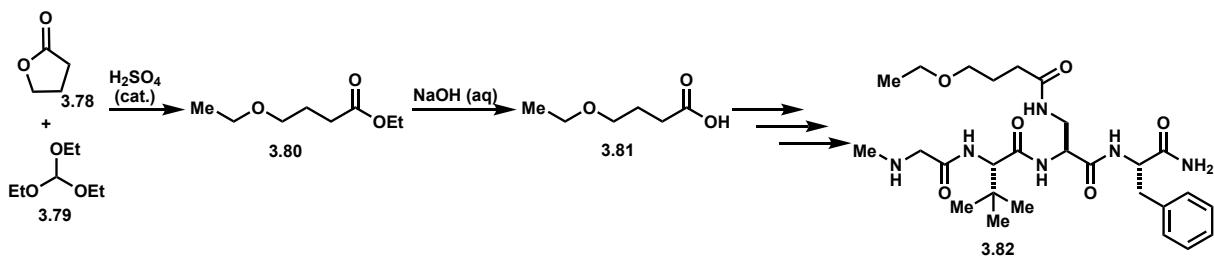
To a solution of **3.75** (1.26 g, 8.58 mmol) in THF/water (1:1, 5 mL) was added LiOH (306 mg, 12.75 mmol). The resulting mixture was stirred at room temperature overnight and then the THF was removed under reduced pressure. Resultant mixture was acidified to pH 2 with 1N HCl. The aqueous was then extracted with EtOAc (x2). Organics were combined, dried (MgSO<sub>4</sub>), filtered, and concentrated under reduced pressure to afford **3.76** (803 mg) in 71% yield. <sup>1</sup>H NMR (500 MHz, CDCl<sub>3</sub>) δ 11.29 (s, 1H), 3.70 (t, *J* = 6.3 Hz, 2H), 3.41 (t, *J* = 6.7 Hz, 2H), 2.62 (t, *J* = 6.3 Hz, 2H), 1.58 (quint., *J* = 7.1 Hz, 2H), 0.90 (t, *J* = 7.4 Hz, 3H). <sup>13</sup>C NMR (126 MHz, CDCl<sub>3</sub>) δ 177.47, 72.91, 65.63, 34.92, 22.69, 10.45.



**(S)-N-((S)-1-(((S)-1-amino-1-oxo-3-phenylpropan-2-yl)amino)-1-oxo-3-(3-propoxypropanamido)propan-2-yl)-3,3-dimethyl-2-(2-(methylamino)acetamido)butanamide (3.77):**

Following GP 11, Fmoc-Phe-OH, Fmoc-Dap(Alloc), Fmoc-Tle-OH, and Fmoc-Sar-OH were coupled. Following GP 7, the Alloc protecting group was removed and then **X** was coupled on resin following conditions outlined in GP 11 to afford **3.77**. <sup>1</sup>H NMR (500 MHz, MeOD) δ 7.25 (m, 5H), 4.60 (m, 1H), 4.40 (t, *J* = 6.1 Hz, 1H), 4.19 (s, 1H), 3.85 (d, *J* = 3.8 Hz, 2H), 3.65 (t, *J* = 6.4 Hz, 1H), 3.61 (m, 1H), 3.55 (m, 1H), 3.44 (m, 1H), 3.39 (t, *J* = 6.7 Hz, 2H), 3.32 (s, 2H), 3.15 (m, 1H), 3.13 (d, *J* = 5.7 Hz, 1H), 2.96 (m, 4H), 2.92 (m, 1H), 2.71 (s, 3H), 2.43 (t, *J* = 6.4 Hz, 2H), 1.56 (q, *J* = 7.0 Hz, 2H), 0.97 (s, 9H), 0.90 (t, *J* = 7.4 Hz, 3H). <sup>13</sup>C NMR (126 MHz, MeOD) δ 174.43, 173.43, 170.73, 170.09, 165.20, 136.93, 128.87, 128.08, 126.42, 72.34, 66.20, 61.67, 54.51, 53.23, 49.24, 40.36, 37.44, 36.15, 33.64, 32.23, 25.77, 22.39, 9.46. HPLC/MS MH<sup>+</sup> 550.3.

**Preparation of 3.82**



**ethyl 4-ethoxybutanoate (3.80):**

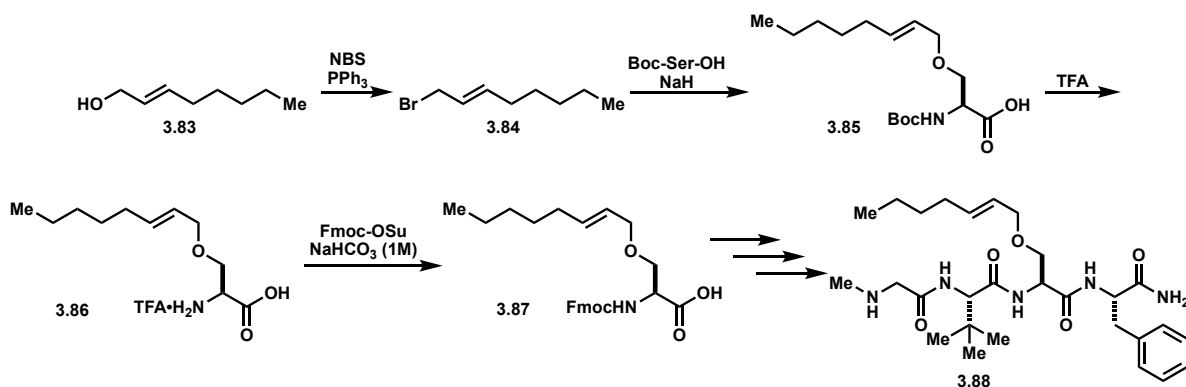
To a solution of  $\gamma$ -butyrolactone (1.77 mL, 23.2 mmol) and triethyl orthoformate (7.41 mL, 44.5 mmol) in EtOH (18 mL) at 0 °C was added  $\text{H}_2\text{SO}_4$  (0.04 mL, 0.81 mmol). Resulting solution was stirred at 50 °C for 12 hours and then cooled to room temperature. The reaction mixture was then concentrated under reduced pressure and quenched with saturated aqueous  $\text{NaHCO}_3$  and extracted with EtOAc (x2). Organics were combined, dried ( $\text{Na}_2\text{SO}_4$ ), filtered, and concentrated under reduced pressure to afford **3.80** (3.67 g)

in 99% yield.  $^1\text{H}$  NMR (500 MHz,  $\text{CDCl}_3$ )  $\delta$  4.11 (m, 2H), 3.44 (m, 4H), 2.37 (t,  $J = 7.4$  Hz, 2H), 1.88 (m, 2H), 1.24 (t,  $J = 7.1$  Hz, 3H), 1.17 (t,  $J = 7.0$  Hz, 3H).

#### 4-ethoxybutanoic acid (**3.81**):

To a solution of **3.80** (3.67g, 22.9 mmol) in THF (35 mL) at 0 °C was slowly added a solution of NaOH (2.17 g) in  $\text{H}_2\text{O}$  (21 mL). The resulting solution was allowed to warm to room temperature and then stir at room temperature overnight. The THF was removed under reduced pressure and the resultant solution was diluted with water and then acidified to pH 2 using 1N HCl. The solution was extracted with EtOAc (x3) and the combined organic extracts were dried ( $\text{Na}_2\text{SO}_4$ ), filtered, and concentrated under reduced pressure to afford **3.81** (2.76g) as a yellow oil which was used without further purification.  $^1\text{H}$  NMR (500 MHz,  $\text{CDCl}_3$ )  $\delta$  11.37 (br, 1H), 3.47 (m,  $J = 3.5$  Hz, 4H), 2.46 (t,  $J = 7.2$  Hz, 2H), 1.90 (quintet,  $J = 6.7$  Hz, 2H), 1.18 (t,  $J = 7.0$  Hz, 3H).  $^{13}\text{C}$  NMR (126 MHz,  $\text{CDCl}_3$ )  $\delta$  179.45, 69.33, 66.25, 31.08, 24.75, 15.07. HPLC/MS  $\text{MH}^+$  550.3.

#### Preparation of **3.88**



#### (E)-1-bromooct-2-ene (**3.84**):

To a solution of (E)-2-octen-1-ol (1.0 mL, 6.58 mmol) and  $\text{PPh}_3$  (1.9 g, 7.24 mmol) in  $\text{CH}_2\text{Cl}_2$  (34 mL) at -20 °C was added NBS (1.4g, 7.90 mmol). Resultant mixture was allowed to warm to room temperature and stir for 2h. Reaction mixture was then

concentrated to half the volume and diluted with hexanes and filtered. Filtrate was washed with H<sub>2</sub>O, brine, and organics were dried (MgSO<sub>4</sub>), filtered and concentrated under reduced pressure. Residue was passed through a plug of silica to afford **3.84** (1.2 g) in 93% yield. <sup>1</sup>H NMR (400 MHz, CDCl<sub>3</sub>) δ 5.73 (m, 2H), 3.95 (d, *J* = 7.4 Hz, 2H), 2.05 (q, *J* = 7.0 Hz, 2H), 1.38 (m, 1H), 1.28 (m, 4H), 0.88 (t, *J* = 6.9 Hz, 3H).

**(*E*)-*N*-(*tert*-butoxycarbonyl)-*O*-(*oct*-2-en-1-yl)-*L*-serine (**3.85**):**

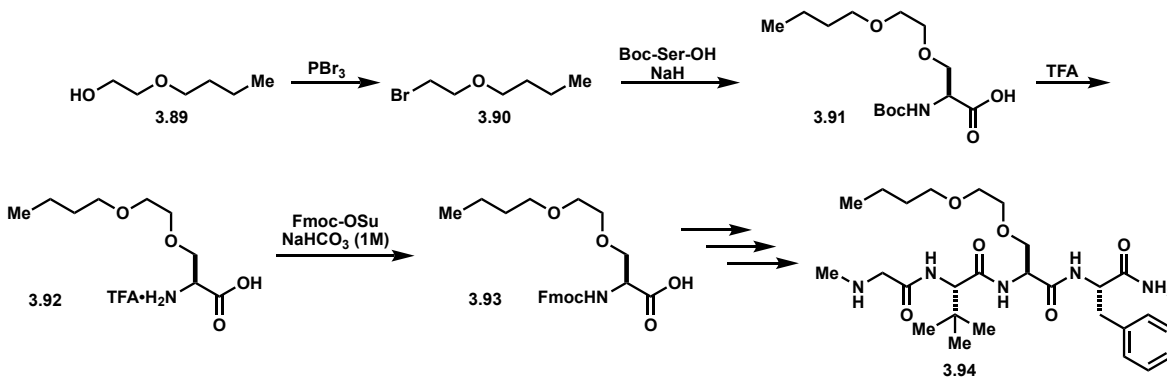
To a solution of Boc-Ser-OH (205 mg, 1.0 mmol) in DMF (5 mL) at 0 °C was added NaH (60% in mineral oil, 88 mg, 2.2 mmol). After evolution of H<sub>2</sub> ceased, **3.84** (0.17 mL, 1.0 mmol) was added and resultant mixture was allowed to stir at room temperature for 4 hours. Reaction mixture was concentrated under reduced pressure and dissolved in H<sub>2</sub>O (10 mL) and washed with ether (10 mL). The aqueous layer was acidified to pH 2 with 1N HCl and extracted with EtOAc (x3). Organics were dried (MgSO<sub>4</sub>), filtered and concentrated under reduced pressure to afford **3.85** (207 mg) in 66% yield. <sup>1</sup>H NMR (500 MHz, CDCl<sub>3</sub>) δ 5.69 (m, 1H), 5.49 (m, 1H), 5.38 (d, *J* = 7.6 Hz, 1H), 4.43 (s, 1H), 3.96 (d, *J* = 6.4 Hz, 2H), 3.87 (d, *J* = 6.6 Hz, 1H), 3.63 (dd, *J* = 4.4, 9.6 Hz, 2H), 2.04 (m, 2H), 1.45 (s, 9H), 1.37 (q, 2H), 1.28 (m, 4H), 0.88 (t, *J* = 7.0 Hz, 3H). HPLC/MS MH<sup>+</sup> 338.2 (+Na).

**(*S*)-*N*-(((*S*)-1-(((*S*)-1-amino-1-oxo-3-phenylpropan-2-yl)amino)-3-(((*E*)-hept-2-en-1-yl)oxy)-1-oxopropan-2-yl)-3,3-dimethyl-2-(2-(methylamino)acetamido)butanamide (**3.88**):**

Following GP 4, **3.85** was deprotected to afford **3.86** as the TFA salt which was used without purification. To a solution of **3.86** (142 mg, 0.66 mmol) in acetone:H<sub>2</sub>O (1:1, 3.4 mL) was added NaHCO<sub>3</sub> (1M, 0.73 mL, 0.73 mmol) followed by Fmoc-OSu (245 mg, 0.73 mmol) and resulting solution was allowed to stir at room temperature overnight. Reaction mixture was concentrated to dryness and residue was partitioned between CH<sub>2</sub>Cl<sub>2</sub> and H<sub>2</sub>O. Layers were separated and aqueous was extracted with CH<sub>2</sub>Cl<sub>2</sub> (x3). Organics were combined, dried (MgSO<sub>4</sub>), filtered, and concentrated under reduced pressure to afford the desired Fmoc-protected product **3.87** as a white solid that was used directly for solid phase peptide synthesis following GP 11 to afford **3.88**. <sup>1</sup>H NMR (500 MHz, MeOD) δ

7.24 (t,  $J = 3.0$  Hz, 8H), 5.71 (m,  $J = 7.2$  Hz, 1H), 5.49 (m,  $J = 7.0$  Hz, 1H), 4.59 (q,  $J = 4.7$  Hz, 3H), 4.50 (t,  $J = 6.3$  Hz, 2H), 4.27 (s, 2H), 3.93 (d,  $J = 6.3$  Hz, 3H), 3.82 (q,  $J = 14.9$  Hz, 3H), 3.57 (m,  $J = 5.6$  Hz, 3H), 3.19 (q,  $J = 6.4$  Hz, 2H), 2.92 (q,  $J = 7.6$  Hz, 2H), 2.69 (s, 6H), 2.04 (q,  $J = 6.9$  Hz, 4H), 1.38 (m,  $J = 7.3$  Hz, 4H), 1.30 (m,  $J = 4.7$  Hz, 10H), 0.95 (s, 17H), 0.89 (t,  $J = 7.0$  Hz, 7H).  $^{13}\text{C}$  NMR (126 MHz, MeOD)  $\delta$  135.36, 128.86, 128.07, 126.37, 71.67, 68.77, 54.33, 52.98, 37.09, 31.89, 31.16, 28.54, 25.75, 22.16, 12.97. HPLC/MS  $\text{MH}^+$  546.3, 568.3 (+  $\text{Na}^+$ ).

### Preparation of 3.94



#### 1-(2-bromoethoxy)butane (3.90):

In a round-bottom flask, 2-butoxyethanol (2.05 mL, 15.60 mmol) was cooled to 0 °C. After 15 minutes at 0 °C,  $\text{PBr}_3$  (0.73 mL, 7.81 mmol) was added dropwise over 10 minutes. The resultant mixture was allowed to slowly warm to room temperature and then stirred at room temperature overnight. Reaction mixture was carefully quenched with water and extracted with EtOAc (x3). Organics were dried ( $\text{MgSO}_4$ ), filtered, and concentrated under reduced pressure to afford **3.90** (2.4 g) in 85% yield.  $^1\text{H}$  NMR (500 MHz,  $\text{CDCl}_3$ )  $\delta$  3.73 (t,  $J = 6.3$  Hz, 2H), 3.49 (t,  $J = 6.6$  Hz, 2H), 3.45 (t,  $J = 6.3$  Hz, 2H), 1.57 (quintet,  $J = 6.8$  Hz, 2H), 1.38 (sextet,  $J = 7.3$  Hz, 2H), 0.92 (t,  $J = 7.4$  Hz, 3H).  $^{13}\text{C}$  NMR (126 MHz,  $\text{CDCl}_3$ )  $\delta$  71.04, 70.61, 31.69, 30.53, 19.25, 13.89.

#### N-(tert-butoxycarbonyl)-O-(2-butoxyethyl)-L-serine (3.91):

To a solution of Boc-Ser-OH (205 mg, 1.00 mmol) in DMF (5 mL) at 0 °C was added NaH (60% in mineral oil, 88 mg, 2.2 mmol). After evolution of H<sub>2</sub> ceased, **3.90** (181 mg, 1 mmol) was added and resulting mixture was allowed to stir at room temperature until completion as determined by TLC. Reaction mixture was concentrated under reduced pressure and resultant residue was dissolved in water (10 mL) and washed with ether (10 mL). Aqueous layer was then acidified to pH 2 with 1N HCl and extracted with EtOAc (x3). Organics were combined, dried (MgSO<sub>4</sub>), filtered, and concentrated under reduced pressure to afford **3.91**. Resultant residue was used without further purification. <sup>1</sup>H NMR (500 MHz, CDCl<sub>3</sub>) δ 4.41 (s, 1H), 3.95 (dd, *J* = 3.8, 10.1 Hz, 1H), 3.69 (m, 3H), 3.57 (m, 2H), 3.47 (m, 2H), 1.57 (quintet, *J* = 6.6 Hz, 2H), 1.45 (s, 9H), 1.35 (sextet, *J* = 7.6 Hz, 2H), 0.91 (t, *J* = 7.4 Hz, 3H).

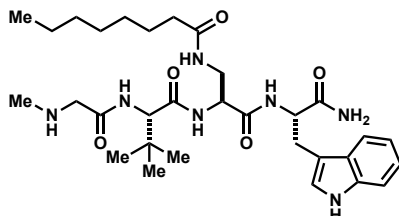
**(S)-N-((S)-1-(((S)-1-amino-1-oxo-3-phenylpropan-2-yl)amino)-3-(2-butoxyethoxy)-1-oxopropan-2-yl)-3,3-dimethyl-2-(2-(methylamino)acetamido)butanamide (3.94):**

Following GP 4, **3.91** was deprotected to afford **3.92** as the TFA salt which was used without purification. To a solution of **3.92** (166 mg, 0.81 mmol) in acetone:H<sub>2</sub>O (1:1, 4 mL) was added NaHCO<sub>3</sub> (1M, 0.81 mL, 0.81 mmol) followed by Fmoc-OSu (301 mg, 0.89 mmol) and resulting solution was allowed to stir at room temperature overnight. Reaction mixture was concentrated to dryness and residue was partitioned between CH<sub>2</sub>Cl<sub>2</sub> and H<sub>2</sub>O. Layers were separated and aqueous was extracted with CH<sub>2</sub>Cl<sub>2</sub> (x3). Organics were combined, dried (MgSO<sub>4</sub>), filtered, and concentrated under reduced pressure to afford the desired Fmoc-protected product **3.93** as a white solid that was used directly for solid phase peptide synthesis following GP 11 to afford **3.94**. <sup>1</sup>H NMR (500 MHz, Acetone) δ 7.24 (m, 5H), 4.58 (dd, *J* = 5.3, 8.8 Hz, 1H), 4.45 (t, *J* = 5.9 Hz, 1H), 4.19 (s, 1H), 3.66 (m, 2H), 3.58 (m, 3H), 3.52 (m, 3H), 3.46 (m, 2H), 3.21 (dd, *J* = 4.7, 14.0 Hz, 2H), 2.97 (dd, *J* = 9.0, 14.0 Hz, 1H), 2.50 (s, 1H), 1.49 (m, 2H), 1.33 (m, 2H), 0.97 (s, 9H), 0.87 (t, *J* = 7.4 Hz, 3H). <sup>13</sup>C NMR (126 MHz, CDCl<sub>3</sub>) δ 173.20, 170.64, 169.48, 137.89, 129.17, 128.16, 126.33, 70.56, 70.26, 70.17, 69.62, 61.24, 54.27, 53.53, 53.01, 37.13, 35.05, 33.86, 31.60, 26.20, 19.03, 13.26. HPLC/MS MH<sup>+</sup> 536.3.

## PREPARATION OF LINEAR TETRAPEPTIDES

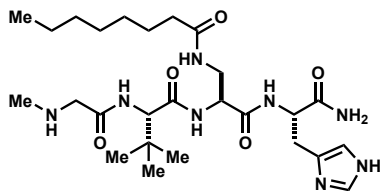
Unless otherwise noted, linear peptides were synthesized *via* solid phase peptide synthesis following GP 11.

### Sar-Tle-Dap(octanoyl)-Trp-NH<sub>2</sub> (3.96):

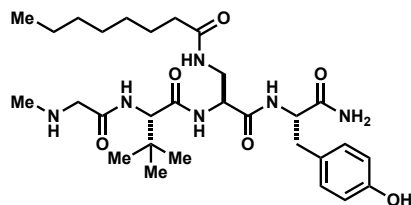


<sup>1</sup>H NMR (500 MHz, MeOD)  $\delta$  7.61 (d,  $J$  = 7.8 Hz, 1H), 7.31 (d,  $J$  = 8.1 Hz, 1H), 7.11 (s, 1H), 7.08 (t,  $J$  = 7.6 Hz, 1H), 7.00 (t,  $J$  = 7.4 Hz, 1H), 4.66 (t,  $J$  = 6.8 Hz, 1H), 4.58 (s, 1H), 4.35 (t,  $J$  = 5.9 Hz, 1H), 4.15 (s, 1H), 3.75 (m, 2H), 3.52 (dd,  $J$  = 6.7, 13.8 Hz, 1H), 3.41 (d,  $J$  = 5.6 Hz, 1H), 3.20 (dd,  $J$  = 7.4, 14.3 Hz, 2H), 2.64 (s, 3H), 2.09 (m, 2H), 1.54 (m, 2H), 1.28 (s, 8H), 0.96 (s, 9H), 0.89 (t,  $J$  = 7.0 Hz, 3H). HPLC/MS MH<sup>+</sup> 602.4.

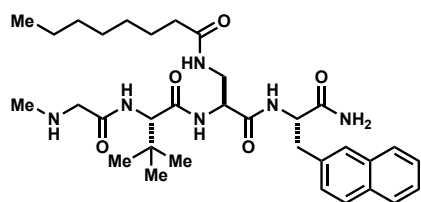
### Sar-Tle-Dap(octanoyl)-His-NH<sub>2</sub> (3.97):



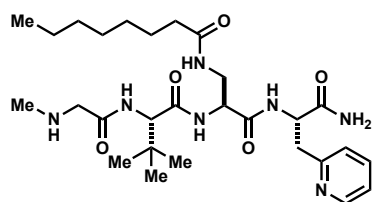
<sup>1</sup>H NMR (500 MHz, MeOD)  $\delta$  8.72 (s, 1H), 7.35 (s, 1H), 4.66 (dd,  $J$  = 5.5, 7.4 Hz, 1H), 4.34 (t,  $J$  = 5.8 Hz, 1H), 4.22 (s, 1H), 3.89 (dd,  $J$  = 15.5, 20.5 Hz, 2H), 3.59 (dd,  $J$  = 6.4, 14.1 Hz, 1H), 3.44 (dd,  $J$  = 5.3, 14.0 Hz, 1H), 3.08 (dd,  $J$  = 7.6, 14.4 Hz, 1H), 2.73 (s, 3H), 2.17 (t,  $J$  = 7.7 Hz, 2H), 1.57 (m, 2H), 1.30 (s, 8H), 1.02 (s, 9H), 0.89 (t,  $J$  = 6.9 Hz, 3H). HPLC/MS MH<sup>+</sup> 552.4.

**Sar-Tle-Dap(octanoyl)-Tyr-NH<sub>2</sub> (3.98):**

<sup>1</sup>H NMR (500 MHz, MeOD) δ 7.06 (d, *J* = 8.4 Hz, 2H), 6.67 (d, *J* = 8.5 Hz, 2H), 4.51 (dd, *J* = 5.4, 8.1 Hz, 1H), 4.38 (t, *J* = 5.9 Hz, 1H), 4.19 (s, 1H), 3.84 (dd, *J* = 15.7, 22.0 Hz, 2H), 3.54 (dd, *J* = 6.3, 13.9 Hz, 1H), 3.41 (dd, *J* = 5.4, 13.9 Hz, 1H), 3.03 (dd, *J* = 5.8, 13.9 Hz, 1H), 2.87 (dd, *J* = 8.1, 13.9 Hz, 1H), 2.71 (s, 3H), 2.16 (m, 2H), 1.57 (m, 2H), 1.30 (s, 8H), 0.98 (s, 9H), 0.89 (t, *J* = 6.7 Hz, 3H). HPLC/MS MH<sup>+</sup> 579.5.

**Sar-Tle-Dap(octanoyl)-2-Nal-NH<sub>2</sub> (3.99):**

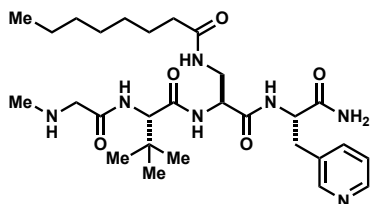
<sup>1</sup>H NMR (500 MHz, MeOD) δ 8.23 (t, *J* = 8.5 Hz, 2H), 8.14 (d, *J* = 7.7 Hz, 1H), 7.85 (d, *J* = 8.0 Hz, 1H), 7.74 (q, *J* = 3.1 Hz, 1H), 7.54 (m, 1H), 7.48 (m, 1H), 7.36 (m, 2H), 4.76 (q, *J* = 7.4 Hz, 1H), 4.36 (q, *J* = 6.2 Hz, 1H), 4.16 (s, 1H), 3.86 (q, *J* = 5.8 Hz, 2H), 3.58 (m, 2H), 3.46 (dd, *J* = 6.2, 14.0 Hz, 1H), 3.40 (dd, *J* = 5.2, 13.7 Hz, 2H), 2.70 (s, 3H), 2.15 (t, *J* = 7.6 Hz, 2H), 1.57 (q, *J* = 7.3 Hz, 2H), 1.29 (s, 8H), 0.97 (s, 9H), 0.89 (t, *J* = 7.0 Hz, 3H). <sup>13</sup>C NMR (126 MHz, MeOD) δ 171.2, 132.86, 128.44, 127.24, 127.92, 125.90, 125.32, 125.02, 123.30, 61.94, 54.05, 49.23, 40.5 38.70, 35.64, 32.19, 31.50, 29.00, 25.77, 25.50, 22.3. HPLC/MS MH<sup>+</sup> 611.3.

**Sar-Tle-Dap(octanoyl)-2-Pal-NH<sub>2</sub> (3.101):**

<sup>1</sup>H NMR (500 MHz, MeOD) δ 8.72 (s, 1H), 8.42 (t, *J* = 7.8 Hz, 1H), 7.94 (d, *J* = 7.6 Hz, 1H), 7.86 (t, *J* = 6.4 Hz, 1H), 4.84 (t, *J* = 4.0 Hz, 1H), 4.29 (t, *J* = 5.6 Hz, 1H), 4.18 (s, 1H), 3.90 (s, 2H), 3.61 (m, 2H), 3.39 (dd, *J* = 4.9, 14.0 Hz, 1H), 3.33 (d, *J* = 8.3 Hz, 1H), 3.10

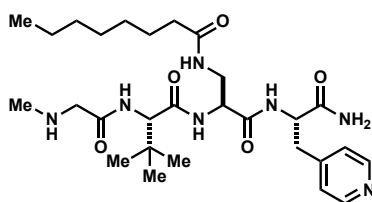
(s, 1H), 2.74 (s, 3H), 2.16 (t,  $J = 7.6$  Hz, 2H), 1.56 (t,  $J = 6.9$  Hz, 2H), 1.29 (s, 8H), 0.99 (s, 9H), 0.89 (t,  $J = 6.8$  Hz, 3H).  $^{13}\text{C}$  NMR (126 MHz, MeOD)  $\delta$  146.7, 141.6, 128.3, 125.2, 62.7, 55.0, 52.7, 49.5, 48.1, 41.1, 40.6, 39.7, 38.3, 36.3, 32.5, 30.5, 26.2, 25.6, 25.0.

**Sar-Tle-Dap(octanoyl)-3-Pal-NH<sub>2</sub> (3.196):**



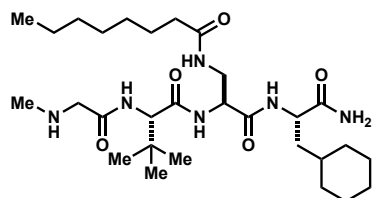
$^1\text{H}$  NMR (500 MHz, MeOD)  $\delta$  8.78 (s, 1H), 8.72 (d,  $J = 5.3$  Hz, 1H), 8.52 (d,  $J = 8.1$  Hz, 1H), 8.38 (d,  $J = 8.1$  Hz, 1H), 8.17 (d,  $J = 6.5$  Hz, 1H), 7.97 (t,  $J = 6.9$  Hz, 1H), 4.75 (m, 1H), 4.29 (q,  $J = 5.5$  Hz, 1H), 4.18 (s, 1H), 3.90 (q,  $J = 5.8$  Hz, 2H), 3.56 (dd,  $J = 6.3, 13.8$  Hz, 1H), 3.43 (t,  $J = 4.5$  Hz, 1H), 3.41 (t,  $J = 4.4$  Hz, 1H), 3.15 (dd,  $J = 8.5, 14.1$  Hz, 1H), 2.73 (s, 3H), 2.17 (t,  $J = 7.6$  Hz, 2H), 1.57 (m, 2H), 1.29 (s, 8H), 0.98 (s, 9H), 0.89 (t,  $J = 6.9$  Hz, 3H).  $^{13}\text{C}$  NMR (126 MHz, MeOD)  $\delta$  144.7, 142.6, 139.2, 126.7, 62.7, 54.8, 54.3, 53.3, 49.4, 48.3, 40.5, 40.2, 35.8, 35.3, 35.0, 30.6, 26.4, 25.3, 24.3.

**Sar-Tle-Dap(octanoyl)-4-Pal-NH<sub>2</sub> (3.102):**

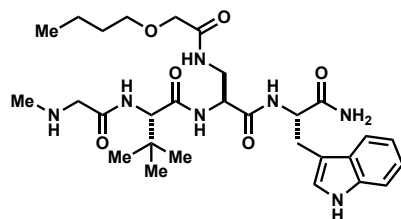


$^1\text{H}$  NMR (500 MHz, MeOD)  $\delta$  8.72 (d,  $J = 5.6$  Hz, 2H), 8.45 (d,  $J = 8.4$  Hz, 1H), 8.15 (d,  $J = 6.7$  Hz, 1H), 7.98 (d,  $J = 6.1$  Hz, 2H), 4.83 (dd,  $J = 5.1, 9.1$  Hz, 1H), 4.29 (q,  $J = 5.5$  Hz, 1H), 4.16 (s, 1H), 3.89 (q,  $J = 12.7$  Hz, 2H), 3.58 (dd,  $J = 6.5, 14.0$  Hz, 1H), 3.52 (dd,  $J = 4.8, 14.2$  Hz, 1H), 3.41 (dd,  $J = 5.4, 14.0$  Hz, 1H), 3.20 (dd,  $J = 9.2, 13.8$  Hz, 1H), 2.73 (s, 3H), 2.17 (t,  $J = 7.6$  Hz, 2H), 1.57 (m, 2H), 1.29 (s, 8H), 0.98 (s, 9H), 0.89 (t,  $J = 6.9$  Hz, 3H).  $^{13}\text{C}$  NMR (126 MHz, MeOD)  $\delta$  177.2, 175.7, 169.6, 141.6, 128.2, 62.4, 54.4, 52.8, 49.4, 48.2, 41.3, 39.4, 38.3, 36.4, 32.2, 25.6, 25.3, 24.5.

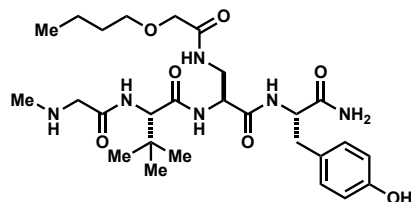


**Sar-Tle-Dap(octanoyl)-Cha-NH<sub>2</sub> (3.104):**

<sup>1</sup>H NMR (500 MHz, MeOD) δ 8.27 (d, *J* = 7.2 Hz, 1H), 8.13 (d, *J* = 7.6 Hz, 1H), 7.98 (t, *J* = 6.0 Hz, 1H), 4.42 (m, 2H), 4.25 (s, 1H), 3.86 (q, *J* = 5.1 Hz, 1H), 3.57 (m, 1H), 3.44 (m, 1H), 2.72 (s, 3H), 2.19 (t, *J* = 7.7 Hz, 3H), 1.81 (d, *J* = 12.4 Hz, 1H), 1.70 (d, *J* = 10.0 Hz, 3H), 1.60 (m, 5H), 1.39 (m, 1H), 1.30 (m, 9H), 1.21 (m, 3H), 1.02 (s, 9H), 0.89 (t, *J* = 7.0 Hz, 3H). <sup>13</sup>C NMR (126 MHz, MeOD) δ 171.7, 160.3, 61.5, 53.3, 51.0, 49.0, 33.6, 32.2, 31.4, 28.7, 26.0, 25.6, 25.4. HPLC/MS MH<sup>+</sup> 567.5.

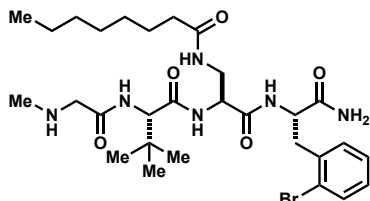
**Sar-Tle-Dap(2-butoxyacetyl)-Trp-NH<sub>2</sub> (3.197):**

<sup>1</sup>H NMR (500 MHz, MeOD) δ 8.22 (d, *J* = 6.9 Hz, 1H), 7.92 (d, *J* = 7.5 Hz, 1H), 7.88 (t, *J* = 6.2 Hz, 1H), 7.61 (d, *J* = 7.9 Hz, 1H), 7.32 (d, *J* = 8.1 Hz, 1H), 7.11 (s, 1H), 7.08 (dt, *J* = 1.1, 7.3 Hz, 1H), 7.00 (dt, *J* = 1.0, 7.2 Hz, 1H), 4.66 (m, 1H), 4.44 (m, 1H), 4.18 (s, 1H), 3.83 (m, 5H), 3.56 (m, 2H), 3.48 (t, *J* = 6.6 Hz, 2H), 3.26 (dd, *J* = 6.3, 15.1 Hz, 1H), 3.19 (dd, *J* = 6.8, 14.6 Hz, 1H), 2.70 (m, 1H), 2.67 (s, 1H), 1.58 (m, 2H), 1.37 (m, 2H), 0.96 (s, 9H), 0.92 (t, *J* = 7.4 Hz, 3H). <sup>13</sup>C NMR (126 MHz, MeOD) δ 174.86, 172.56, 171.10, 170.09, 165.30, 136.65, 127.44, 123.12, 121.08, 118.47, 118.01, 110.92, 109.39, 71.28, 69.37, 61.81, 54.01, 53.71, 49.25, 39.78, 33.50, 32.18, 31.20, 27.64, 25.70, 18.78, 12.83.

**Sar-Tle-Dap(2-butoxyacetyl)-Tyr-NH<sub>2</sub> (3.198):**

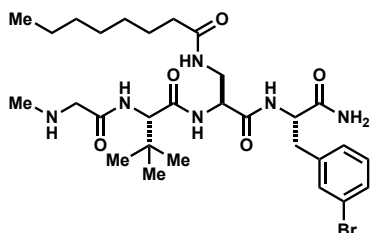
$^1\text{H}$  NMR (500 MHz, MeOD)  $\delta$  7.05 (d,  $J$  = 8.5 Hz, 2H), 6.67 (d,  $J$  = 8.5 Hz, 2H), 4.51 (t,  $J$  = 7.0 Hz, 1H), 4.42 (t,  $J$  = 5.8 Hz, 1H), 4.20 (s, 1H), 3.91 (d,  $J$  = 1.6 Hz, 2H), 3.85 (d,  $J$  = 2.7 Hz, 2H), 3.55 (m, 2H), 3.50 (t,  $J$  = 6.6 Hz, 2H), 3.02 (dd,  $J$  = 5.8, 14.0 Hz, 1H), 2.87 (dd,  $J$  = 8.0, 14.0 Hz, 1H), 2.72 (s, 3H), 1.59 (m, 2H), 1.39 (m, 2H), 0.99 (s, 9H), 0.93 (t,  $J$  = 7.4 Hz, 3H). HPLC/MS  $\text{MH}^+$  566.2.

**Sar-Tle-Dap(octanoyl)-2-Br-Phe-NH<sub>2</sub> (3.105):**



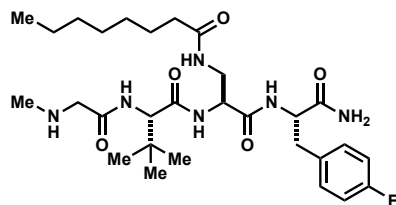
$^1\text{H}$  NMR (500 MHz, MeOD)  $\delta$  8.29 (d,  $J$  = 7.9 Hz, 1H), 8.16 (d,  $J$  = 7.2 Hz, 1H), 7.93 (t,  $J$  = 5.6 Hz, 1H), 7.53 (d,  $J$  = 7.9 Hz, 1H), 7.29 (d,  $J$  = 6.9 Hz, 1H), 7.24 (t,  $J$  = 7.4 Hz, 1H), 7.11 (t,  $J$  = 7.1 Hz, 1H), 4.73 (m, 1H), 4.44 (q,  $J$  = 5.3 Hz, 1H), 4.23 (s, 1H), 3.88 (q,  $J$  = 13.8 Hz, 2H), 3.56 (dd,  $J$  = 6.0, 13.8 Hz, 3H), 3.39 (dd,  $J$  = 5.2, 13.8 Hz, 1H), 3.34 (m, 2H), 3.07 (dd,  $J$  = 8.8, 13.9 Hz, 3H), 2.72 (s, 3H), 2.16 (t,  $J$  = 7.6 Hz, 2H), 1.57 (m, 2H), 1.29 (s, 8H), 0.97 (s, 9H), 0.89 (t,  $J$  = 6.8 Hz, 3H). HPLC/MS  $\text{MH}^+$  639.2, 641.2.

**Sar-Tle-Dap(octanoyl)-3-Br-Phe-NH<sub>2</sub> (3.106):**



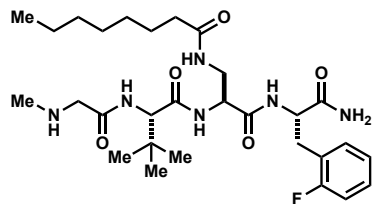
$^1\text{H}$  NMR (500 MHz, MeOD)  $\delta$  8.19 (d,  $J$  = 7.2 Hz, 1H), 8.17 (d,  $J$  = 7.9 Hz, 1H), 7.94 (t,  $J$  = 5.8 Hz, 1H), 7.45 (s, 1H), 7.35 (d,  $J$  = 8.0 Hz, 1H), 7.24 (d,  $J$  = 7.7 Hz, 1H), 7.18 (t,  $J$  = 7.8 Hz, 1H), 4.60 (m, 1H), 4.41 (m, 1H), 4.21 (s, 1H), 3.87 (q,  $J$  = 13.4 Hz, 2H), 3.54 (dd,  $J$  = 6.2, 13.6 Hz, 1H), 3.41 (dd,  $J$  = 5.5, 13.7 Hz, 1H), 3.15 (dd,  $J$  = 5.5, 13.7 Hz, 1H), 2.93 (dd,  $J$  = 8.2, 13.7 Hz, 1H), 2.72 (s, 3H), 2.16 (t,  $J$  = 7.6 Hz, 2H), 1.57 (m, 2H), 1.29 (s, 8H), 0.97 (s, 9H), 0.89 (t,  $J$  = 6.9 Hz, 3H). HPLC/MS  $\text{MH}^+$  639.2, 641.2.

**Sar-Tle-Dap(octanoyl)-4-F-Phe-NH<sub>2</sub> (3.107):**



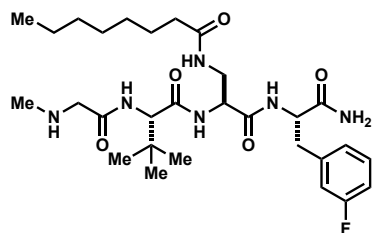
<sup>1</sup>H NMR (500 MHz, MeOD) δ 8.17 (d, *J* = 7.1 Hz, 1H), 8.11 (d, *J* = 7.8 Hz, 1H), 7.93 (t, *J* = 6.1 Hz, 1H), 7.26 (q, *J* = 4.7 Hz, 2H), 6.97 (t, *J* = 8.8 Hz, 2H), 4.57 (m, 1H), 4.38 (m, 1H), 4.19 (s, 1H), 3.84 (q, *J* = 11.1 Hz, 2H), 3.55 (dd, *J* = 6.2, 13.8 Hz, 1H), 3.41 (dd, *J* = 5.7, 13.8 Hz, 1H), 3.13 (dd, *J* = 5.2, 13.8 Hz, 1H), 2.92 (dd, *J* = 8.6, 13.8 Hz, 1H), 2.72 (s, 3H), 2.17 (t, *J* = 7.7 Hz, 2H), 1.57 (m, *J* = 7.4 Hz, 2H), 1.30 (s, 8H), 0.97 (s, 9H), 0.89 (t, *J* = 7.0 Hz, 3H). <sup>13</sup>C NMR (126 MHz, MeOD) δ 172.94, 170.77, 170.14, 165.10, 137.7, 132.9, 130.68, 130.61, 114.76, 114.59, 61.68, 54.52, 49.23, 40.41, 36.69, 35.66, 33.64, 32.19, 31.49, 28.95, 28.76, 25.72, 25.42, 22.28. HPLC/MS MH<sup>+</sup> 579.3.

**Sar-Tle-Dap(octanoyl)-2-F-Phe-NH<sub>2</sub> (3.108):**



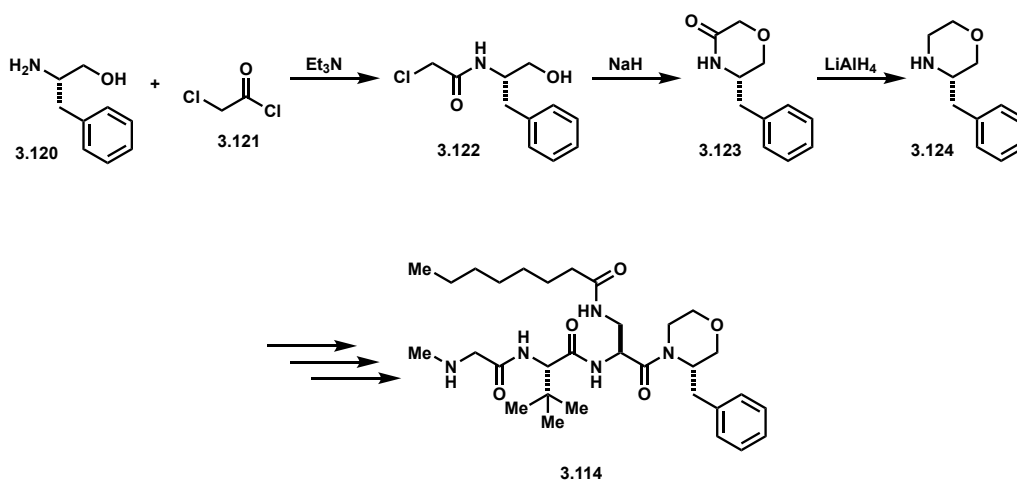
<sup>1</sup>H NMR (500 MHz, MeOD) δ 8.15 (dd, *J* = 9.8 Hz, 2H), 7.28 (dt, *J* = 1.6, 7.6 Hz, 1H), 7.22 (m, 1H), 7.07 (m, 1H), 7.02 (m, 1H), 4.63 (m, 1H), 4.37 (q, *J* = 4.7 Hz, 1H), 4.18 (s, 1H), 3.86 (q, *J* = 6.0 Hz, 2H), 3.56 (dd, *J* = 6.3, 13.8 Hz, 1H), 3.39 (dd, *J* = 5.1, 13.8 Hz, 1H), 3.20 (dd, *J* = 5.9, 13.8 Hz, 1H), 3.01 (dd, *J* = 8.3, 14.2 Hz, 1H), 2.72 (s, 3H), 2.17 (t, *J* = 7.7 Hz, 2H), 1.58 (m, 2H), 1.30 (s, 8H), 0.98 (s, 9H), 0.89 (t, *J* = 7.0 Hz, 3H). <sup>13</sup>C NMR (126 MHz, MeOD) δ 131.30, 130.90, 128.50, 124.00, 114.90, 112.30, 61.86, 53.32, 49.23, 40.41, 36.69, 35.66, 33.64, 32.20, 31.49, 28.95, 28.75, 25.77, 25.42, 22.28. HPLC/MS MH<sup>+</sup> 579.3.

### Sar-Tle-Dap(octanoyl)-3-F-Phe-NH<sub>2</sub> (3.109):



<sup>1</sup>H NMR (500 MHz, MeOD)  $\delta$  8.19 (d,  $J = 7.1$  Hz, 1H), 8.14 (d,  $J = 7.8$  Hz, 1H), 7.26 (m, 1H), 7.07 (d,  $J = 7.7$  Hz, 1H), 7.02 (m, 1H), 6.92 (m, 1H), 4.61 (m, 1H), 4.39 (m, 1H), 4.19 (s, 1H), 3.86 (q,  $J = 6.3$  Hz, 2H), 3.54 (dd,  $J = 5.6, 13.8$  Hz, 1H), 3.42 (dd,  $J = 5.6, 13.8$  Hz, 1H), 3.16 (dd,  $J = 5.1, 13.8$  Hz, 1H), 2.95 (dd,  $J = 8.7, 13.8$  Hz, 1H), 2.72 (s, 3H), 2.17 (t,  $J = 7.6$  Hz, 2H), 1.57 (m, 2H), 1.30 (s, 8H), 0.97 (s, 9H), 0.89 (t,  $J = 7.0$  Hz, 3H). HPLC/MS MH<sup>+</sup> 579.3.

### Preparation of 3.114:



### (S)-2-chloro-N-(1-hydroxy-3-phenylpropan-2-yl)acetamide (3.122):

To a solution of L-phenylalaninol (500 mg, 3.31 mmol) in CH<sub>2</sub>Cl<sub>2</sub> (8.7 mL) at 0 °C was added a solution of Et<sub>3</sub>N (0.55 mL, 3.97 mmol) in CH<sub>2</sub>Cl<sub>2</sub> (2.2 mL). The resultant solution was stirred at 0 °C for ten minutes. A solution of chloroacetyl chloride (0.32 mL, 3.97 mmol) in CH<sub>2</sub>Cl<sub>2</sub> (4.4 mL) was added dropwise over 20 minutes. The resultant mixture was allowed to stir at 0 °C for thirty minutes and then slowly warmed to room temperature.

Upon completion, as determined by TLC, the reaction mixture was quenched with water. The organic phase was separated and the aqueous was extracted with CH<sub>2</sub>Cl<sub>2</sub> (x2). Organics were combined, washed with brine (x2), dried (MgSO<sub>4</sub>), filtered, and concentrated under reduced pressure to afford **3.122**. Resultant residue was used directly in the next step without further purification.

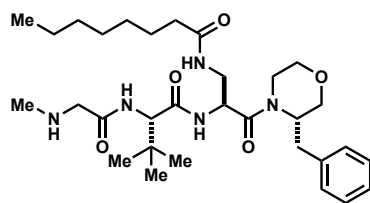
**(S)-5-benzylmorpholin-3-one (3.123):**

NaH (60% in mineral oil, 212 mg, 5.30 mmol) was suspended in THF (9.3 mL) at -10 °C for ten minutes. A solution of **3.122** (754 mg, 3.31 mmol) in THF (7 mL) was added dropwise over 20 minutes and resulting mixture was allowed to stir at -10 °C for 30 minutes and then slowly warmed to room temperature. Upon completion, as determined by TLC, water was carefully added to quench the reaction, followed by EtOAc. The organic phase was separated and the aqueous was extracted with EtOAc (x3). Organics were combined, dried (MgSO<sub>4</sub>), filtered, and concentrated under reduced pressure to produce **3.123** as a yellow solid that was used without further purification.

**(S)-3-benzylmorpholine (3.124):**

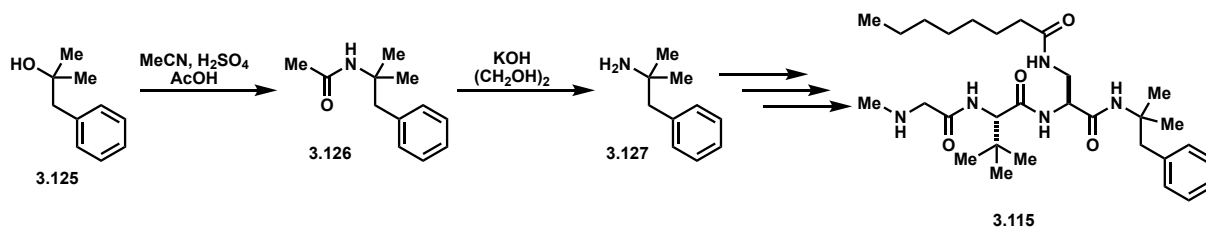
To a suspension of LiAlH<sub>4</sub> (432 mg, 11.32 mmol) in THF (12 mL) at 0 °C was slowly added a solution of **3.123** (633 mg, 3.31 mmol) in THF (9 mL). The resultant mixture was slowly warmed to room temperature and then refluxed for 48 h. After 48 h, the reaction mixture was cooled to -10 °C and carefully quenched with water followed by 2N NaOH. The resultant white precipitate was filtered through celite and filter cake washed with EtOAc (x6). Filtrate was dried (MgSO<sub>4</sub>), filtered, and concentrated under reduced pressure. Resultant residue was purified by column chromatography to afford **3.124** (365 mg) in 62% yield (over 3 steps). <sup>1</sup>H NMR (500 MHz, CDCl<sub>3</sub>) δ 7.31 (m, 2H), 7.22 (m, 3H), 3.80 (m, 2H), 3.55 (dt, *J* = 3.4, 10.3 Hz, 1H), 3.28 (dd, *J* = 9.7, 10.7 Hz, 1H), 3.01 (m, 1H), 2.87 (m, 2H), 2.67 (dd, *J* = 4.8, 13.5 Hz, 1H), 2.47 (dd, *J* = 9.0, 13.1 Hz, 1H). HPLC/MS MH<sup>+</sup> 178.2.

***N*-((*S*)-3-((*S*)-3-benzylmorpholino)-2-((*S*)-3,3-dimethyl-2-(2-(methylamino)acetamido)butanamido)-3-oxopropyl)octanamide (3.114):**



$^1\text{H}$  NMR (500 MHz, MeOD)  $\delta$  7.27 (m, 5H), 4.95 (m, 1H), 4.78 (m, 1H), 4.44 (m, 1H), 4.21 (s, 1H), 3.97 (m, 1H), 3.84 (m, 3H), 3.70 (q,  $J = 12.4$  Hz, 1H), 3.60 (m, 1H), 3.47 (m, 1H), 3.39 (m, 2H), 3.17 (m, 2H), 3.05 (m, 1H), 2.83 (m, 1H), 2.71 (s, 3H), 2.15 (m, 2H), 1.55 (m, 2H), 1.28 (m, 8H), 0.98 (d,  $J = 17.0$  Hz, 9H), 0.87 (t,  $J = 5.0$  Hz, 3H).  $^{13}\text{C}$  NMR (126 MHz, MeOD)  $\delta$  170.45, 168.97, 164.93, 129.33, 129.05, 128.46, 128.19, 126.54, 126.22, 67.82, 66.43, 61.45, 55.44, 51.56, 49.20, 41.71, 37.48, 35.60, 33.81, 32.18, 31.46, 28.93, 28.76, 25.80, 25.70, 25.47, 22.28, 12.99. HPLC/MS  $\text{MH}^+$  575.4.

**Preparation of 3.115:**



***N*-(2-methyl-1-phenylpropan-2-yl)acetamide (3.126):**

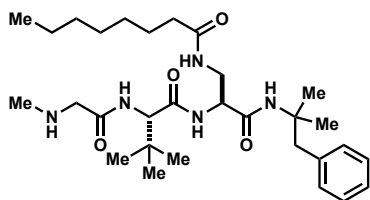
To a solution of **3.125** (1.54 mL, 10 mmol) and MeCN (3 mL) in acetic acid (15 mL) was added  $\text{H}_2\text{SO}_4$  (3 mL) dropwise. Resultant mixture was stirred at  $65^\circ\text{C}$  for 3 h and then poured into ice-water (~200 mL). The aqueous solution was brought to pH >11 using saturated aqueous NaOH. The resulting suspension was stirred for 30 minutes and the precipitate was filtered and washed with water. The solid was dried overnight to afford 1 g (52%) of **3.126**.  $^1\text{H}$  NMR (500 MHz,  $\text{CDCl}_3$ )  $\delta$  7.27 (m, 2H), 7.22 (m, 1H), 7.13 (m, 2H),

5.07 (s, 1H), 3.04 (s, 2H), 1.90 (s, 3H), 1.31 (s, 6H). <sup>13</sup>C NMR (126 MHz, MeOD) δ 169.92, 138.10, 130.51, 127.97, 126.31, 54.07, 44.51, 27.40, 24.57.

### 2-methyl-1-phenylpropan-2-amine (3.127):

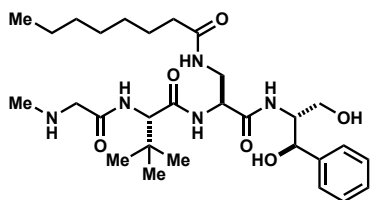
A mixture of **3.126** (191 mg, 1 mmol) and KOH (1 g) in ethylene glycol (10 mL) was refluxed for 8 hours and then cooled to rt. The mixture was diluted with ice-water and extracted with EtOAc (x2). Organics were combined, washed with water (x1), dried (MgSO<sub>4</sub>), filtered and concentrated under reduced pressure to afford crude **3.127** as a brown oil that was used without further purification. <sup>1</sup>H NMR (500 MHz, CDCl<sub>3</sub>) δ 7.20 (m, 5H), 2.65 (s, 2H), 1.30 (s, 2H), 1.11 (s, 6H). <sup>13</sup>C NMR (126 MHz, MeOD) δ 138.13, 130.44, 128.06, 126.36, 50.87, 50.19, 30.05.

### *N*-((*S*)-2-(((*S*)-3,3-dimethyl-2-(2-(methylamino)acetamido)butanamido)-3-((2-methyl-1-phenylpropan-2-yl)amino)-3-oxopropyl)octanamide (3.115):



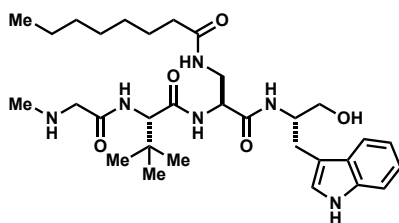
<sup>1</sup>H NMR (500 MHz, Acetone-d<sub>6</sub>) δ 7.23 (m, 2H), 7.16 (m, 3H), 4.44 (m, 1H), 4.20 (s, 1H), 4.07 (dd, *J* = 15.7, 40.2 Hz, 2H), 3.56 (m, 1H), 3.46 (m, 1H), 3.12 (d, *J* = 13.0 Hz, 1H), 2.97 (d, *J* = 13.1 Hz, 1H), 2.86 (s, 3H), 2.17 (dt, *J* = 3.2, 7.3 Hz, 2H), 2.07 (s, 1H), 2.05 (m, 2H), 1.55 (m, 2H), 1.27 (m, 12H), 1.22 (s, 2H), 0.99 (s, 9H), 0.86 (t, *J* = 6.9 Hz, 3H). <sup>13</sup>C NMR (126 MHz, Acetone-d<sub>6</sub>) δ 170.07, 169.74, 165.72, 160.79, 138.27, 130.54, 127.79, 126.04, 62.36, 55.03, 53.92, 49.76, 44.06, 40.85, 35.86, 33.57, 32.89, 31.59, 26.48, 26.35, 26.22, 25.50, 22.40, 13.45. HPLC/MS MH<sup>+</sup> 546.3.

### *N*-((*S*)-3-(((1*R*,2*R*)-1,3-dihydroxy-1-phenylpropan-2-yl)amino)-2-(((*S*)-3,3-dimethyl-2-(2-(methylamino)acetamido)butanamido)-3-oxopropyl)octanamide (3.199):



$^1\text{H}$  NMR (500 MHz, Acetone)  $\delta$  9.28 (s, 1H), 8.60 (d,  $J$  = 6.8 Hz, 1H), 8.35 (d,  $J$  = 6.0 Hz, 1H), 7.84 (s, 1H), 7.68 (s, 1H), 7.40 (d,  $J$  = 7.3 Hz, 1H), 7.26 (t,  $J$  = 7.4 Hz, 2H), 7.20 (d,  $J$  = 7.3 Hz, 1H), 5.00 (s, 1H), 4.71 (s, 1H), 4.51 (s, 1H), 4.17 (s, 3H), 3.65 (m, 4H), 3.45 (s, 3H), 2.85 (s, 3H), 2.14 (t,  $J$  = 7.1 Hz, 2H), 2.06 (t,  $J$  = 4.2 Hz, 1H), 1.53 (s, 2H), 1.25 (s, 8H), 0.97 (s, 9H), 0.85 (t,  $J$  = 6.8 Hz, 3H).  $^{13}\text{C}$  NMR (126 MHz, Acetone)  $\delta$  170.70, 170.11, 166.27, 166.14, 142.68, 127.94, 127.07, 126.42, 71.98, 61.83, 57.35, 53.48, 49.92, 40.89, 40.78, 35.85, 34.12, 33.11, 31.61, 26.38, 25.54, 22.41, 13.47. HPLC/MS  $\text{MH}^+$  564.3.

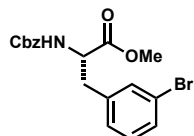
***N*-((*S*)-2-((*S*)-3,3-dimethyl-2-(2-(methylamino)acetamido)butanamido)-3-(((*S*)-1-hydroxy-3-(1*H*-indol-3-yl)propan-2-yl)amino)-3-oxopropyl)octanamide (3.200):**



$^1\text{H}$  NMR (500 MHz, MeOD)  $\delta$  8.18 (d,  $J$  = 7.2 Hz, 1H), 7.92 (t,  $J$  = 5.9 Hz, 1H), 7.88 (d,  $J$  = 8.3 Hz, 1H), 7.60 (d,  $J$  = 7.9 Hz, 1H), 7.31 (d,  $J$  = 8.1 Hz, 1H), 7.09 (s, 1H), 7.07 (t,  $J$  = 7.6 Hz, 1H), 6.99 (t,  $J$  = 7.3 Hz, 1H), 4.43 (m, 1H), 4.22 (s, 1H), 4.20 (m, 1H), 3.86 (q,  $J$  = 13.8 Hz, 2H), 3.59 (dd,  $J$  = 4.5, 10.9 Hz, 1H), 3.49 (m, 3H), 2.95 (m, 2H), 2.69 (s, 3H), 2.14 (t,  $J$  = 7.4 Hz, 2H), 1.57 (m, 2H), 1.29 (s, 9H), 1.00 (s, 9H), 0.88 (t,  $J$  = 6.8 Hz, 3H). HPLC/MS  $\text{MH}^+$  587.4.

**C3. Macrocyclic Peptidomimetic Inhibitors**

**Z-3-Br-Phe-OMe (3.137):**

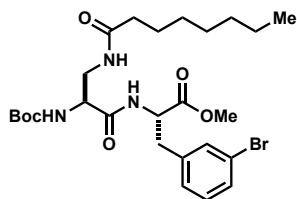


To a solution of 3-Br-Phe-OMe (1.4 g, 5.4 mmol) in saturated aqueous  $\text{NaHCO}_3$  (22 mL) was added Cbz-Cl (0.77 mL, 5.4 mmol) dropwise. Resulting reaction mixture was allowed to stir at room temperature overnight and then extracted with ether (x3). Organics were combined, washed with water (x2), dried ( $\text{MgSO}_4$ ), filtered, and concentrated under



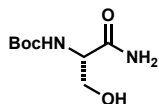
reduced pressure to afford **3.137** (1.76 g).  $^1\text{H}$  NMR (500 MHz,  $\text{CDCl}_3$ )  $\delta$  7.35 (m,  $J = 4.5$  Hz, 6H), 7.27 (s, 1H), 7.14 (t,  $J = 7.8$  Hz, 1H), 7.03 (d,  $J = 7.6$  Hz, 1H), 5.26 (d,  $J = 5.8$  Hz, 1H), 5.11 (d,  $J = 7.6$  Hz, 2H), 4.65 (q,  $J = 6.5$  Hz, 1H), 3.73 (s, 3H), 3.12 (q,  $J = 6.5$  Hz, 1H), 3.04 (q,  $J = 6.6$  Hz, 1H).

**Boc-Dap(octanoyl)-3-Br-Phe-OMe (3.138):**



Following GP2, Boc-Dap(octanoyl)-OH was coupled to 3-Br-Phe-OMe to afford **3.138**.  $^1\text{H}$  NMR (500 MHz,  $\text{CDCl}_3$ )  $\delta$  7.49 (t,  $J = 9.3$  Hz, 1H), 7.36 (m,  $J = 1.8$  Hz, 1H), 7.29 (t,  $J = 1.6$  Hz, 1H), 7.15 (t,  $J = 7.8$  Hz, 1H), 7.08 (d,  $J = 7.7$  Hz, 1H), 6.27 (s, 1H), 5.92 (s, 1H), 4.75 (d,  $J = 6.3$  Hz, 1H), 4.15 (d,  $J = 4.2$  Hz, 1H), 3.72 (s, 3H), 3.68 (m, 1H), 3.47 (m, 1H), 3.15 (q,  $J = 6.5$  Hz, 1H), 3.00 (q,  $J = 7.1$  Hz, 1H), 2.16 (t,  $J = 3.9$  Hz, 2H), 1.60 (d,  $J = 7.3$  Hz, 2H), 1.42 (s, 9H), 1.27 (s, 8H), 0.87 (t,  $J = 4.6$  Hz, 3H).  $^{13}\text{C}$  NMR (126 MHz,  $\text{CDCl}_3$ )  $\delta$  175.16, 171.31, 170.72, 156.37, 146.75, 138.40, 132.25, 130.23, 130.10, 127.79, 122.52, 85.20, 80.49, 55.84, 53.39, 52.53, 41.66, 37.46, 36.52, 31.67, 29.22, 28.99, 28.26, 27.42, 25.62, 22.61, 14.07. HPLC/MS  $\text{MH}^+$  604.2, 606.3.

**Boc-Ser-NH $_2$  (3.139):**



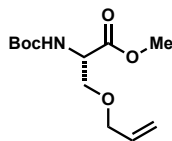
Tert-butyl (S)-(2-oxooxetan-3-yl)carbamate (94 mg, 0.5 mmol) was dissolved in liquid ammonia (35 mL) at  $-78$   $^\circ\text{C}$  and was allowed to stir for 20 minutes and then warmed to room temperature. Excess ammonia was allowed to evaporate and the resultant oil was triturated with ether to afford **3.139** (102 mg, 100%) as a white solid.  $^1\text{H}$  NMR (500 MHz,

MeOD)  $\delta$  6.95 (s, 1H), 6.46 (s, 1H), 5.91 (s, 1H), 4.10 (d,  $J = 6.1$  Hz, 1H), 3.80 (q,  $J = 5.3$  Hz, 1H), 3.70 (q,  $J = 5.5$  Hz, 1H), 1.40 (s, 9H).

**allyl (tert-butoxycarbonyl)-L-serinate (3.140):**

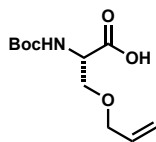
To a solution of allyl bromide (2.23 mL, 25.81 mmol) and aliquat 336 (4.39 mL, 9.60 mmol) in DCM (35 mL) was added a solution of Boc-Ser-OH (1.00 g, 4.87 mmol) and  $\text{NaHCO}_3$  (417 mg, 4.97 mmol) in  $\text{H}_2\text{O}$  (16 mL). The resulting mixture was stirred vigorously at room temperature for 48 hours. Reaction was then diluted with  $\text{H}_2\text{O}$  (50 mL) and extracted with DCM (x3). Organics were combined, dried ( $\text{MgSO}_4$ ), filtered, and concentrated under reduced pressure. Resulting oil was purified by column chromatography using 3:2 hexanes:EtOAc as eluents to afford **3.140** (901 mg) as a colorless oil.  $^1\text{H}$  NMR (500 MHz,  $\text{CDCl}_3$ )  $\delta$  5.91 (m, 1H), 5.45 (s, 1H), 5.34 (m, 1H), 5.26 (m, 1H), 4.67 (d,  $J = 5.7$  Hz, 2H), 4.40 (s, 1H), 3.97 (q,  $J = 5.0$  Hz, 3H), 3.92 (q,  $J = 4.9$  Hz, 3H), 2.33 (t,  $J = 5.5$  Hz, 1H), 1.45 (s, 9H).

**Boc-Ser(O-allyl)-OMe (3.201):**



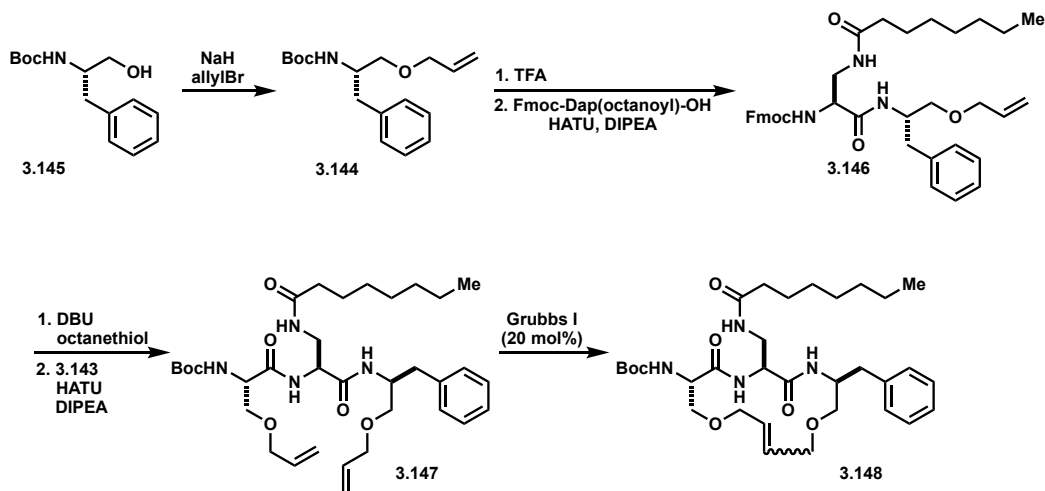
To a solution of Boc-Ser-OMe (1.28 g, 5.85 mmol) in THF (11.7 mL) was added a solution of allyl ethyl carbonate (1.54 mL, 11.7 mmol), allyl palladium chloride dimer (43 mg, 0.12 mmol) and  $\text{PPh}_3$  (138 mg, 0.53 mmol) in THF (5.85 mL) dropwise. The resulting reaction mixture was refluxed under argon overnight. Reaction mixture was concentrated under reduced pressure and the resultant residue was purified by column chromatography using 9:1 hexanes:EtOAc as eluents to afford **3.201** (1.24 g, 82%) as a clear oil.  $^1\text{H}$  NMR (500 MHz,  $\text{CDCl}_3$ )  $\delta$  5.82 (m, 1H), 5.37 (d,  $J = 8.1$  Hz, 1H), 5.23 (m, 1H), 5.17 (d,  $J = 10.4$  Hz, 1H), 4.42 (t,  $J = 4.4$  Hz, 1H), 3.97 (t,  $J = 5.7$  Hz, 2H), 3.84 (q,  $J = 4.1$  Hz, 1H), 3.75 (s, 9H), 3.64 (q,  $J = 4.2$  Hz, 1H).  $^{13}\text{C}$  NMR (126 MHz,  $\text{CDCl}_3$ )  $\delta$  171.23, 155.51, 134.06, 117.40, 79.99, 72.24, 69.94, 53.99, 52.48, 28.32. HPLC/MS  $\text{MH}^+$  1601.1 (-Boc).

### Boc-Ser(O-allyl)-OH (3.143):



To a solution of **3.201** (1.24 g, 4.78 mmol) in a mixture of THF/MeOH/H<sub>2</sub>O (1:1:1, 75 mL) was added LiOH·H<sub>2</sub>O (502 mg, 11.96 mmol) and the reaction was stirred at room temperature until completion as determined by TLC. THF and MeOH were removed under reduced pressure and the resulting solution was partitioned between 1N HCl (70 mL) and DCM (150 mL). The aqueous layer was extracted with DCM (x2) and the combined organics were dried (MgSO<sub>4</sub>), filtered, and concentrated under reduced pressure to afford **3.143** (1.1 g) as a colorless oil which was used without further purification. <sup>1</sup>H NMR (500 MHz, CDCl<sub>3</sub>) δ 5.85 (m, 1H), 5.40 (d, *J* = 7.9 Hz, 1H), 5.25 (m, 1H), 5.19 (q, *J* = 3.9 Hz, 1H), 4.45 (t, *J* = 3.9 Hz, 1H), 4.01 (d, *J* = 5.7 Hz, 2H), 3.90 (d, *J* = 4.5 Hz, 1H), 3.67 (q, *J* = 4.4 Hz, 1H). <sup>13</sup>C NMR (126 MHz, CDCl<sub>3</sub>) δ 175.96, 156.15, 134.25, 118.21, 80.77, 72.80, 69.96, 54.16, 28.70.

### Preparation of 3.148



***tert*-butyl (S)-(1-(allyloxy)-3-phenylpropan-2-yl)carbamate (3.144):**

To a solution of **3.145** (1.0 g, 3.98 mmol) in DMF (22 mL) at 0 °C was added NaH (60% in mineral oil, 365 mg, 9.12 mmol) followed by allyl bromide (0.77 mL, 9.72 mmol). The resulting mixture was allowed to stir at room temperature for 4 hours. Reaction was quenched with saturated aqueous NH<sub>4</sub>Cl and extracted with EtOAc (x2). Organics were dried (MgSO<sub>4</sub>), filtered, and concentrated under reduced pressure. Resultant oil was purified by column chromatography using 9:1 hexanes:EtOAc as eluents to afford **3.144** (526 mg, 45%) as a clear oil. <sup>1</sup>H NMR (500 MHz, CDCl<sub>3</sub>) δ 7.28 (q, *J* = 4.9 Hz, 2H), 7.21 (d, *J* = 7.4 Hz, 3H), 5.91 (m, 1H), 5.27 (q, *J* = 6.3 Hz, 1H), 5.19 (q, *J* = 4.0 Hz, 1H), 4.86 (s, 1H), 3.96 (m, 2H), 3.34 (m, 2H), 2.87 (m, 2H), 1.42 (s, 9H). <sup>13</sup>C NMR (126 MHz, CDCl<sub>3</sub>) δ 155.1, 138.0, 134.3, 129.2, 128.1, 126.0, 116.7, 78.7, 71.8, 69.8, 51.4, 37.6, 28.1. HPLC/MS MH<sup>+</sup> 192.1 (-Boc).

**(9H-fluoren-9-yl)methyl ((S)-1-(((S)-1-(allyloxy)-3-phenylpropan-2-yl)amino)-3-octanamido-1-oxopropan-2-yl)carbamate (3.146):**

Following GP 4, **3.144** could be deprotected and the resultant TFA salt was used without further purification. Following GP 2, the resultant residue could be coupled to Fmoc-Dap(octanoyl)-OH to afford **3.146** (178 mg, 95%). <sup>1</sup>H NMR (500 MHz, CDCl<sub>3</sub>) δ 7.77 (d, *J* = 7.5 Hz, 2H), 7.60 (d, *J* = 7.2 Hz, 2H), 7.40 (t, *J* = 7.5 Hz, 2H), 7.32 (m, 2H), 7.25 (d, *J* = 14.7 Hz, 2H), 7.19 (q, *J* = 3.5 Hz, 3H), 6.97 (d, *J* = 7.8 Hz, 1H), 6.41 (d, *J* = 4.3 Hz, 1H), 6.12 (s, 1H), 5.84 (m, 1H), 5.22 (d, *J* = 17.1 Hz, 1H), 5.12 (d, *J* = 10.3 Hz, 1H), 4.37 (t, *J* = 8.9 Hz, 1H), 4.31 (m, 2H), 4.21 (t, *J* = 7.1 Hz, 2H), 3.94 (s, 2H), 3.69 (d, *J* = 11.6 Hz, 1H), 3.49 (t, *J* = 7.0 Hz, 1H), 3.37 (s, 2H), 2.87 (m, 2H), 2.13 (t, *J* = 7.2 Hz, 2H), 1.74 (s, 1H), 1.60 (s, 2H), 1.26 (t, *J* = 5.2 Hz, 8H), 0.85 (t, *J* = 7.0 Hz, 3H). <sup>13</sup>C NMR (126 MHz, CDCl<sub>3</sub>) δ 175.37, 169.47, 143.74, 141.29 (d, *J* = 2.4 Hz), 137.81, 134.40, 129.30, 128.44, 127.80, 127.15 (d, *J* = 2.7 Hz), 126.53, 125.20, 120.03, 117.20, 72.14, 69.90, 67.52, 56.73, 50.35, 47.07, 42.15, 37.54, 36.51, 31.67, 29.24, 29.01, 25.66, 22.62, 14.06. HPLC/MS MH<sup>+</sup> 626.1.

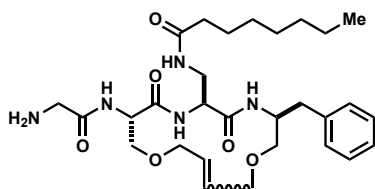
***tert*-butyl ((6*S*,9*S*,12*S*)-6-benzyl-9-(octanamidomethyl)-8,11-dioxo-4,14-dioxa-7,10-diazaheptadeca-1,16-dien-12-yl)carbamate (3.147):**

Following GP 8, the Fmoc group could be removed and following purification the resulting amine could be coupled to **3.143** following GP 2 to afford **3.147** (195 mg). <sup>1</sup>H NMR (500 MHz, CDCl<sub>3</sub>) δ 7.98 (d, *J* = 4.7 Hz, 1H), 7.28 (t, *J* = 3.8 Hz, 2H), 7.20 (q, *J* = 3.4 Hz, 3H), 7.08 (d, *J* = 8.6 Hz, 1H), 6.01 (s, 1H), 5.87 (m, 2H), 5.42 (d, *J* = 4.9 Hz, 1H), 5.28 (m, 1H), 5.24 (m, 1H), 5.19 (dd, *J* = 1.5, 10.5 Hz, 1H), 5.16 (dd, *J* = 1.5, 10.5 Hz, 1H), 4.40 (m, 1H), 4.35 (t, *J* = 3.8 Hz, 1H), 4.23 (t, *J* = 4.9 Hz, 1H), 3.98 (m, 4H), 3.78 (q, *J* = 4.8 Hz, 1H), 3.65 (q, *J* = 5.7 Hz, 1H), 3.58 (q, *J* = 4.9 Hz, 1H), 3.46 (m, 1H), 3.38 (m, 2H), 2.94 (q, *J* = 7.0 Hz, 1H), 2.77 (q, *J* = 7.2 Hz, 1H), 2.01 (q, *J* = 4.9 Hz, 1H), 1.64 (s, 6H), 1.56 (s, 1H), 1.46 (s, 9H), 1.26 (s, 8H), 0.87 (t, *J* = 6.9 Hz, 3H). <sup>13</sup>C NMR (126 MHz, CDCl<sub>3</sub>) δ 175.55, 170.73, 134.72, 133.96, 129.31, 129.16, 128.37, 126.38, 117.78, 117.02, 72.29, 72.26, 72.16, 70.33, 69.43, 55.64, 54.95, 50.17, 41.78, 37.50, 36.29, 31.66, 29.22, 28.98, 28.34, 25.57, 22.61, 14.05. HPLC/MS MH<sup>+</sup> 631.1.

***tert*-butyl ((3*S*,6*S*,9*S*)-3-benzyl-6-(octanamidomethyl)-5,8-dioxo-1,11-dioxa-4,7-diazacyclopentadec-13-en-9-yl)carbamate (3.148):**

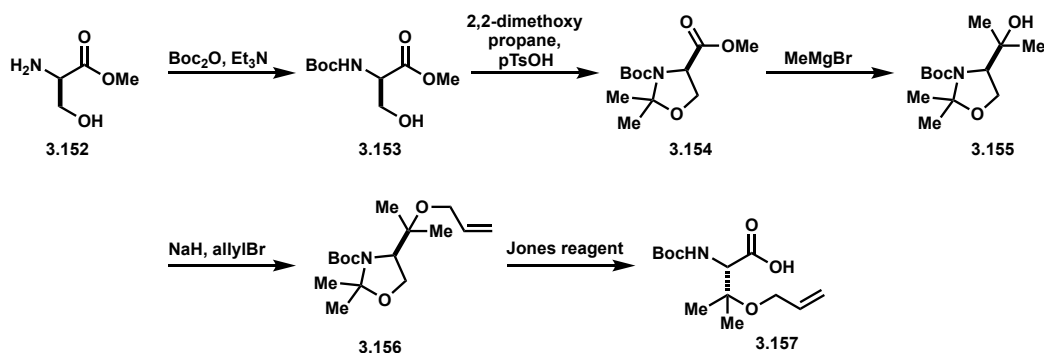
Following GP 10, **3.147** (158 mg, 0.25 mmol) could undergo RCM to afford **3.148** (134 mg) as a mixture of alkene isomers which co-elutes with minor leftover **3.147**. <sup>1</sup>H NMR (500 MHz, CDCl<sub>3</sub>) δ 7.25 (m, 2H), 7.18 (m, 3H), 5.83 (m, 1H), 5.49 (dd, *J* = 8.5, 32.0 Hz, 1H), 5.20 (m, 1H), 4.33 (m, 2H), 4.12 (m, 1H), 3.97 (m, 2H), 3.85 (q, *J* = 5.7 Hz, 1H), 3.77 (m, 1H), 3.69 (q, *J* = 5.1 Hz, 1H), 3.57 (m, 2H), 3.44 (m, 1H), 3.31 (m, 2H), 2.91 (m, 1H), 2.76 (m, 1H), 2.25 (s, 1H), 2.13 (q, *J* = 7.2 Hz, 1H), 2.04 (m, 1H), 1.90 (d, *J* = 12.7 Hz, 3H), 1.82 (s, 5H), 1.71 (s, 2H), 1.56 (m, 2H), 1.50 (s, 1H), 1.42 (m, 11H), 1.23 (s, 13H), 0.85 (t, *J* = 4.1 Hz, 3H). <sup>13</sup>C NMR (126 MHz, CDCl<sub>3</sub>) δ 176.40, 175.77, 175.58, 175.52, 171.65, 170.67, 170.57, 169.48, 169.24, 169.00, 168.77, 155.24, 155.18, 138.20, 129.37, 129.31, 129.15, 128.43, 128.42, 128.38, 128.34, 126.47, 126.44, 117.74, 72.23, 72.13, 71.19, 70.31, 70.22, 69.23, 69.46, 69.34, 69.02, 68.69, 67.29, 67.18, 56.44, 54.34, 50.95, 41.74, 37.45, 36.37, 36.32, 35.54, 35.06, 31.68, 31.66, 29.30, 29.27, 29.01, 28.33, 26.95, 26.86, 26.34, 26.32, 26.13, 22.61, 14.06. HPLC/MS MH<sup>+</sup> 603.1.

***N*-(((3*S*,6*S*,9*S*)-9-(2-aminoacetamido)-3-benzyl-5,8-dioxo-1,11-dioxa-4,7-diazacyclopentadec-13-en-6-yl)methyl)octanamide (3.151):**



Following GP 4, **3.148** could be deprotected. The resultant TFA salt was immediately coupled with Boc-Gly-OH following GP 2 to afford Boc-**3.151**. The Boc group could then be removed following GP 4 to afford **3.151** (50 mg) which was purified by preparative HPLC to separate the alkene isomers. **Z-3.151**:  $^1\text{H}$  NMR (500 MHz, MeOD)  $\delta$  8.35 (d,  $J$  = 7.3 Hz, 1H), 7.26 (d,  $J$  = 6.6 Hz, 3H), 7.18 (m, 2H), 5.79 (m, 2H), 4.46 (d,  $J$  = 2.3 Hz, 1H), 4.38 (m, 1H), 4.17 (d,  $J$  = 14.1 Hz, 1H), 4.03 (m, 3H), 3.83 (dd,  $J$  = 3.2, 9.8 Hz, 1H), 3.76 (dd,  $J$  = 8.1, 14.3 Hz, 1H), 3.54 (dd,  $J$  = 5.2, 10.5 Hz, 1H), 3.48 (q,  $J$  = 5.2 Hz, 1H), 3.35 (dd,  $J$  = 2.2, 10.5 Hz, 1H), 3.19 (dd,  $J$  = 2.4, 14.2 Hz, 1H), 2.92 (dd,  $J$  = 6.5, 13.0 Hz, 1H), 2.78 (dd,  $J$  = 8.7, 13.4 Hz, 1H), 2.20 (m, 2H), 1.93 (m, 2H), 1.85 (m, 2H), 1.75 (s, 1H), 1.59 (t,  $J$  = 6.7 Hz, 2H), 1.42 (d,  $J$  = 12.2 Hz, 2H), 1.31 (m, 11H), 0.88 (t,  $J$  = 6.7 Hz, 3H).  $^{13}\text{C}$  NMR (126 MHz, MeOD)  $\delta$  172.09, 170.08, 166.86, 138.15, 130.16, 129.01, 128.04, 127.50, 126.12, 69.47, 69.22, 69.02, 66.63, 57.29, 57.19, 55.21, 52.59, 41.30, 41.25, 40.60, 36.47, 35.67, 34.96, 34.47, 31.48, 29.01, 28.76, 26.41, 26.32, 25.82 (d,  $J$  = 2.9 Hz, 1C), 25.75, 25.65, 22.30. **E-3.151**:  $^1\text{H}$  NMR (500 MHz, DMSO)  $\delta$  7.35 (d,  $J$  = 8.4 Hz, 1H), 7.28 (t,  $J$  = 7.4 Hz, 2H), 7.24 (t,  $J$  = 4.1 Hz, 2H), 7.20 (m, 1H), 5.87 (m, 2H), 4.57 (t,  $J$  = 5.4 Hz, 1H), 4.35 (m, 2H), 4.10 (dd,  $J$  = 4.7, 12.2 Hz, 2H), 4.01 (dd,  $J$  = 5.7, 11.4 Hz, 1H), 3.94 (dd,  $J$  = 6.3, 12.7 Hz, 1H), 3.77 (m, 2H), 3.72 (s, 2H), 3.47 (m, 2H), 3.37 (dq,  $J$  = 3.2, 9.5 Hz, 2H), 2.92 (q,  $J$  = 6.5 Hz, 1H), 2.82 (q,  $J$  = 7.4 Hz, 1H), 2.19 (m, 2H), 1.89 (m, 1H), 1.59 (m, 2H), 1.42 (m, 1H), 1.31 (s, 9H), 0.89 (t,  $J$  = 6.9 Hz, 3H). HPLC/MS  $\text{MH}^+$  560.3.

## Preparation of 3.157



### Boc-D-Ser-OMe (3.153):

To a solution of **3.152** (1.0 g, 8.39 mmol) and Et<sub>3</sub>N (2.51 mL, 18.04 mmol) in THF (22 mL) at 0 °C was added a solution of Boc<sub>2</sub>O (1.81 g, 8.31 mmol) in THF (7 mL) dropwise over 20 minutes. The resulting solution was allowed to warm to room temperature and stir at that temperature overnight and then at 50 °C for 3 h. The solvent was removed under reduced pressure and the resultant residue was taken up in ether (15 mL) and saturated aqueous NaHCO<sub>3</sub> (20 mL). The aqueous phase was extracted with ether (x3). Organics were combined, dried (MgSO<sub>4</sub>), filtered, and concentrated under reduced pressure to afford **3.153** (1.61 g, 87%) as a colorless oil which was used without further purification. <sup>1</sup>H NMR (500 MHz, CDCl<sub>3</sub>) δ 5.46 (s, 1H), 4.38 (s, 1H), 3.95 (m, 1H), 3.89 (m, 1H), 3.77 (s, 3H), 2.46 (t, *J* = 6.2 Hz, 1H), 1.44 (s, 9H). <sup>13</sup>C NMR (126 MHz, CDCl<sub>3</sub>) δ 171.4, 155.7, 80.2, 63.3, 55.6, 52.5, 28.2.

### 3-(*tert*-butyl) 4-methyl (*R*)-2,2-dimethyloxazolidine-3,4-dicarboxylate (3.154):

To a solution of **3.153** (1.67 g, 7.33 mmol) in CH<sub>2</sub>Cl<sub>2</sub> (9 mL) at 0 °C was added 2,2-dimethoxypropane (4.50 mL, 36.66 mmol) and pTsOH (140 mg, 0.73 mmol). The resulting mixture was allowed to warm to room temperature and then stirred at room temperature overnight. The reaction mixture was then poured into saturated aqueous NaHCO<sub>3</sub> (10 mL) and extracted with ether (x3). Organics were combined and washed with NaHCO<sub>3</sub> and brine, dried (MgSO<sub>4</sub>), filtered, and concentrated under reduced pressure. Residue

was purified by column chromatography using 1:1 hexanes:EtOAc as eluents to afford **3.154** (1.63 g, 86%) as a colorless oil. <sup>1</sup>H NMR (500 MHz, CDCl<sub>3</sub>) δ 4.48 (dd, *J* = 2.4, 6.8 Hz, 0.4H), 4.37 (dd, *J* = 3.0, 6.8 Hz, 0.6H), 4.13 (m, 1H), 4.03 (m, 1H), 3.75 (s, 3H), 1.66 (s, 1.89H), 1.63 (s, 1.42H), 1.52 (s, 1.77H), 1.49 (s, 5.11H), 1.40 (s, 5.29H).

**tert-butyl (R)-4-(2-hydroxypropan-2-yl)-2,2-dimethyloxazolidine-3-carboxylate (3.155):**

To a solution of **3.154** (1.63 g, 6.29 mmol) in THF (50 mL) at -20 °C was added MeMgBr (1.95 M in Et<sub>2</sub>O, 10.8 mL, 21.13 mmol) dropwise. The resulting mixture was allowed to stir at 0 °C for 4 hours. To the reaction mixture was added saturated aqueous NH<sub>4</sub>Cl to quench the reaction and then extracted with EtOAc (x3). Organics were combined, washed with brine (x2), dried (MgSO<sub>4</sub>), filtered, and concentrated under reduced pressure. Residue was purified by column chromatography using 3:1 hexanes:EtOAc as eluents to afford **3.155** (982 mg, 60%). <sup>1</sup>H NMR (500 MHz, CDCl<sub>3</sub>) δ 4.00 (m, 2H), 3.79 (s, 1H), 1.59 (s, 3H), 1.50 (s, 12H), 1.17 (d, *J* = 7.0 Hz, 6H). HPLC/MS MH<sup>+</sup> 186.2 (-Boc +Na).

**tert-butyl (R)-4-(2-(allyloxy)propan-2-yl)-2,2-dimethyloxazolidine-3-carboxylate (3.156):**

To a solution of **3.155** (289 mg, 1.12 mmol) in DMF (5.2 mL) at 0 °C was added NaH (60% in mineral oil, 90 mg, 2.24 mmol) followed by allyl bromide (0.11 mL, 1.25 mmol). The resulting solution was allowed to warm to room temperature and was stirred for 1 hour and cooled back to 0 °C. The reaction was quenched with the addition of saturated aqueous NH<sub>4</sub>Cl and organics were extracted with EtOAc (x3). Organics were combined, washed with brine, dried (MgSO<sub>4</sub>), filtered, and concentrated under reduced pressure. Resultant residue was purified by column chromatography using 3:1 hexanes:EtOAc to afford **3.156** (89 mg). <sup>1</sup>H NMR (500 MHz, CDCl<sub>3</sub>) δ 5.88 (m, 1H), 5.25 (m, 1H), 5.09 (d, 1H), 4.20 (d, *J* = 7.7 Hz, 1H), 3.94 (m, 2H), 3.87 (m, 1H), 1.60 (s, 3H), 1.49 (s, 3H), 1.48 (s, 9H), 1.22 (s, 3H), 1.17 (s, 3H). <sup>13</sup>C NMR (126 MHz, CDCl<sub>3</sub>) δ 145.18, 136.00, 115.46, 80.16, 62.87, 29.71, 28.35. HPLC/MS MH<sup>+</sup> 200.2 (-Boc).

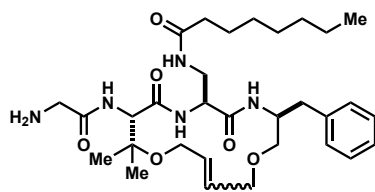


**(S)-3-(allyloxy)-2-((tert-butoxycarbonyl)amino)-3-methylbutanoic acid (3.157):**

To a solution of **3.156** (80 mg, 0.27 mmol) in acetone (3 mL) was added Jones' reagent (2.5 M in H<sub>2</sub>O, 0.16 mL, 0.40 mmol) at 0 °C. Resulting mixture was allowed to warm to room temperature and then was stirred at this temperature overnight. To the reaction mixture was added celite (100 mg) and isopropanol (0.5 mL) and the resulting precipitate was filtered through off through a plug of celite. Filtrate was adjusted to pH 9 with aqueous NaHCO<sub>3</sub> and then concentrated under reduced pressure. The aqueous layer was washed with ether (x2) and acidified to pH 3 with citric acid. The resulting solution was extracted with EtOAc (x3) and the combined extracts were washed with brine (x2), dried (MgSO<sub>4</sub>), filtered, and concentrated under reduced pressure to afford **3.157** (50 mg, 68%) which was used without further purification. <sup>1</sup>H NMR (500 MHz, CDCl<sub>3</sub>) δ 5.89 (m, *J* = 5.5 Hz, 1H), 5.30 (q, *J* = 6.2 Hz, 1H), 5.20 (q, *J* = 3.8 Hz, 1H), 4.38 (s, 1H), 4.04 (m, 2H), 1.44 (s, 9H), 1.35 (s, 3H), 1.24 (s, 3H). <sup>13</sup>C NMR (126 MHz, CDCl<sub>3</sub>) δ 172.36, 56.00, 133.90, 117.54, 80.37, 78.67, 63.60, 28.26, 22.64, 21.11.

**Preparation of Macrocycle Derivatives:** Macrocycle derivatives were synthesized in the same manner as **3.151** with the modified residue substituted in where necessary.

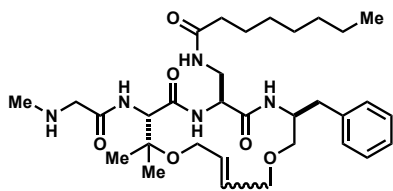
***N*-(((3*S*,6*S*,9*S*)-9-(2-aminoacetamido)-3-benzyl-10,10-dimethyl-5,8-dioxo-1,11-dioxo-4,7-diazacyclopentadec-13-en-6-yl)methyl)octanamide (3.171):**



**Z-3.171:** <sup>1</sup>H NMR (500 MHz, MeOD) δ 8.06 (q, *J* = 3.7 Hz, 1H), 7.64 (m, 1H), 7.54 (t, *J* = 4.0 Hz, 1H), 7.27 (t, *J* = 7.3 Hz, 2H), 7.23 (t, *J* = 4.1 Hz, 2H), 7.19 (m, 1H), 5.79 (m, 2H), 4.56 (s, 1H), 4.49 (m, 1H), 4.02 (m, 2H), 3.94 (t, *J* = 5.3 Hz, 2H), 3.90 (t, *J* = 3.8 Hz, 1H), 3.74 (q, *J* = 13.5 Hz, 2H), 3.62 (m, 1H), 3.45 (q, *J* = 4.2 Hz, 1H), 3.36 (q, *J* = 4.6 Hz, 1H),

3.34 (s, 1H), 2.97 (q,  $J = 7.1$  Hz, 1H), 2.82 (q,  $J = 7.0$  Hz, 1H), 2.14 (t,  $J = 7.6$  Hz, 2H), 1.57 (m,  $J = 7.3$  Hz, 2H), 1.43 (s, 2H), 1.29 (m, 9H), 1.27 (s, 3H), 1.24 (s, 3H), 0.89 (t,  $J = 7.0$  Hz, 3H).  $^{13}\text{C}$  NMR (126 MHz, MeOD)  $\delta$  175.69, 170.13, 169.79, 165.86, 138.42, 131.02, 128.93, 128.09, 127.22, 126.12, 77.02, 69.39, 67.88, 60.51, 60.33, 54.35, 53.18, 41.01, 40.15, 35.83, 35.70, 31.51, 29.00, 28.80, 25.47, 22.62, 22.31, 18.77, 13.02. **E-3.171**:  $^1\text{H}$  NMR (500 MHz, MeOD)  $\delta$  7.25 (m, 5H), 5.82 (m, 2H), 4.50 (s, 1H), 4.41 (t,  $J = 5.4$  Hz, 1H), 4.24 (q,  $J = 5.6$  Hz, 1H), 4.17 (q,  $J = 6.3$  Hz, 1H), 4.05 (m, 2H), 3.96 (q,  $J = 5.5$  Hz, 1H), 3.73 (d,  $J = 4.3$  Hz, 2H), 3.52 (t,  $J = 4.7$  Hz, 2H), 3.43 (q,  $J = 4.4$  Hz, 1H), 3.34 (q,  $J = 4.2$  Hz, 1H), 2.97 (m, 1H), 2.78 (q,  $J = 7.5$  Hz, 1H), 2.18 (m, 2H), 1.60 (t,  $J = 7.2$  Hz, 2H), 1.36 (s, 3H), 1.30 (m, 11H), 0.89 (t,  $J = 6.9$  Hz, 3H).  $^{13}\text{C}$  NMR (126 MHz, MeOD)  $\delta$  176.54, 169.93, 138.18, 131.29, 129.02, 128.82, 128.13, 126.14, 77.43, 68.71, 65.98, 60.13, 58.53, 55.14, 51.81, 40.56, 36.52, 35.57, 31.49, 29.04, 28.84, 25.54, 22.47, 22.33, 21.13, 13.03. HPLC/MS  $\text{MH}^+$  588.3.

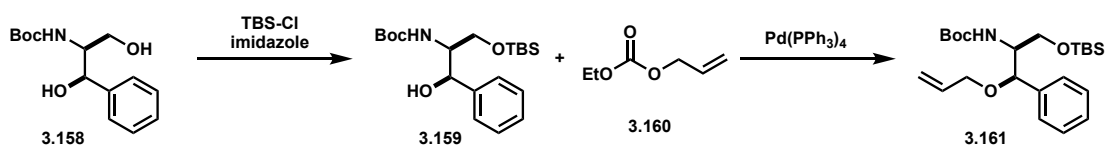
***N*-(((3*S*,6*S*,9*S*)-3-benzyl-10,10-dimethyl-9-(2-(methylamino)acetamido)-5,8-dioxo-1,11-dioxo-4,7-diazacyclopentadec-13-en-6-yl)methyl)octanamide (3.172):**



**Z-3.172**:  $^1\text{H}$  NMR (500 MHz, MeOD)  $\delta$  7.24 (m,  $J = 6.3$  Hz, 5H), 5.78 (m, 2H), 4.57 (s, 1H), 4.49 (t,  $J = 6.2$  Hz, 1H), 4.03 (q,  $J = 12.2$  Hz, 2H), 3.94 (t,  $J = 4.1$  Hz, 2H), 3.85 (q,  $J = 14.8$  Hz, 2H), 3.62 (m, 1H), 3.45 (q,  $J = 4.3$  Hz, 1H), 3.36 (t,  $J = 5.9$  Hz, 1H), 3.34 (s, 1H), 2.96 (q,  $J = 6.8$  Hz, 1H), 2.82 (q,  $J = 7.0$  Hz, 1H), 2.72 (s, 3H), 2.13 (t,  $J = 7.6$  Hz, 2H), 1.57 (m, 2H), 1.30 (s, 8H), 1.26 (s, 3H), 1.23 (s, 3H), 0.89 (t,  $J = 7.0$  Hz, 3H).  $^{13}\text{C}$  NMR (126 MHz, MeOD)  $\delta$  175.67, 170.03, 169.82, 165.05, 138.42, 131.03, 128.93, 128.09, 127.21, 126.12, 77.06, 69.39, 67.90, 60.52, 60.26, 54.35, 53.17, 49.26, 41.01, 35.85, 35.70, 32.19, 31.50, 28.99, 28.80, 25.47, 22.61, 22.31, 18.82, 13.03. **E-3.172**:  $^1\text{H}$  NMR (500 MHz, MeOD)  $\delta$  8.45 (d,  $J = 7.3$  Hz, 1H), 7.59 (d,  $J = 7.7$  Hz, 1H), 7.25 (m, 5H), 5.82 (m, 2H), 4.51 (s, 1H), 4.41 (m, 1H), 4.24 (q,  $J = 5.7$  Hz, 1H), 4.17 (m, 1H), 4.06 (q,  $J$

= 5.6 Hz, 1H), 3.96 (q,  $J$  = 5.6 Hz, 1H), 3.85 (q,  $J$  = 13.0 Hz, 2H), 3.52 (d,  $J$  = 5.4 Hz, 2H), 3.43 (q,  $J$  = 4.5 Hz, 1H), 3.34 (q,  $J$  = 4.2 Hz, 1H), 2.97 (q,  $J$  = 6.2 Hz, 1H), 2.78 (q,  $J$  = 7.5 Hz, 1H), 2.72 (s, 3H), 2.18 (m, 2H), 1.60 (m, 2H), 1.36 (s, 3H), 1.31 (s, 5H), 1.29 (s, 7H), 0.89 (q,  $J$  = 4.6 Hz, 3).  $^{13}\text{C}$  NMR (126 MHz, MeOD)  $\delta$  176.56, 170.12, 169.92, 165.02, 138.18, 131.25, 129.02, 128.81, 128.13, 126.14, 77.43, 68.72, 65.99, 60.06, 58.55, 55.19, 51.80, 49.23, 40.56, 36.51, 35.57, 32.15, 31.49, 29.04, 28.84, 25.54, 22.46, 22.33, 21.18, 13.02. HPLC/MS  $\text{MH}^+$  602.4.

### Preparation of 3.173



### ***tert*-butyl ((1*R*,2*S*)-3-((*tert*-butyldimethylsilyl)oxy)-1-hydroxy-1-phenylpropan-2-yl)carbamate (3.159):**

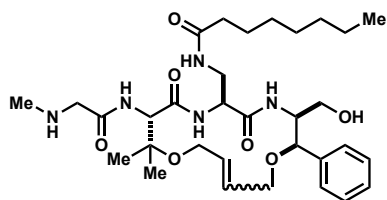
To a solution of **3.158** (400 mg, 1.50 mmol) and imidazole (103 mg, 1.52 mmol) in DMF (1.43 mL) was added TBS-Cl (226 mg, 1.50 mmol). Resulting mixture was allowed to stir at room temperature for 1 hour. Reaction mixture was concentrated under reduced pressure and resultant residue diluted with water and extracted with EtOAc (x3). Organics were combined, washed with brine, dried ( $\text{MgSO}_4$ ), filtered, and concentrated under reduced pressure. Residue was purified by column chromatography using 2:1 hexanes:EtOAc as eluents to afford **3.159** (488 mg, 85%) as a light yellow oil.  $^1\text{H}$  NMR (400 MHz,  $\text{CDCl}_3$ )  $\delta$  7.32 (m, 5H), 5.16 (d,  $J$  = 7.0 Hz, 1H), 5.01 (t,  $J$  = 3.1 Hz, 1H), 3.78 (m, 3H), 1.37 (s, 6H), 0.93 (s, 9H), 0.08 (s, 6H).  $^{13}\text{C}$  NMR (101 MHz,  $\text{CDCl}_3$ )  $\delta$  128.27, 127.55, 126.12, 28.31, 25.87, 18.21, -5.55 (d,  $J$  = 2.6 Hz, 1C). HPLC/MS  $\text{MH}^+$  282.3.

### ***tert*-butyl ((1*R*,2*S*)-1-allyloxy-3-((*tert*-butyldimethylsilyl)oxy)-1-phenylpropan-2-yl)carbamate (3.161):**

Following the procedure outlined in the synthesis of **3.201**, **3.159** (250 mg, 0.66 mmol) was allylated to afford **3.161** (266 mg, 95%).  $^1\text{H}$  NMR (400 MHz,  $\text{CDCl}_3$ )  $\delta$  7.30 (m, 5H),

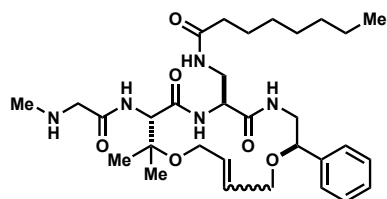
5.89 (m, 1H), 5.23 (d,  $J = 17.2$  Hz, 1H), 5.14 (q,  $J = 3.9$  Hz, 1H), 4.90 (d,  $J = 8.6$  Hz, 1H), 4.66 (d,  $J = 3.2$  Hz, 1H), 3.98 (m, 1H), 3.78 (q,  $J = 6.2$  Hz, 2H), 3.66 (q,  $J = 5.9$  Hz, 1H), 3.50 (q,  $J = 4.7$  Hz, 2H), 1.34 (s, 9H), 0.92 (s, 9H), 0.06 (s, 6H).

***N*-(((2*R*,3*S*,6*S*,9*S*)-3-(hydroxymethyl)-10,10-dimethyl-9-(2-(methylamino)acetamido)-5,8-dioxo-2-phenyl-1,11-dioxo-4,7-diazacyclopentadec-13-en-6-yl)methyl)octanamide (3.173):**



**Z-3.173:** <sup>1</sup>H NMR (500 MHz, MeOD)  $\delta$  8.14 (d,  $J = 7.4$  Hz, 1H), 7.79 (d,  $J = 8.9$  Hz, 1H), 7.36 (m, 5H), 5.91 (m, 1H), 5.78 (m, 1H), 4.60 (m, 2H), 4.29 (d,  $J = 10.0$  Hz, 1H), 4.13 (m, 1H), 4.03 (m, 2H), 3.93 (q,  $J = 5.8$  Hz, 1H), 3.86 (d,  $J = 1.6$  Hz, 2H), 3.55 (d,  $J = 5.7$  Hz, 2H), 3.32 (q,  $J = 2.1$  Hz, 1H), 3.14 (m, 1H), 2.73 (s, 3H), 2.21 (m, 2H), 1.60 (t,  $J = 7.0$  Hz, 2H), 1.30 (m, 16H), 1.25 (s, 3H), 0.89 (t,  $J = 7.0$  Hz, 3H). HPLC/MS MH<sup>+</sup> 618.3.

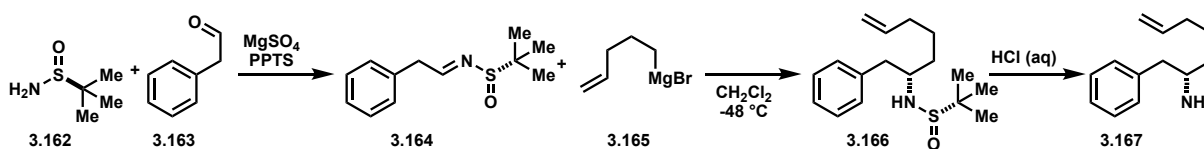
***N*-(((2*R*,6*S*,9*S*)-10,10-dimethyl-9-(2-(methylamino)acetamido)-5,8-dioxo-2-phenyl-1,11-dioxo-4,7-diazacyclopentadec-13-en-6-yl)methyl)octanamide (3.174):**



**Z-174:** <sup>1</sup>H NMR (500 MHz, MeOD)  $\delta$  8.19 (d,  $J = 8.0$  Hz, 1H), 7.36 (d,  $J = 4.4$  Hz, 4H), 7.29 (m, 1H), 5.87 (m, 2H), 4.67 (d,  $J = 2.4$  Hz, 1H), 4.59 (m, 1H), 4.41 (q,  $J = 4.1$  Hz, 1H), 4.10 (m, 1H), 4.00 (q,  $J = 5.6$  Hz, 1H), 3.90 (s, 2H), 3.64 (m, 2H), 3.52 (q,  $J = 6.8$  Hz, 1H), 3.41 (q,  $J = 6.5$  Hz, 1H), 3.06 (d,  $J = 14.0$  Hz, 1H), 2.77 (s, 3H), 2.16 (t,  $J = 7.5$  Hz, 2H), 1.57 (m, 2H), 1.28 (m, 15H), 0.86 (t,  $J = 6.9$  Hz, 3H). <sup>13</sup>C NMR (126 MHz, MeOD)  $\delta$  175.61, 170.32, 170.10, 165.19, 139.82, 130.31, 128.24, 127.71, 127.17, 126.06, 80.34,

77.19, 68.30, 60.81, 60.26, 54.08, 49.38, 45.95, 40.68, 35.67, 32.31, 31.51, 28.92, 28.81, 25.57, 22.57, 22.29, 18.95, 13.00. **E-174**:  $^1\text{H}$  NMR (500 MHz, MeOD)  $\delta$  8.44 (d,  $J$  = 7.2 Hz, 1H), 7.72 (t,  $J$  = 4.9 Hz, 1H), 7.34 (m, 5H), 5.85 (m, 1H), 5.72 (m, 1H), 4.54 (s, 1H), 4.44 (m, 2H), 4.25 (d,  $J$  = 7.1 Hz, 2H), 3.99 (q,  $J$  = 6.3 Hz, 1H), 3.86 (d,  $J$  = 7.1 Hz, 2H), 3.81 (m, 1H), 3.51 (m, 2H), 3.38 (q,  $J$  = 4.4 Hz, 2H), 2.73 (s, 3H), 2.19 (t,  $J$  = 7.6 Hz, 2H), 1.59 (t,  $J$  = 7.0 Hz, 2H), 1.37 (s, 3H), 1.33 (s, 3H), 1.30 (m, 10H), 0.89 (t,  $J$  = 6.9 Hz, 3H).  $^{13}\text{C}$  NMR (126 MHz, MeOD)  $\delta$  176.41, 170.49, 170.29, 165.00, 139.06, 131.95, 128.33, 128.07, 127.99, 126.25, 80.24, 77.59, 63.80, 59.95, 58.79, 55.05, 53.40, 49.27, 46.01 (d,  $J$  = 15.6 Hz, 1C), 40.33, 35.60, 32.18, 31.50, 28.95, 28.81, 25.57, 22.55, 22.32, 21.34, 13.01. HPLC/MS  $\text{MH}^+$  588.4.

### Preparation of 3.175



### **(S,E)-2-methyl-N-(2-phenylethylidene)propane-2-sulfonamide (3.164):**

To a solution of phenylacetaldehyde (2.00 g, 16.5 mmol) in  $\text{CH}_2\text{Cl}_2$  (28 mL) was added **3.162** (3.86 mL, 33.0 mmol), PPTS (200 mg, 0.80 mmol) and  $\text{MgSO}_4$  (9.88 g, 82.10 mmol). The reaction was heated at reflux for 18 hours and then cooled to room temperature. The solids were filtered off and washed with  $\text{CH}_2\text{Cl}_2$  (x2). The filtrate was concentrated under reduced pressure and resultant residue was purified by column chromatography using hexanes:EtOAc as eluents to afford **3.164** (3.3 g, 90%) as a colorless oil. *Note*: product appears to decompose readily in air, so column was run with low pressure and obtained product was used immediately or stored under argon at  $-20$   $^\circ\text{C}$ .  $^1\text{H}$  NMR (500 MHz,  $\text{CDCl}_3$ )  $\delta$  8.13 (t,  $J$  = 5.2 Hz, 1H), 7.33 (m, 2H), 7.27 (d,  $J$  = 7.4 Hz, 1H), 7.22 (m, 2H), 3.83 (t,  $J$  = 5.1 Hz, 2H), 1.18 (s, 9H).  $^{13}\text{C}$  NMR (126 MHz,  $\text{CDCl}_3$ )  $\delta$  167.46, 134.80, 129.23, 128.86, 127.15, 56.89, 42.67, 22.40. HPLC/MS  $\text{MH}^+$  224.2.

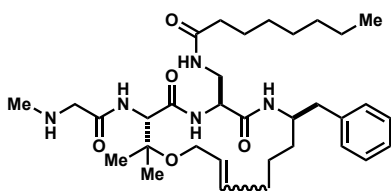
### **(S)-2-methyl-N-((S)-1-phenylhept-6-en-2-yl)propane-2-sulfonamide (3.166):**

To a solution of **3.164** (3.3 g, 14.8 mmol) in CH<sub>2</sub>Cl<sub>2</sub> (74 mL) at -48 °C was added **3.165** (2.7 M in Et<sub>2</sub>O, 11 mL, 29.6 mmol) dropwise. Resulting mixture was stirred at -48 °C for 4 hours and then allowed to stir at room temperature overnight. Reaction was quenched with saturated aqueous NH<sub>4</sub>Cl and then extracted with EtOAc (x2). Organics were combined, washed with H<sub>2</sub>O (x2), dried (MgSO<sub>4</sub>), filtered, and concentrated under reduced pressure. Resultant residue was purified by column chromatography using hexanes:EtOAc as eluents to afford **3.166**. <sup>1</sup>H NMR (500 MHz, MeOD) δ 7.89 (s, 1H), 7.20 (m, 5H), 5.80 (m, 1H), 4.99 (m, 1H), 4.91 (m, 1H), 3.41 (m, 1H), 2.85 (q, *J* = 6.5 Hz, 1H), 2.70 (q, *J* = 7.5 Hz, 1H), 2.06 (m, 2H), 1.64 (m, 3H), 1.51 (m, 1H), 1.00 (s, 9H). HPLC/MS MH<sup>+</sup> 294.3.

**(S)-1-phenylhept-6-en-2-amine (3.167):**

**3.166** (1 equiv) in was dissolved in a methanolic HCl solution (0.5 M in MeOH) and stirred at room temperature for 5 hours. Resulting mixture was concentrated under reduced pressure to afford **3.167** as the HCl salt. <sup>1</sup>H NMR (400 MHz, MeOD) δ 7.29 (m, *J* = 5.4 Hz, 1H), 5.75 (m, *J* = 4.5 Hz, 1H), 4.97 (q, *J* = 6.3 Hz, 1H), 4.92 (m, *J* = 2.4 Hz, 1H), 3.43 (t, *J* = 6.5 Hz, 1H), 2.91 (d, *J* = 6.8 Hz, 1H), 2.04 (m, *J* = 3.0 Hz, 1H), 1.57 (m, *J* = 3.9 Hz, 1H), 1.45 (m, *J* = 3.9 Hz, 1H).

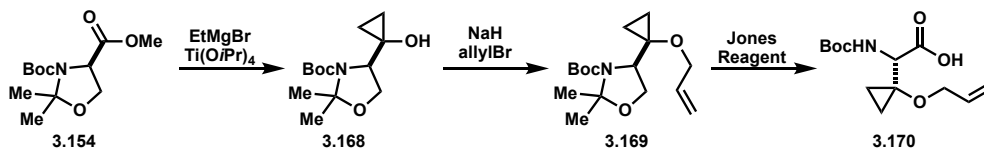
***N*-(((3*S*,6*S*,9*R*)-9-benzyl-2,2-dimethyl-3-(2-(methylamino)acetamido)-4,7-dioxo-1-oxa-5,8-diazacyclopentadec-13-en-6-yl)methyl)octanamide (3.175):**



***E*-3.175:** <sup>1</sup>H NMR (500 MHz, MeOD) δ 7.22 (m, ), 5.59 (m, 1H), 5.50 (m, 1H), 4.54 (s, 1H), 4.47 (t, *J* = 6.2 Hz, 1H), 4.11 (m, 1H), 3.96 (q, *J* = 5.4 Hz, 1H), 3.88 (q, *J* = 5.9 Hz, 1H), 3.84 (d, *J* = 3.6 Hz, 2H), 3.36 (m, 2H), 2.73 (s, 1H), 2.71 (s, 3H), 2.10 (m, 2H), 1.99 (m, 2H), 1.63 (m, 1H), 1.55 (t, *J* = 7.2 Hz, 2H), 1.49 (m, 1H), 1.42 (q, *J* = 4.3 Hz, 1H), 1.37 (q, *J* = 7.8 Hz, 1H), 1.29 (s, 9H), 1.26 (s, 3H), 1.20 (s, 3H), 0.88 (t, *J* = 7.0 Hz, 3H). <sup>13</sup>C NMR

(126 MHz, MeOD)  $\delta$  172.6, 132.4, 128.9, 128.0, 126.1, 93.0, 87.0, 61.7, 59.8, 53.8, 40.8, 35.6, 32.1, 31.5, 29.0, 28.8, 25.4, 22.3, 19.8, 13.0. HPLC/MS  $MH^+$  600.4.

### Preparation of 3.176



#### **tert-butyl (R)-4-(1-hydroxycyclopropyl)-2,2-dimethyl-1,3-oxazolidin-3-carboxylate (3.168):**

To a solution of **3.154** (1.0 g, 3.86 mmol) and  $Ti(O-iPr)_4$  (0.56 mL, 1.89 mmol) in  $Et_2O$  (12 mL) at 0 °C was added  $EtMgBr$  (1.78 M in  $Et_2O$ , 5.36 mL, 9.54 mmol) dropwise. The resulting mixture was allowed to warm to room temperature and stirred at this temperature overnight. The reaction was quenched with saturated aqueous  $NH_4Cl$  and extracted with  $EtOAc$  (x3). Organics were combined, dried ( $MgSO_4$ ), filtered, and concentrated under reduced pressure. Resultant residue was purified *via* column chromatography using 40%  $EtOAc$  in hexanes as eluents to afford **3.168** (463 mg).  $^1H$  NMR (500 MHz,  $CDCl_3$ )  $\delta$  4.00 (m, 2H), 3.69 (d,  $J = 2.7$  Hz, 1H), 1.55 (s, 3H), 1.50 (s, 12H), 0.83 (m, 2H), 0.76 (m, 1H), 0.51 (m, 1H). HPLC/MS  $MH^+$  158.2 (-Boc).

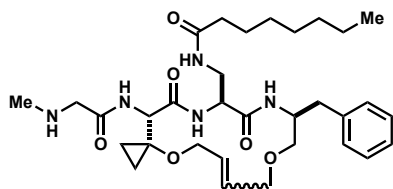
#### **tert-butyl (R)-4-(1-(allyloxy)cyclopropyl)-2,2-dimethyl-1,3-oxazolidin-3-carboxylate (3.169):**

Following the procedure described for the synthesis of **3.156**, **3.168** (350 mg, 1.36 mmol) could be allylated to afford **3.169** (303 mg, 75%).  $^1H$  NMR (400 MHz,  $CDCl_3$ )  $\delta$  5.85 (m, 1H), 5.10 (d,  $J = 9.4$  Hz, 1H), 4.14 (m, 5H), 1.49 (s, 11H), 1.46 (s, 4H), 0.88 (m, 1H), 0.79 (t,  $J = 3.1$  Hz, 2H), 0.50 (s, 1H). HPLC/MS  $MH^+$  198.2 (-Boc).

**(S)-2-(1-(allyloxy)cyclopropyl)-2-((tert-butoxycarbonyl)amino)acetic acid (3.170):**

Following the procedure utilized to synthesize **3.157**, **3.169** (155 mg, 0.52 mmol) could be reacted to afford **3.170** (56 mg) which was used without further purification.  $^1\text{H}$  NMR (500 MHz,  $\text{CDCl}_3$ )  $\delta$  5.83 (m, 1H), 5.40 (d,  $J = 6.7$  Hz, 1H), 5.23 (q,  $J = 6.3$  Hz, 1H), 5.14 (q,  $J = 4.0$  Hz, 1H), 4.22 (d,  $J = 7.0$  Hz, 1H), 4.16 (t,  $J = 4.0$  Hz, 1H), 4.06 (m, 1H), 1.45 (s, 9H), 1.04 (m, 1H), 0.92 (m, 2H), 0.78 (m, 1H).  $^{13}\text{C}$  NMR (126 MHz,  $\text{CDCl}_3$ )  $\delta$  173.85, 155.72, 134.17, 117.69, 116.95, 80.44, 69.70, 63.40, 56.75, 53.43, 28.27, 11.57, 11.01.

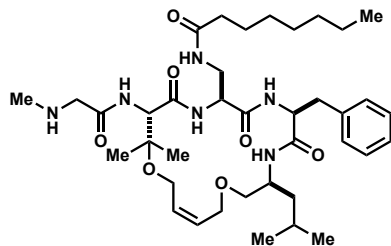
**N-(((11S,14S,17S)-11-benzyl-17-(2-(methylamino)acetamido)-13,16-dioxo-4,9-dioxo-12,15-diazaspiro[2.14]heptadec-6-en-14-yl)methyl)octanamide (3.176):**



**Z-3.176:**  $^1\text{H}$  NMR (500 MHz, MeOD)  $\delta$  7.25 (m, 5H), 5.61 (q,  $J = 2.3$  Hz, 2H), 4.31 (m, 3H), 4.17 (m, 1H), 4.09 (s, 1H), 3.94 (m, 2H), 3.88 (s, 2H), 3.52 (q,  $J = 7.3$  Hz, 1H), 3.44 (q,  $J = 6.0$  Hz, 1H), 3.40 (q,  $J = 4.5$  Hz, 1H), 3.32 (d,  $J = 2.9$  Hz, 1H), 2.92 (q,  $J = 6.6$  Hz, 1H), 2.81 (q,  $J = 7.4$  Hz, 1H), 2.72 (s, 3H), 2.19 (m, 2H), 1.60 (m, 2H), 1.30 (d,  $J = 6.0$  Hz, 10H), 1.20 (m, ), 0.94 (m, 1H), 0.88 (t,  $J = 6.9$  Hz, 3H).  $^{13}\text{C}$  NMR (126 MHz, MeOD)  $\delta$  138.03, 131.36, 128.97, 128.16, 126.23, 126.08, 69.09, 66.99, 66.63, 63.90, 58.70, 57.40, 51.33, 49.21, 40.65, 37.06, 35.42, 32.16, 31.51, 29.02, 28.81, 25.54, 22.32, 13.01, 12.71, 11.97. HPLC/MS  $\text{MH}^+$  600.4.

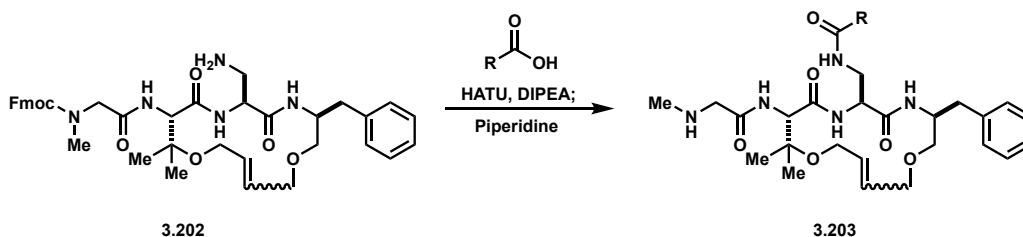


***N*-(((3*S*,6*S*,9*S*,12*S*,*Z*)-6-benzyl-3-isobutyl-13,13-dimethyl-12-(2-(methylamino)acetamido)-5,8,11-trioxo-1,14-dioxo-4,7,10-triazacyclooctadec-16-en-9-yl)methyl)octanamide (3.177):**



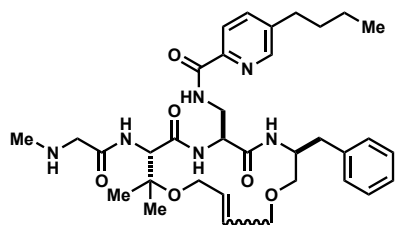
**Z-3.177:**  $^1\text{H}$  NMR (500 MHz, MeOD)  $\delta$  8.22 (d,  $J = 5.3$  Hz, 1H), 8.09 (d,  $J = 8.0$  Hz, 1H), 7.47 (d,  $J = 8.5$  Hz, 1H), 7.28 (m, 4H), 7.21 (m, 1H), 5.87 (m, 2H), 4.52 (s, 1H), 4.44 (m, 1H), 4.36 (m, 1H), 4.09 (q,  $J = 5.5$  Hz, 1H), 4.02 (q,  $J = 5.8$  Hz, 1H), 3.98 (t,  $J = 3.8$  Hz, 1H), 3.96 (d,  $J = 4.7$  Hz, 1H), 3.90 (d,  $J = 2.3$  Hz, 1H), 3.86 (d,  $J = 2.2$  Hz, 2H), 3.71 (q,  $J = 6.4$  Hz, 1H), 3.48 (m, 3H), 3.16 (q,  $J = 6.7$  Hz, 1H), 3.01 (m, 1H), 2.70 (s, 3H), 2.23 (m, 1H), 2.16 (m, 1H), 1.59 (m, 3H), 1.52 (q,  $J = 6.7$  Hz, 1H), 1.31 (q,  $J = 2.8$  Hz, 7H), 1.27 (s, 7H), 1.22 (m, 1H), 0.89 (m, 9H).  $^{13}\text{C}$  NMR (126 MHz, MeOD)  $\delta$  175.72, 172.21 (d,  $J = 2.8$  Hz, 1C), 172.13 (d,  $J = 2.7$  Hz, 1C), 169.92, 165.43, 159.74, 159.44, 136.96, 128.66, 128.57 (d,  $J = 4.4$  Hz, 1C), 128.23, 126.53, 116.91, 114.62, 77.18, 71.54, 70.23, 61.63, 60.74, 57.42 (d,  $J = 11.1$  Hz, 1C), 52.80 (d,  $J = 10.3$  Hz, 1C), 49.21, 41.01, 39.72 (d,  $J = 4.0$  Hz, 1C), 36.36 (d,  $J = 6.3$  Hz, 1C), 35.60, 32.15, 31.48, 28.97, 28.76, 25.41, 24.48, 22.30, 22.13, 21.84, 21.08, 19.35, 13.02. HPLC/MS  $\text{MH}^+$  715.4.

**Preparation of Side Chain Derivatives**



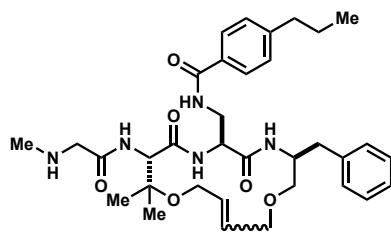
**General Procedure:** For side chain derivatives, **3.202** is coupled with the acid of the desired side chain following GP 2. After completion of coupling reaction as determined by LCMS, the Fmoc group is removed following GP 9. Resultant reaction mixtures were used directly for preparative HPLC purification.

***N*-(((3*S*,6*S*,9*S*)-3-benzyl-10,10-dimethyl-9-(2-(methylamino)acetamido)-5,8-dioxo-1,11-dioxo-4,7-diazacyclopentadec-13-en-6-yl)methyl)-5-butylpicolinamide (**3.178**):**



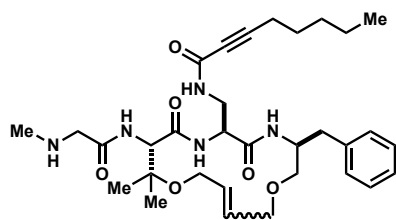
**Z-3.178:**  $^1\text{H}$  NMR (500 MHz, MeOD)  $\delta$  8.46 (d,  $J$  = 1.6 Hz, 1H), 8.22 (t,  $J$  = 4.0 Hz, 1H), 7.99 (q,  $J$  = 2.8 Hz, 1H), 7.78 (q,  $J$  = 3.4 Hz, 1H), 7.61 (d,  $J$  = 7.5 Hz, 1H), 7.18 (m, 5H), 5.76 (m, 2H), 4.62 (m, 2H), 4.04 (t,  $J$  = 7.8 Hz, 1H), 3.95 (m, 2H), 3.85 (t,  $J$  = 6.8 Hz, 2H), 3.81 (s, 1H), 3.74 (s, 1H), 3.65 (m, 1H), 3.58 (d,  $J$  = 5.7 Hz, 2H), 3.45 (m, 1H), 2.96 (q,  $J$  = 7.2 Hz, 1H), 2.77 (t,  $J$  = 6.8 Hz, 1H), 2.72 (t,  $J$  = 7.8 Hz, 2H), 2.69 (s, 3H), 1.64 (m, 2H), 1.37 (q,  $J$  = 7.5 Hz, 2H), 1.26 (s, 3H), 1.23 (s, 3H), 0.95 (t,  $J$  = 7.4 Hz, 3H).  $^{13}\text{C}$  NMR (126 MHz, MeOD)  $\delta$  170.13, 169.99, 166.04, 164.92, 148.57, 147.07, 141.94, 138.34, 137.00, 130.91, 128.83, 128.00, 127.29, 126.05, 121.63, 77.06, 69.44, 68.09, 60.57, 60.06, 54.12, 53.58, 49.24, 41.11, 35.71, 32.99, 32.13, 32.09, 22.62, 21.85, 18.91, 12.74. **E-3.178:**  $^1\text{H}$  NMR (500 MHz, MeOD)  $\delta$  8.45 (q,  $J$  = 2.7 Hz, 1H), 8.01 (q,  $J$  = 2.8 Hz, 1H), 7.78 (m, 1H), 7.58 (d,  $J$  = 7.7 Hz, 1H), 7.18 (m, 5H), 5.81 (m, 1H), 5.72 (m, 1H), 4.57 (s, 1H), 4.52 (q,  $J$  = 3.7 Hz, 1H), 4.23 (q,  $J$  = 6.1 Hz, 1H), 4.16 (q,  $J$  = 6.6 Hz, 1H), 4.01 (q,  $J$  = 6.1 Hz, 1H), 3.91 (q,  $J$  = 5.9 Hz, 1H), 3.81 (m, 3H), 3.71 (q,  $J$  = 6.3 Hz, 1H), 3.43 (m, 1H), 2.90 (q,  $J$  = 6.4 Hz, 1H), 2.71 (q,  $J$  = 3.7 Hz, 3H), 2.68 (s, 3H), 2.61 (q,  $J$  = 7.5 Hz, 1H), 1.62 (m, 3H), 1.38 (m, 2H), 1.35 (s, 3H), 1.27 (s, 3H), 0.94 (t,  $J$  = 7.3 Hz, 3H). HPLC/MS  $\text{MH}^+$  637.4.

***N*-(((3*S*,6*S*,9*S*)-3-benzyl-10,10-dimethyl-9-(2-(methylamino)acetamido)-5,8-dioxo-1,11-dioxo-4,7-diazacyclopentadec-13-en-6-yl)methyl)-4-propylbenzamide (3.179):**



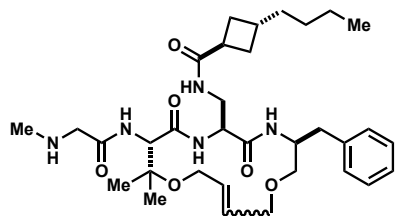
**Z-3.179:**  $^1\text{H}$  NMR (500 MHz, MeOD)  $\delta$  7.69 (d,  $J$  = 8.3 Hz, 2H), 7.29 (d,  $J$  = 8.2 Hz, 2H), 7.20 (m, 4H), 7.14 (m, 1H), 5.78 (q,  $J$  = 3.5 Hz, 2H), 4.65 (q,  $J$  = 4.2 Hz, 1H), 4.61 (s, 1H), 4.00 (m, 2H), 3.92 (m, 3H), 3.73 (d,  $J$  = 15.8 Hz, 1H), 3.63 (m, 2H), 3.44 (m, 2H), 3.33 (t,  $J$  = 7.9 Hz, 1H), 2.93 (q,  $J$  = 7.2 Hz, 1H), 2.80 (m, 1H), 2.65 (t,  $J$  = 7.6 Hz, 2H), 2.58 (s, 3H), 1.66 (q,  $J$  = 7.5 Hz, 2H), 1.28 (s, 1H), 1.24 (s, 6H), 0.95 (t,  $J$  = 7.4 Hz, 3H).  $^{13}\text{C}$  NMR (126 MHz, MeOD)  $\delta$  170.16, 169.71, 169.37, 164.64, 146.92, 138.30, 131.51, 130.86, 128.89, 128.34, 128.02, 127.29, 127.19, 126.08, 77.11, 69.44, 68.20, 60.51, 60.03, 54.42, 53.20, 49.05, 41.89, 37.41, 35.89, 32.09, 24.15, 22.65, 18.71, 12.65. **E-3.179:**  $^1\text{H}$  NMR (500 MHz, MeOD)  $\delta$  7.72 (d,  $J$  = 8.4 Hz, 2H), 7.27 (d,  $J$  = 8.4 Hz, 2H), 7.20 (m,  $J$  = 5.3 Hz, 5H), 5.80 (m, 2H), 4.56 (q,  $J$  = 4.2 Hz, 1H), 4.52 (s, 1H), 4.33 (s, 1H), 4.23 (q,  $J$  = 5.9 Hz, 1H), 4.14 (q,  $J$  = 6.4 Hz, 1H), 4.04 (m, 1H), 3.98 (q,  $J$  = 7.3 Hz, 2H), 3.73 (m, 2H), 3.43 (m, 1H), 3.36 (d,  $J$  = 2.4 Hz, 2H), 3.33 (t,  $J$  = 3.5 Hz, 2H), 2.92 (q,  $J$  = 6.4 Hz, 1H), 2.70 (q,  $J$  = 7.5 Hz, 1H), 2.64 (t,  $J$  = 7.6 Hz, 2H), 2.41 (s, 3H), 1.91 (s, 1H), 1.65 (q,  $J$  = 7.5 Hz, 2H), 1.34 (s, 3H), 1.28 (s, 4H), 0.93 (t,  $J$  = 7.4 Hz, 3H).  $^{13}\text{C}$  NMR (126 MHz, MeOD)  $\delta$  177.42, 170.52, 169.95, 169.64, 168.73, 146.93, 138.20, 131.51, 131.24, 129.02, 128.91, 128.27, 128.05, 127.19, 126.05, 77.54, 73.59, 68.81, 65.76, 60.02, 58.30, 54.78, 51.71, 51.13, 40.84, 37.42, 36.61, 33.52, 24.12, 22.55, 20.77, 12.64. HPLC/MS  $\text{MH}^+$  622.3.

***N*-(((3*S*,6*S*,9*S*)-3-benzyl-10,10-dimethyl-9-(2-(methylamino)acetamido)-5,8-dioxo-1,11-dioxo-4,7-diazacyclopentadec-13-en-6-yl)methyl)oct-2-ynamide (3.181):**



**Z-3.181:**  $^1\text{H}$  NMR (500 MHz, MeOD)  $\delta$  7.23 (m, 5H), 5.78 (m, 2H), 4.61 (s, 1H), 4.55 (m,  $J = 5.0$  Hz, 1H), 4.33 (s, 1H), 4.00 (m, 2H), 3.92 (q,  $J = 3.3$  Hz, 3H), 3.61 (q,  $J = 5.9$  Hz, 1H), 3.58 (d,  $J = 2.3$  Hz, 2H), 3.45 (q,  $J = 4.3$  Hz, 1H), 3.38 (q,  $J = 5.2$  Hz, 1H), 3.34 (s, 1H), 2.94 (m, 1H), 2.82 (m, 1H), 2.56 (s, 3H), 2.33 (t,  $J = 7.1$  Hz, 2H), 1.55 (m, 2H), 1.34 (m, 6H), 1.25 (s, 6H), 0.90 (t,  $J = 7.2$  Hz, 3H).  $^{13}\text{C}$  NMR (126 MHz, MeOD)  $\delta$  177.83, 170.36, 169.59, 168.64, 154.98, 138.36, 131.00, 128.97, 128.07, 127.17, 126.10, 88.30, 77.14, 74.77, 73.82, 69.51, 68.00, 60.44, 59.82, 53.97, 53.14, 51.16, 41.37, 36.03, 33.57, 30.74, 27.29, 22.76, 21.81, 18.78, 17.81, 12.85. **E-3.181:**  $^1\text{H}$  NMR (500 MHz, MeOD)  $\delta$  7.24 (m, 5H), 5.84 (m, 2H), 4.49 (s, 1H), 4.44 (q,  $J = 4.0$  Hz, 1H), 4.32 (s, 1H), 4.26 (q,  $J = 5.5$  Hz, 1H), 4.14 (m, 1H), 4.02 (m, 3H), 3.61 (q,  $J = 6.2$  Hz, 1H), 3.50 (m, 2H), 3.44 (s, 2H), 3.34 (m, 2H), 2.94 (m, 1H), 2.80 (q,  $J = 7.5$  Hz, 1H), 2.48 (s, 3H), 2.32 (t,  $J = 7.1$  Hz, 2H), 1.54 (m, 2H), 1.38 (m, 3H), 1.34 (s, 3H), 1.32 (m, 3H), 1.28 (s, 4H), 0.89 (t,  $J = 7.3$  Hz, 3H).  $^{13}\text{C}$  NMR (126 MHz, MeOD)  $\delta$  178.04, 170.47, 169.68, 155.34, 138.23, 131.46, 129.08, 128.96, 128.09, 126.09, 88.48, 77.52, 74.61, 73.74, 68.72, 65.92, 59.91, 58.38, 54.26, 51.90 (d,  $J = 12.0$  Hz, 1C), 40.47, 36.60, 34.07, 30.70, 27.25, 22.56, 22.21, 21.79, 20.92, 17.76, 12.83. HPLC/MS  $\text{MH}^+$  598.3.

**(1*s*,3*S*)-*N*-(((3*S*,6*S*,9*S*)-3-benzyl-10,10-dimethyl-9-(2-(methylamino)acetamido)-5,8-dioxo-1,11-dioxo-4,7-diazacyclopentadec-13-en-6-yl)methyl)-3-butylcyclobutane-1-carboxamide (3.182):**



**Z-3.182:**  $^1\text{H}$  NMR (500 MHz, MeOD)  $\delta$  7.23 (m, 5H), 5.78 (t,  $J$  = 3.2 Hz, 2H), 4.59 (s, 1H), 4.52 (t,  $J$  = 6.4 Hz, 1H), 4.34 (s, 1H), 4.01 (m, 1H), 3.92 (m, 3H), 3.71 (q,  $J$  = 14.3 Hz, 2H), 3.62 (q,  $J$  = 5.8 Hz, 1H), 3.44 (q,  $J$  = 4.3 Hz, 1H), 3.35 (t,  $J$  = 4.5 Hz, 2H), 2.95 (m, 1H), 2.82 (q,  $J$  = 7.0 Hz, 1H), 2.64 (s, 3H), 2.28 (m, 3H), 1.80 (m, 2H), 1.45 (q,  $J$  = 7.4 Hz, 2H), 1.30 (m, 3H), 1.26 (s, 3H), 1.23 (s, 3H), 1.20 (m, 2H), 0.89 (t,  $J$  = 7.3 Hz, 3H).  $^{13}\text{C}$  NMR (126 MHz, MeOD)  $\delta$  177.86, 177.66, 170.15, 169.90, 167.07, 138.44, 131.04, 128.94, 128.08, 127.14, 126.10, 77.18, 73.75, 69.38, 67.91, 60.52, 60.08, 54.36, 53.14, 50.33, 41.18, 35.91 (d,  $J$  = 1.3 Hz, 1C), 35.88, 33.02, 31.67, 29.90 (d,  $J$  = 1.6 Hz, 1C), 29.19, 22.66, 22.35, 18.88, 13.08. **E-3.182:**  $^1\text{H}$  NMR (500 MHz, MeOD)  $\delta$  7.24 (m, 5H), 5.83 (m, 2H), 4.49 (s, 1H), 4.43 (q,  $J$  = 4.0 Hz, 1H), 4.32 (s, 1H), 4.27 (q,  $J$  = 5.7 Hz, 1H), 4.17 (q,  $J$  = 6.3 Hz, 1H), 4.04 (m, 2H), 3.97 (q,  $J$  = 5.6 Hz, 1H), 3.60 (q,  $J$  = 6.1 Hz, 1H), 3.52 (t,  $J$  = 5.6 Hz, 1H), 3.46 (q,  $J$  = 5.0 Hz, 1H), 3.43 (q,  $J$  = 3.2 Hz, 1H), 3.35 (d,  $J$  = 5.5 Hz, 3H), 3.33 (t,  $J$  = 2.2 Hz, 1H), 3.00 (m, 1H), 2.95 (q,  $J$  = 6.3 Hz, 2H), 2.77 (q,  $J$  = 7.5 Hz, 1H), 2.43 (s, 3H), 2.31 (m, 3H), 1.89 (s, 1H), 1.81 (m, 2H), 1.65 (m, 1H), 1.53 (m, 1H), 1.46 (m, 3H), 1.35 (s, 3H), 1.31 (m, 4H), 1.28 (s, 3H), 1.21 (m, 3H), 0.89 (t,  $J$  = 4.8 Hz, 3H).  $^{13}\text{C}$  NMR (126 MHz, MeOD)  $\delta$  178.49, 177.86, 170.87, 170.50, 169.92, 138.21, 131.41, 129.04, 128.86, 128.10, 126.10, 77.60, 73.76, 68.74, 65.94, 59.77, 58.53, 54.87, 52.44, 51.74, 45.92, 42.65, 40.34, 36.60, 35.88 (t,  $J$  = 3.4 Hz, 1C), 34.43, 33.48, 31.71, 31.17, 30.00, 29.87, 29.75, 29.18, 26.14, 25.39, 24.13, 22.48, 22.33, 21.07, 13.05. HPLC/MS  $\text{MH}^+$  614.3.

## D. References

- (1) *Fmoc Solid Phase Peptide Synthesis*; Chan, W. C., White, P. D., Eds.; Oxford University Press, 2000.

## Experimental Procedures Supporting Chapter 4

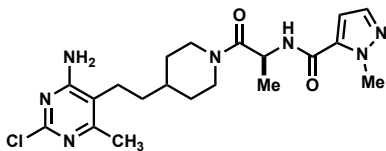
### A. Materials and Methods

All reactions were carried out using oven- or flame-dried glassware and a magnetic stir bar under an atmosphere of argon (Ar) unless otherwise indicated. Methylene chloride ( $\text{CH}_2\text{Cl}_2$ ), tetrahydrofuran (THF), diethyl ether ( $\text{Et}_2\text{O}$ ), toluene, and acetonitrile (MeCN) were dried by passage through activate alumina using a GlassContour<sup>®</sup> solvent drying system. Commercial reagents and catalysts were used as received unless otherwise indicated.

NMR spectra were recorded on Bruker Advance spectrometers (300 MHz, 400 MHz, 500 MHz) and are reported as  $\delta$  values in ppm relative to  $\text{CDCl}_3$  (calibrated to 7.26 ppm in  $^1\text{H}$  NMR and 77.16 ppm in  $^{13}\text{C}$  NMR, unless otherwise indicated). Splitting patterns are abbreviated as follows: singlet (s), doublet (d), triplet (t), quartet (q), multiplet (m), broad (br), and combinations thereof. Column chromatography was conducted on silica gel 60 (240–400 mesh) purchased from Silicycle. Thin layer chromatography (TLC) was performed using pre-coated, glass-backed plates (silica gel 60 PF254, 0.25 mm) and visualized using a combination of UV and potassium permanganate staining. HPLC analyses were carried out using an Agilent 1200 HPLC system equipped with an Agilent Quadrupole 6130 ESI-MS detector. Mobile phase was prepared with 0.1% TFA.

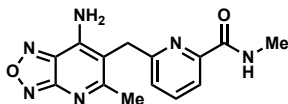
## B. Reported GOAT Inhibitors

### (S)-N-(1-(4-(2-(4-amino-2-chloro-6-methylpyrimidin-5-yl)ethyl)piperidin-1-yl)-1-oxopropan-2-yl)-1-methyl-1H-pyrazole-5-carboxamide (4.1):



Compound **4.1** was synthesized according to the patented protocol.<sup>1</sup> <sup>1</sup>H NMR (500 MHz, MeOD)  $\delta$  7.45 (d,  $J$  = 2.0 Hz, 1H), 6.85 (d,  $J$  = 2.1 Hz, 1H), 5.00 (q,  $J$  = 6.5 Hz, 1H), 4.52 (m, 1H), 4.08 (s, 4H), 3.18 (m, 1H), 2.70 (m, 1H), 2.54 (m, 2H), 2.35 (d,  $J$  = 6.6 Hz, 3H), 1.90 (m, 2H), 1.70 (m, 1H), 1.40 (m, 6H), 1.19 (m, 2H). <sup>13</sup>C NMR (126 MHz, Acetone)  $\delta$  163.90, 158.70, 137.10, 135.15, 113.36, 106.68, 45.48, 45.09, 44.87, 42.25, 41.92, 38.48, 36.10, 33.70, 32.49, 32.43, 31.65, 22.80, 22.70, 20.17, 18.05, 17.54. HPLC/MS MH<sup>+</sup> 435.0.

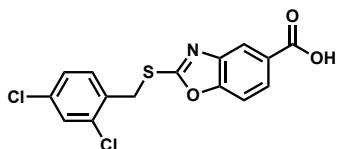
### 6-((7-amino-5-methyl-[1,2,5]oxadiazolo[3,4-*b*]pyridin-6-yl)methyl)-*N*-methylpicolinamide (4.2):



Compound **4.2** was prepared according to the patented protocol.<sup>2</sup> <sup>1</sup>H NMR (500 MHz, MeOD)  $\delta$  7.96 (q,  $J$  = 2.9 Hz, 1H), 7.91 (m, 1H), 7.51 (q,  $J$  = 2.9 Hz, 1H), 4.32 (s, 2H), 2.92 (s, 3H), 2.62 (s, 3H). HPLC/MS MH<sup>+</sup> 299.0.



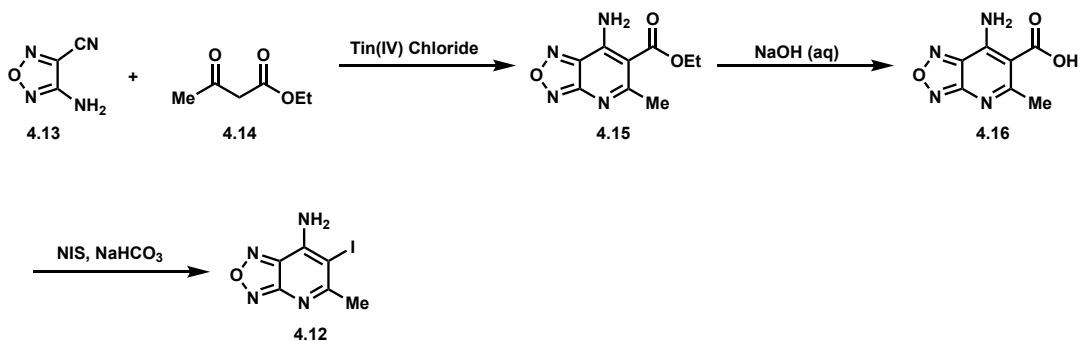
## 2-((2,4-dichlorobenzyl)thio)benzo[d]oxazole-5-carboxylic acid (4.3)



Compound **4.3** was prepared according to literature protocol.<sup>3</sup> Spectral data were in accordance with reported values. <sup>1</sup>H NMR (500 MHz, DMSO)  $\delta$  13.10 (s, 1H), 8.14 (dd,  $J = 0.6, 1.7$  Hz, 1H), 7.93 (dd,  $J = 1.8, 8.6$  Hz, 1H), 7.73 (m, 2H), 7.68 (d,  $J = 2.2$  Hz, 1H), 7.42 (dd,  $J = 2.2, 8.2$  Hz, 1H), 4.69 (s, 2H). HPLC/MS  $MH^+$  354.0, 356.0.

## C. Preparation of Small-Molecule Heterocyclic Inhibitors

### Preparation of 4.12



### ethyl 7-amino-5-methyl-[1,2,5]oxadiazolo[3,4-b]pyridine-6-carboxylate (4.15):

To a solution of **4.13** (1.0 g, 9.08 mmol) and ethyl acetoacetate (1.16 mL, 9.08 mmol) in toluene (10 mL) was added tin(IV) chloride (2.13 mL, 18.2 mmol). The resulting mixture is stirred at reflux for 30 minutes and then cooled to room temperature. Reaction mixture is concentrated under reduced pressure and resultant residue diluted with a half saturated aqueous solution of  $NaHCO_3$ . The aqueous is extracted with  $CH_2Cl_2$  (x3) and organics are combined, dried ( $MgSO_4$ ), filtered, and concentrated under reduced pressure to afford **4.15** (1.82 g, 90%). <sup>1</sup>H NMR (500 MHz, DMSO)  $\delta$  8.57 (br, 2H), 4.33 (q,  $J = 7.1$  Hz, 2H),

2.59 (s, 3H), 1.31 (t,  $J = 7.1$  Hz, 3H).  $^{13}\text{C}$  NMR (126 MHz, DMSO)  $\delta$  170.08, 167.06, 158.50, 145.91, 140.31, 103.05, 61.56, 28.10, 14.43.

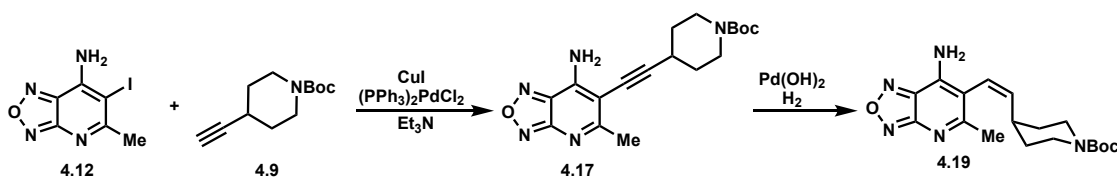
### 7-amino-5-methyl-[1,2,5]oxadiazolo[3,4-*b*]pyridine-6-carboxylic acid (**4.16**):

To a solution of **4.15** (1.58 g, 7.13 mmol) in THF (14.3 mL) and NaOH (1 M aq., 10.8 mL, 10.8 mmol) was added. The resultant mixture was allowed to stir at room temperature for 18 hours and then HCl (4 M aq., 2.6 mL, 10.4 mmol) is added. Resulting solution was concentrated under reduced pressure and resultant residue is filtered, rinsed with water and dried under reduced pressure to afford **4.16** which was used without further purification.  $^1\text{H}$  NMR (500 MHz, DMSO)  $\delta$  8.87 (br, 2H), 2.66 (s, 3H).  $^{13}\text{C}$  NMR (126 MHz, DMSO)  $\delta$  170.74, 168.93, 157.86, 147.17, 140.53, 102.81, 28.41. HPLC/MS  $\text{MH}^+$  195.1.

### 6-iodo-5-methyl-[1,2,5]oxadiazolo[3,4-*b*]pyridin-7-amine (**4.12**):

To a solution of **4.16** (1.38 g, 7.13 mmol) in DMF (17 mL) was added NIS (1.93 g, 8.56 mmol) and  $\text{NaHCO}_3$  (719 mg, 8.56 mmol). The resulting mixture was allowed to stir at room temperature for 18 hours and then concentrated under reduced pressure. The resultant residue was diluted with water and stirred for 10 minutes. The mixture was filtered to collect the precipitate which was dried under reduced pressure to afford **4.12** (1.35 g, 69% over 2 steps).  $^1\text{H}$  NMR (500 MHz, DMSO)  $\delta$  7.85 (br, 2H), 2.72 (s, 3H).  $^{13}\text{C}$  NMR (126 MHz, DMSO)  $\delta$  170.72, 158.92, 144.54, 138.41, 74.59, 32.60.

### Preparation of **4.19**



***tert*-butyl 4-((7-amino-5-methyl-[1,2,5]oxadiazolo[3,4-*b*]pyridin-6-yl)ethynyl)piperidine-1-carboxylate (4.17):**

A solution of **4.12** (1.35 g, 4.89 mmol), **4.9** (1.45 g, 7.15 mmol), (PPh<sub>3</sub>)<sub>2</sub>PdCl<sub>2</sub> (687 mg, 0.98 mmol), and CuI (93 mg, 0.49 mmol) in Et<sub>3</sub>N (20 mL) was degassed with argon for 15 minutes and then heated at 80 °C for 24 hours. The mixture was then allowed to stir at room temperature for 2 days and then diluted with EtOAc and filtered through a pad of celite. Filter cake was rinsed with EtOAc. Organics were washed with brine (x2), dried (MgSO<sub>4</sub>), filtered, and concentrated under reduced pressure. Resultant residue was purified via column chromatography using hexanes:EtOAc as eluents to afford **4.17** (889 mg, 51%). <sup>1</sup>H NMR (500 MHz, DMSO) δ 3.63 (m, *J* = 3.3 Hz, 2H), 3.15 (s, 2H), 2.94 (m, *J* = 4.0 Hz, 1H), 2.53 (s, 3H), 1.83 (m, *J* = 3.3 Hz, 2H), 1.61 (m, *J* = 4.3 Hz, 2H), 1.38 (s, 9H). HPLC/MS MH<sup>+</sup> 358.3.

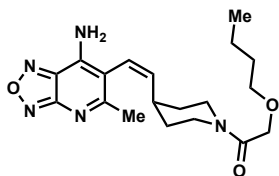
***tert*-butyl (Z)-4-(2-(7-amino-5-methyl-[1,2,5]oxadiazolo[3,4-*b*]pyridin-6-yl)vinyl)piperidine-1-carboxylate (4.19):**

To a solution of **4.17** (250 mg, 0.70 mmol) in EtOH (7 mL) under argon was added Pd(OH)<sub>2</sub> (20% on carbon, 150 mg, 0.21 mmol). Argon was removed and reaction was put under an H<sub>2</sub> atmosphere and stirred at room temperature. Upon completion, as determined by LCMS, reaction mixture was diluted with EtOH and filtered through a pad of celite to remove the catalyst. Filter cake was rinsed with EtOH and filtrate was concentrated under reduced pressure to afford **4.19** (276 mg crude) which was used without further purification. <sup>1</sup>H NMR (400 MHz, DMSO) δ 6.04 (d, *J* = 10.9 Hz, 1H), 5.75 (t, *J* = 10.3 Hz, 1H), 3.79 (d, *J* = 10.5 Hz, 2H), 3.40 (m, 1H), 2.60 (m, 3H), 2.33 (s, 3H), 2.03 (m, 2H), 1.33 (s, 11H), 1.15 (m, 4H).

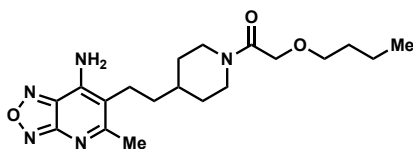
**(Z)-1-(4-(2-(7-amino-5-methyl-[1,2,5]oxadiazolo[3,4-*b*]pyridin-6-yl)vinyl)piperidin-1-yl)-2-butoxyethan-1-one (4.22) and 1-(4-(2-(7-amino-5-methyl-[1,2,5]oxadiazolo[3,4-*b*]pyridin-6-yl)ethyl)piperidin-1-yl)-2-butoxyethan-1-one (4.7):**

To a solution of **4.19** (252 mg, 0.70 mmol) in CH<sub>2</sub>Cl<sub>2</sub> (16 mL) was added TFA (10% v/v, 1.61 mL, 21.0 mmol). Resulting mixture was allowed to stir at room temperature until

completion as determined by LCMS. Upon completion, reaction mixture was concentrated under reduced pressure to afford **4.21** as the TFA salt which was used immediately without purification. **4.21** (0.70 mmol), n-butoxyacetic acid (0.10 mL, 0.77 mmol), and HATU (293 mg, 0.77 mmol) were suspended in DMF (3 mL). To suspension was added DIPEA (0.37 mL, 2.10 mmol) and resulting mixture was allowed to stir at room temperature until completion as determined by LCMS. Upon completion, reaction was diluted with EtOAc and washed with saturated aqueous NH<sub>4</sub>Cl (x2), water (x2), saturated aqueous NaHCO<sub>3</sub> (x2), and brine (x2). Organics were dried (MgSO<sub>4</sub>), filtered, and concentrated under reduced pressure. Residue was purified by column chromatography using hexanes:EtOAc as eluents to afford **4.22** (300 mg) and **4.7** (10 mg) as yellow residues.



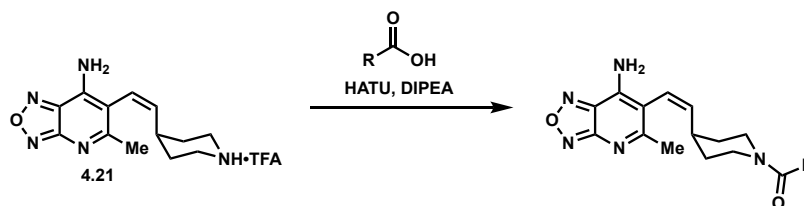
**4.22:** <sup>1</sup>H NMR (500 MHz, MeOD) δ 7.89 (s, 2H), 6.15 (d, *J* = 10.9 Hz, 1H), 5.87 (dd, *J* = 9.7, 10.7 Hz, 1H), 4.39 (d, *J* = 13.0 Hz, 1H), 4.12 (q, *J* = 18.1 Hz, 2H), 3.88 (s, 1H), 3.85 (d, *J* = 12.8 Hz, 1H), 3.51 (t, *J* = 6.6 Hz, 1H), 3.46 (q, *J* = 6.7 Hz, 2H), 2.98 (s, 1H), 2.94 (d, *J* = 12.0 Hz, 1H), 2.85 (d, *J* = 0.6 Hz, 1H), 2.80 (s, 1H), 2.58 (t, *J* = 11.7 Hz, 1H), 2.44 (s, 3H), 2.26 (m, 1H), 1.57 (m, 4H), 1.38 (m, 5H), 0.92 (t, *J* = 7.4 Hz, 3H). <sup>13</sup>C NMR (126 MHz, MeOD) δ 169.65, 168.58, 158.30, 141.64, 140.78, 139.02, 120.46, 109.81, 78.08, 71.12, 70.88, 69.36, 44.37, 41.23, 37.48, 36.17, 31.33, 31.25, 23.91, 18.89, 12.79.



**4.7:** <sup>1</sup>H NMR (500 MHz, CDCl<sub>3</sub>) δ 5.13 (br s, 2H), 4.62 (d, *J* = 13.2 Hz, 1H), 4.13 (d, *J* = 12.3 Hz, 2H), 4.00 (d, *J* = 13.6 Hz, 1H), 3.49 (q, *J* = 7.1 Hz, 2H), 3.03 (t, *J* = 12.0 Hz, 1H), 2.62 (s, 3H), 2.59 (d, *J* = 8.5 Hz, 1H), 1.87 (t, *J* = 12.8 Hz, 2H), 1.66 (m, 1H), 1.58 (m,

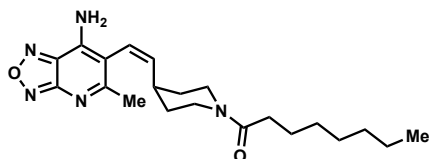
2H), 1.49 (m, 2H), 1.37 (m, 2H), 1.24 (s, 2H), 1.21 (s, 1H), 1.20 (s, 1H), 0.91 (t,  $J = 7.4$  Hz, 3H).  $^{13}\text{C}$  NMR (126 MHz,  $\text{CDCl}_3$ )  $\delta$  170.01, 167.86, 157.97, 139.23, 138.21, 114.14, 71.29, 70.72, 45.33, 42.13, 36.51, 34.10, 32.81, 31.67, 29.71, 25.37, 25.00, 24.02, 19.28, 13.88. HPLC/MS  $\text{MH}^+$  376.1, 398.0 (+Na).

### Side Chain Screening



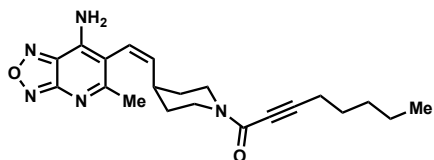
**General Procedure:** 4.21 (1.0 equiv), side chain carboxylic acid (1.1 equiv), and HATU (1.1 equiv) are suspended in DMF (0.3 M). To suspension is added DIPEA (3 equiv) and resulting solution is stirred at room temperature until completion as determined by LCMS. Reaction mixture is diluted with EtOAc and washed with saturated aqueous  $\text{NH}_4\text{Cl}$  (x2), water (x2), saturated aqueous  $\text{NaHCO}_3$  (x2), and brine (x2). Organics are dried ( $\text{MgSO}_4$ ), filtered, and concentrated under reduced pressure. Residue is purified by preparative HPLC.

### (Z)-1-(4-(2-(7-amino-5-methyl-[1,2,5]oxadiazolo[3,4-b]pyridin-6-yl)vinyl)piperidin-1-yl)octan-1-one (4.29):



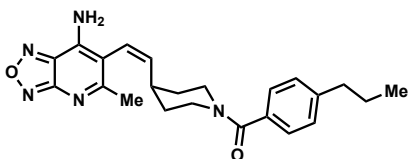
$^1\text{H}$  NMR (500 MHz, MeOD)  $\delta$  6.14 (d,  $J = 10.9$  Hz, 1H), 5.86 (t,  $J = 10.4$  Hz, 1H), 4.42 (d,  $J = 12.9$  Hz, 1H), 3.87 (d,  $J = 13.3$  Hz, 1H), 3.62 (s, 1H), 3.52 (m, 1H), 2.97 (t,  $J = 11.8$  Hz, 1H), 2.52 (t,  $J = 11.8$  Hz, 1H), 2.43 (s, 3H), 2.32 (m, 2H), 2.24 (t,  $J = 7.4$  Hz, 3H), 1.56 (m, 2H), 1.28 (m, 8H), 0.88 (m, 3H). HPLC/MS  $\text{MH}^+$  386.4.

**(Z)-1-(4-(2-(7-amino-5-methyl-[1,2,5]oxadiazolo[3,4-*b*]pyridin-6-yl)vinyl)piperidin-1-yl)oct-2-yn-1-one (4.30):**



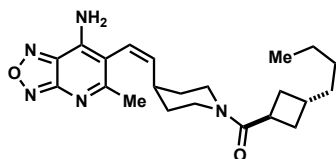
$^1\text{H}$  NMR (500 MHz, MeOD)  $\delta$  6.15 (d,  $J$  = 10.9 Hz, 1H), 5.86 (q,  $J$  = 6.9 Hz, 1H), 4.33 (q,  $J$  = 13.1 Hz, 2H), 3.61 (s, 1H), 3.52 (m, 1H), 3.06 (t,  $J$  = 11.9 Hz, 1H), 2.64 (m, 1H), 2.43 (s, 3H), 2.37 (t,  $J$  = 7.1 Hz, 2H), 2.27 (m, 1H), 1.56 (m, 2H), 1.35 (m, 6H), 0.90 (t,  $J$  = 7.2 Hz, 3H). HPLC/MS  $\text{MH}^+$  382.5.

**(Z)-4-(2-(7-amino-5-methyl-[1,2,5]oxadiazolo[3,4-*b*]pyridin-6-yl)vinyl)piperidin-1-yl)(4-propylphenyl)methanone (4.31):**



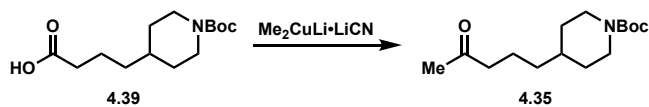
$^1\text{H}$  NMR (500 MHz, MeOD)  $\delta$  7.25 (q,  $J$  = 7.8 Hz, 4H), 6.15 (d,  $J$  = 10.9 Hz, 1H), 5.90 (t,  $J$  = 10.4 Hz, 1H), 4.53 (s, 1H), 3.68 (d,  $J$  = 10.4 Hz, 1H), 3.61 (s, 2H), 3.56 (q,  $J$  = 5.4 Hz, 1H), 3.49 (q,  $J$  = 5.7 Hz, 1H), 3.00 (s, 1H), 2.73 (t,  $J$  = 6.4 Hz, 1H), 2.60 (t,  $J$  = 7.7 Hz, 3H), 2.43 (s, 3H), 2.28 (m,  $J$  = 8.0 Hz, 2H), 1.63 (m,  $J$  = 7.4 Hz, 4H), 0.92 (t,  $J$  = 7.4 Hz, 3H). HPLC/MS  $\text{MH}^+$  406.3.

**4-((Z)-2-(7-amino-5-methyl-[1,2,5]oxadiazolo[3,4-*b*]pyridin-6-yl)vinyl)piperidin-1-yl)((1*s*,3*R*)-3-butylcyclobutyl)methanone (4.32):**



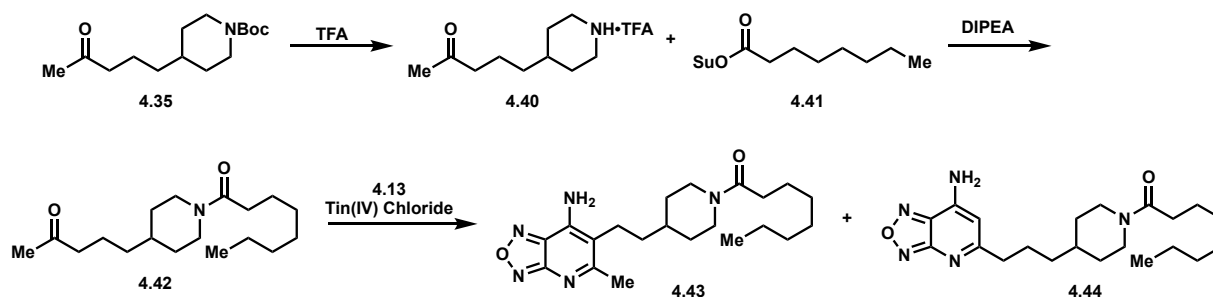
$^1\text{H}$  NMR (500 MHz, MeOD)  $\delta$  6.13 (d,  $J$  = 11.0 Hz, 1H), 5.85 (t,  $J$  = 10.4 Hz, 1H), 4.41 (d,  $J$  = 13.3 Hz, 1H), 3.63 (q,  $J$  = 9.6 Hz, 2H), 3.52 (m, 1H), 2.88 (t,  $J$  = 12.0 Hz, 1H), 2.53 (q,  $J$  = 8.7 Hz, 1H), 2.43 (s, 3H), 2.25 (m, 5H), 1.83 (m, 4H), 1.45 (q,  $J$  = 7.6 Hz, 2H), 1.29 (q,  $J$  = 7.7 Hz, 8H), 1.20 (m, 3H), 0.88 (t,  $J$  = 7.2 Hz, 3H). HPLC/MS  $\text{MH}^+$  398.5.

### Preparation of 4.35:



To a flask containing CuCN (1.65 g, 18.42 mmol) was added dry Et<sub>2</sub>O (30 mL). The resulting suspension was cooled to 0 °C and MeLi (1.6 M in Et<sub>2</sub>O, 23 mL, 36.85 mmol) was added dropwise. After addition, resulting mixture was allowed to stir at 0 °C for 5 min before the addition of a solution of **4.39** (1.00 g, 3.68 mmol) in Et<sub>2</sub>O (18.4 mL) dropwise. The resulting reaction mixture was allowed to warm to room temperature over an hour and then stirred at room temperature overnight. Reaction was quenched with saturated aqueous NH<sub>4</sub>Cl and then extracted with CH<sub>2</sub>Cl<sub>2</sub> (x2). Organics were dried (MgSO<sub>4</sub>), filtered, and concentrated under reduced pressure to afford **4.35** (703 mg, 71%) as a colorless oil. <sup>1</sup>H NMR (500 MHz, CDCl<sub>3</sub>) δ 4.05 (d, *J* = 13.2 Hz, 2H), 2.65 (dt, *J* = 2.6, 12.8 Hz, 2H), 2.40 (t, *J* = 7.4 Hz, 2H), 2.12 (s, 3H), 1.63 (m, *J* = 3.9 Hz, 2H), 1.58 (m, *J* = 6.2 Hz, 2H), 1.44 (s, 9H), 1.36 (m, *J* = 3.6 Hz, 1H), 1.21 (m, *J* = 3.0 Hz, 2H), 1.05 (m, *J* = 5.2 Hz, 2H). <sup>13</sup>C NMR (126 MHz, CDCl<sub>3</sub>) δ 208.99, 154.90, 79.20, 43.99, 43.82, 35.98, 35.91, 32.07, 29.93, 28.48, 20.88. HPLC/MS MH<sup>+</sup> 170.2 (-Boc).

### Preparation of 4.43 and 4.44:



### 1-(4-(4-oxopentyl)piperidin-1-yl)octan-1-one (4.42):

To a solution of **4.35** (200 mg, 0.74 mmol) in CH<sub>2</sub>Cl<sub>2</sub> (10 mL) at 0 °C was added TFA (10% v/v, 1.14 mL, 14.85 mmol). Resulting solution was allowed to stir at 0 °C until

completion as determined by TLC. Reaction mixture was concentrated under reduced pressure and resultant residue was immediately used. **4.40** (188 mg, 0.74 mmol) and **4.41** (172 mg, 0.71 mmol) were dissolved in MeCN (3 mL). To resulting solution was added DIPEA (0.39 mL, 2.22 mmol) at 0 °C and resulting reaction mixture was allowed to stir at 0 °C for 2h. Reaction mixture was then diluted with EtOAc and washed with saturated aqueous NH<sub>4</sub>Cl (x1) and H<sub>2</sub>O (x3). Organics were dried (MgSO<sub>4</sub>), filtered, and concentrated under reduced pressure to afford **4.42** which was used without further purification. <sup>1</sup>H NMR (500 MHz, CDCl<sub>3</sub>) δ 2.42 (t, *J* = 7.3 Hz, 2H), 2.33 (t, *J* = 7.8 Hz, 2H), 2.13 (s, 3H), 1.73 (d, *J* = 12.6 Hz, 2H), 1.60 (m, *J* = 5.4 Hz, 4H), 1.54 (t, *J* = 7.2 Hz, 1H), 1.48 (m, 1H), 1.44 (d, *J* = 6.6 Hz, 1H), 1.26 (m, 12H), 1.07 (m, 2H), 0.87 (t, *J* = 7.0 Hz, 3H). <sup>13</sup>C NMR (126 MHz, CDCl<sub>3</sub>) δ 208.88, 172.01, 60.41, 53.65, 43.72, 36.03, 35.80, 33.38, 31.71, 29.97, 29.48, 29.07, 25.59, 22.62, 20.82, 14.09.

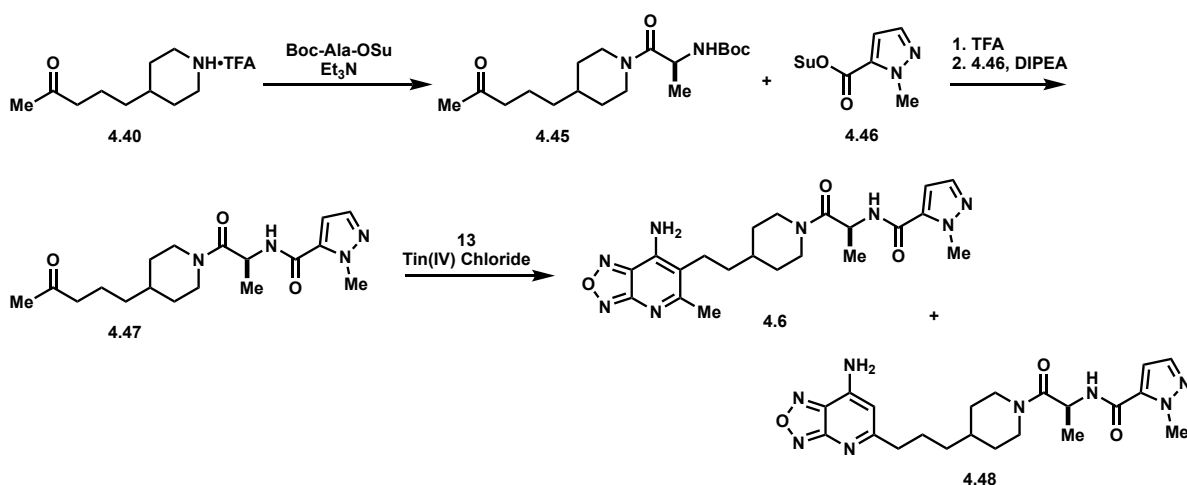
**1-(4-(2-(7-amino-5-methyl-[1,2,5]oxadiazolo[3,4-*b*]pyridin-6-yl)ethyl)piperidin-1-yl)octan-1-one (4.43) and 1-(4-(3-(7-amino-[1,2,5]oxadiazolo[3,4-*b*]pyridin-5-yl)propyl)piperidin-1-yl)octan-1-one (4.44):**

To a suspension of **4.42** (210 mg, 0.71 mmol) and **4.13** (79 mg, 0.71 mmol) in toluene (4 mL) was added tin(IV) chloride (0.17 mL, 1.42 mmol). The resulting mixture was allowed to stir at room temperature for 30 minutes and then refluxed for 18 hours. Reaction was cooled to room temperature and concentrated under reduced pressure. The resultant residue was dissolved in CH<sub>2</sub>Cl<sub>2</sub> and washed with saturated aqueous NaHCO<sub>3</sub> (x1). Aqueous was extracted with CH<sub>2</sub>Cl<sub>2</sub> (x3). Organics were combined, washed with brine (x1), dried (MgSO<sub>4</sub>), filtered, and concentrated under reduced pressure. Residue was purified by column chromatography using 5% MeOH in CH<sub>2</sub>Cl<sub>2</sub> as eluents to afford **4.43** (52 mg), **4.44** (35 mg), and mixed fractions enriched in **4.43** (49 mg) as yellow solids. **4.43**: <sup>1</sup>H NMR (500 MHz, MeOD) δ 4.54 (d, *J* = 13.0 Hz, 1H), 3.97 (d, *J* = 13.6 Hz, 1H), 3.10 (m, *J* = 5.6 Hz, 1H), 2.70 (m, *J* = 4.3 Hz, 2H), 2.64 (s, 3H), 2.60 (s, 1H), 2.37 (t, *J* = 7.6 Hz, 2H), 1.89 (q, *J* = 11.4 Hz, 2H), 1.73 (m, *J* = 4.4 Hz, 1H), 1.57 (t, *J* = 6.7 Hz, 2H), 1.45 (q, *J* = 7.9 Hz, 2H), 1.31 (m, *J* = 4.6 Hz, 8H), 1.16 (m, *J* = 6.1 Hz, 2H), 0.88 (t, *J* = 7.0 Hz, 3H). <sup>13</sup>C NMR (126 MHz, MeOD) δ 172.69, 164.07, 151.89, 147.77, 45.92, 41.80,



35.91, 33.27, 32.81, 32.42, 31.50, 31.47, 29.04, 28.81, 25.32, 22.75, 22.26, 20.06, 12.99. HPLC/MS  $MH^+$  388.3, 410.3 (+Na). **4.44**:  $^1H$  NMR (500 MHz, MeOD)  $\delta$  6.47 (s, 1H), 4.49 (d,  $J$  = 13.2 Hz, 1H), 3.93 (d,  $J$  = 13.7 Hz, 1H), 3.05 (dt,  $J$  = 2.8, 13.0 Hz, 1H), 2.82 (t,  $J$  = 7.6 Hz, 2H), 2.58 (dt,  $J$  = 2.7, 13.0 Hz, 1H), 2.35 (t,  $J$  = 7.6 Hz, 2H), 2.20 (t,  $J$  = 7.5 Hz, 1H), 1.81 (m, 3H), 1.75 (d,  $J$  = 13.0 Hz, 1H), 1.57 (m, 3H), 1.38 (q,  $J$  = 7.6 Hz, 2H), 1.31 (m, 10H), 1.07 (m,  $J$  = 5.8 Hz, 1H), 0.88 (t,  $J$  = 7.0 Hz, 3H).  $^{13}C$  NMR (126 MHz, MeOD)  $\delta$  172.61, 169.17, 154.01, 150.63, 139.42, 100.46, 45.92, 41.80, 36.09, 35.52, 35.44, 32.80, 32.54, 31.59, 31.49, 29.02, 28.80 (t,  $J$  = 9.7 Hz), 25.80, 25.51, 25.32, 22.26. HPLC/MS  $MH^+$  388.3, 410.3 (+Na).

### Preparation of 4.6 and 4.48:



### **tert-butyl (S)-(1-oxo-1-(4-(4-oxopentyl)piperidin-1-yl)propan-2-yl)carbamate (4.45):**

To a solution of **4.40** (188 mg, 0.74 mmol) and Boc-Ala-OSu (203 mg, 0.71 mmol) in MeCN (3 mL) was added DIPEA (0.39 mL, 2.22 mmol) at 0 °C. Resulting mixture was allowed to stir at 0 °C for 2 hours and then was diluted with EtOAc and washed with saturated aqueous  $NH_4Cl$  and  $H_2O$  (x3). Organics were dried ( $MgSO_4$ ), filtered, and concentrated under reduced pressure. Residue was purified by column chromatography using 1:1 hexanes:EtOAc as eluents to afford **4.45** (122 mg, 50%) as a colorless oil.  $^1H$  NMR (500 MHz,  $CDCl_3$ )  $\delta$  5.59 (s, 1H), 4.56 (m, 2H), 3.83 (t,  $J$  = 12.4 Hz, 1H), 3.00 (m,

1H), 2.57 (m, 1H), 2.42 (t,  $J = 6.7$  Hz, 2H), 2.13 (s, 3H), 1.77 (m, 2H), 1.59 (t,  $J = 3.8$  Hz, 2H), 1.49 (m, 2H), 1.43 (d,  $J = 4.0$  Hz, 9H), 1.28 (dd,  $J = 6.9, 8.5$  Hz, 1H), 1.10 (m, 3H).

**(S)-1-methyl-N-(1-oxo-1-(4-(4-oxopentyl)piperidin-1-yl)propan-2-yl)-1H-pyrazole-5-carboxamide (4.47):**

To a solution of **4.45** (122 mg, 0.36 mmol) in  $\text{CH}_2\text{Cl}_2$  (5 mL) at 0 °C was added TFA (10% v/v, 0.55 mL, 7.16 mmol). Resulting mixture was allowed to stir at 0 °C until completion as determined by TLC. Reaction mixture was concentrated under reduced pressure and resultant residue was used immediately without purification. The deprotected material (0.36 mmol) and **4.46** (80 mg, 0.36 mmol) were suspended in MeCN (1.5 mL) at 0 °C. To the suspension was added DIPEA (0.19 mL, 1.08 mmol) and resulting reaction mixture was allowed to stir at 0 °C for 2 hours and then was diluted with EtOAc. Organics were washed with saturated aqueous  $\text{NH}_4\text{Cl}$  and  $\text{H}_2\text{O}$  (x3), dried ( $\text{MgSO}_4$ ), filtered, and concentrated under reduced pressure. Residue was purified by column chromatography using 1:1 hexanes:EtOAc as eluents to afford **4.47** (90 mg, 72%). \*rotational isomers present\*  $^1\text{H}$  NMR (500 MHz,  $\text{CDCl}_3$ )  $\delta$  7.44 (d,  $J = 1.5$  Hz, 1H), 7.28 (s, 1H), 6.60 (q,  $J = 2.6$  Hz, 1H), 4.97 (q,  $J = 6.6$  Hz, 1H), 4.56 (t,  $J = 12.9$  Hz, 1H), 4.18 (s, 3H), 3.87 (m, 1H), 3.06 (m, 1H), 2.62 (m, 1H), 2.43 (q,  $J = 7.1$  Hz, 2H), 2.13 (d,  $J = 3.7$  Hz, 3H), 1.81 (m, 2H), 1.58 (m, 2H), 1.52 (m, 1H), 1.40 (q,  $J = 5.5$  Hz, 3H), 1.24 (t,  $J = 18.2$  Hz, 2H), 1.11 (m, 2H).  $^{13}\text{C}$  NMR (126 MHz, MeOD)  $\delta$  208.73, 170.13, 169.94, 158.81, 137.51, 106.76, 60.41, 45.90, 45.52, 45.41, 43.64 (d,  $J = 5.3$  Hz, 1C), 42.85, 42.51, 39.26, 36.06, 35.89, 35.69, 35.62, 32.66, 32.47, 31.71 (d,  $J = 6.5$  Hz, 1C), 29.98, 20.74, 19.42, 18.91, 14.21.

**(S)-N-(1-(4-(2-(7-amino-5-methyl-[1,2,5]oxadiazolo[3,4-*b*]pyridin-6-yl)ethyl)piperidin-1-yl)-1-oxopropan-2-yl)-1-methyl-1H-pyrazole-5-carboxamide (4.6) and (S)-N-(1-(4-(3-(7-amino-[1,2,5]oxadiazolo[3,4-*b*]pyridin-5-yl)propyl)piperidin-1-yl)-1-oxopropan-2-yl)-1-methyl-1H-pyrazole-5-carboxamide (4.48):**

Following the protocol as described for **4.43** and **4.44**, **4.47** (90 mg, 0.26 mmol) could be reacted with **4.13** (28 mg, 0.26 mmol) to afford **4.6** and **4.48**. **4.6**:  $^1\text{H}$  NMR (500 MHz, MeOD)  $\delta$  7.43 (d,  $J = 2.0$  Hz, 1H), 6.83 (s, 1H), 4.97 (m, 1H), 4.47 (m, 1H), 4.06 (d,  $J =$

5.6 Hz, 31H), 4.01 (d,  $J = 10.5$  Hz, 1H), 3.12 (m, 1H), 2.65 (m, 1H), 2.46 (q,  $J = 7.0$  Hz, 2H), 2.10 (d,  $J = 3.6$  Hz, 3H), 1.78 (m, 2H), 1.55 (m, 3H), 1.36 (dd,  $J = 7.1, 13.9$  Hz, 3H), 1.24 (m, 3H), 1.07 (m, 2H).  $^{13}\text{C}$  NMR (126 MHz, MeOD)  $\delta$  210.31, 170.8, 164.8, 137.12, 107.16, 45.69, 45.36, 45.22, 42.74, 42.55, 42.19, 37.73, 35.64, 35.43, 35.35, 35.23, 32.35, 32.21, 31.53, 31.43, 28.29, 20.32, 16.46, 15.98. **4.48**:  $^1\text{H}$  NMR (500 MHz, MeOD)  $\delta$  7.42 (q,  $J = 2.4$  Hz, 1H), 6.83 (m, 1H), 6.29 (d,  $J = 4.5$  Hz, 1H), 4.97 (m, 1H), 4.46 (m, 1H), 4.05 (s, 3H), 4.02 (s, 1H), 3.13 (m, 1H), 2.67 (m, 3H), 2.53 (d,  $J = 9.5$  Hz, 1H), 1.88 (q,  $J = 12.7$  Hz, 1H), 1.75 (m,  $J = 7.8$  Hz, 3H), 1.59 (s, 1H), 1.46 (q,  $J = 8.0$  Hz, 1H), 1.35 (dd,  $J = 7.1, 13.0$  Hz, 3H), 1.25 (s, 2H), 1.08 (m,  $J = 6.5$  Hz, 2H).  $^{13}\text{C}$  NMR (126 MHz, MeOD)  $\delta$  174.48, 159.60, 137.10, 107.15, 100.26, 45.23, 42.56, 38.87, 37.72, 35.53, 35.38, 32.20, 31.53, 31.43, 25.78, 23.05, 16.44, 15.95.

#### D. References

- (1) Galka, C. S.; Hembre, E. J.; Honigschmidt, N. A.; Keding, S. J.; Martinez-Grau, M. A.; Plaza, G. R.; Rubio, A.; Smith, D. L. Ghrelin O-Acyl Transferase Inhibitors. WO2016168225A1. 13 April 2016.
- (2) Godbout, C.; Trieselmann, T.; Vintonyak, V. Oxadiazolopyridine Derivatives for Use as Ghrelin O-Acyl Transferase (GOAT) Inhibitors. WO2018024653A1. 8 February 2018.
- (3) Yoneyama-Hirozane, M.; Deguchi, K.; Hirakawa, T.; Ishii, T.; Odani, T.; Matsui, J.; Nakano, Y.; Imahashi, K.; Takakura, N.; Chisaki, I.; Takekawa, S.; Sakamoto, J. Identification and Characterization of a New Series of Ghrelin O-Acyl Transferase Inhibitors. *SLAS Discov.* **2018**, 23 (2), 154–163.

## Compiled *In Vitro* and Cellular Inhibition Assay Results

### ***In Vitro* Inhibition Data**

All data was collected and processed by Dr. David Strugatsky.

#### **A. Methods**

pFastBac1-mouseGOAT and pGEX-GST-mouseProghrl8His plasmids were a kind gift from the Brown and Goldstein laboratory.

Recombinant proghrelin peptide was produced in *E. coli* from pGEX-GST-mouseProghrl8His plasmid as reported.<sup>1</sup>

#### ***Baculovirus Expression of Mouse GOAT:***

DH10Bac *E. coli* strain (ThermoFisher) was transformed with pFastBac1-mouseGOAT plasmid and Bacmid DNA from 12 white colonies was analyzed by DNA sequencing and PCR reaction. All clones were transfected to sf9 cells and the level of mGOAT expression was compared between clones from cells producing P2. The clone with the highest mGOAT expression level was used to produce P3. For membrane isolation, sf9 cells were seeded at  $2-4 \times 10^6$  /mL in total 1L volume of sf-900 serum-free medium (ThermoFisher) and infected with P3 virus. At day 2 post-infection, cells were harvested and resuspended in 40 mL of buffer containing 50 mM NaPi pH 7.2, 150 mM NaCl, 1 mM EDTA, 100  $\mu$ M bis(4-nitrophenyl) phosphate, 2.5  $\mu$ g/mL aprotinin, 10  $\mu$ g/mL leupeptin, and 10  $\mu$ g/mL pepstatin A. Cell suspension was briefly sonicated and cell debris was removed by centrifugation at 3000g x 10 min. Membrane fraction was collected from supernatant by centrifugation at 100,000g x 1 hour. Membrane pellet was resuspended in storage buffer (50 mM NaPi pH 7.2, 150 mM NaCl and 10% glycerol) and kept at -80 °C.

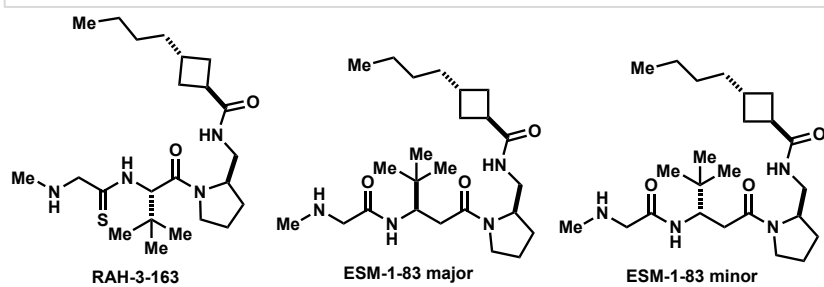
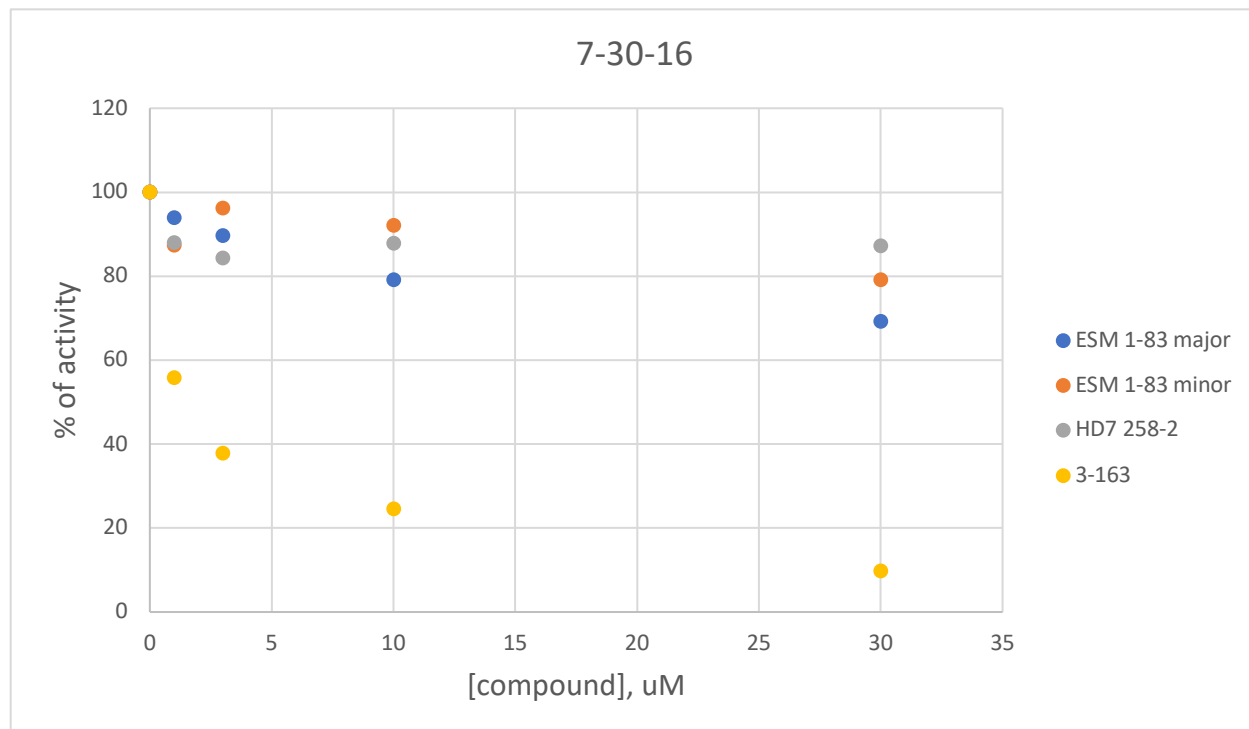
### ***Acyltransferase Assay:***

Assay conditions included are per 50  $\mu$ L reaction:

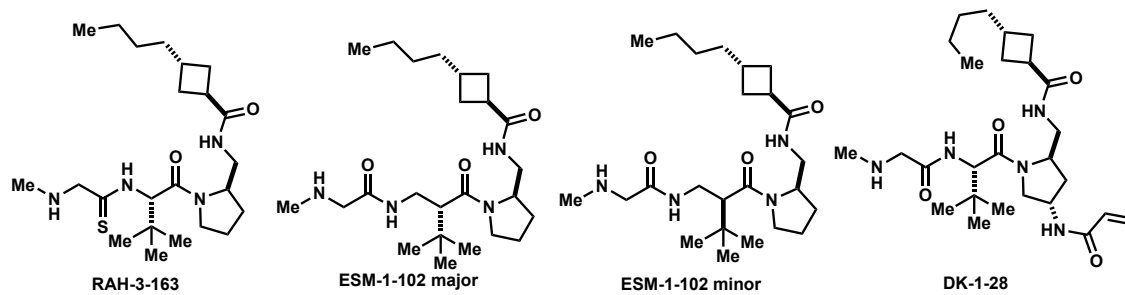
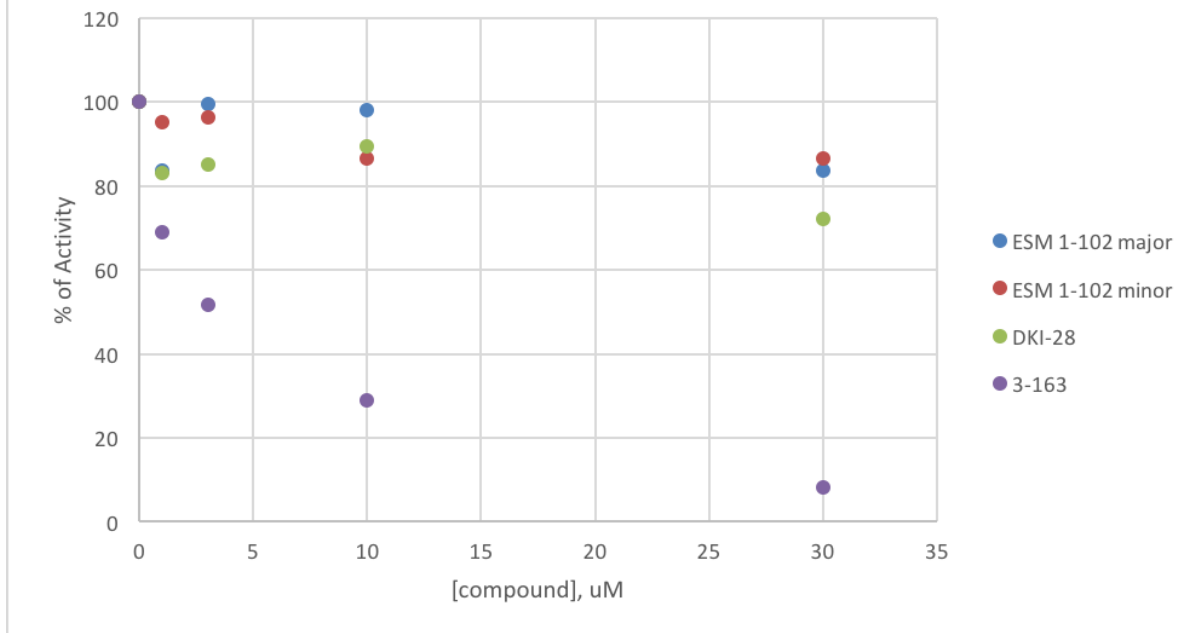
- 50  $\mu$ g of total sf9 membranes
- Various (for modality experiments) or fixed (for IC<sub>50</sub>) concentrations of recombinant proghrelin8His peptide
- Various concentrations of tested compound (for IC<sub>50</sub>)
- 100  $\mu$ M palmitoyl CoA
- 50 mM HEPES pH 7.0
- 1  $\mu$ M [<sup>3</sup>H] octanoyl CoA (~5.5 dpm/fmol – American Radioactive Chemicals)

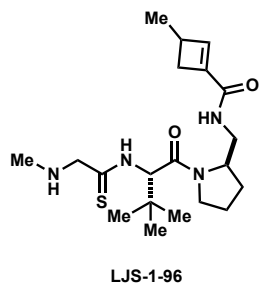
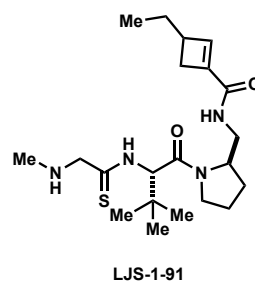
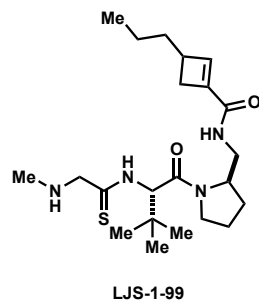
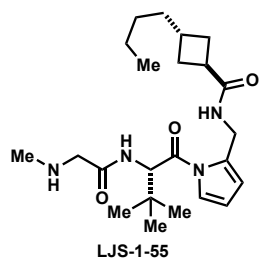
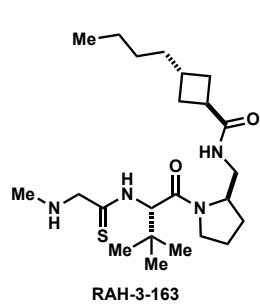
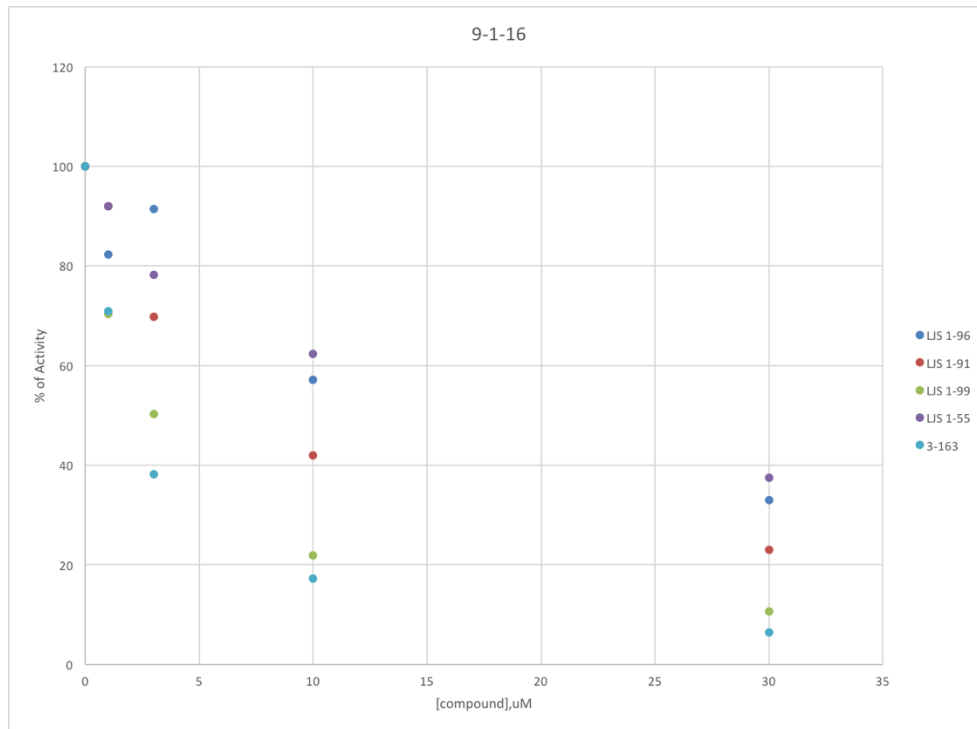
After incubation of the reaction mixture at 37 °C for 10 minutes, reaction tubes were placed on ice and 10  $\mu$ L of 1M HCl were added to each tube. Following addition of 750  $\mu$ L of cold quench buffer (50 mM NaPi pH 7.4, 10 mM imidazole, 150 mM NaCl, 100  $\mu$ M bis(4-nitrophenyl) phosphate, 1 mM phenylmethylsulfonyl fluoride and 0.1% Triton), 0.2 mL of 50% Ni-NTA slurry were added to each reaction. Tubes were incubated at 4 °C for 1 hour with rotation to capture proGhr18His. After washing of Ni resin with 40 mM imidazole, all bound proghrelin8His was eluted with 250 mM imidazole and the amount of octanoylated proghrelin was assessed with scintillation counting.

## B. In Vitro Assay Results

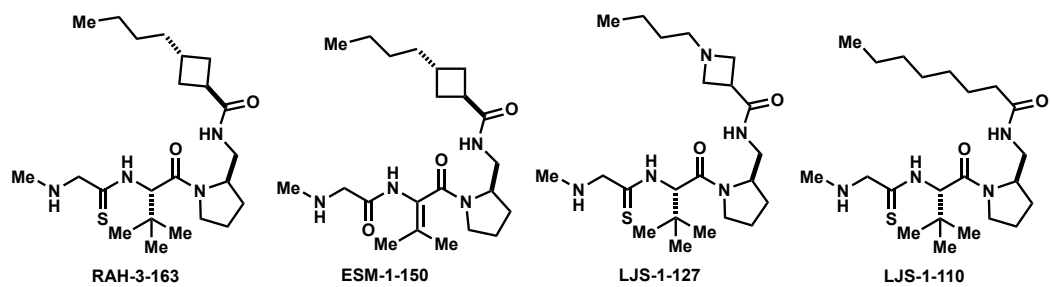
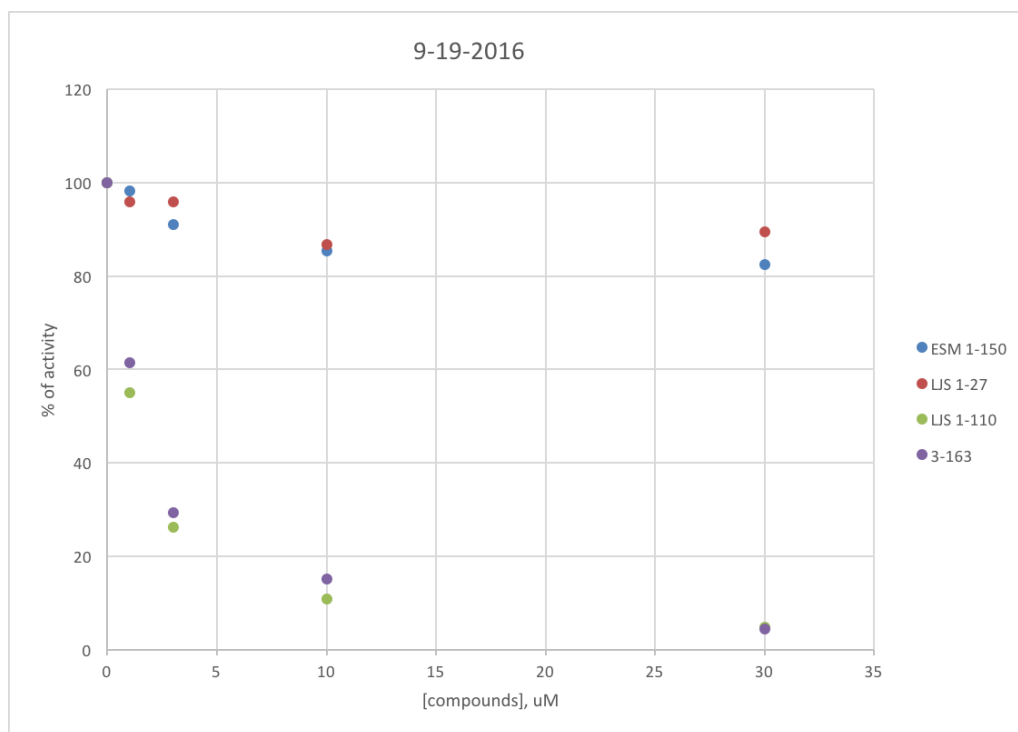


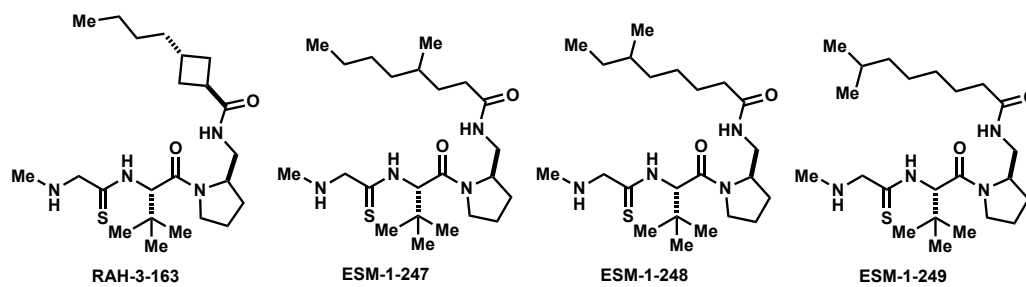
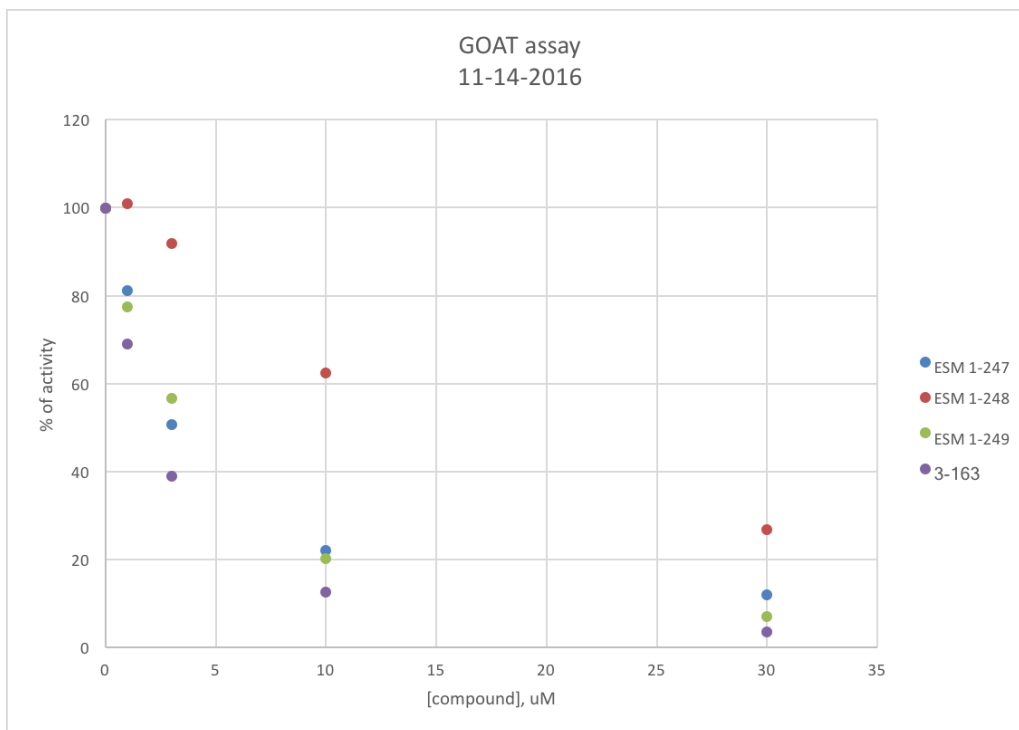
8-31-16

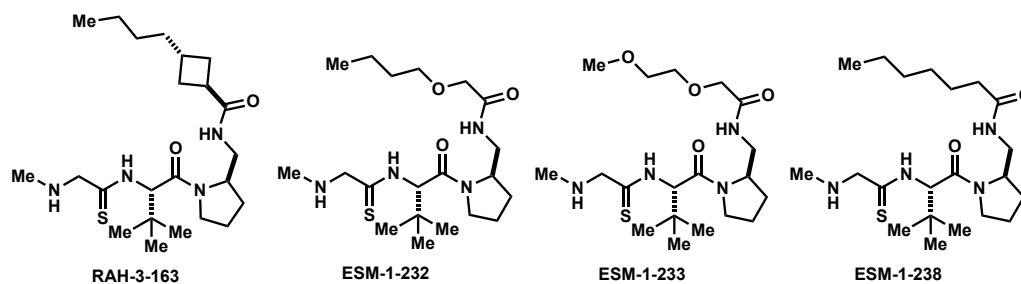
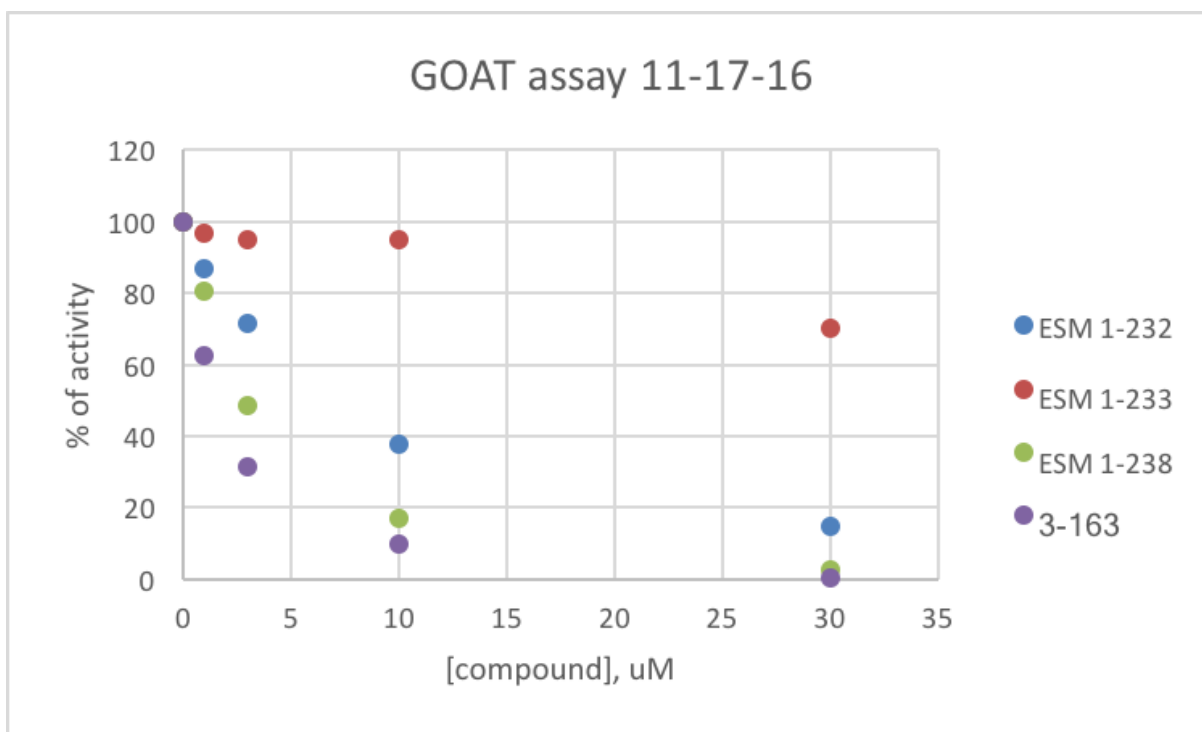


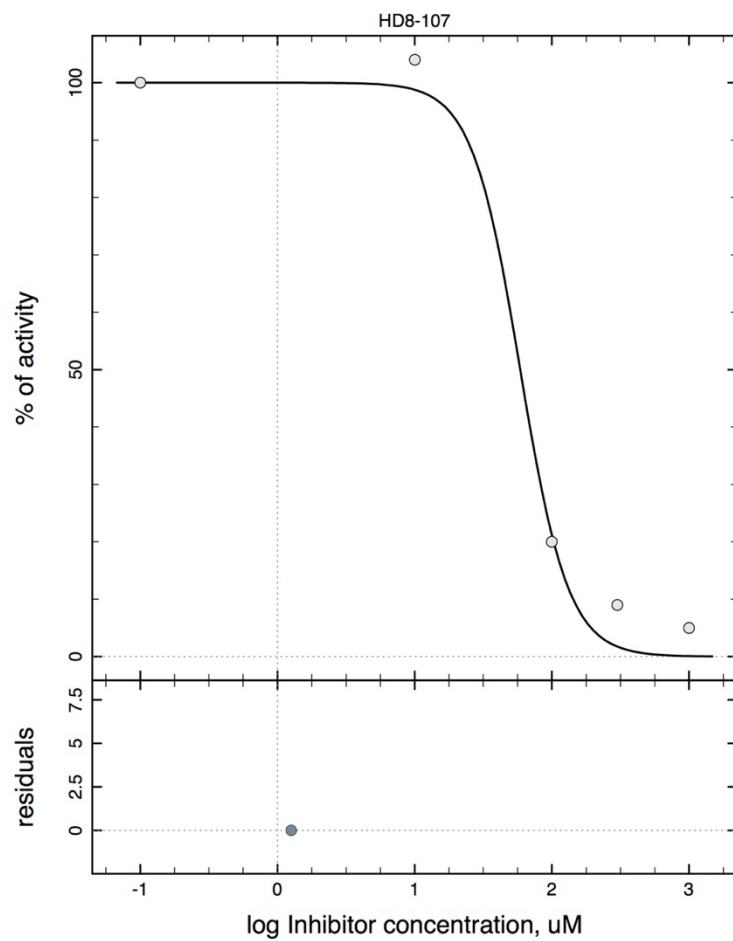




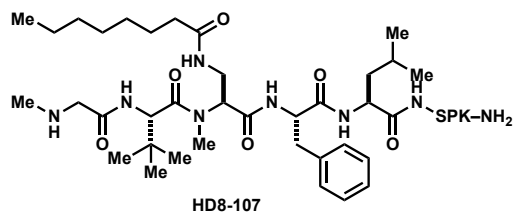


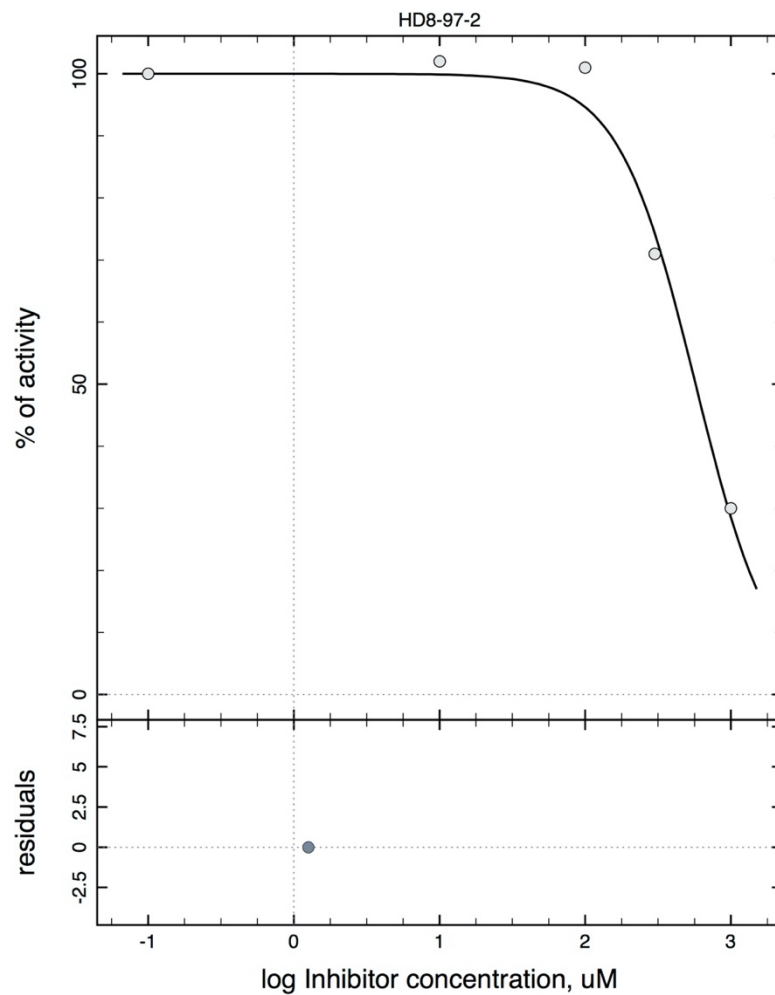




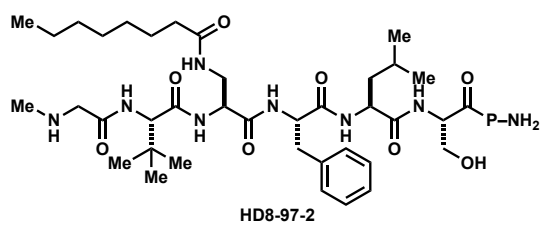


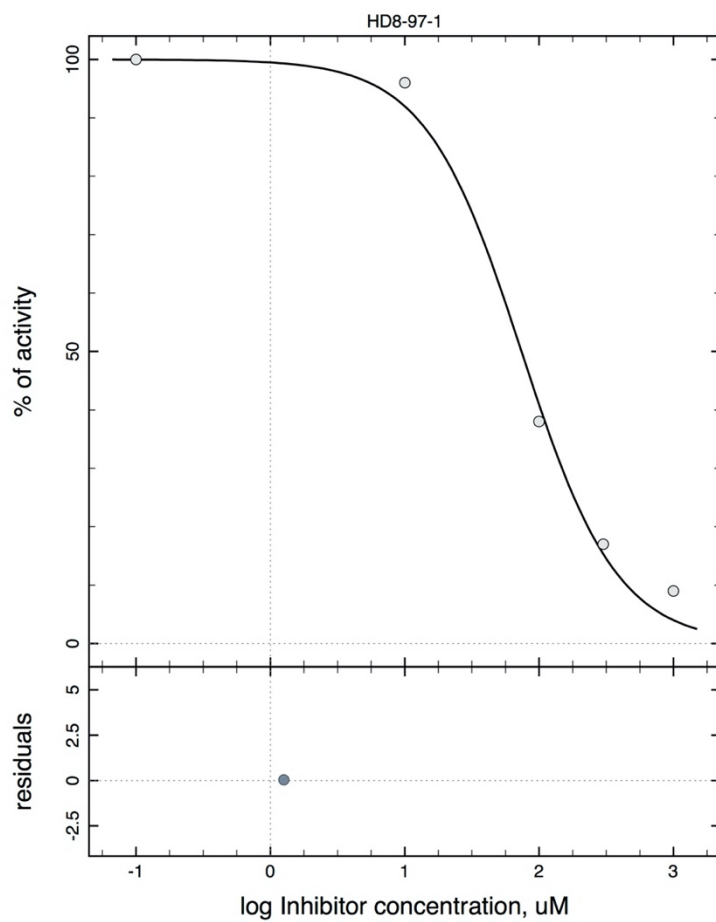
No.	Par#Set	Initial	Final	Std. Error	CV (%)	Note
#1	IC50	100	58.7836	23.6705	40.27	
#2	n	-1	-2.47667	1.75667	70.93	



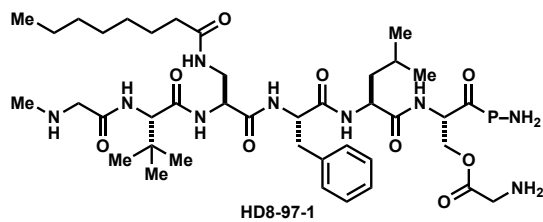


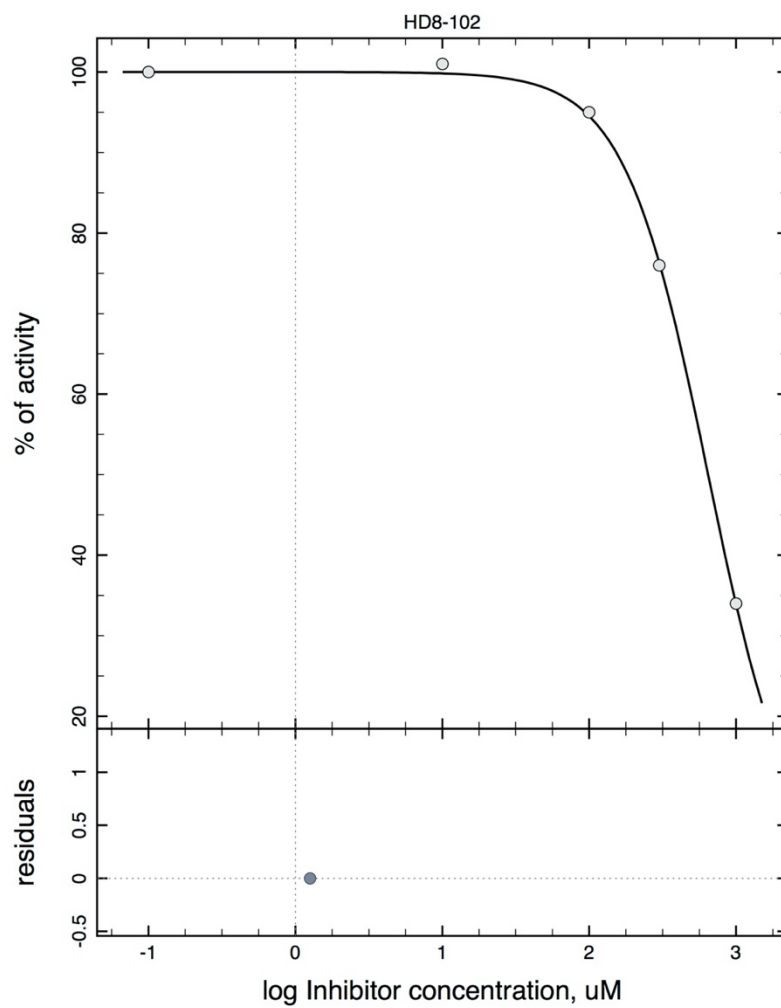
No.	Par# Set	Initial	Final	Std. Error	CV (%)	Note
#1	IC50	100	571.936	54.1611	9.47	
#2	n	-1	-1.64514	0.23299	14.16	



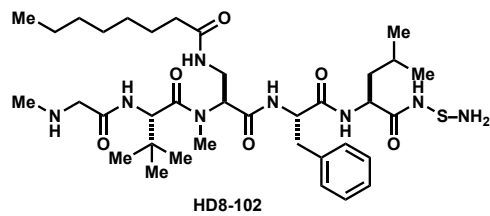


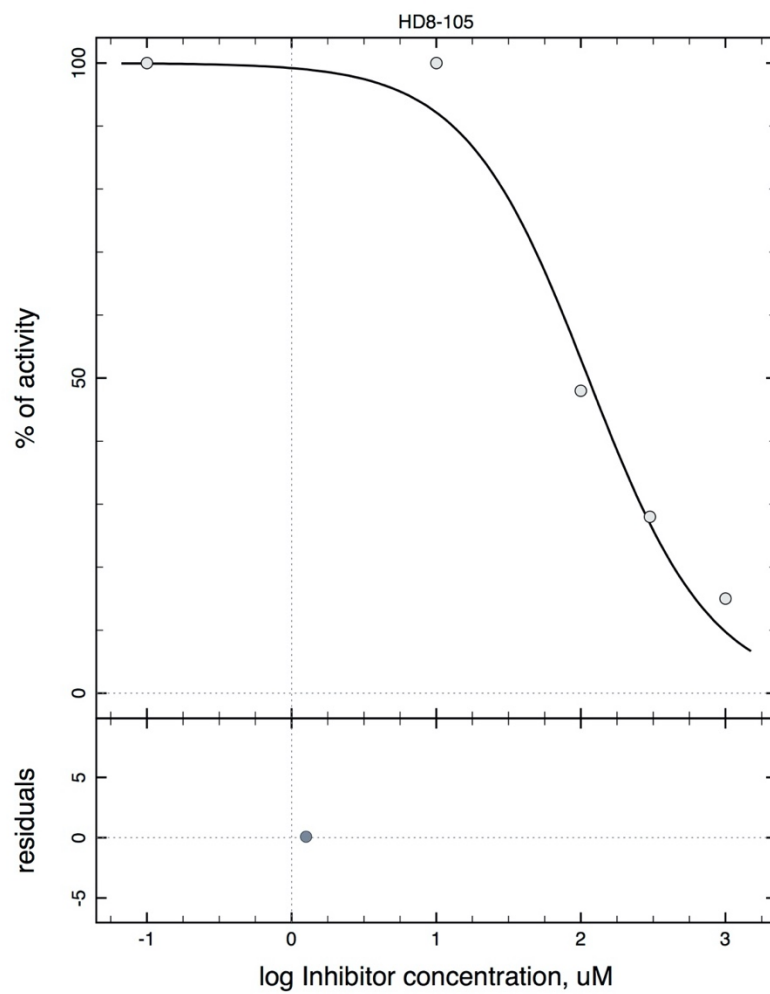
No.	Par#Set	Initial	Final	Std. Error	CV (%)	Note
#1	IC50	100	<b>73.9745</b>	9.88396	13.36	
#2	n	-1	<b>-1.22015</b>	0.176536	14.47	



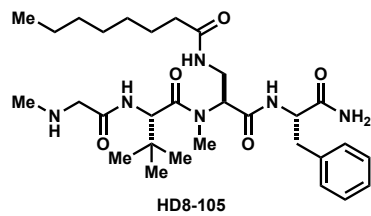


No.	Par#Set	Initial	Final	Std. Error	CV (%)	Note
#1	IC50	100	645.279	11.0399	1.71	
#2	n	-1	-1.52707	0.0391033	2.56	

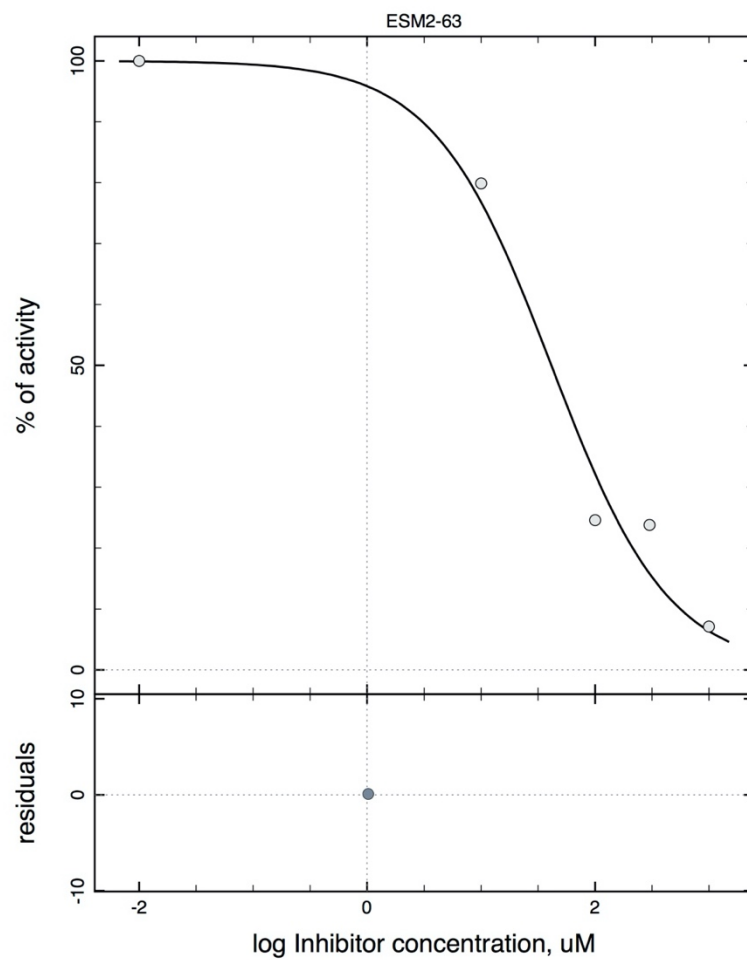




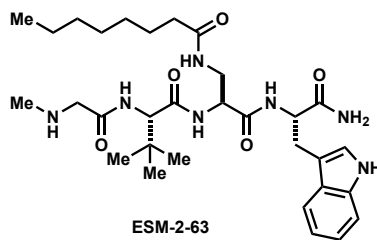
No.	Par#Set	Initial	Final	Std. Error	CV (%)	Note
#1	IC50	100	112.473	21.3959	19.02	
#2	n	-1	-1.01883	0.201148	19.74	



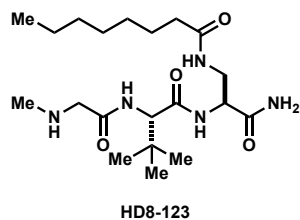
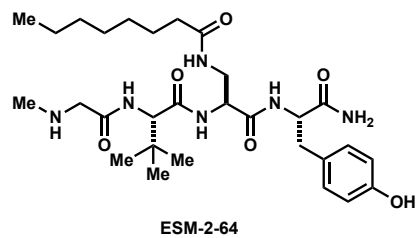
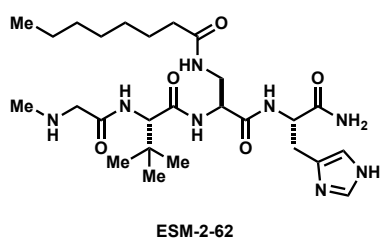
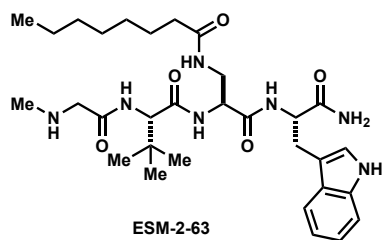
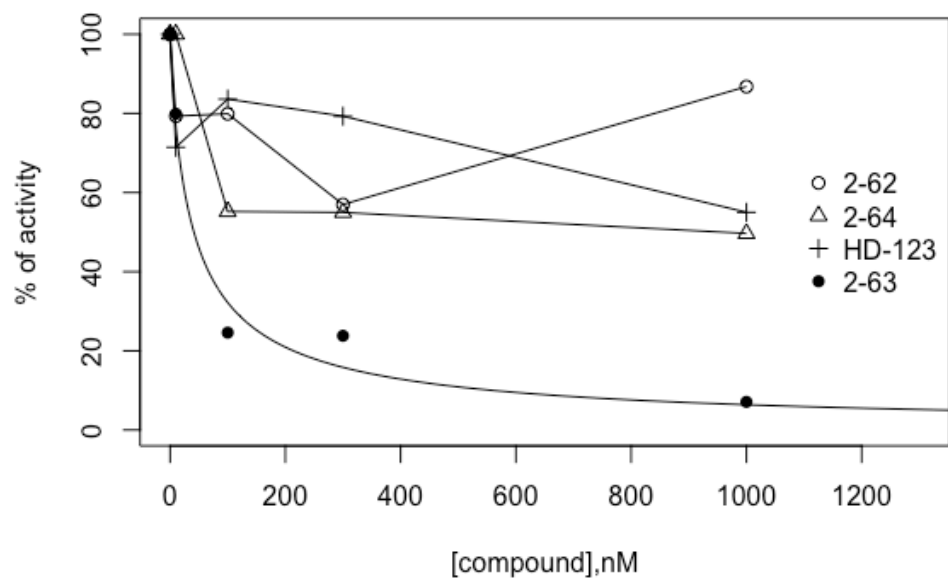


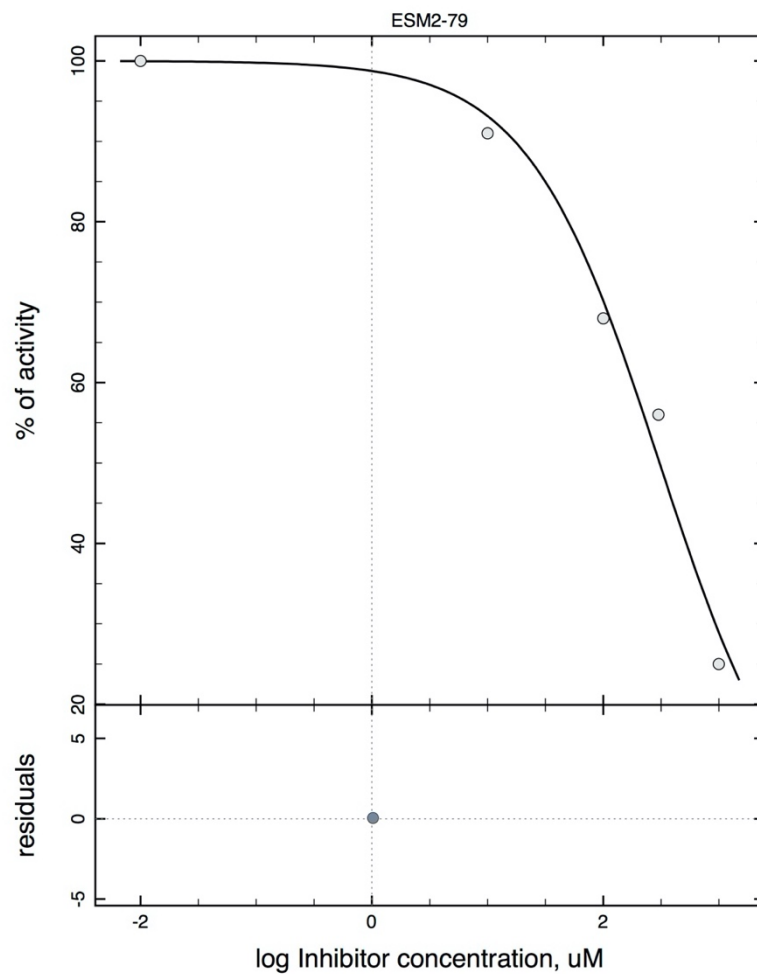


No.	Par#Set	Initial	Final	Std. Error	CV (%)	Note
#1	IC50	100	41.3514	10.7239	25.93	
#2	n	-1	-0.843683	0.152625	18.09	

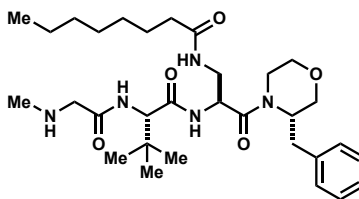


## *in-vitro* GOAT assay

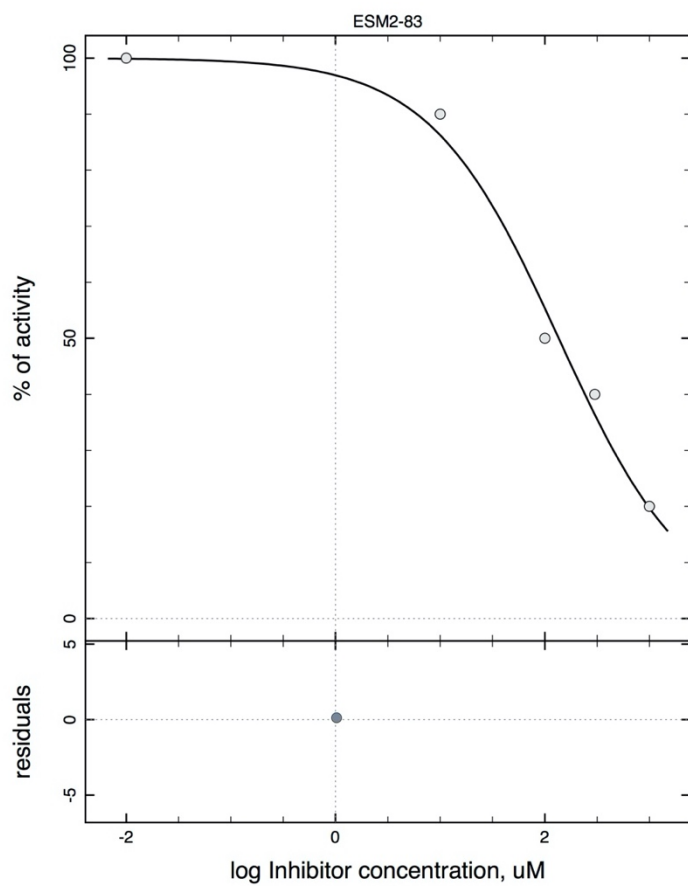




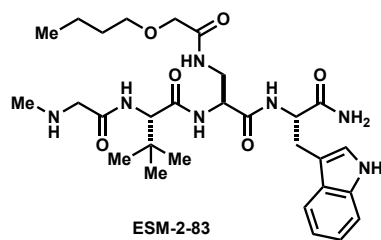
No.	Par#Set	Initial	Final	Std. Error	CV (%)	Note
#1	IC50	100	<b>306.958</b>	44.5051	14.50	
#2	n	-1	-0.762358	0.107357	14.08	



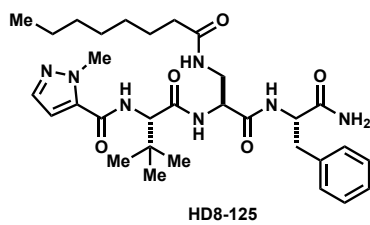
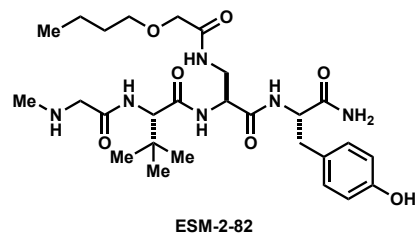
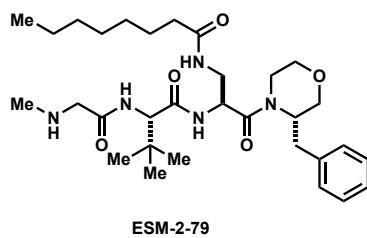
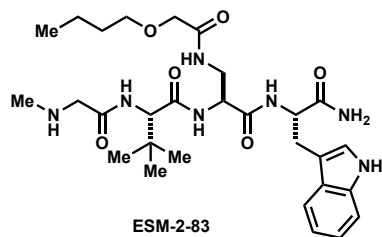
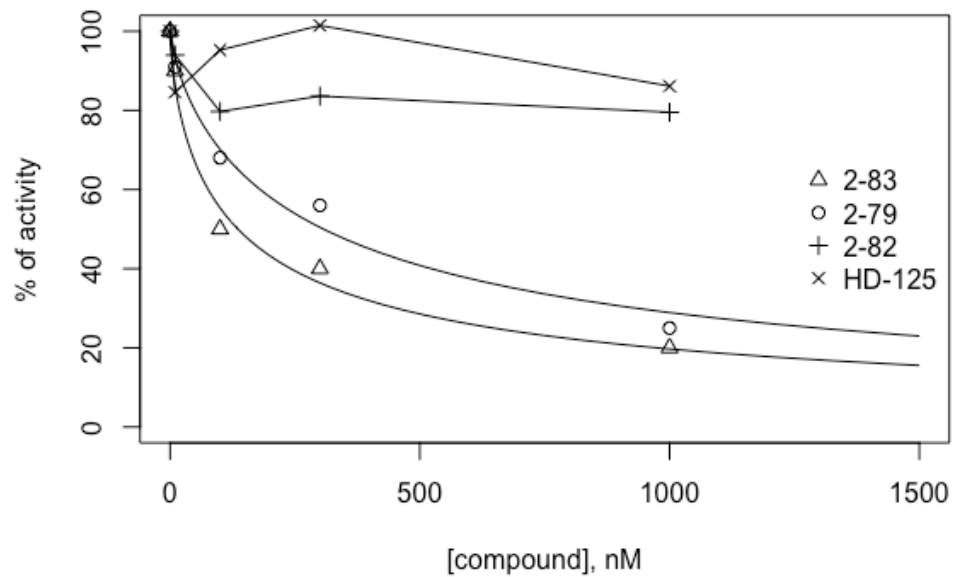
ESM-2-79

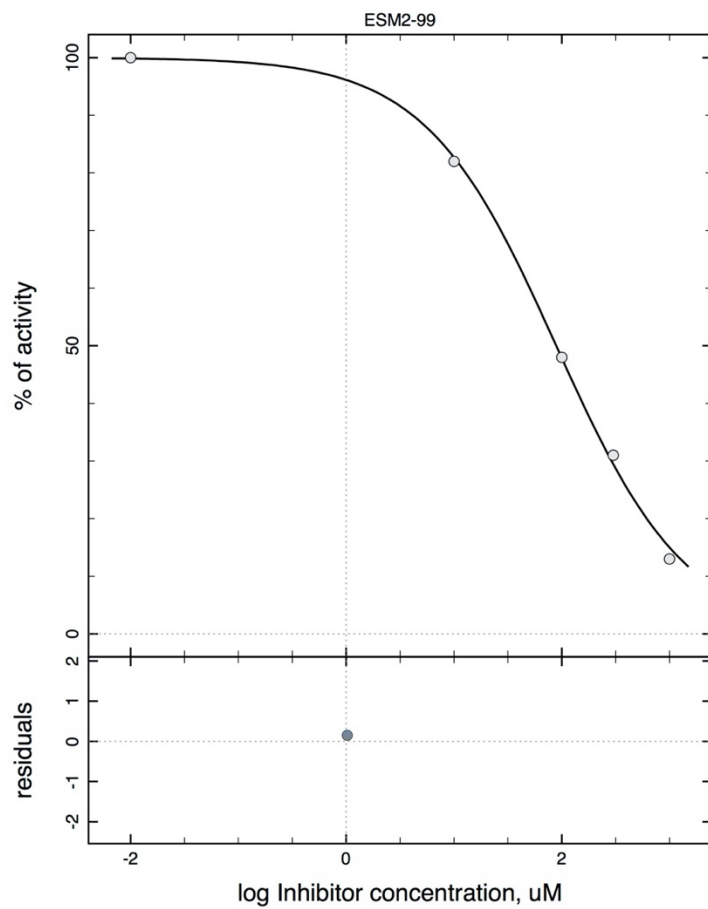


No.	Par#Set	Initial	Final	Std. Error	CV (%)	Note
#1	IC50	100	135.8	21.6509	15.94	
#2	n	-1	-0.703902	0.0907817	12.90	

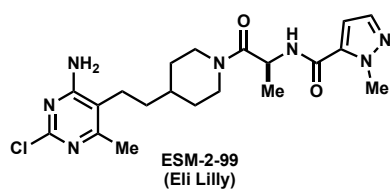


## *in-vitro* GOAT assay

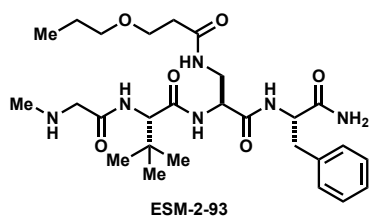
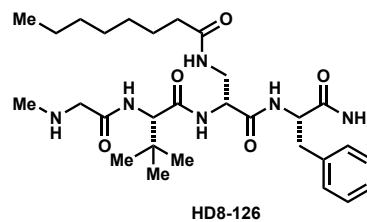
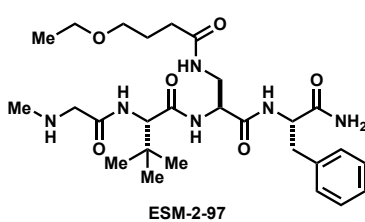
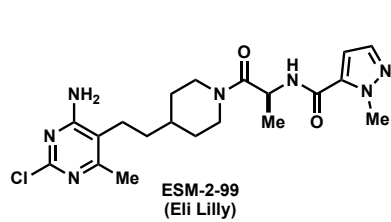
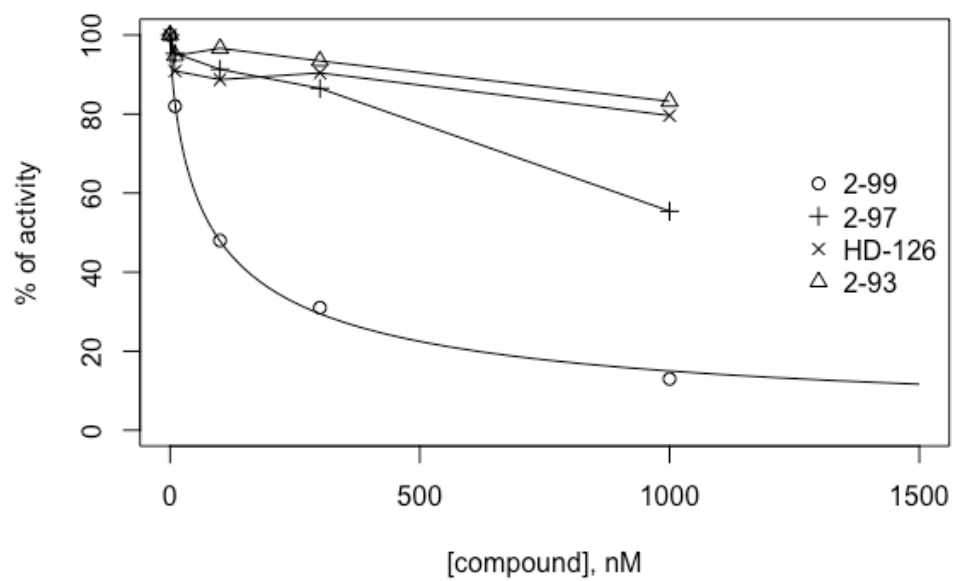


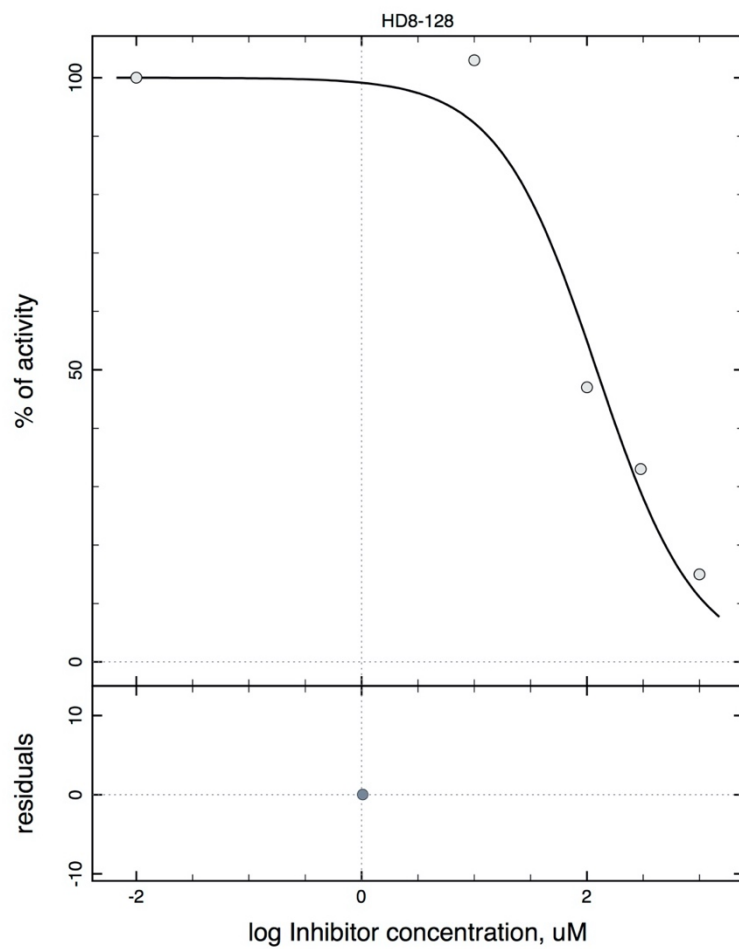


No.	Par# Set	Initial	Final	Std. Error	CV (%)	Note
	#1 IC50	100	<b>88.7551</b>	5.17078	5.83	
	#2 n	-1	<b>-0.716789</b>	0.0310079	4.33	

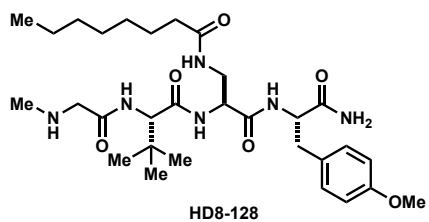


## *in-vitro* GOAT assay

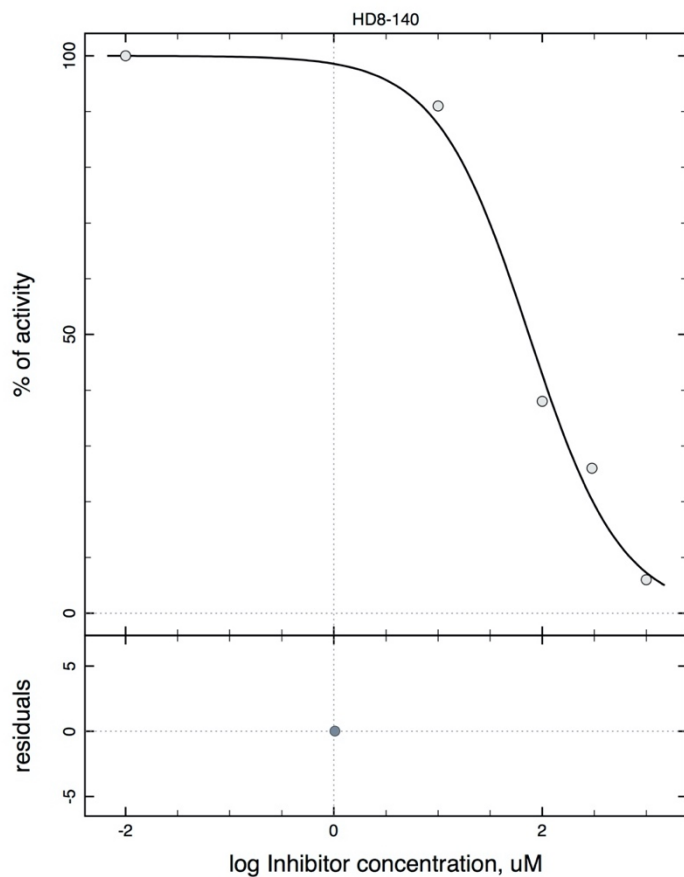




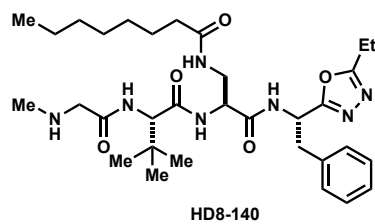
No.	Par# Set	Initial	Final	Std. Error	CV (%)	Note
#1	IC50	100	122.034	31.2164	25.58	
#2	n	-1	-0.989796	0.26079	26.35	

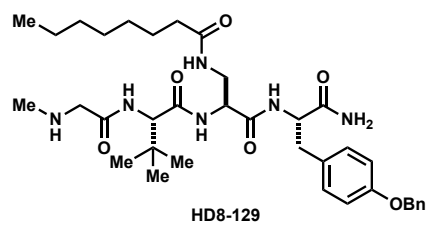
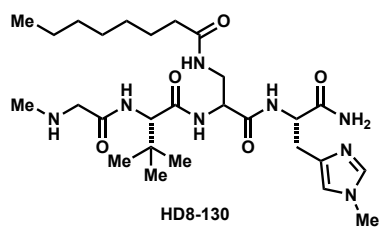
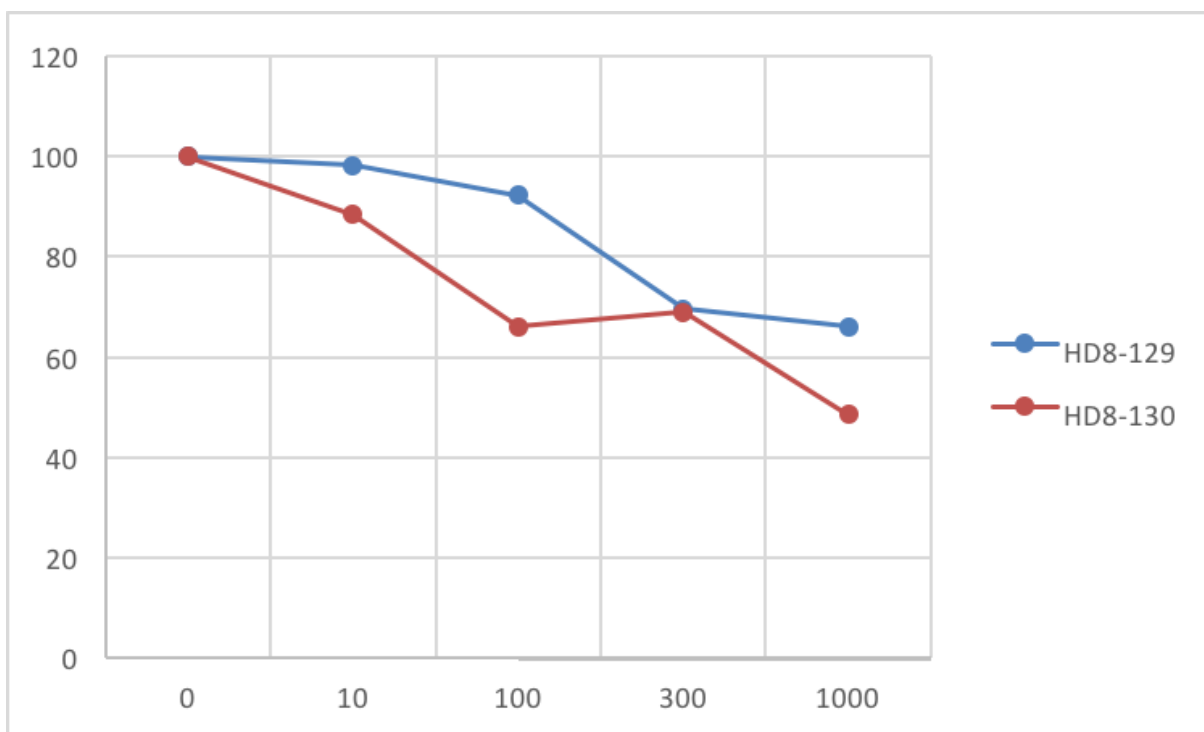


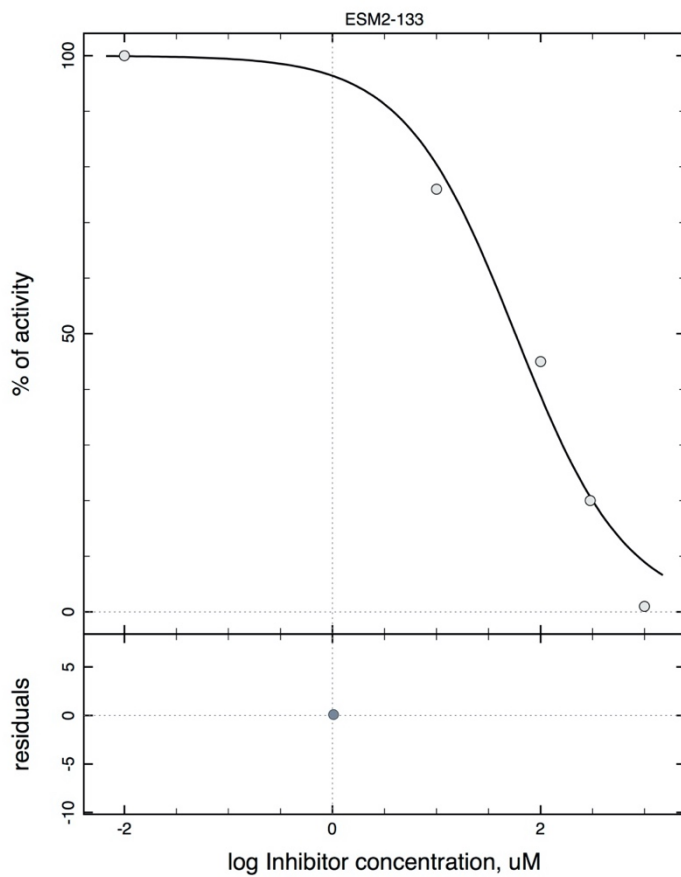




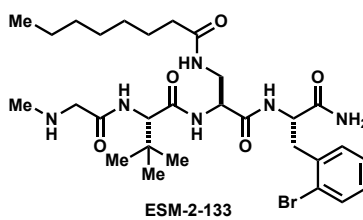
No.	Par# Set	Initial	Final	Std. Error	CV (%)	Note
#1	IC50	100	74.474	12.1272	16.28	
#2	n	-1	-0.979863	0.139665	14.25	

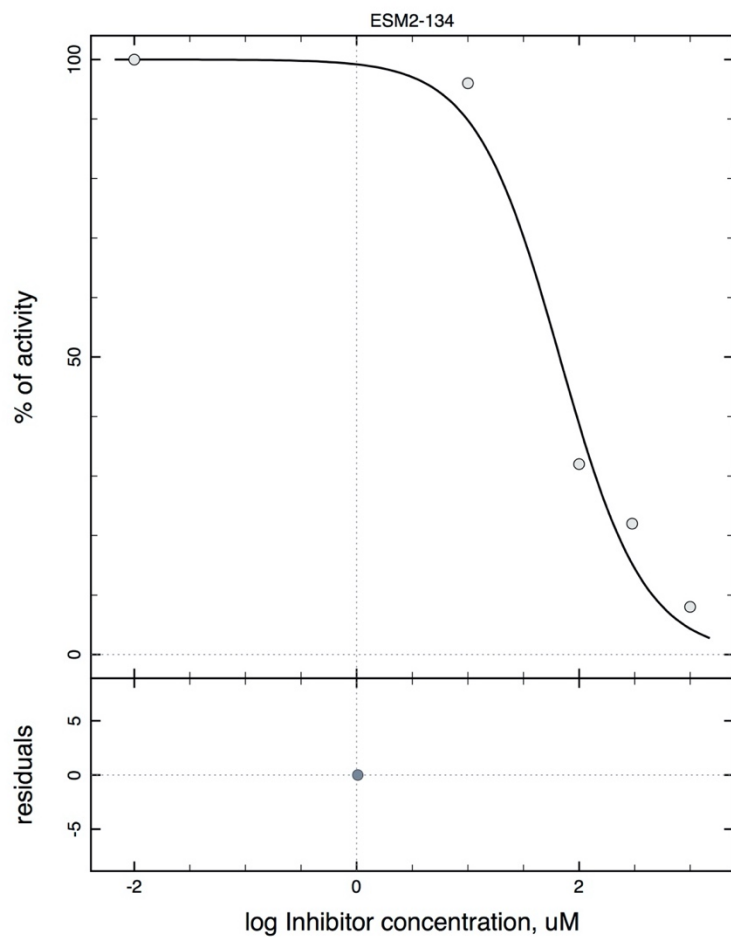




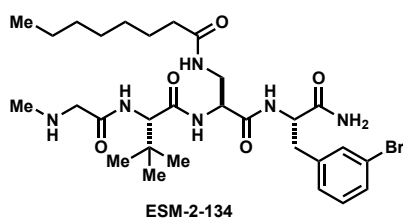


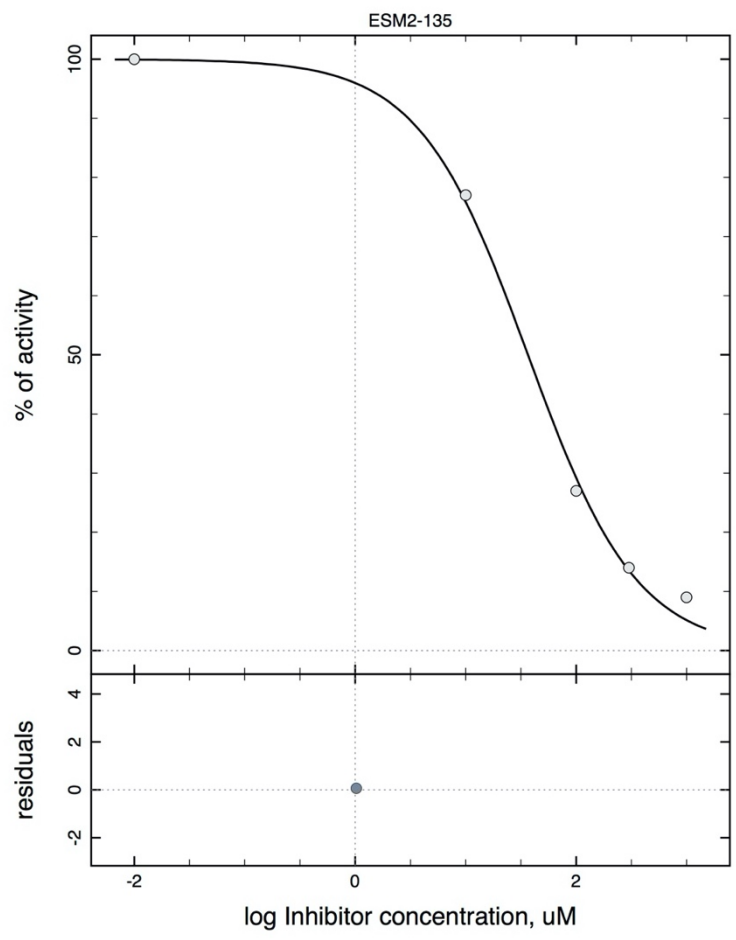
No.	Par#Set	Initial	Final	Std. Error	CV (%)	Note
#1	IC50	100	57.2044	13.9876	24.45	
#2	n	-1	-0.811189	0.142893	17.62	



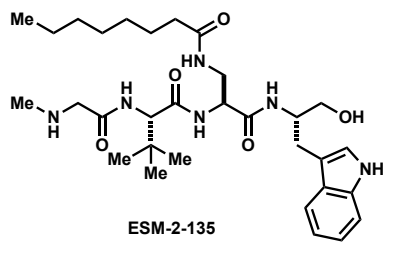


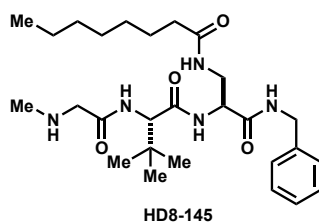
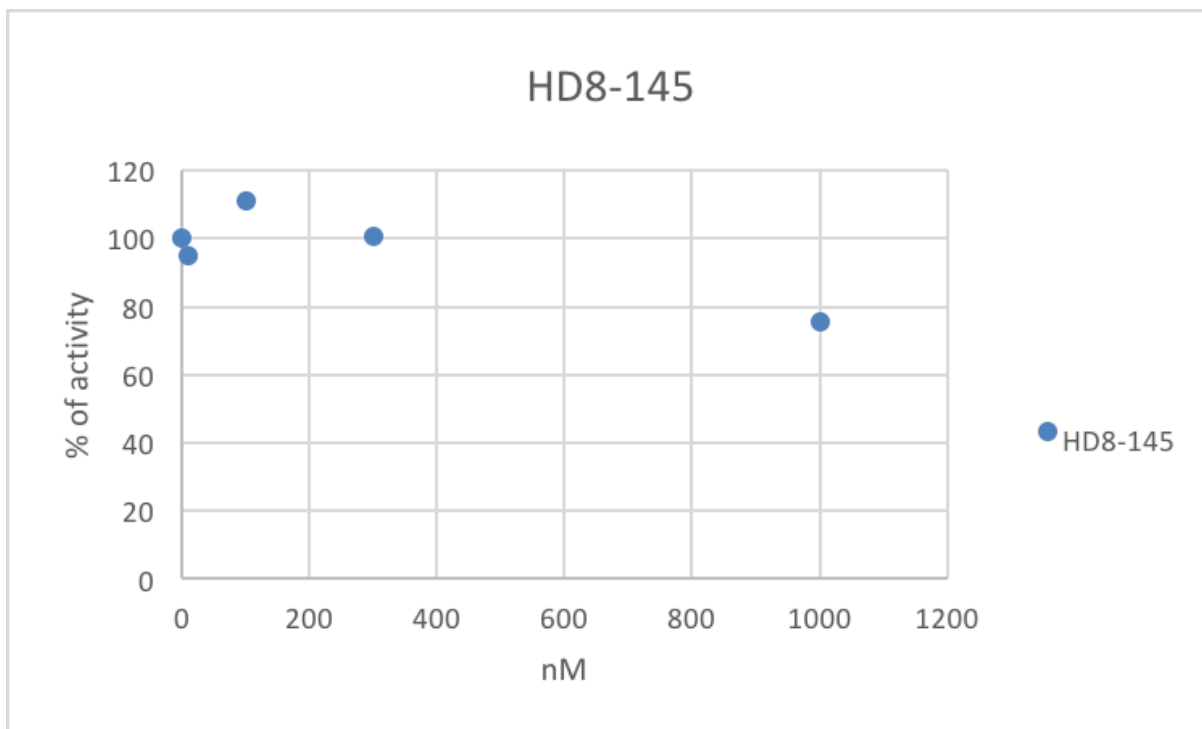
No.	Par#Set	Initial	Final	Std. Error	CV (%)	Note
#1	IC50	100	66.9343	15.4353	23.06	
#2	n	-1	-1.14388	0.254085	22.21	

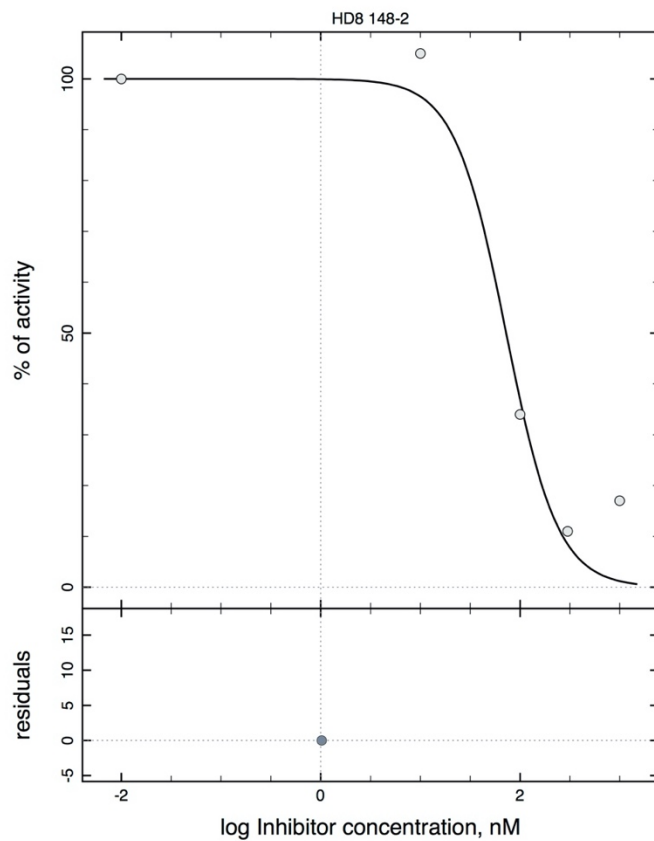




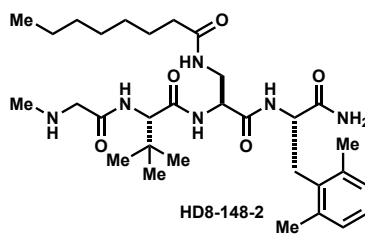
No.	Par#Set	Initial	Final	Std. Error	CV (%)	Note
#1	IC50	100	<b>36.6087</b>	3.78691	10.34	
#2	n	-1	<b>-0.88129</b>	0.064183	7.28	

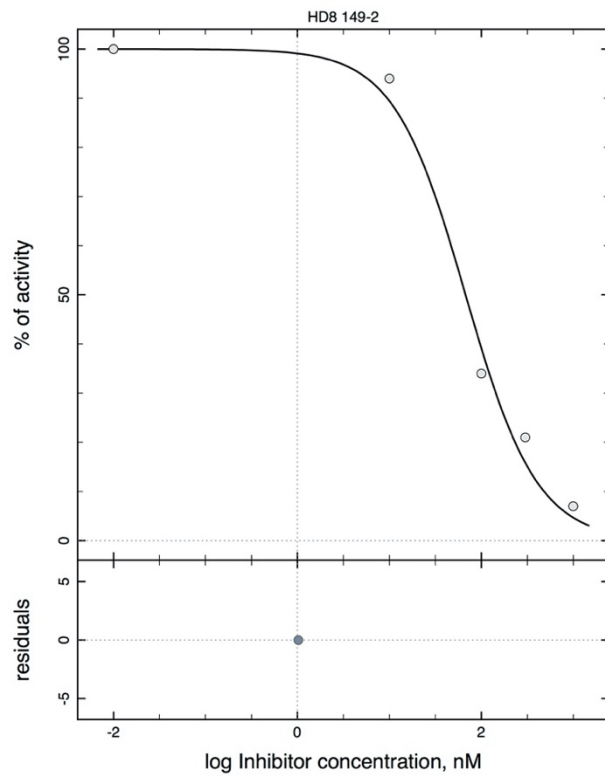




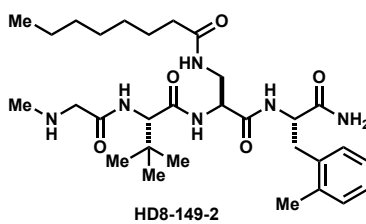


No.	Par#Set	Initial	Final	Std. Error	CV (%)	Note
#1	IC50	100	<b>72.5974</b>	23.9922	33.05	
#2	n	-1	<b>-1.67929</b>	0.907584	54.05	

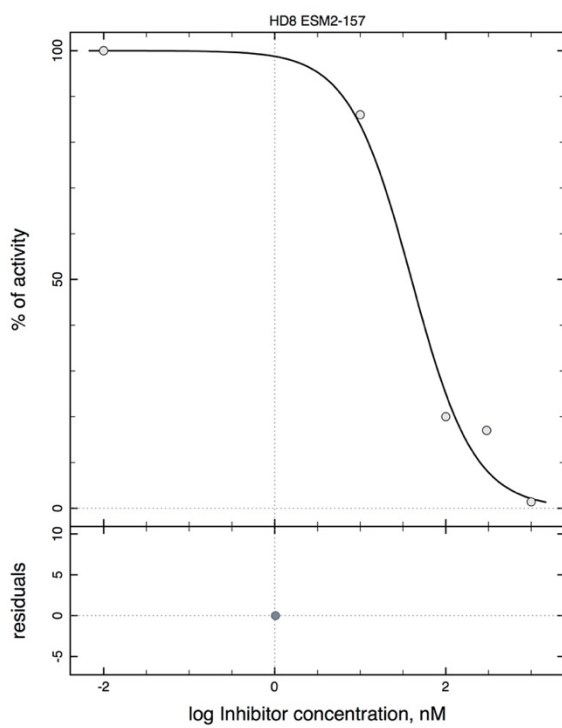




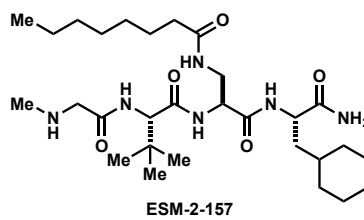
No.	Par# Set	Initial	Final	Std. Error	CV (%)	Note
#1	IC50	100	67.4054	11.644	17.27	
#2	n	-1	-1.11895	0.182958	16.35	

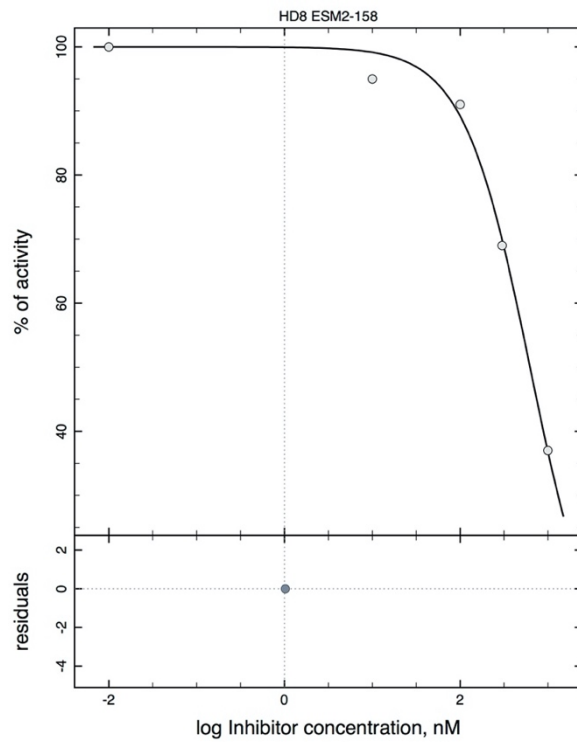




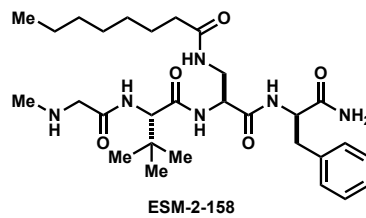


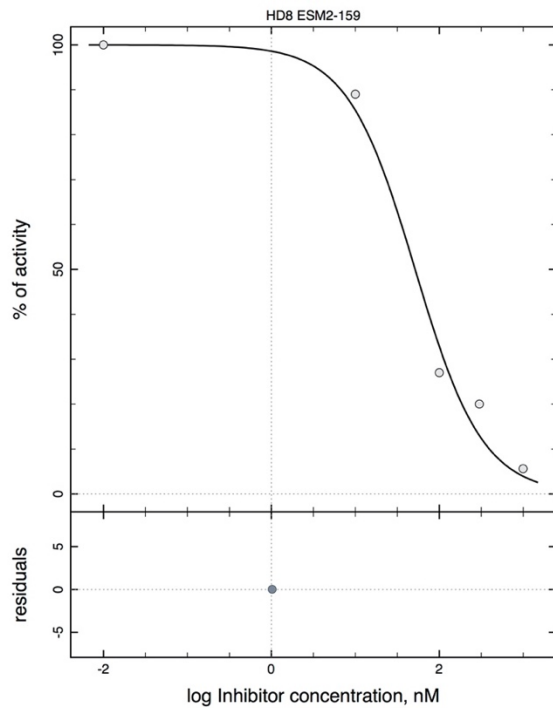
No.	Par#Set	Initial	Final	Std. Error	CV (%)	Note
#1	IC50	100	39.7896	8.45953	21.26	
#2	n	-1	-1.18915	0.202688	17.04	



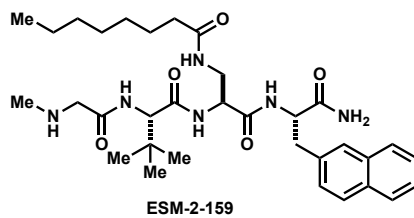


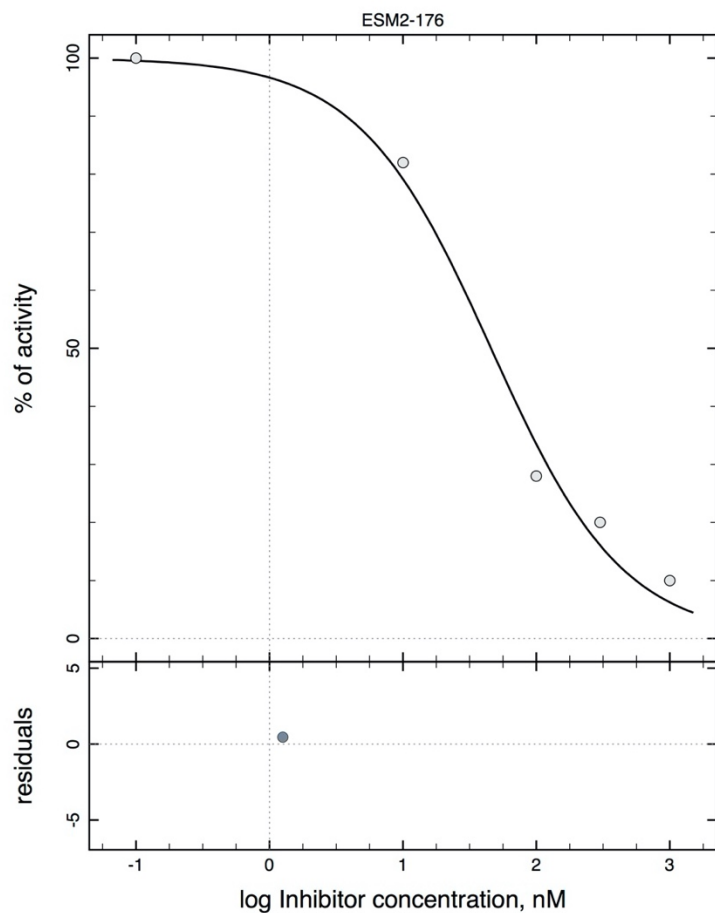
No.	Par# Set	Initial	Final	Std. Error	CV (%)	Note
#1	IC50	100	624.206	46.0492	7.38	
#2	n	-1	-1.15286	0.106928	9.28	



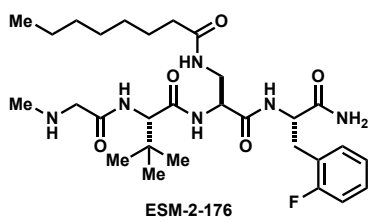


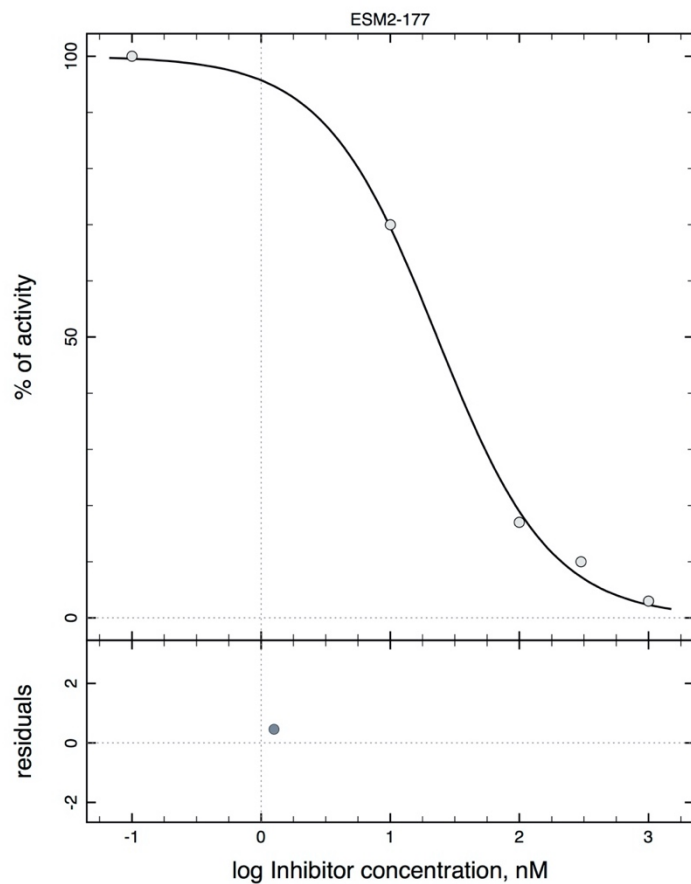
No.	Par# Set	Initial	Final	Std. Error	CV (%)	Note
#1	IC50	100	<b>51.5941</b>	10.4709	20.29	
#2	n	-1	<b>-1.07918</b>	0.18073	16.75	



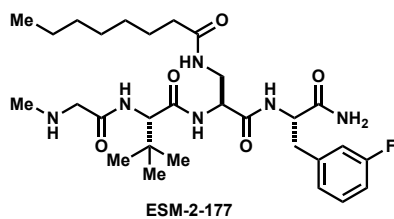


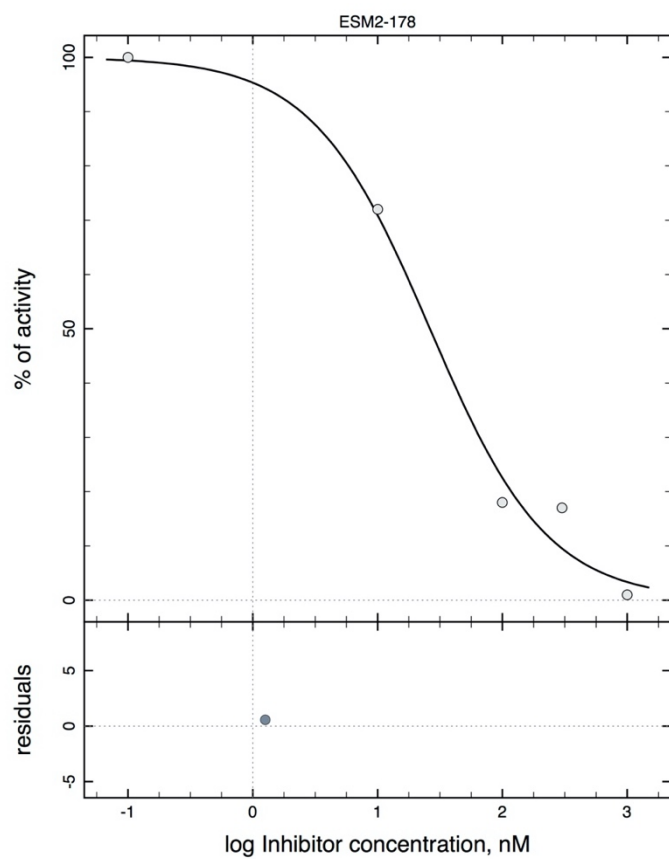
No.	Par#Set	Initial	Final	Std. Error	CV (%)	Note
#1	IC50	100	<b>45.7116</b>	8.26889	18.09	
#2	n	-1	<b>-0.877591</b>	0.114124	13.00	



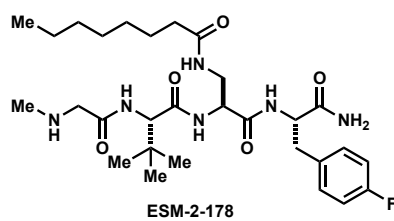


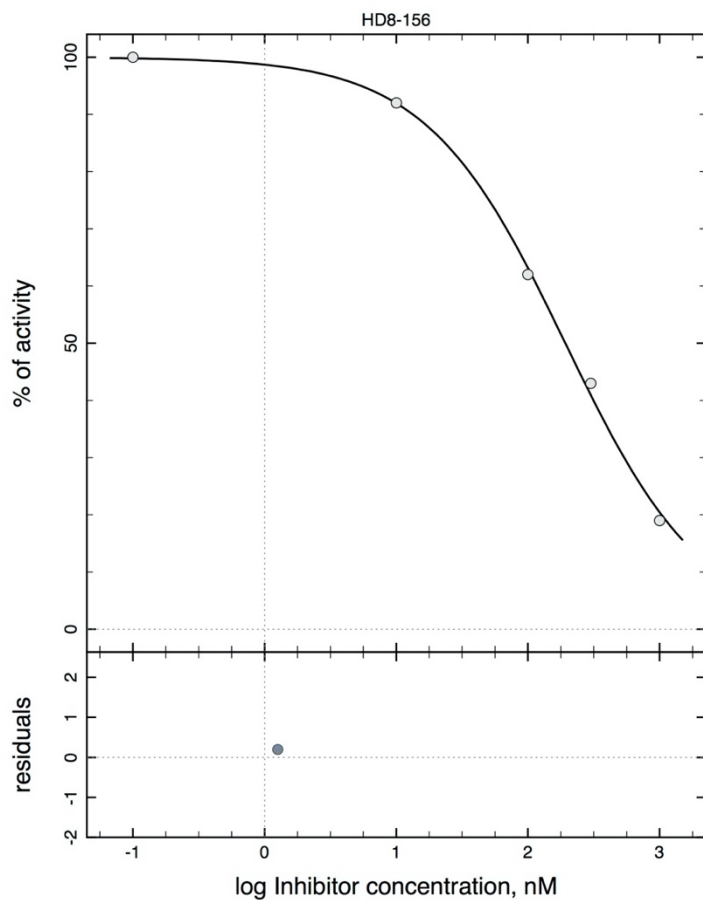
No.	Par#Set	Initial	Final	Std. Error	CV (%)	Note
#1	IC50	100	<b>23.0218</b>	1.71993	7.47	
#2	n	-1	<b>-0.990264</b>	0.0578775	5.84	



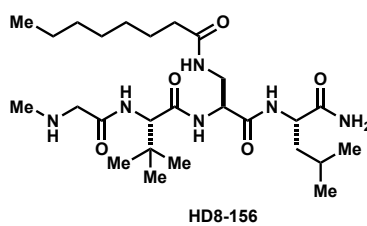


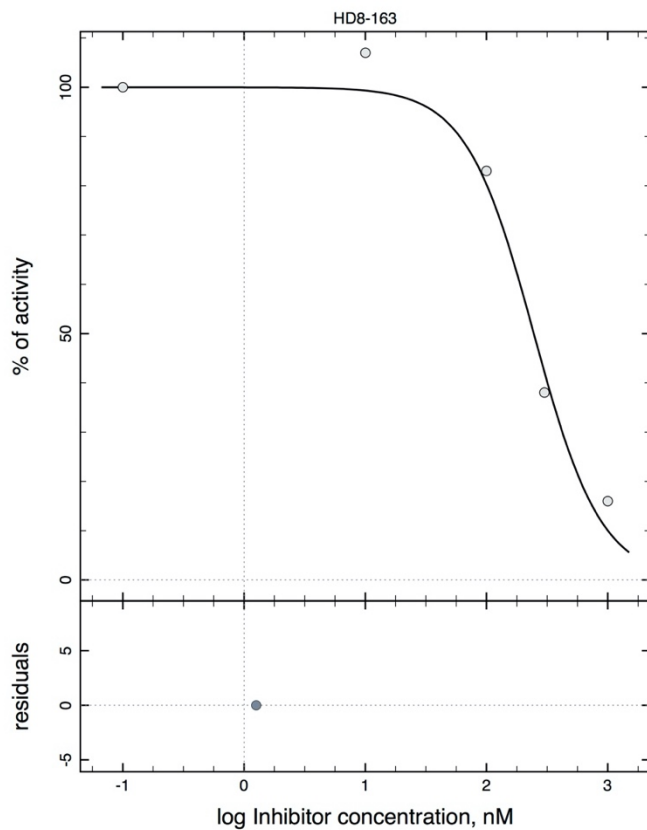
No.	Par#Set	Initial	Final	Std. Error	CV (%)	Note
#1	IC50	100	<b>26.2666</b>	5.3461	20.35	
#2	n	-1	<b>-0.923585</b>	0.137113	14.85	



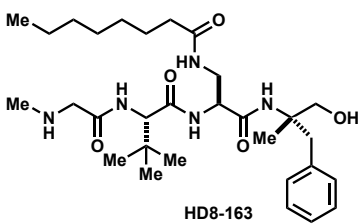


No.	Par#Set	Initial	Final	Std. Error	CV (%)	Note
#1	IC50	100	<b>192.276</b>	9.91041	5.15	
#2	n	-1	<b>-0.824255</b>	0.0410747	4.98	

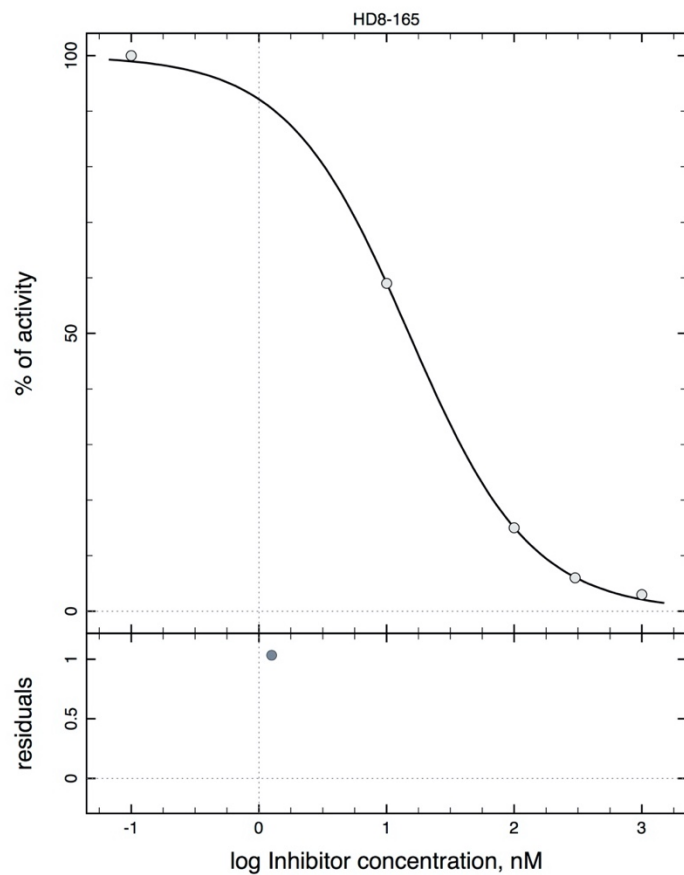




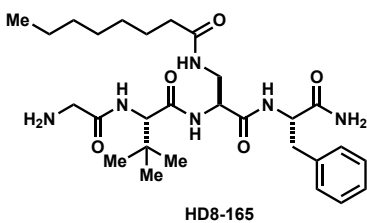
No.	Par#Set	Initial	Final	Std. Error	CV (%)	Note
#1	IC50	100	<b>245.316</b>	32.5762	13.28	
#2	n	-1	<b>-1.56309</b>	0.319745	20.46	

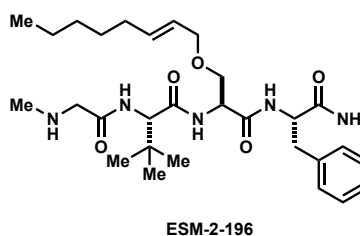
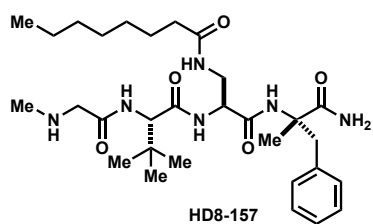
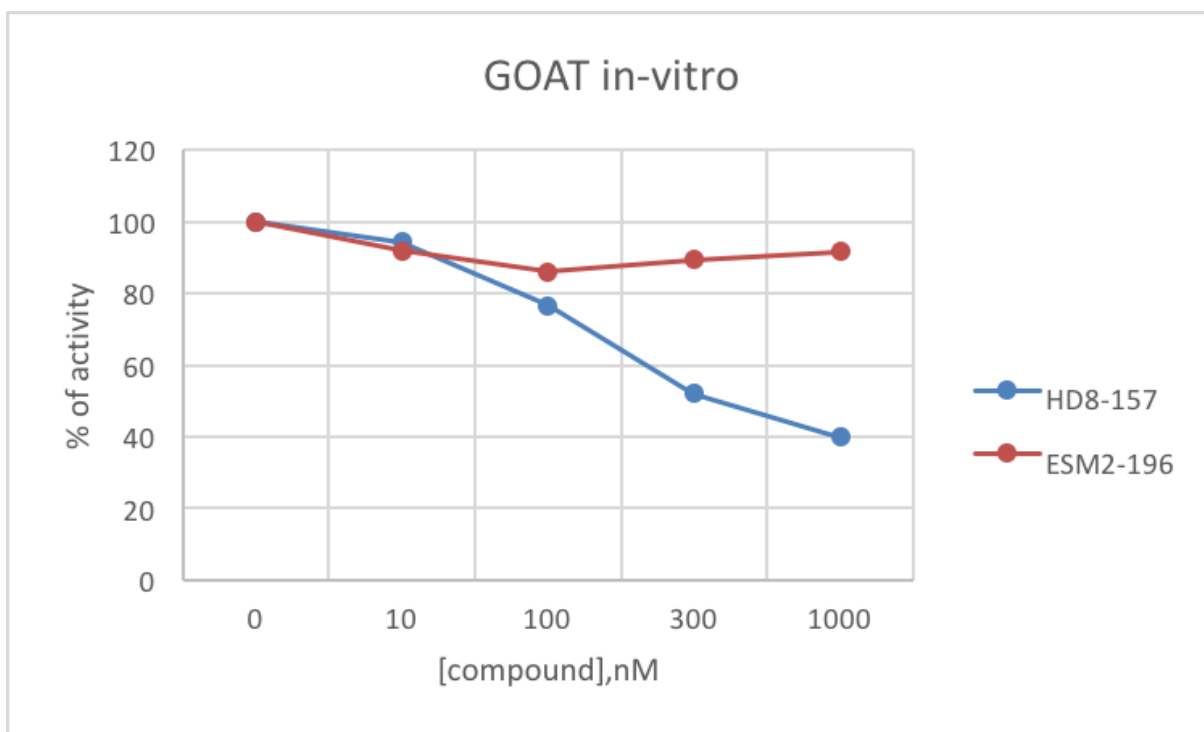


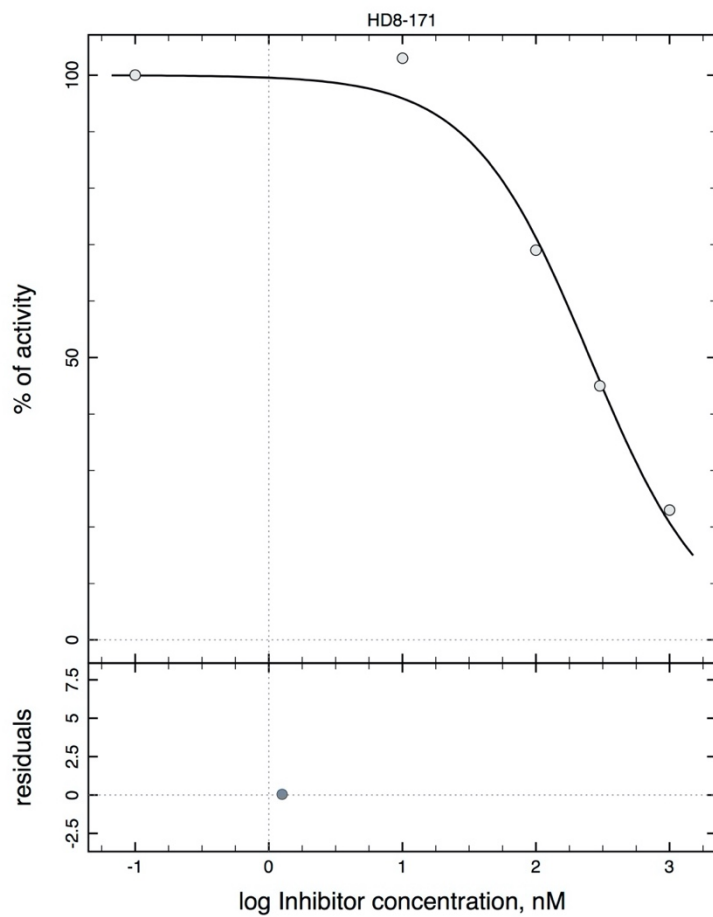




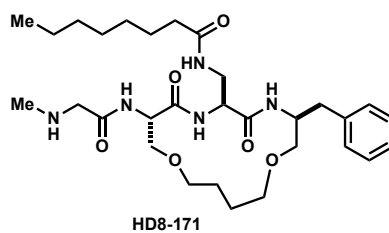
No.	Par#Set	Initial	Final	Std. Error	CV (%)	Note
#1	IC50	100	<b>14.957</b>	0.469196	3.14	
#2	n	-1	<b>-0.911082</b>	0.0243483	2.67	

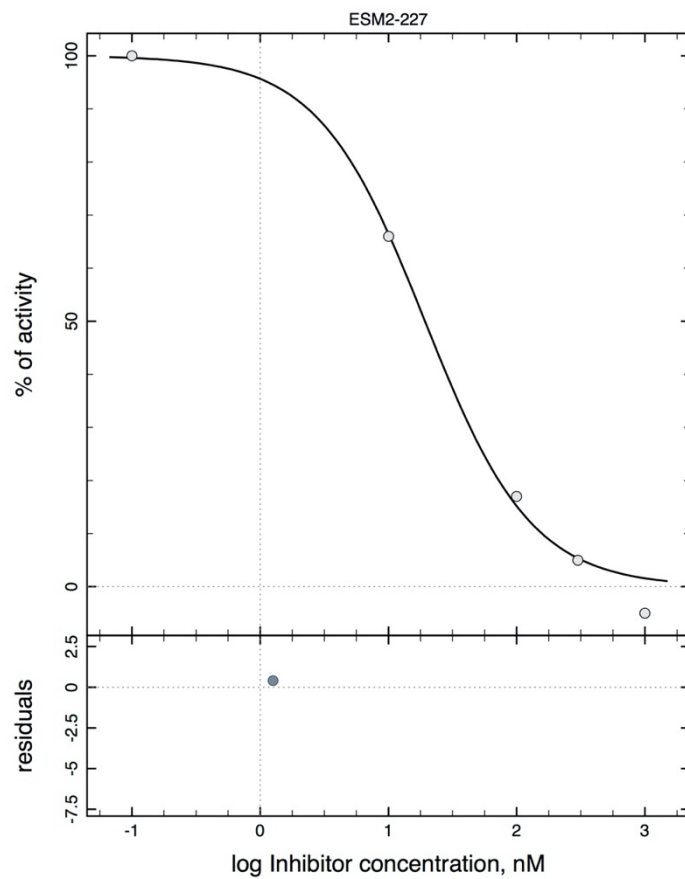




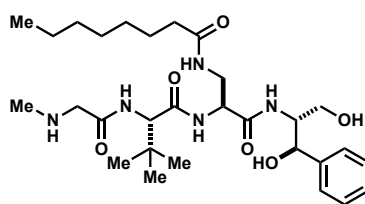


No.	Par# Set	Initial	Final	Std. Error	CV (%)	Note
#1	IC50	100	<b>252.723</b>	32.1657	12.73	
#2	n	-1	<b>-0.978214</b>	0.139355	14.28	

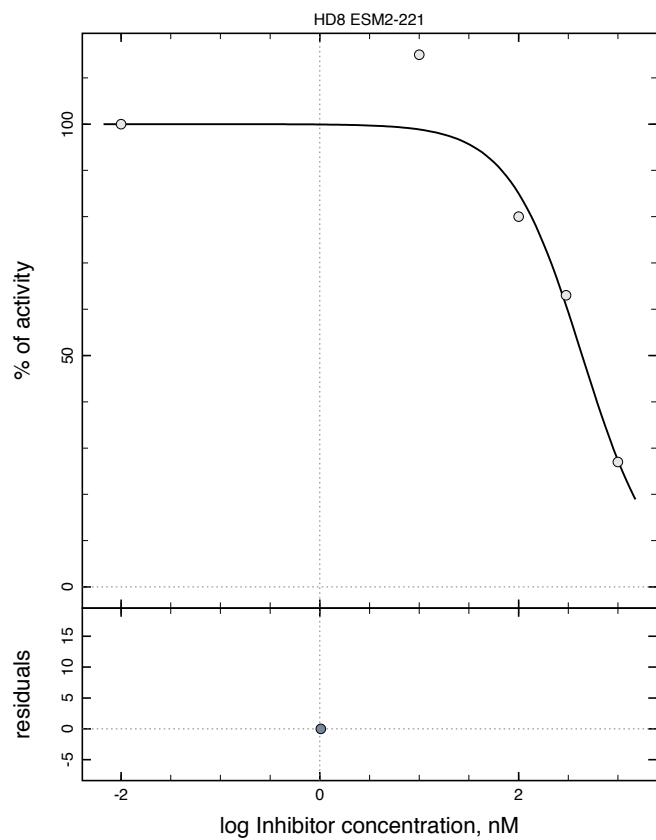




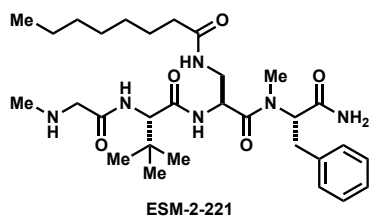
No.	Par#Set	Initial	Final	Std. Error	CV (%)	Note
#1	IC50	100	19.2815	2.78772	14.46	
#2	n	-1	-1.04584	0.13247	12.67	

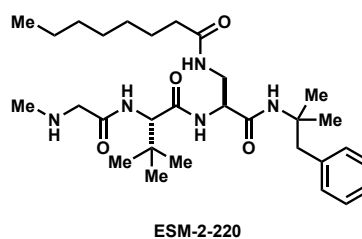
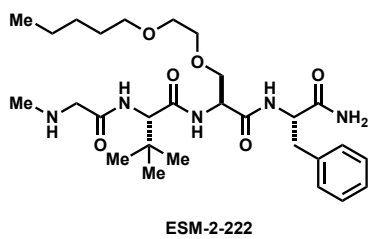
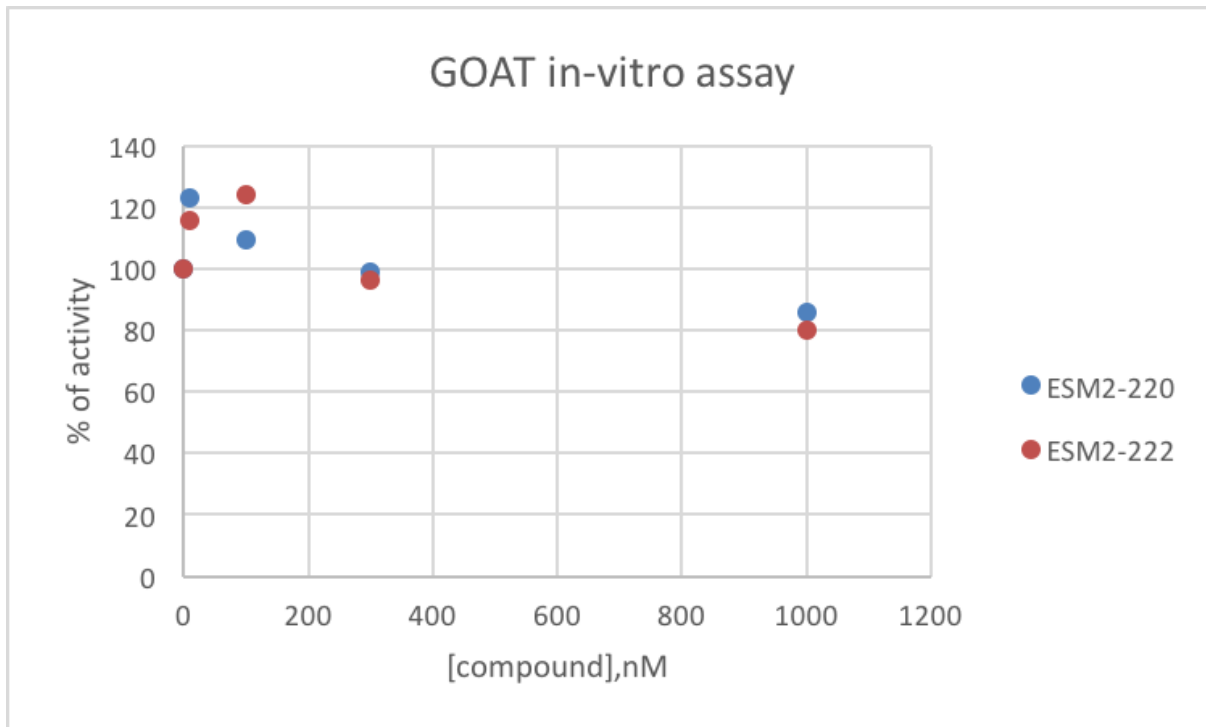


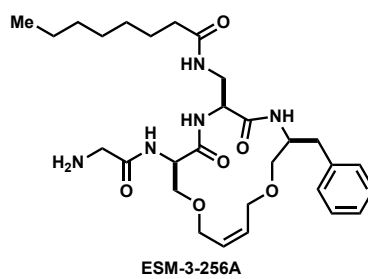
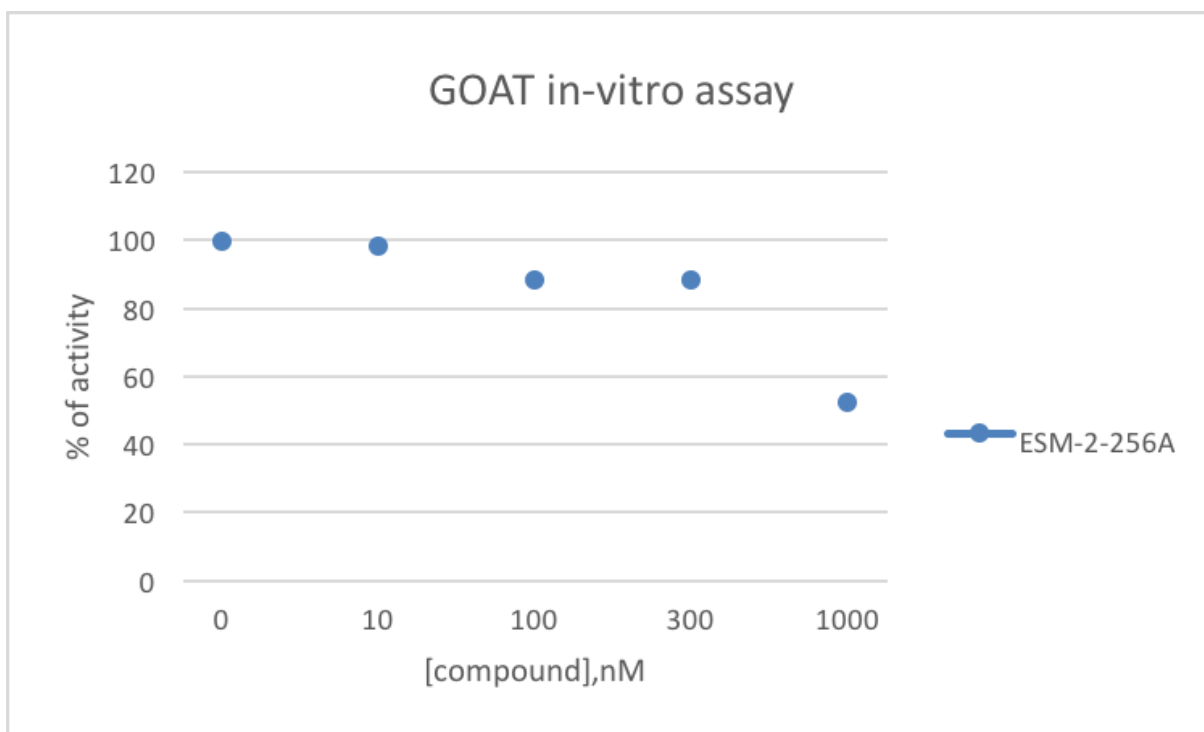
ESM-2-227

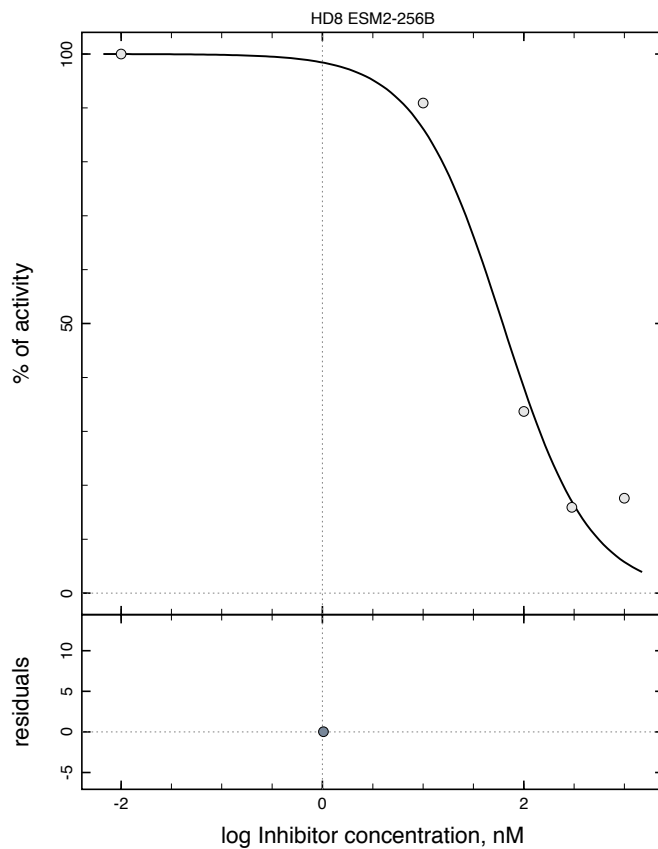


No.	Par#Set	Initial	Final	Std. Error	CV (%)	Note
#1	IC50	100	435.874	109.651	25.16	
#2	n	-1	-1.17882	0.370389	31.42	

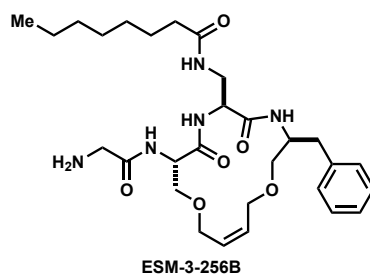




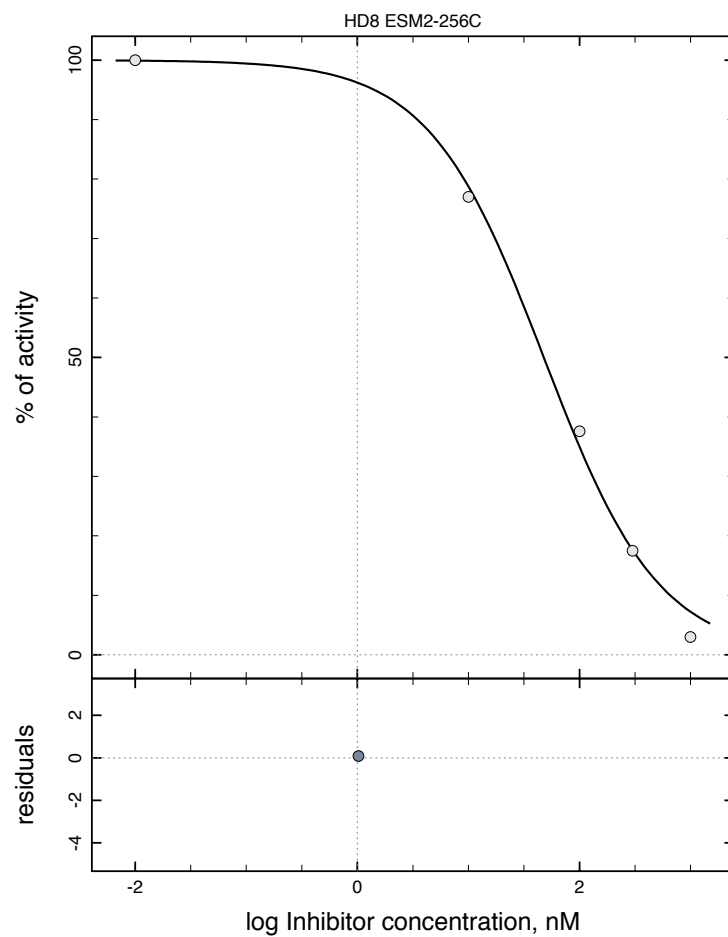




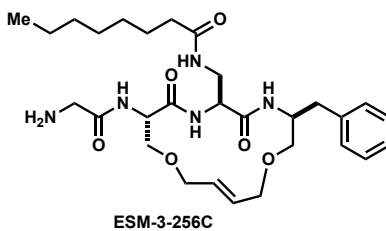
No.	Par#Set	Initial	Final	Std. Error	CV (%)	Note
#1	IC50	100	<b>61.813</b>	16.9992	27.50	
#2	n	-1	<b>-1.00301</b>	0.230566	22.99	

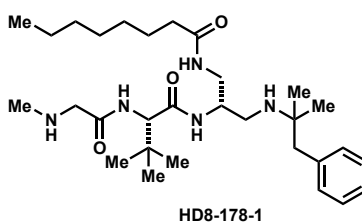
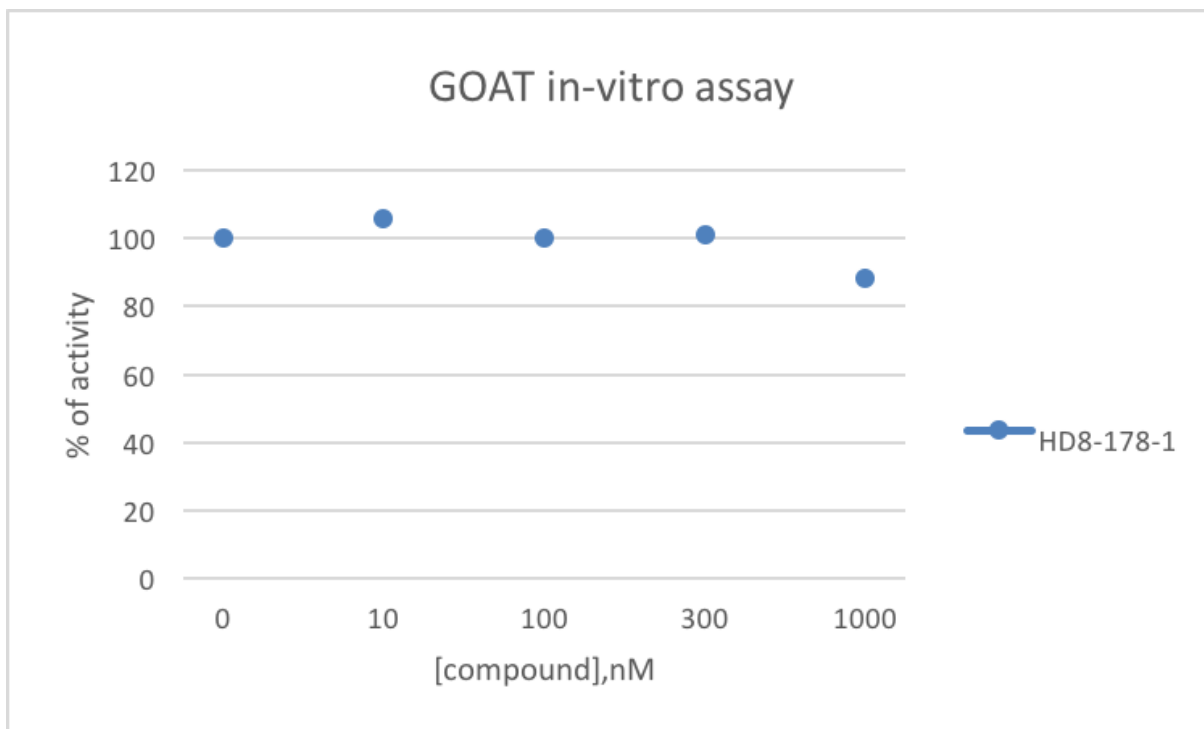


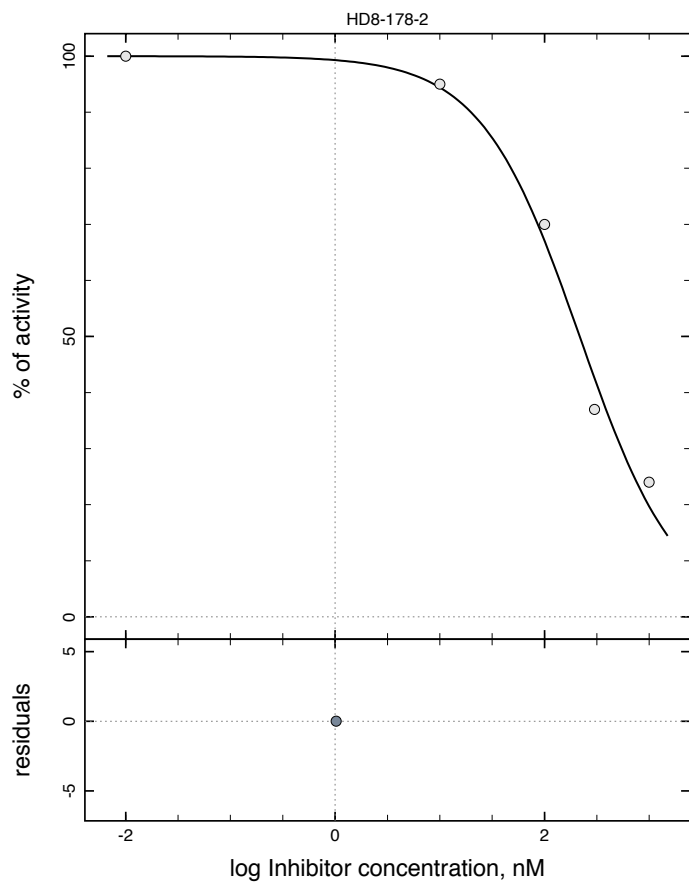




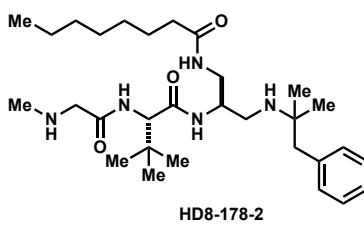
No.	Par#Set	Initial	Final	Std. Error	CV (%)	Note
#1	IC50	100	<b>47.7219</b>	5.64493	11.83	
#2	n	-1	<b>-0.838448</b>	0.07028	8.38	

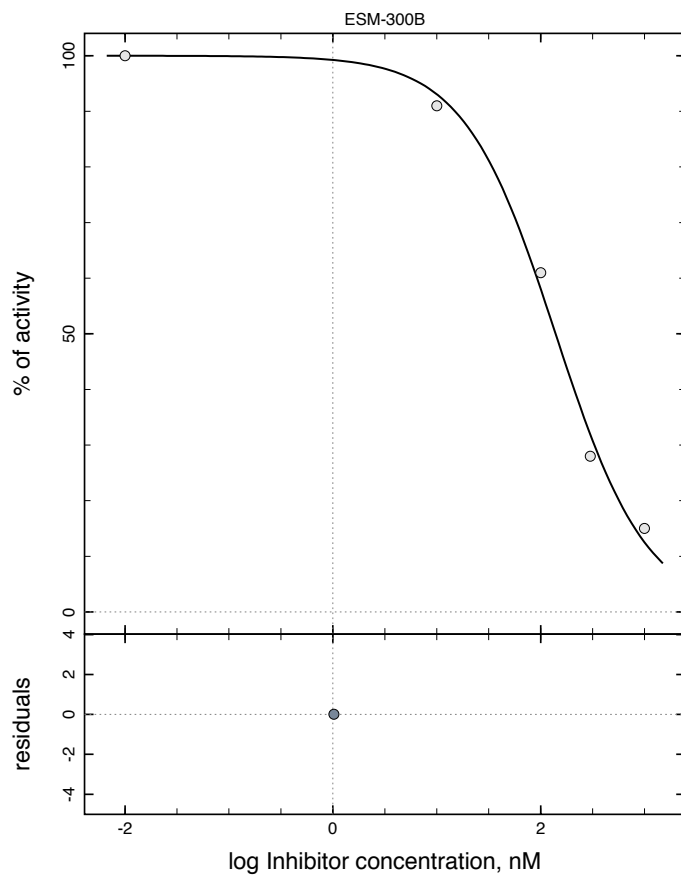




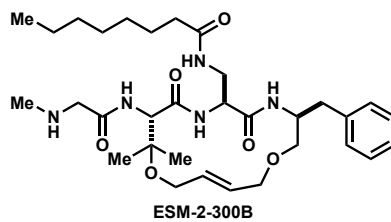


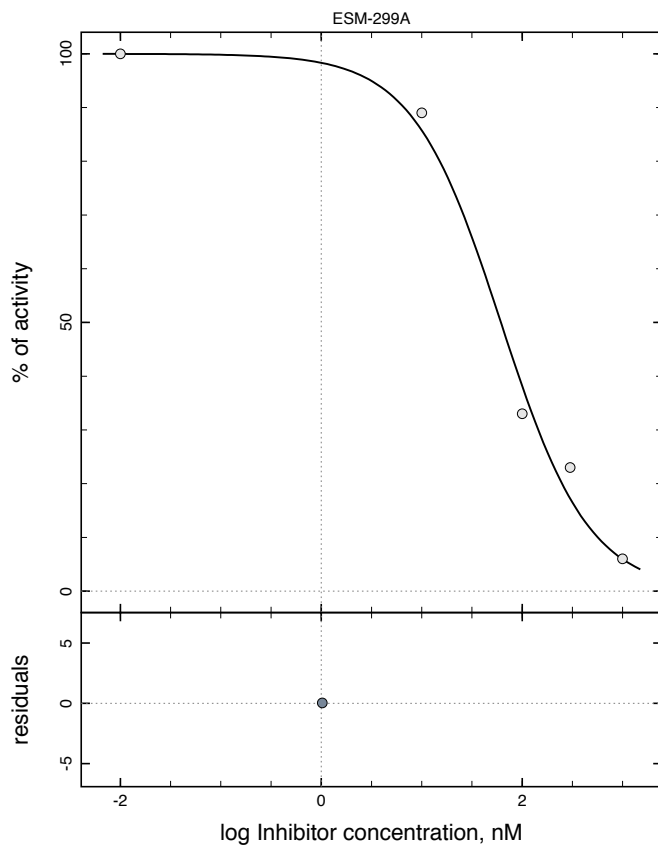
No.	Par# Set	Initial	Final	Std. Error	CV (%)	Note
#1	IC50	100	<b>216.656</b>	28.347	13.08	
#2	n	-1	<b>-0.919143</b>	0.128023	13.93	



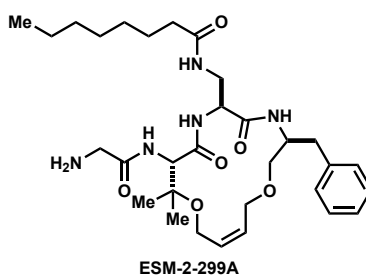


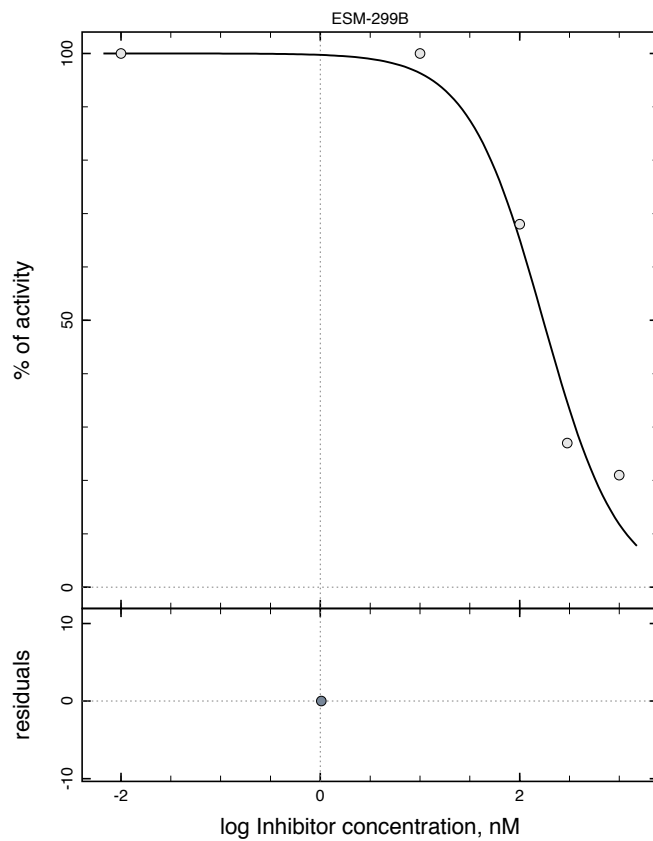
No.	Par# Set	Initial	Final	Std. Error	CV (%)	Note
#1	IC50	100	139.161	14.0925	10.13	
#2	n	-1	-0.986307	0.105567	10.70	



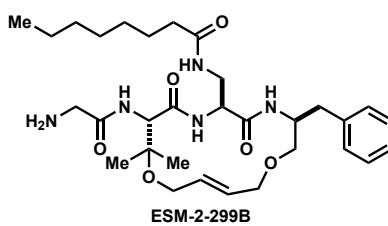


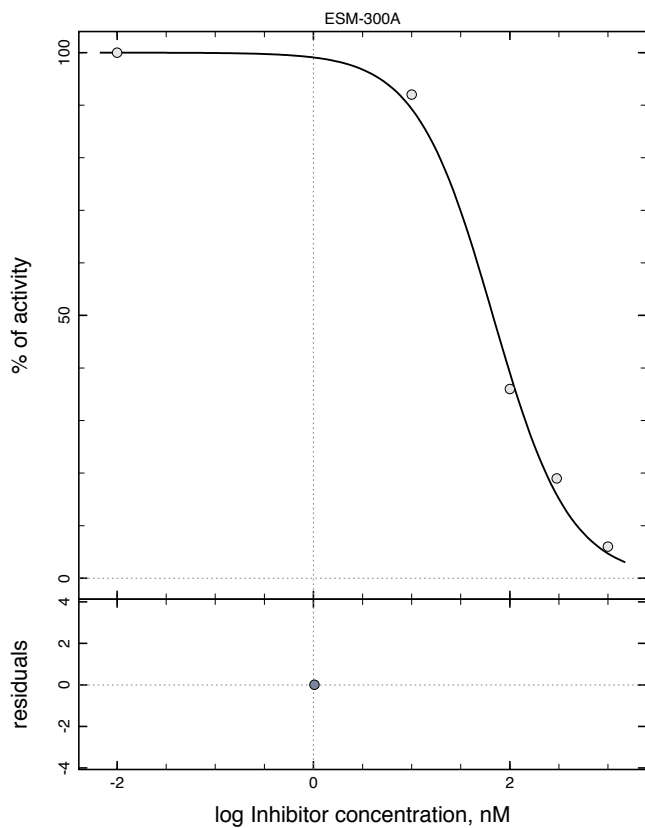
No.	Par#Set	Initial	Final	Std. Error	CV (%)	Note
#1	IC50	100	61.4176	10.518	17.13	
#2	n	-1	-0.989343	0.139939	14.14	



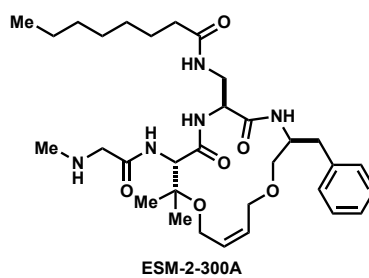


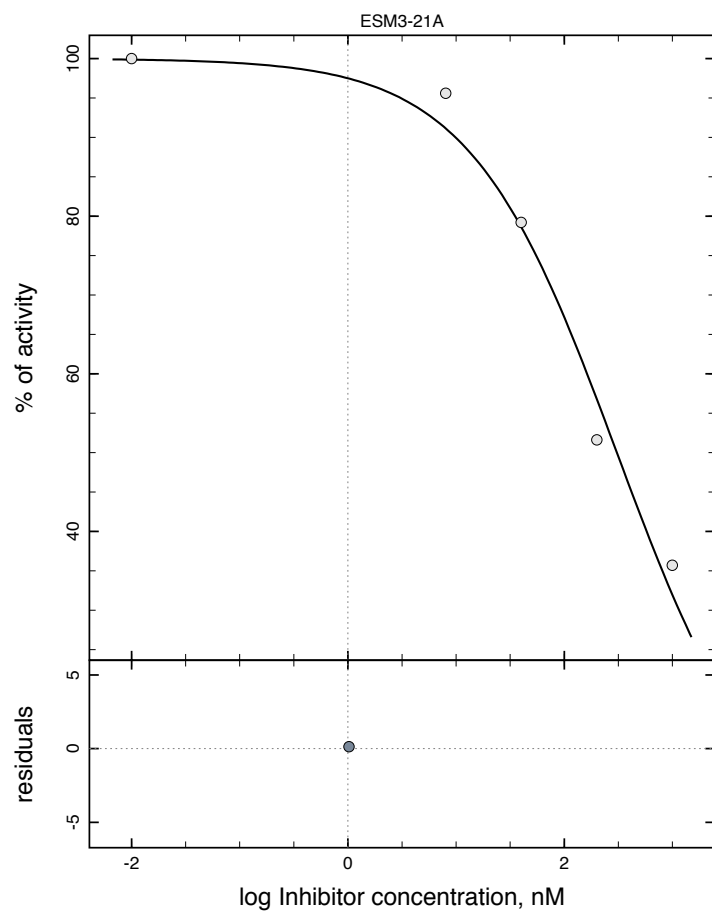
No.	Par# Set	Initial	Final	Std. Error	CV (%)	Note
#1	IC50	100	<b>172.587</b>	33.4701	19.39	
#2	n	-1	<b>-1.14845</b>	0.276075	24.08	



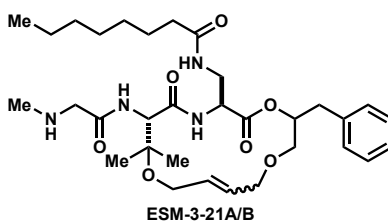


No.	Par# Set	Initial	Final	Std. Error	CV (%)	Note
#1	IC50	100	67.1468	6.9311	10.32	
#2	n	-1	-1.11432	0.10827	9.72	

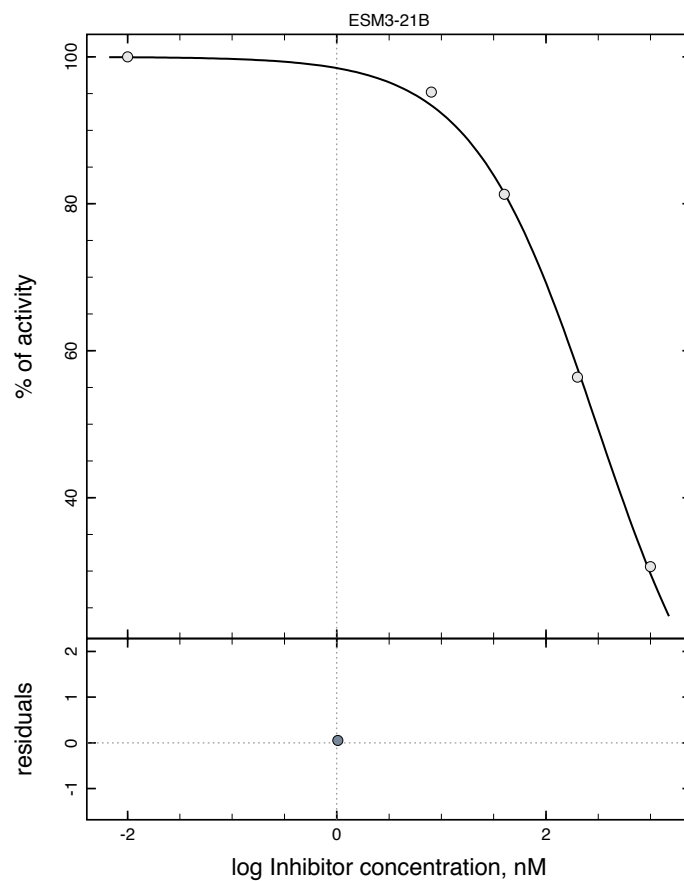




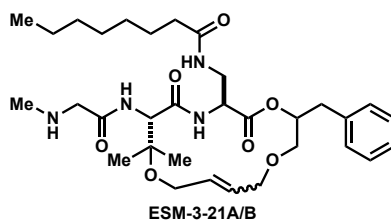
No.	Par#Set	Initial	Final	Std. Error	CV (%)	Note
#1	IC50	100	306.522	59.3434	19.36	
#2	n	-1	-0.639581	0.0881098	13.78	

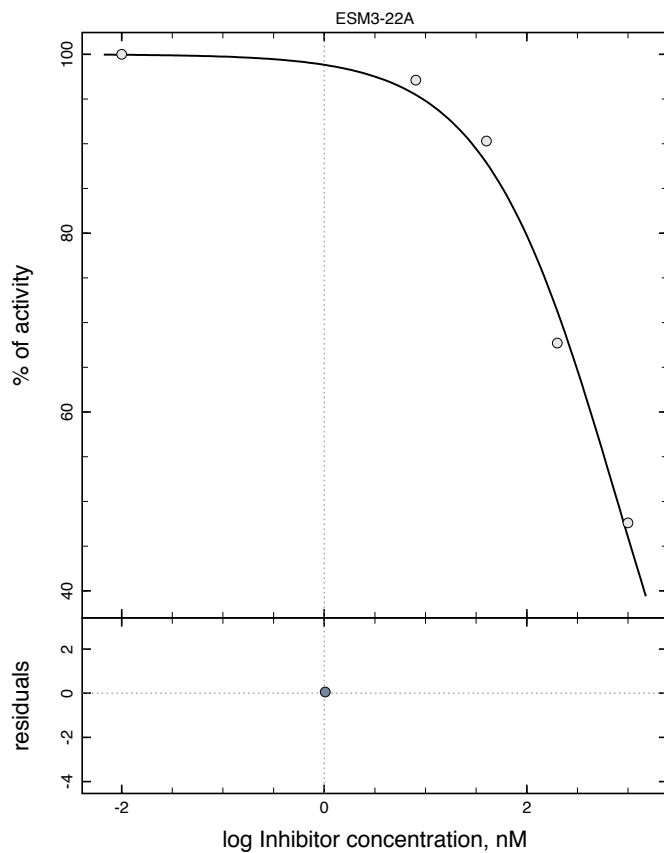




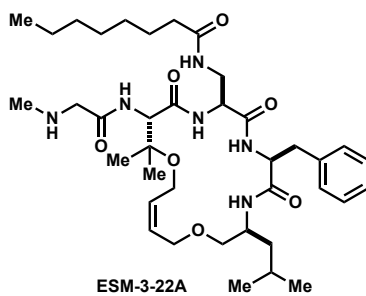


No.	Par# Set	Initial	Final	Std. Error	CV (%)	Note
#1	IC50	100	<b>304.727</b>	16.2866	5.34	
#2	n	-1	<b>-0.72796</b>	0.0301143	4.14	

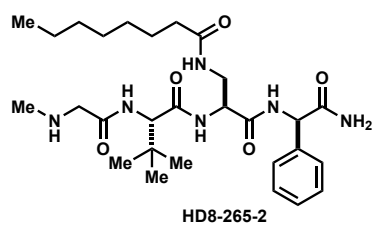
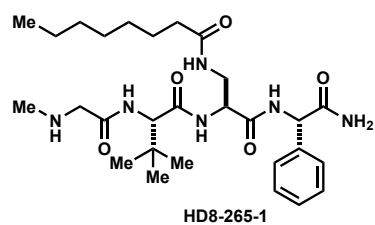
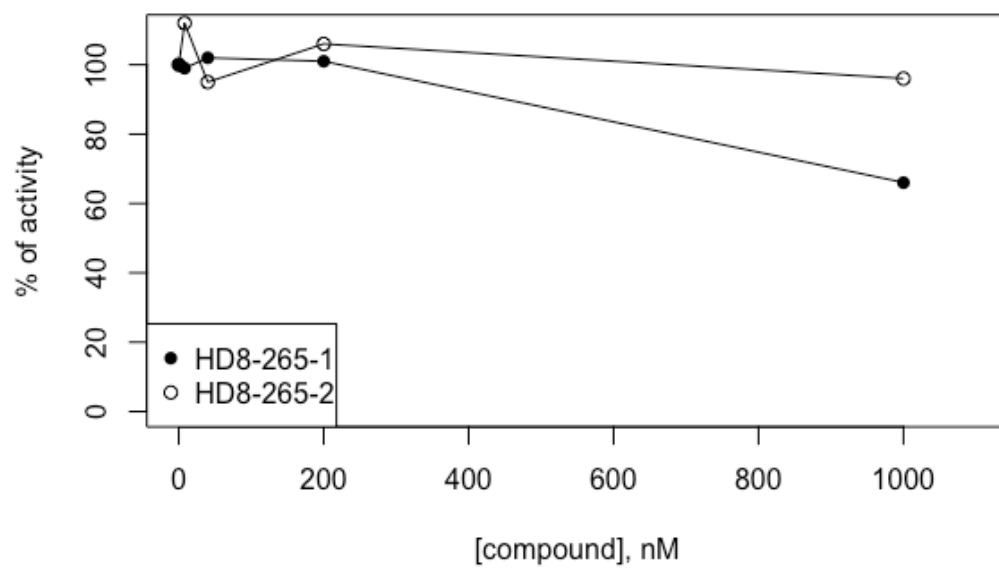


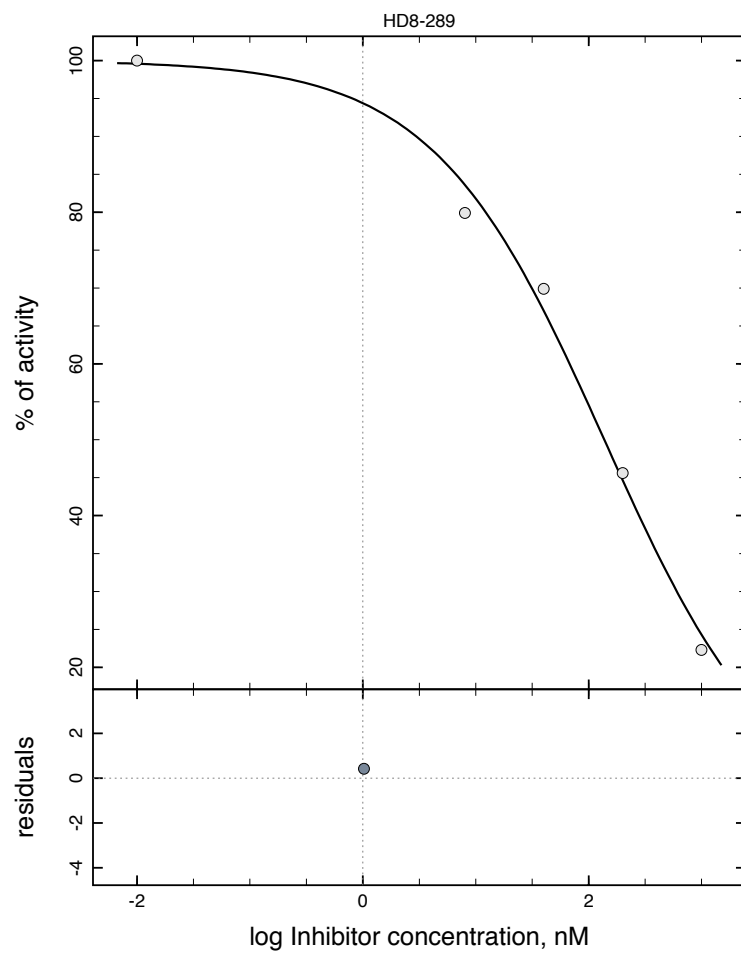


No.	Par#Set	Initial	Final	Std. Error	CV (%)	Note
#1	IC50	100	<b>784.907</b>	114.989	14.65	
#2	n	-1	<b>-0.664797</b>	0.070637	10.63	

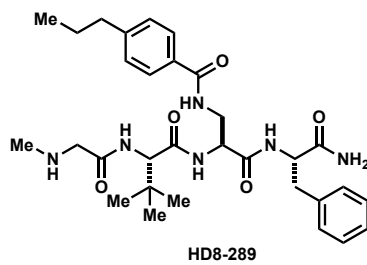


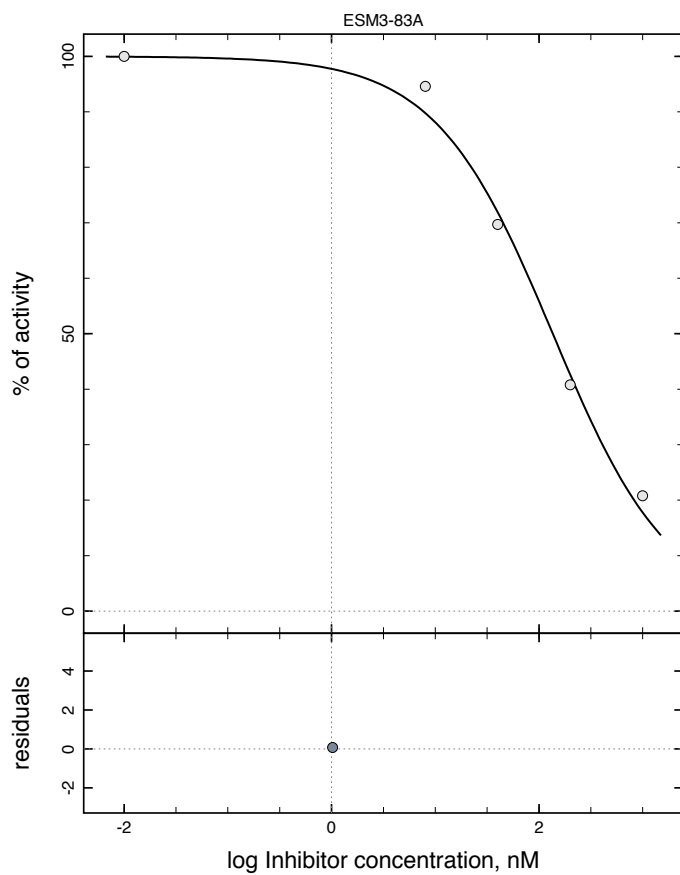
## *in-vitro* GOAT assay



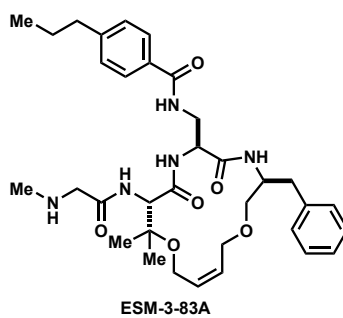


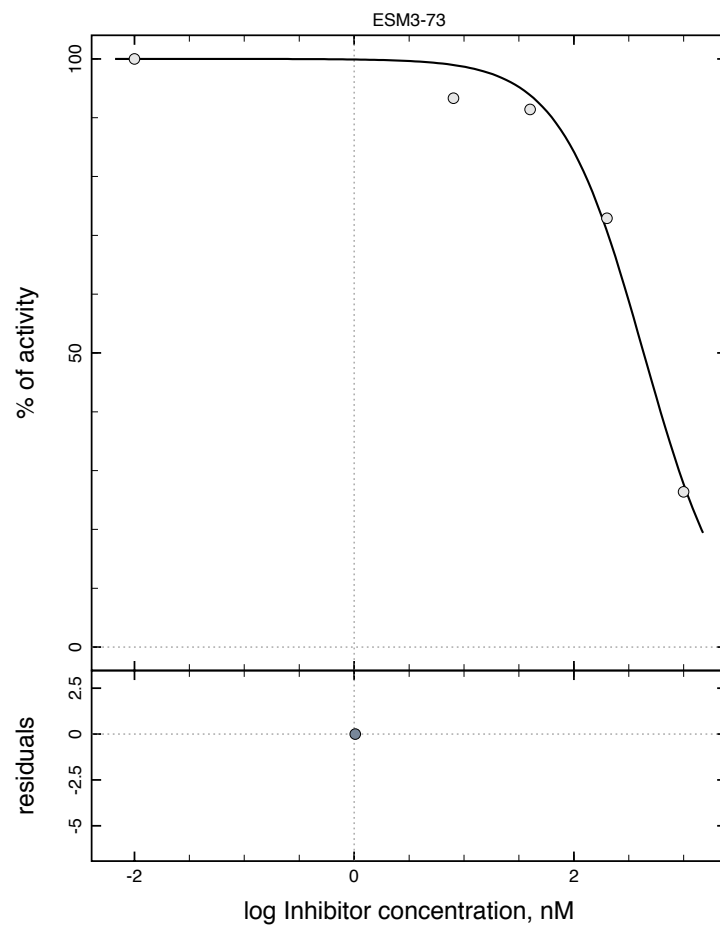
No.	Par# Set	Initial	Final	Std. Error	CV (%)	Note
#1	IC50	100	<b>137.586</b>	18.0532	13.12	
#2	n	-1	<b>-0.573099</b>	0.0498703	8.70	



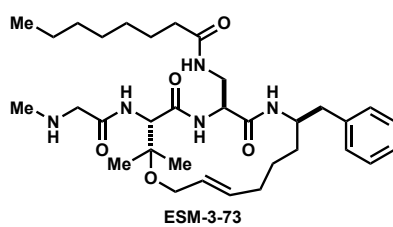


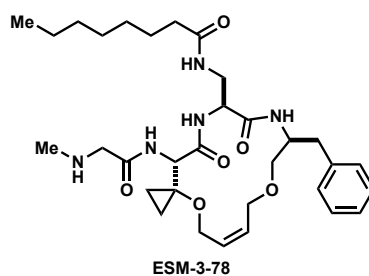
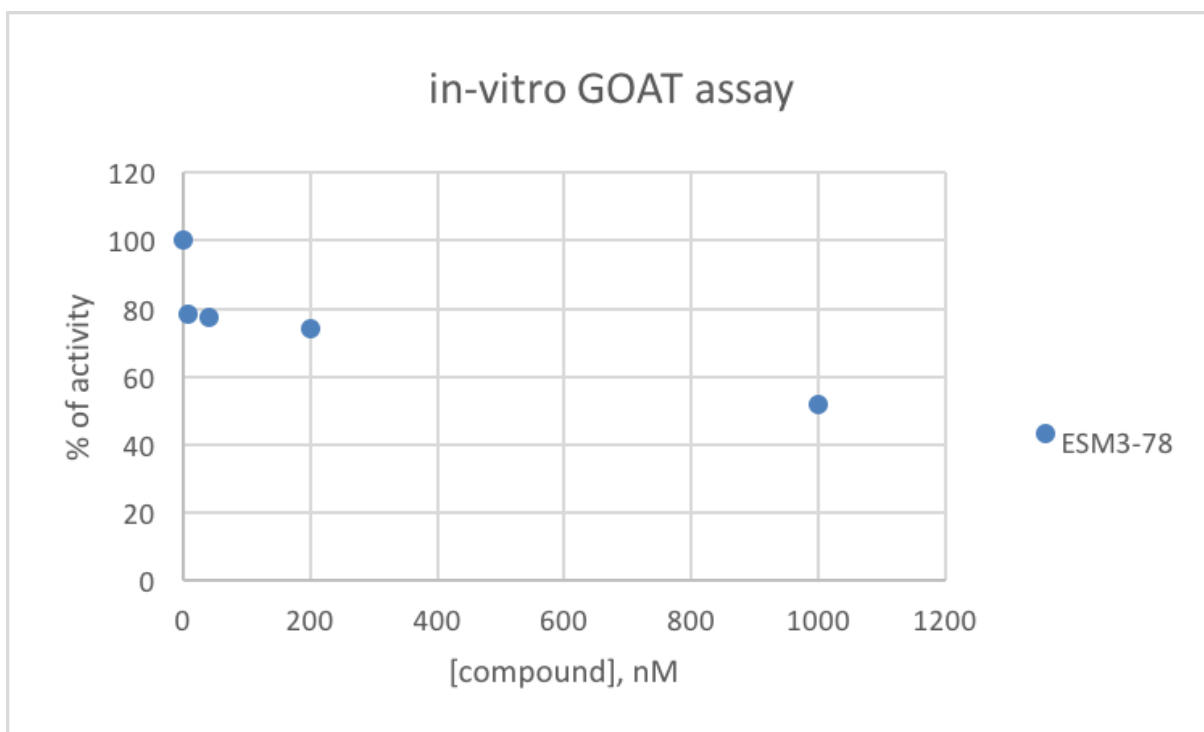
No.	Par#Set	Initial	Final	Std. Error	CV (%)	Note
#1	IC50	100	<b>135.792</b>	18.0115	13.26	
#2	n	-1	<b>-0.76761</b>	0.0779432	10.15	

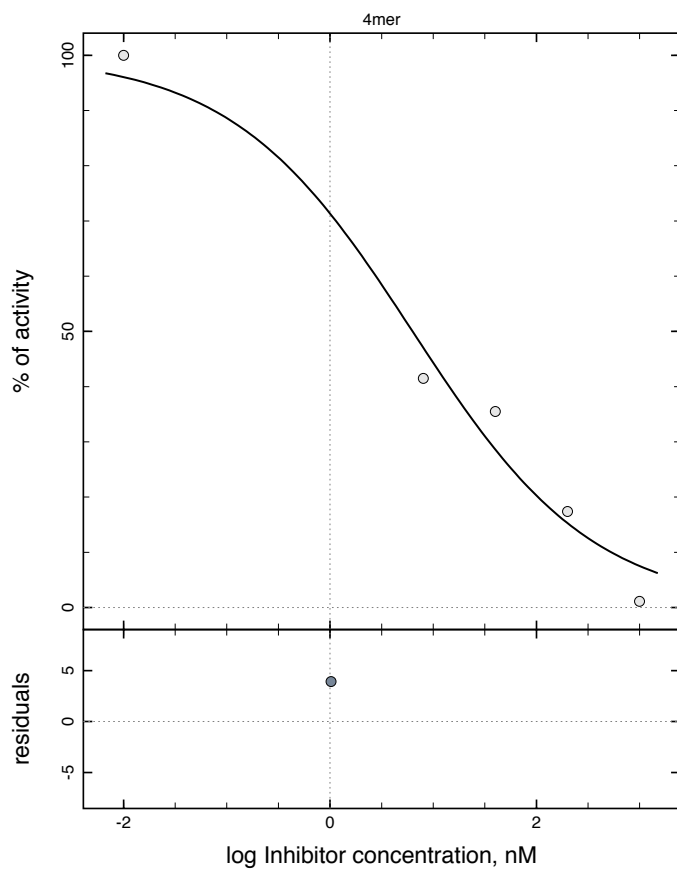




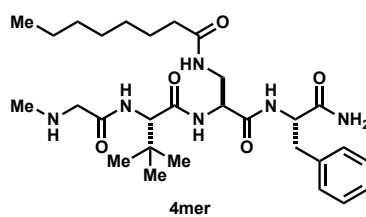
No.	Par# Set	Initial	Final	Std. Error	CV (%)	Note
#1	IC50	100	<b>431.972</b>	49.7088	11.51	
#2	n	-1	<b>-1.14406</b>	0.141998	12.41	



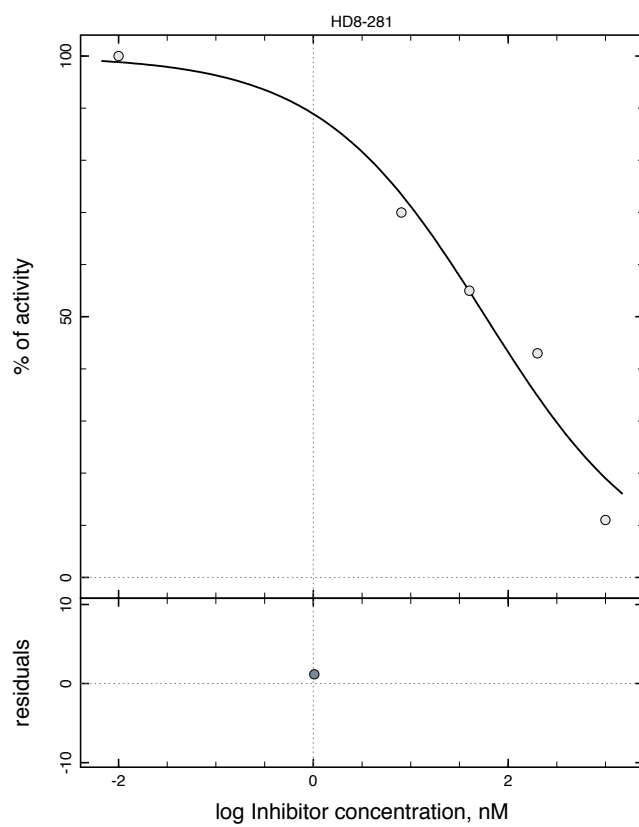




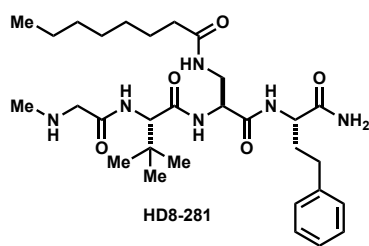
No.	Par# Set	Initial	Final	Std. Error	CV (%)	Note
#1	IC50	100	6.30976	3.16518	50.16	
#2	n	-1	-0.495459	0.121622	24.55	

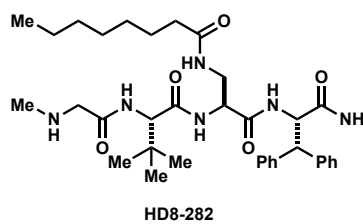
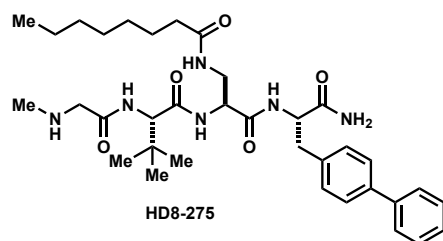
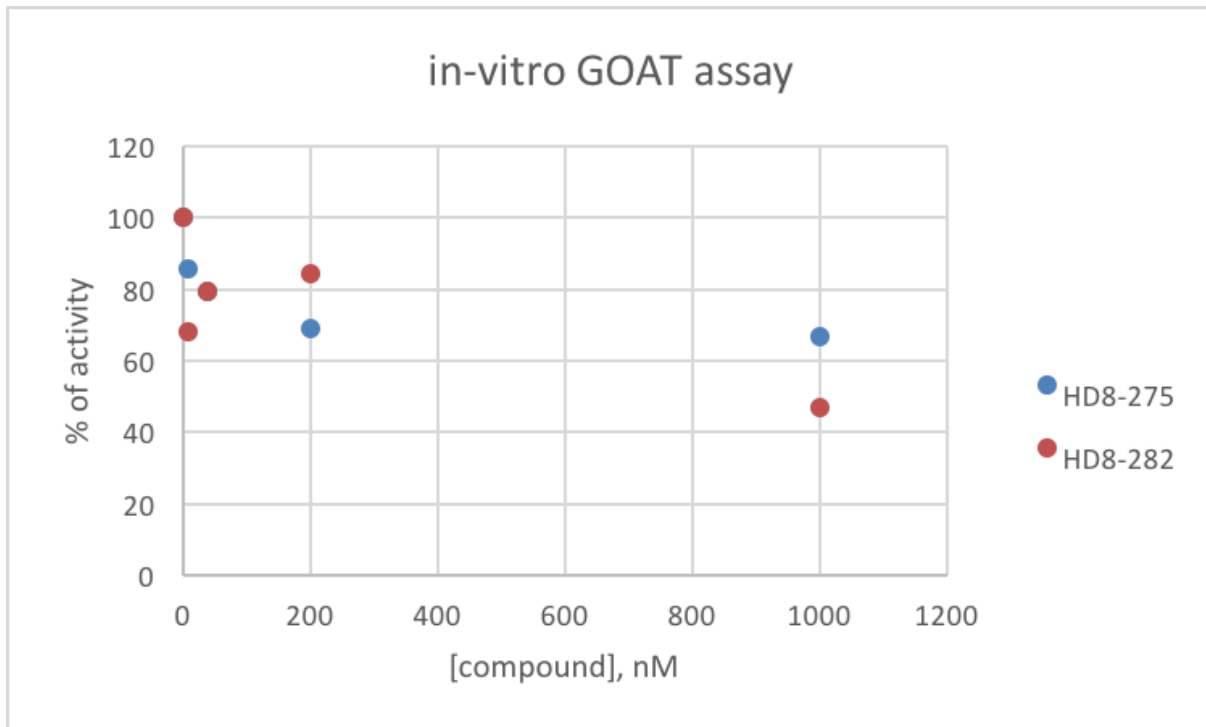




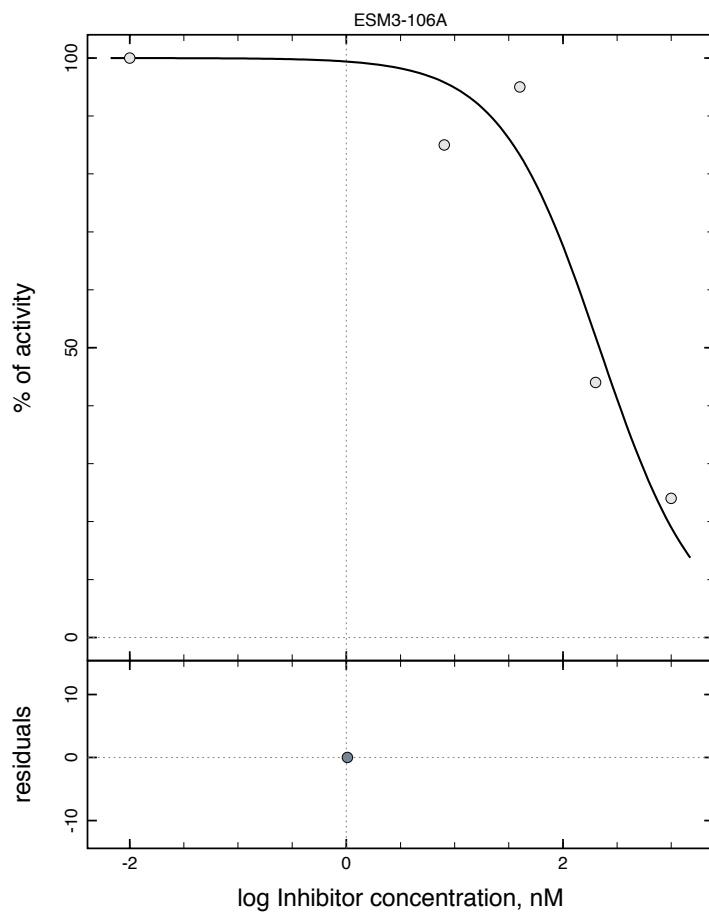


No.	Par#Set	Initial	Final	Std. Error	CV (%)	Note
#1	IC50	100	58.6098	19.1496	32.67	
#2	n	-1	-0.511135	0.105456	20.63	

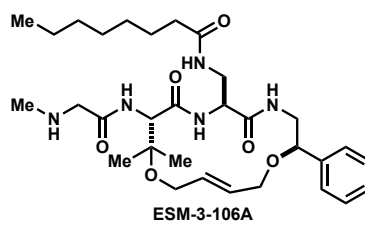


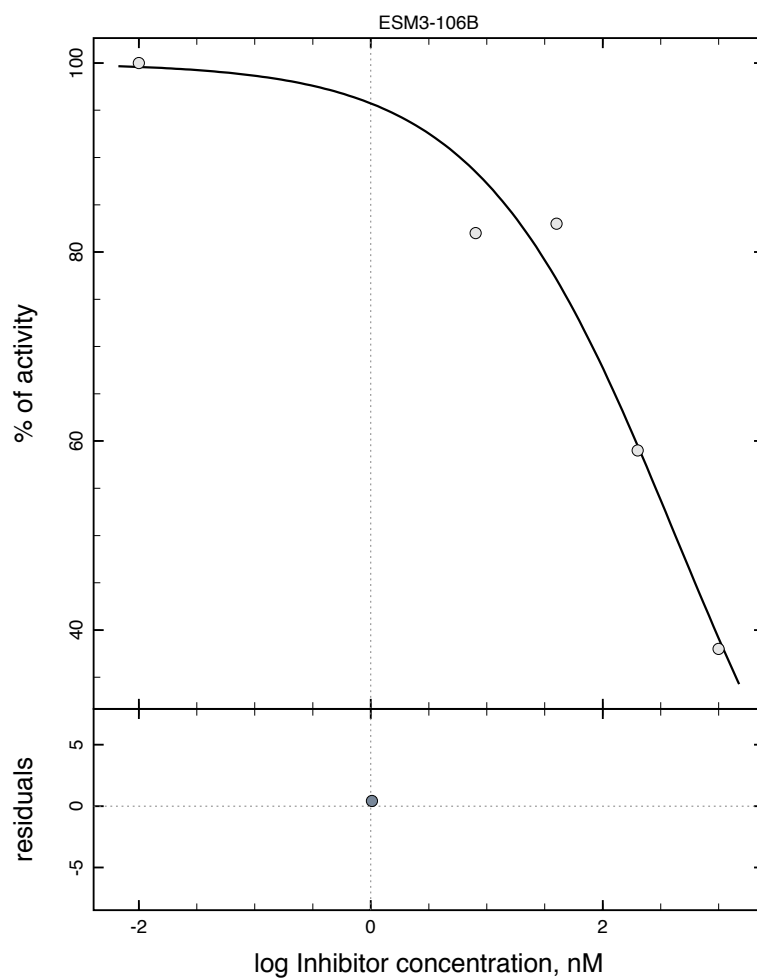




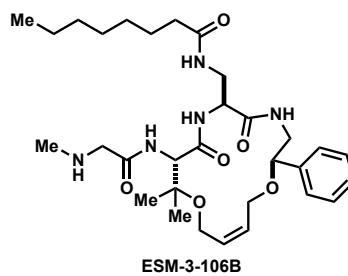


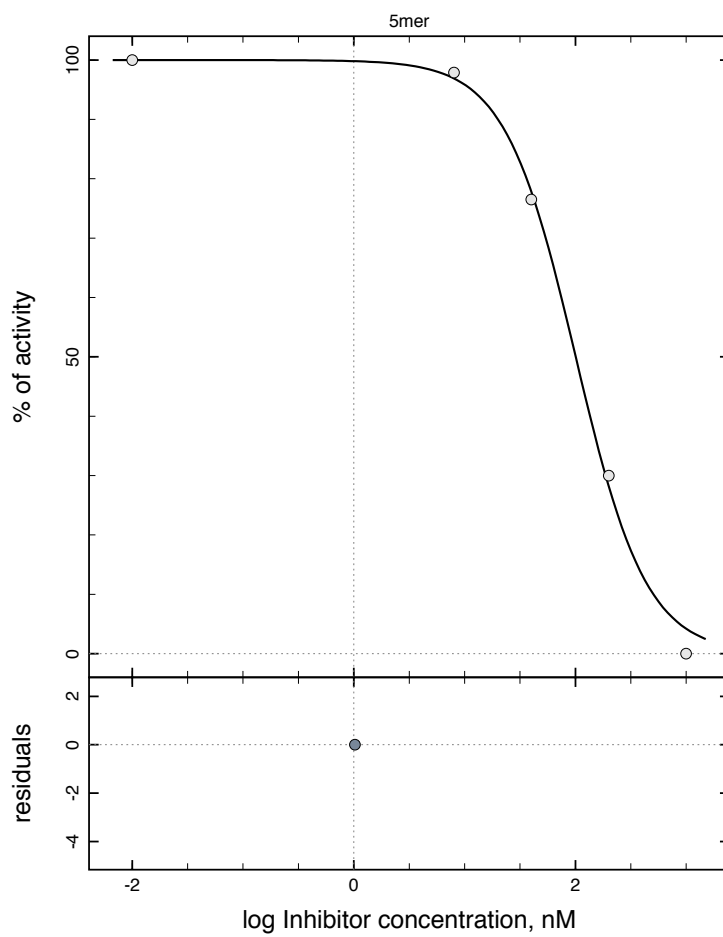
No.	Par#Set	Initial	Final	Std. Error	CV (%)	Note
#1	IC50	100	<b>216.791</b>	74.769	34.49	
#2	n	-1	<b>-0.948837</b>	0.298356	31.44	



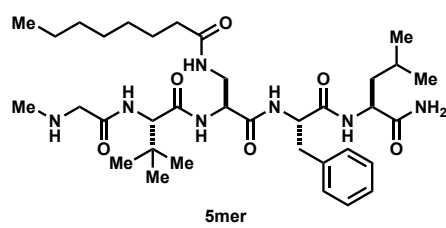


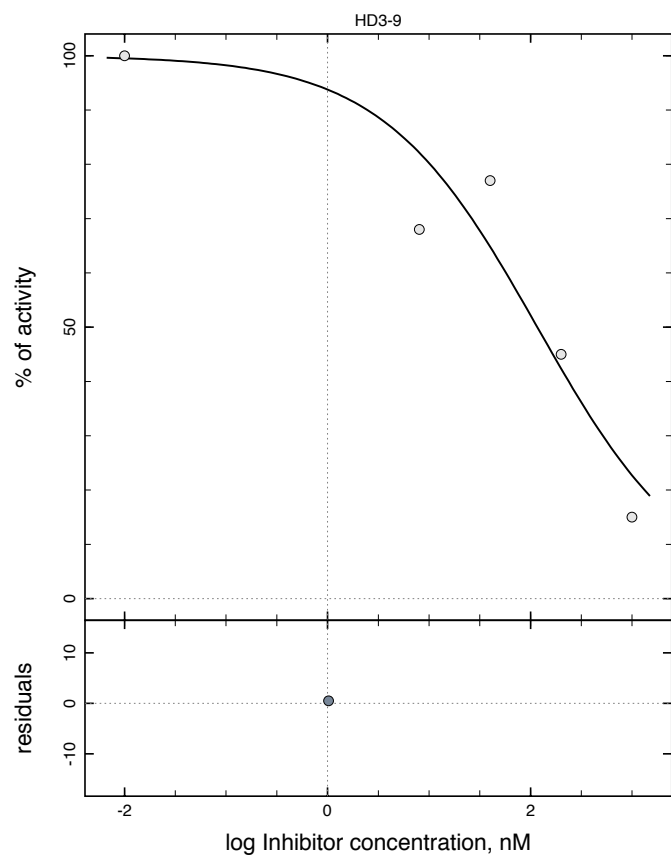
No.	Par#Set	Initial	Final	Std. Error	CV (%)	Note
#1	IC50	100	422.863	118.235	27.96	
#2	n	-1	-0.514196	0.0884348	17.20	



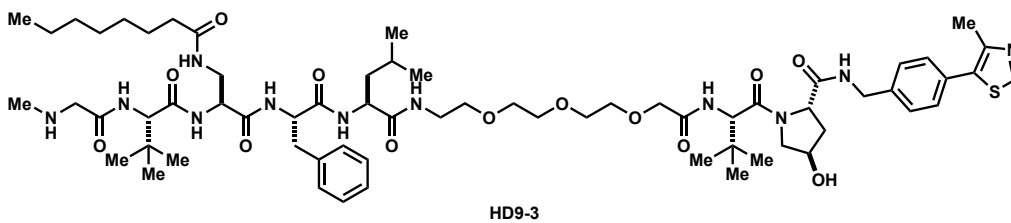


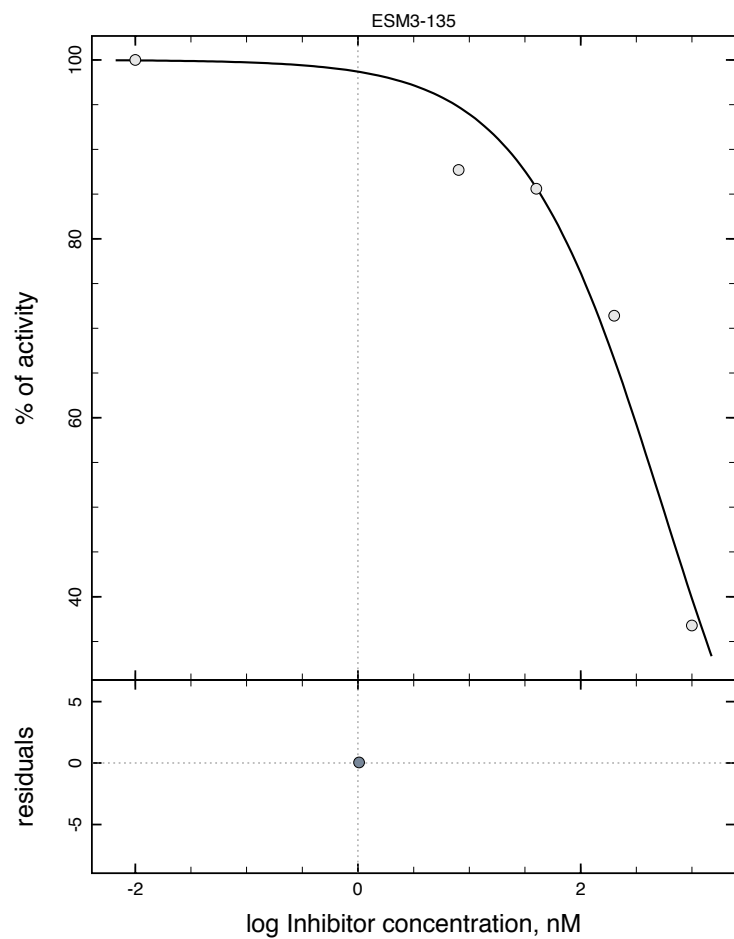
No.	Par# Set	Initial	Final	Std. Error	CV (%)	Note
#1	IC50	100	100.595	7.67793	7.63	
#2	n	-1	-1.36127	0.11581	8.51	



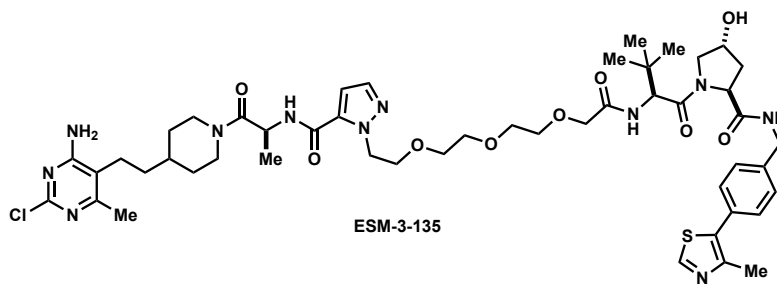


No.	Par#Set	Initial	Final	Std. Error	CV (%)	Note
#1	IC50	100	<b>116.619</b>	59.6127	51.12	
#2	n	-1	<b>-0.570038</b>	0.192586	33.78	

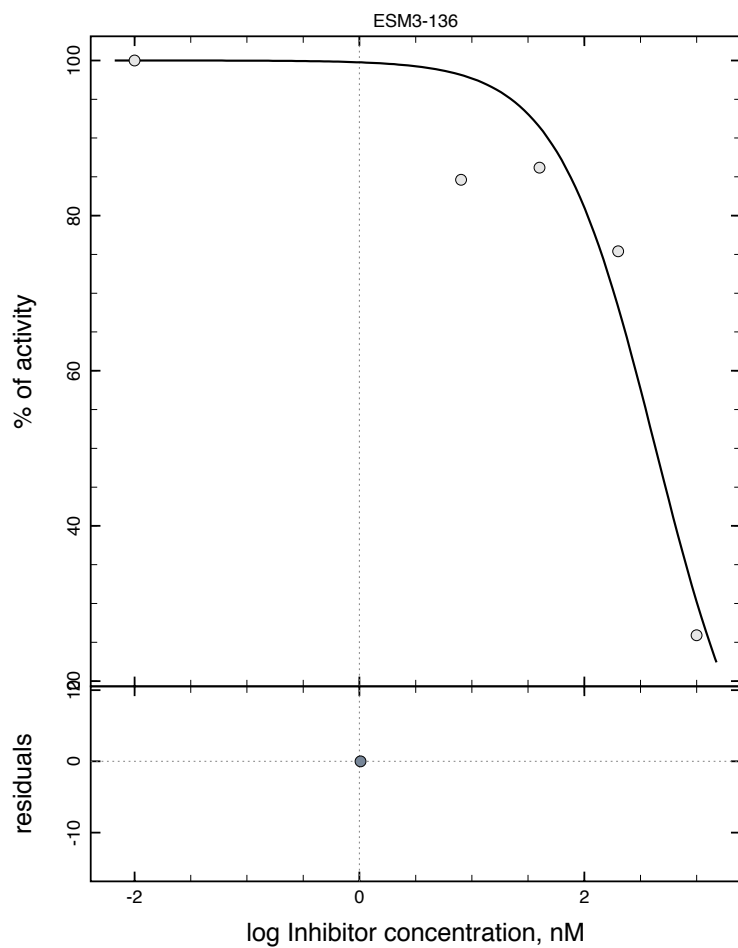




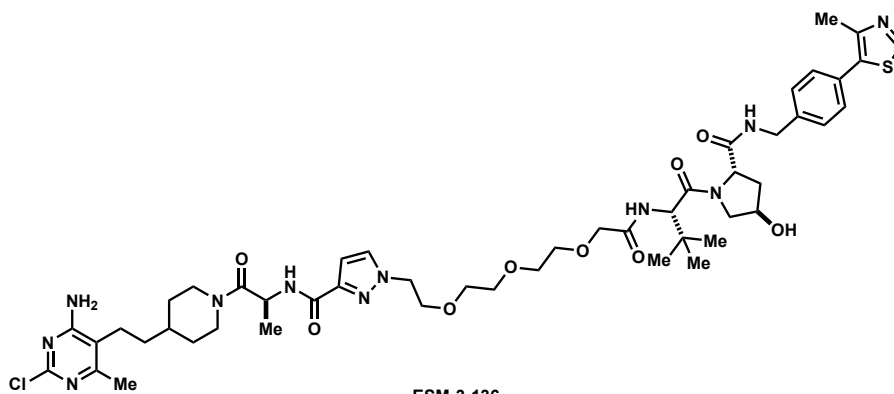
No.	Par#Set	Initial	Final	Std. Error	CV (%)	Note
#1	IC50	100	546.053	128.556	23.54	
#2	n	-1	-0.685246	0.121979	17.80	



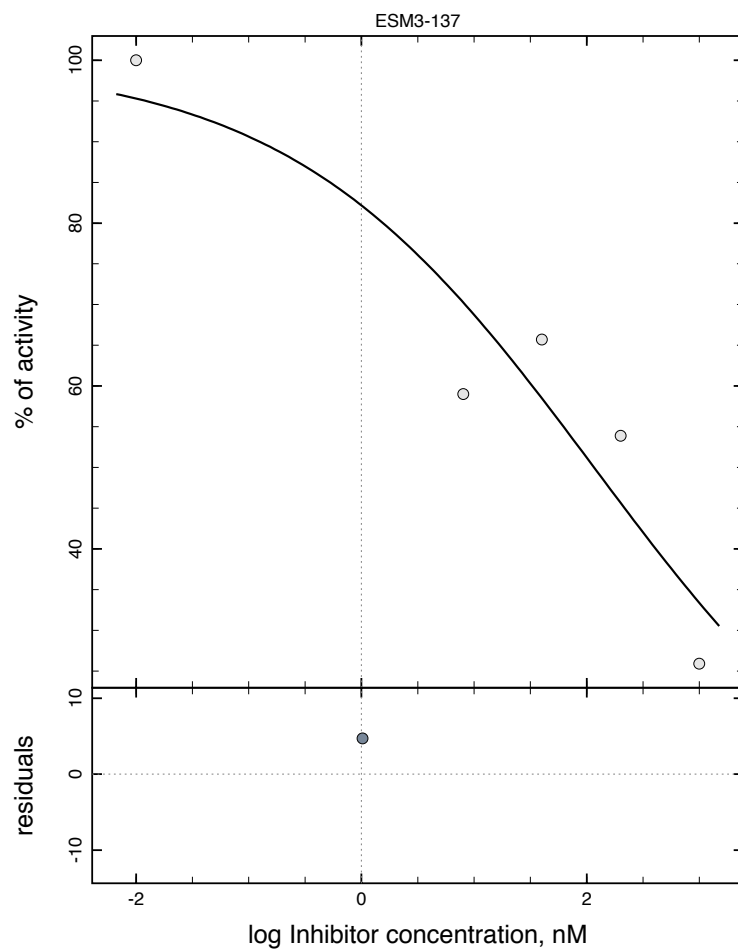




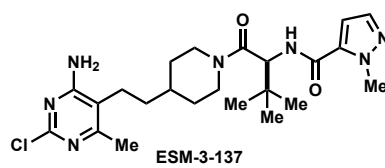
No.	Par# Set	Initial	Final	Std. Error	CV (%)	Note
#1	IC50	100	<b>430.663</b>	135.231	31.40	
#2	n	-1	<b>-0.995354</b>	0.310465	31.19	

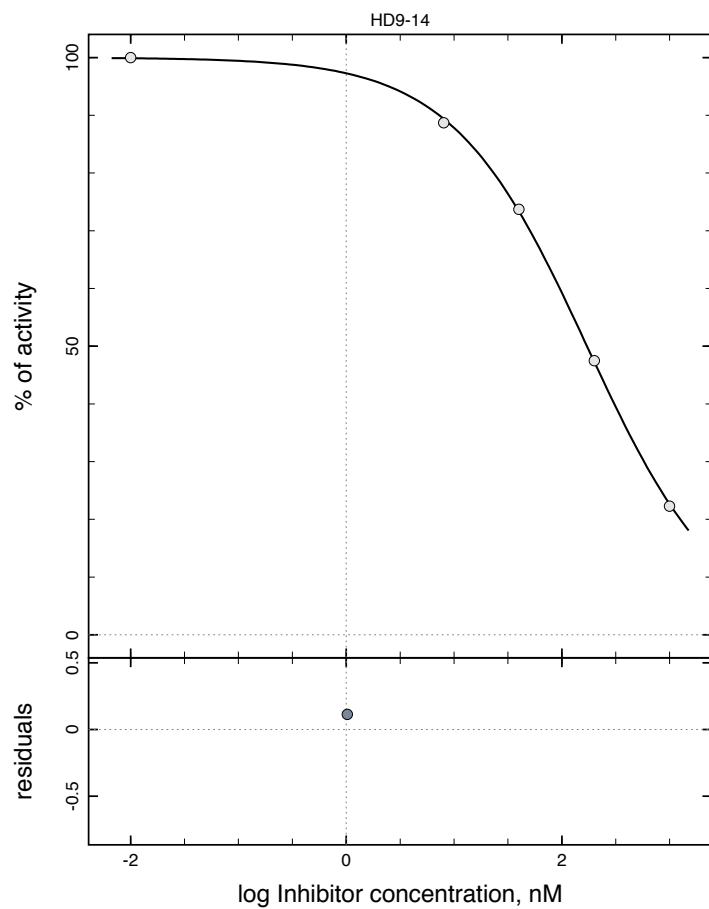


245

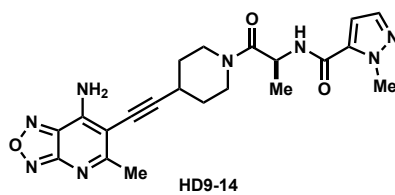


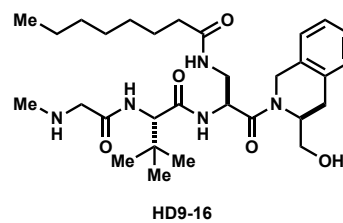
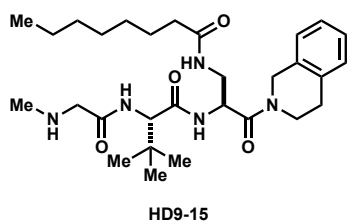
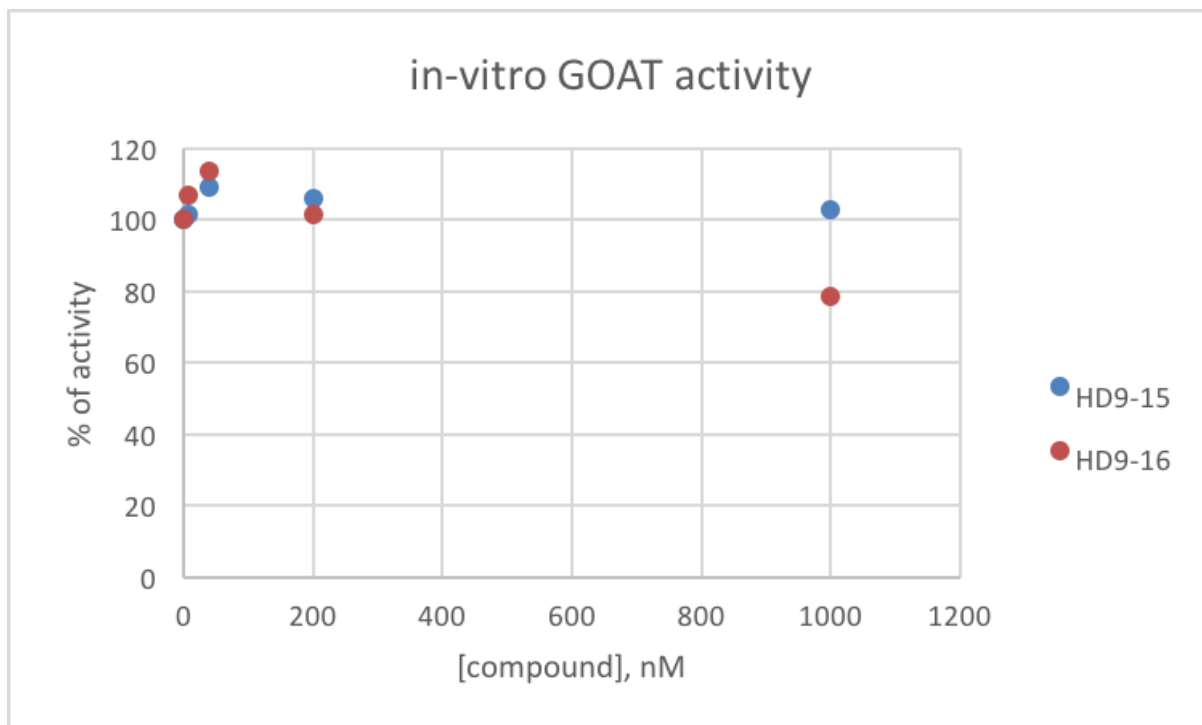
o.	Par#Set	Initial	Final	Std. Error	CV (%)	Note
#1	IC50	100	116.141	81.7976	70.43	
#2	n	-1	-0.321443	0.117327	36.50	

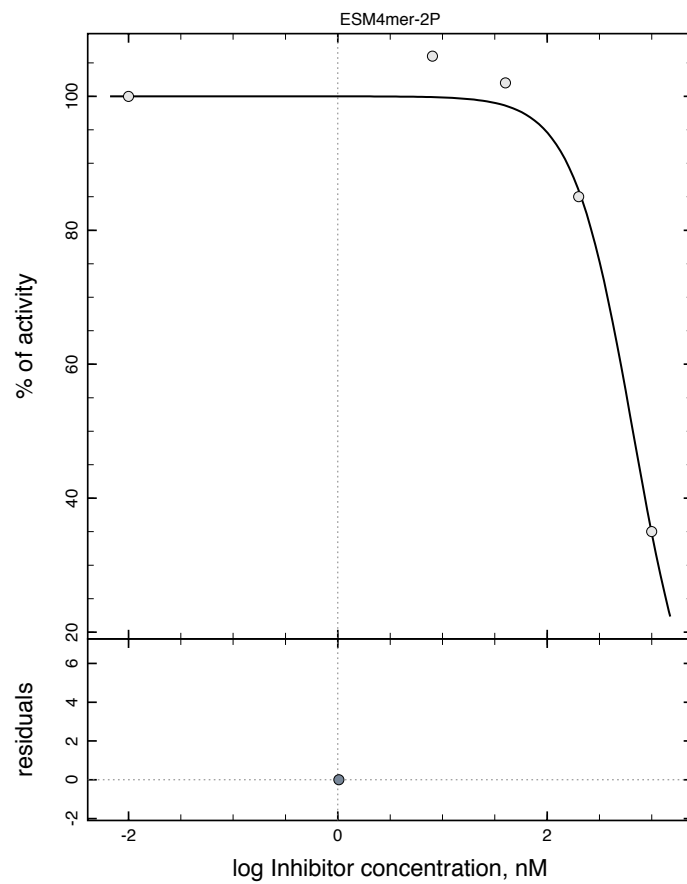




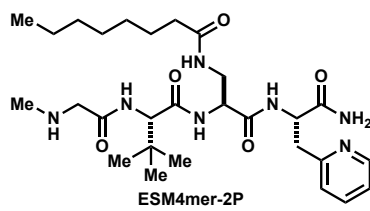
No.	Par# Set	Initial	Final	Std. Error	CV (%)	Note
#1	IC50	100	<b>171.096</b>	3.39058	1.98	
#2	n	-1	-0.696026	0.0100776	1.45	

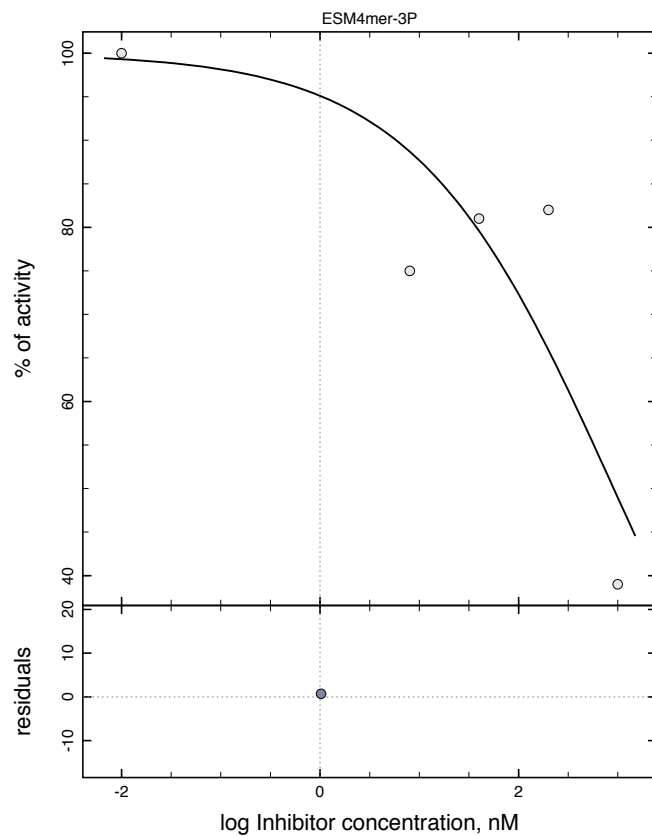




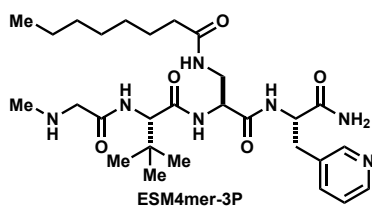


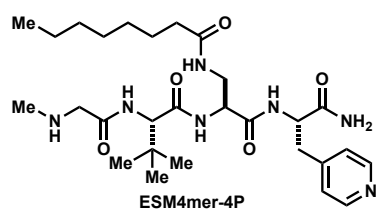
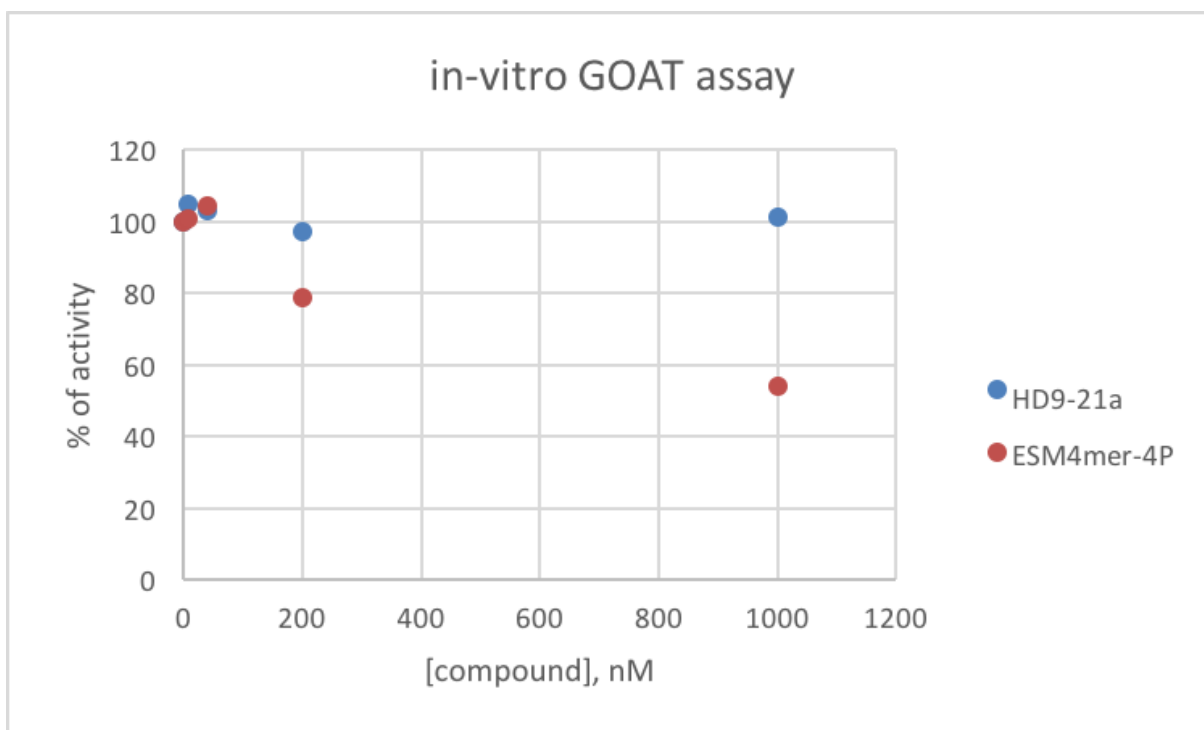
No.	Par#Set	Initial	Final	Std. Error	CV (%)	Note
#1	IC50	100	659.89	69.2352	10.49	
#2	n	-1	-1.51815	0.232088	15.29	

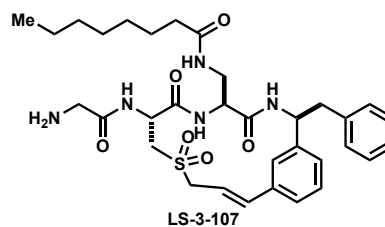
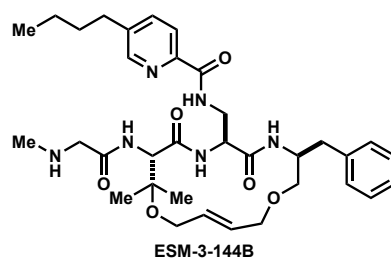
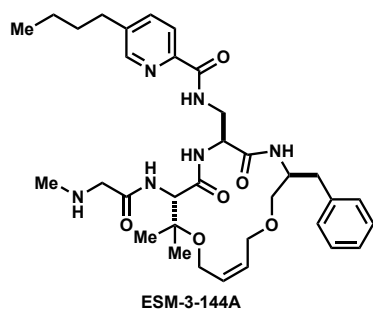
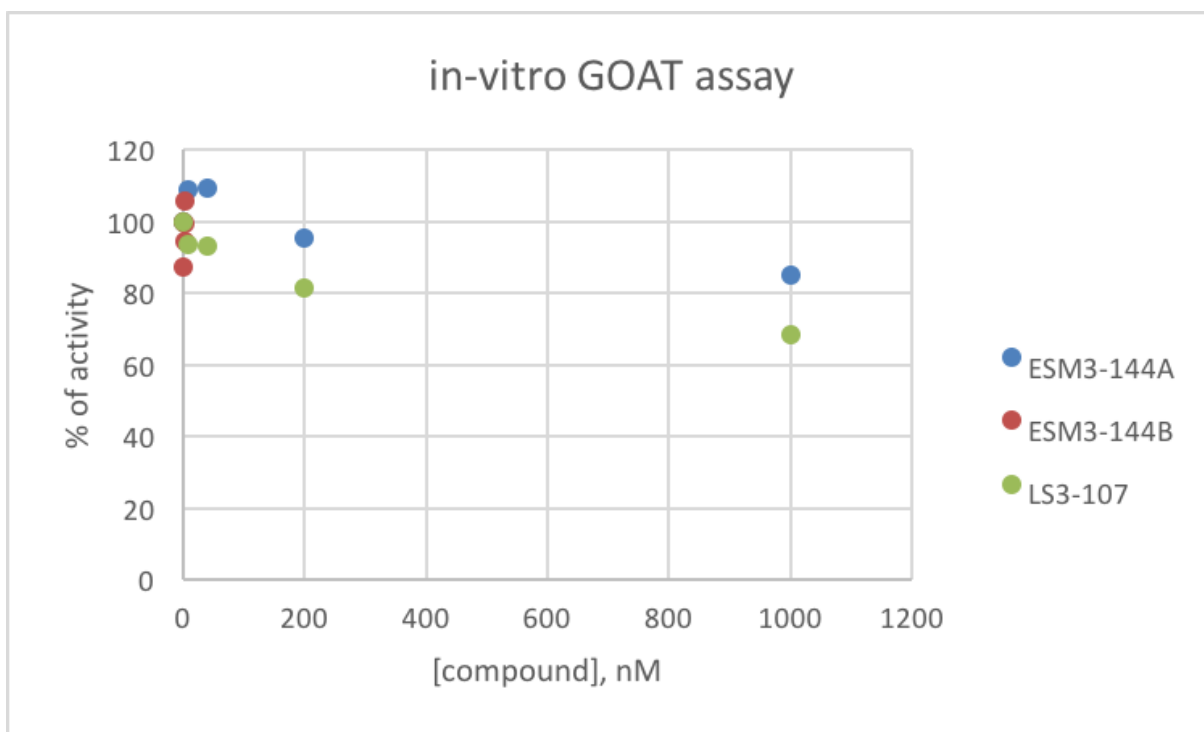




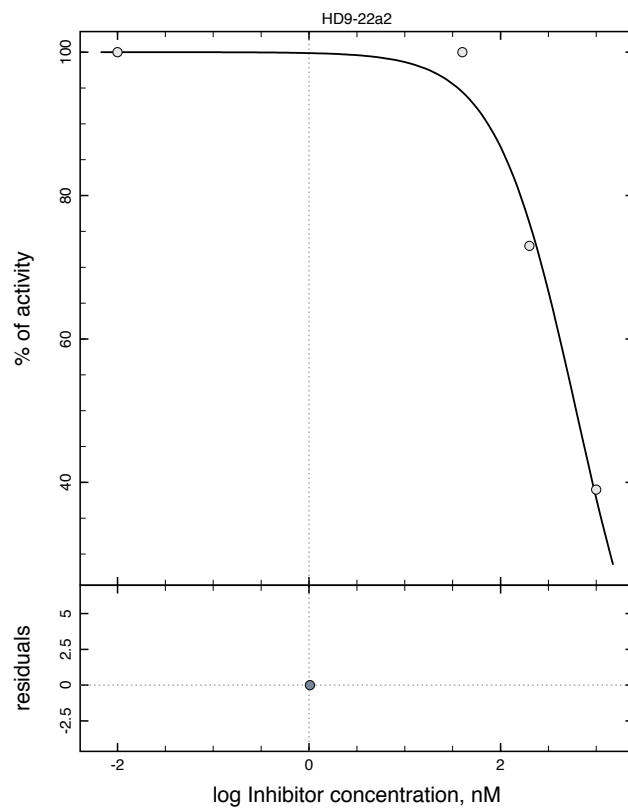
No.	Par#Set	Initial	Final	Std. Error	CV (%)	Note
#1	IC50	100	<b>907.368</b>	979.431	107.94	
#2	n	-1	<b>-0.435481</b>	0.233714	53.67	



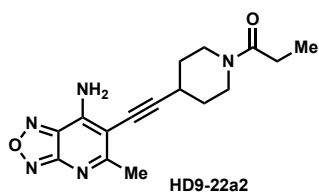


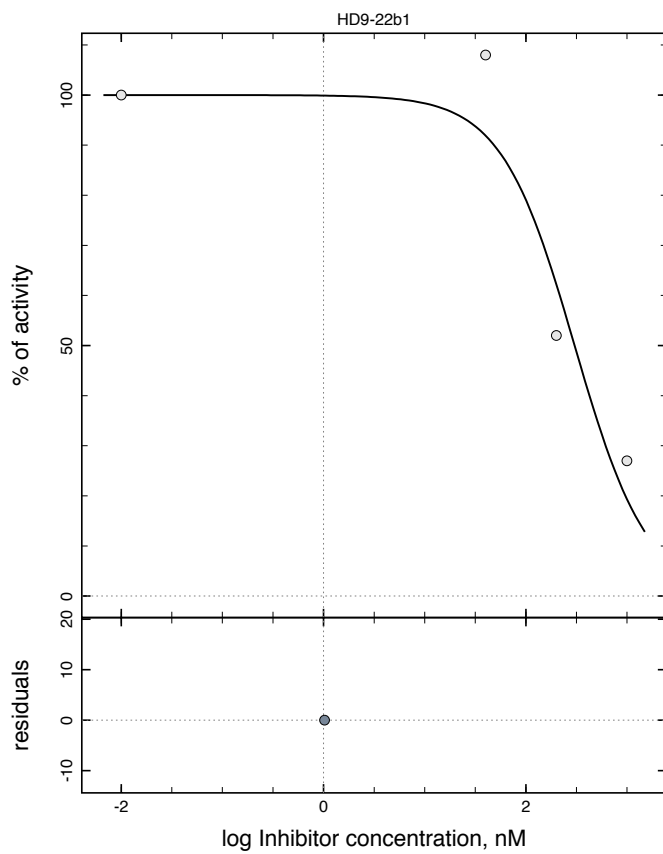




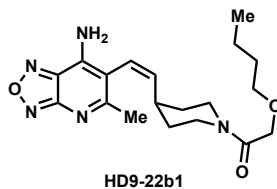


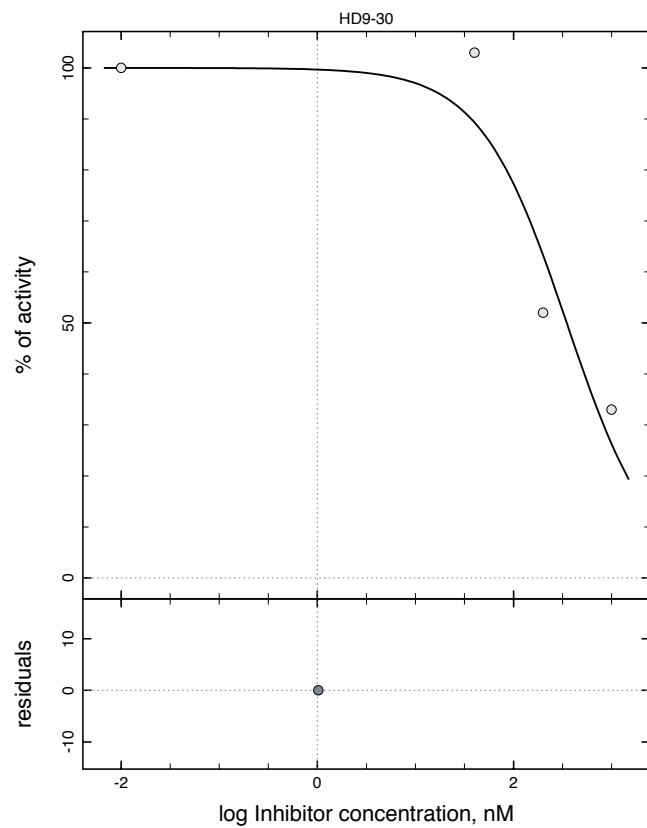
No.	Par# Set	Initial	Final	Std. Error	CV (%)	Note
#1	IC50	100	616.813	93.9284	15.23	
#2	n	-1	-1.03478	0.17314	16.73	



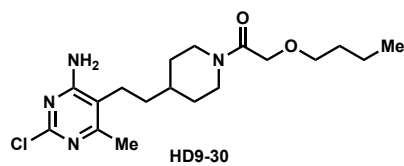


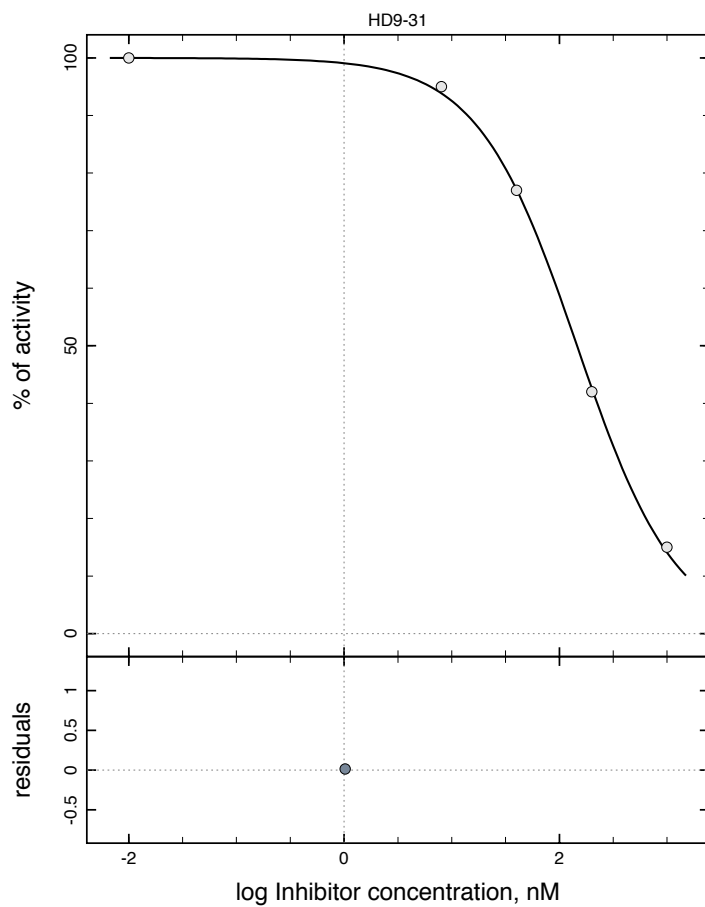
No.	Par#Set	Initial	Final	Std. Error	CV (%)	Note
#1	IC50	100	303.099	126.383	41.70	
#2	n	-1	-1.19884	0.563829	47.03	



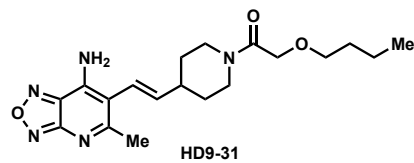


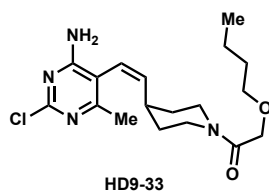
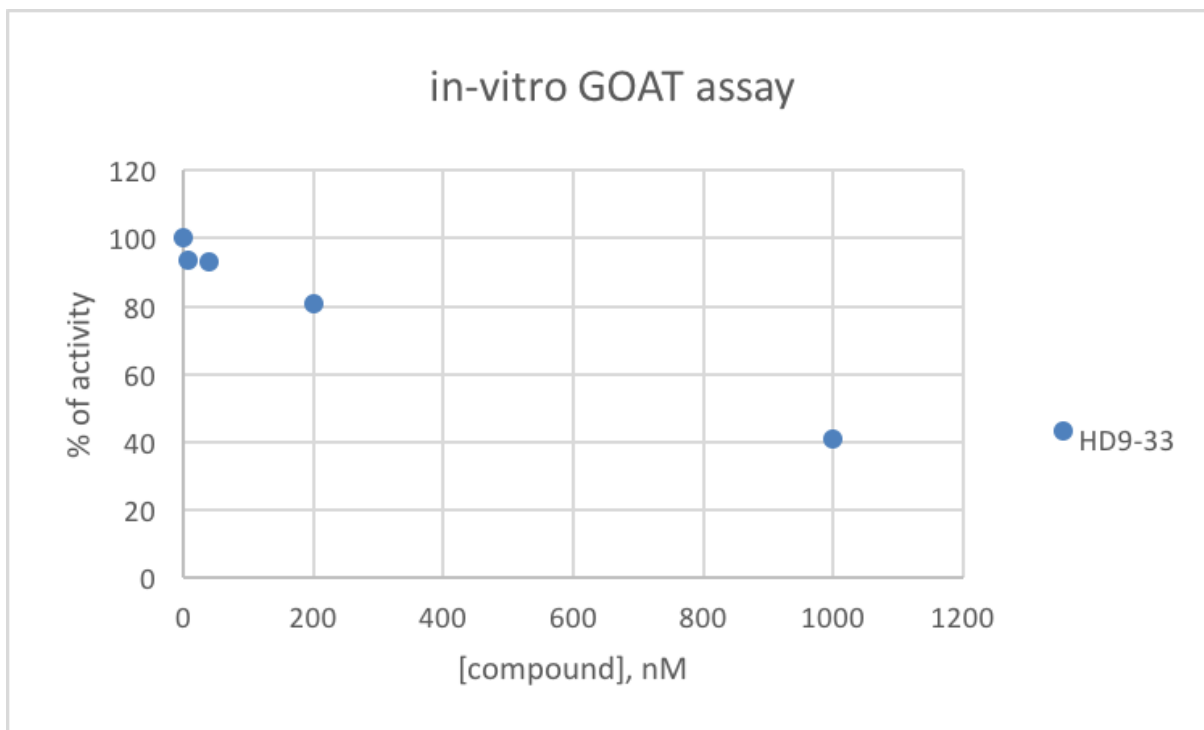
o.	Par# Set	Initial	Final	Std. Error	CV (%)	Note
	#1 IC50	100	348.3	151.2	43.41	
	#2 n	-1	-0.980285	0.424564	43.31	

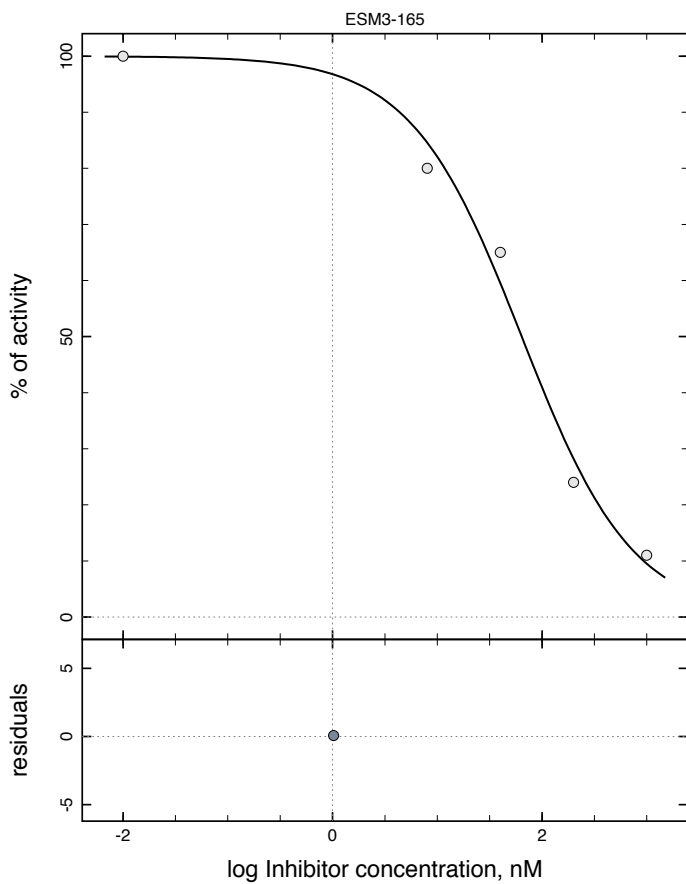




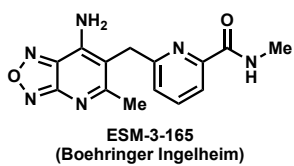
No.	Par# Set	Initial	Final	Std. Error	CV (%)	Note
#1	IC50	100	145.832	4.34959	2.98	
#2	n	-1	-0.939246	0.0246785	2.63	

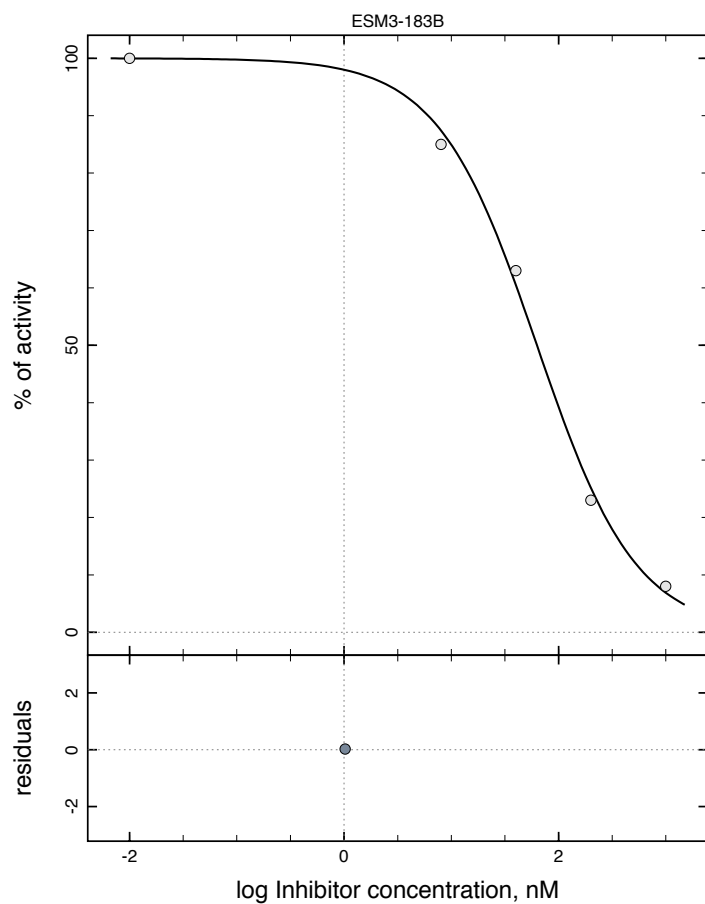




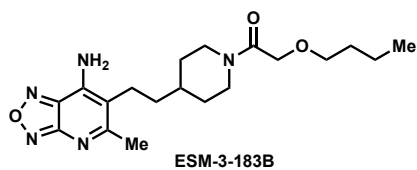


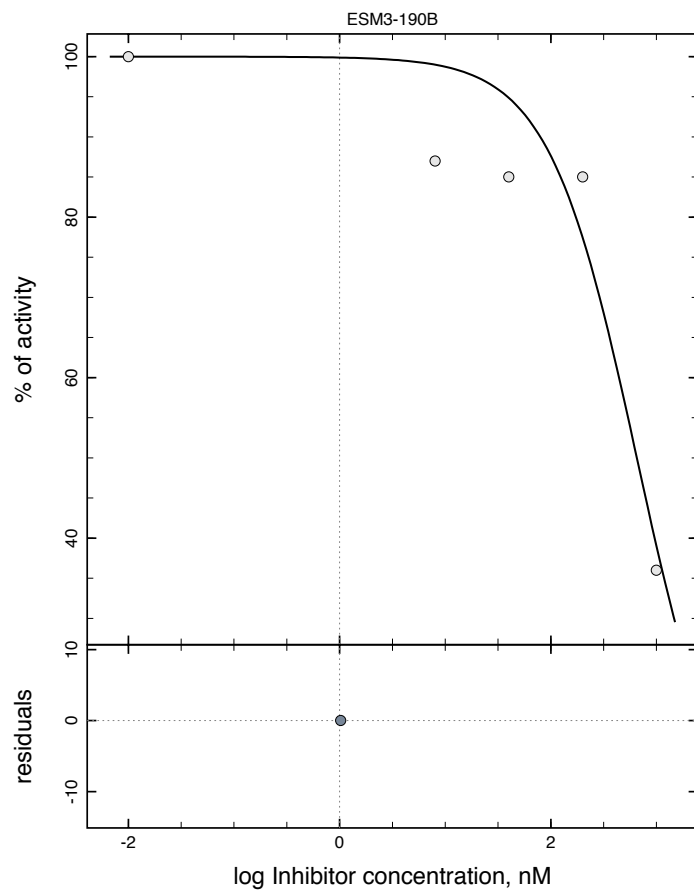
No.	Par# Set	Initial	Final	Std. Error	CV (%)	Note
#1	IC50	100	63.9761	10.8417	16.95	
#2	n	-1	-0.819207	0.110309	13.47	



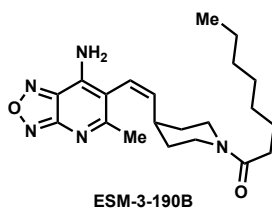


No.	Par#Set	Initial	Final	Std. Error	CV (%)	Note
#1	IC50	100	<b>62.839</b>	4.99599	7.95	
#2	n	-1	<b>-0.940955</b>	0.0654771	6.96	

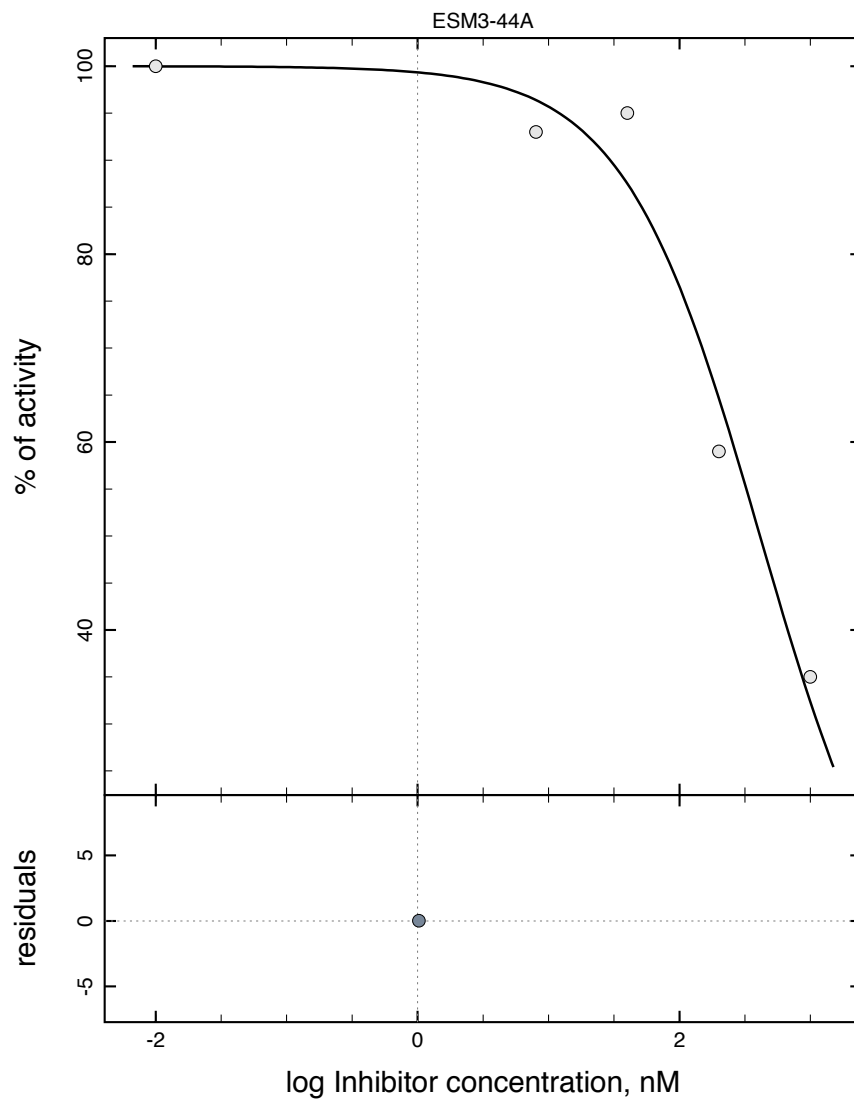




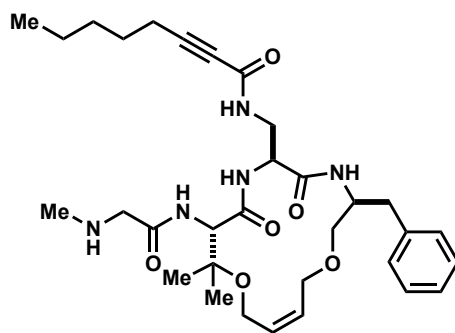
No.	Par# Set	Initial	Final	Std. Error	CV (%)	Note
#1	IC50	100	<b>652.067</b>	217.13	33.30	
#2	n	-1	<b>-1.04409</b>	0.384097	36.79	





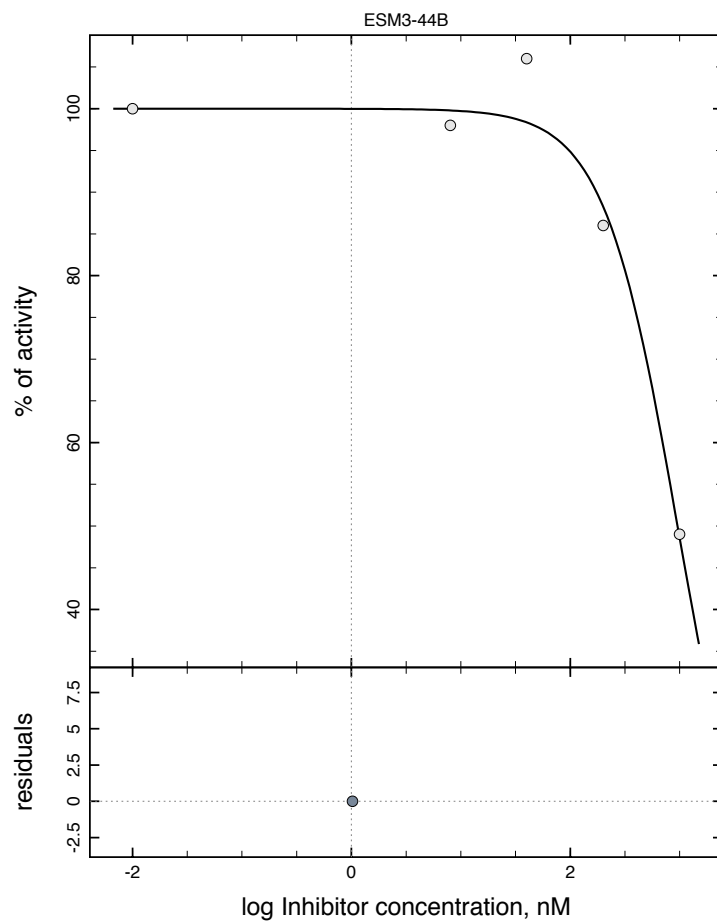


No.	Par# Set	Initial	Final	Std. Error	CV (%)	Note
#1	IC50	100	412.258	89.7893	21.78	
#2	n	-1	-0.833907	0.158473	19.00	

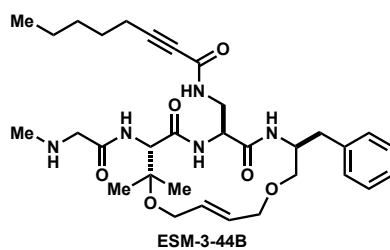


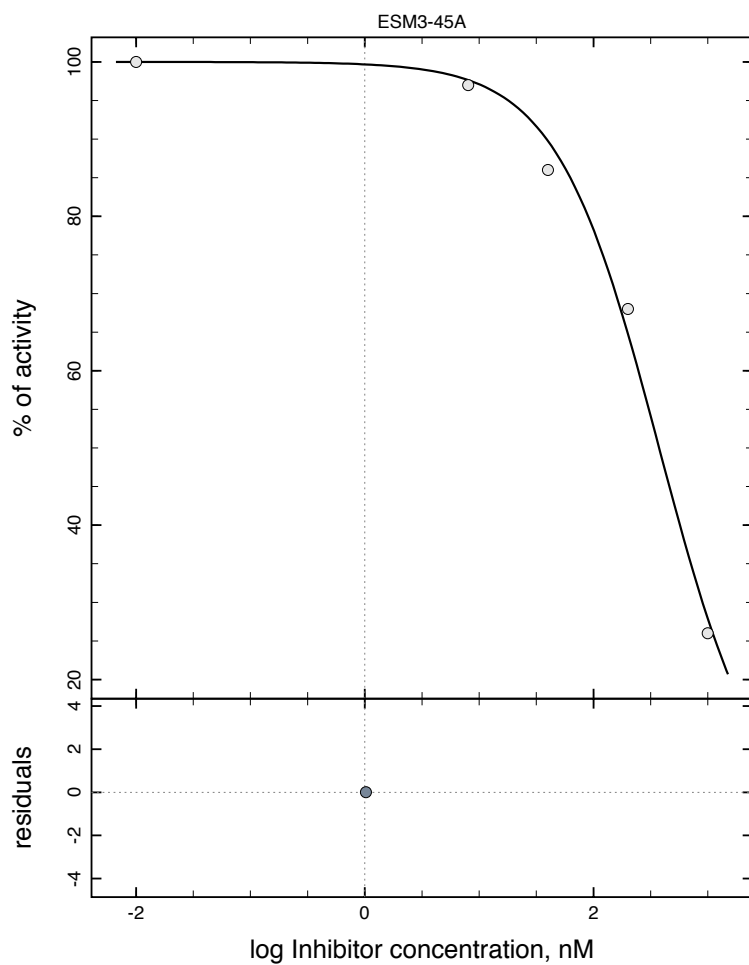
ESM-3-44A

261

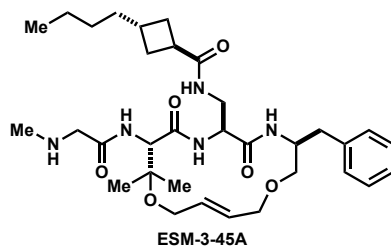


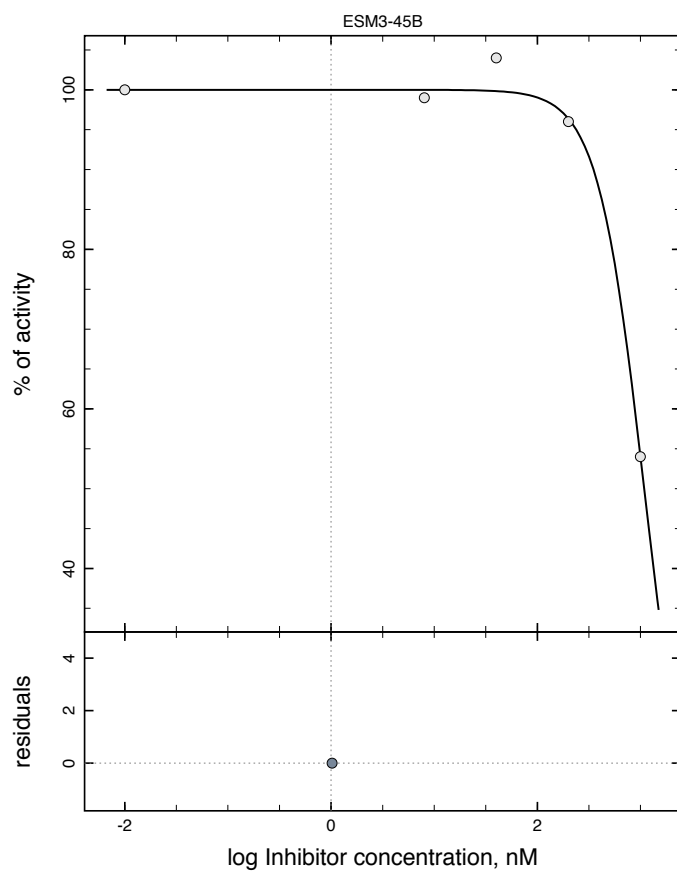
No.	Par# Set	Initial	Final	Std. Error	CV (%)	Note
#1	IC50	100	955.65	136.299	14.26	
#2	n	-1	-1.29036	0.292391	22.66	



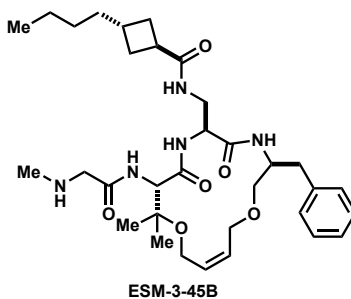


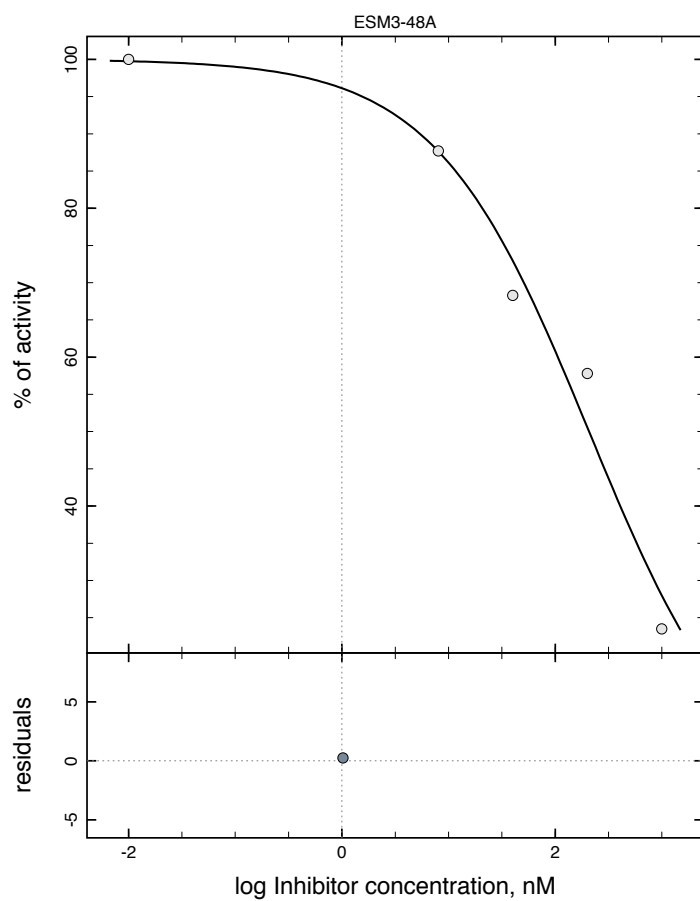
No.	Par# Set	Initial	Final	Std. Error	CV (%)	Note
#1	IC50	100	374.938	37.6617	10.04	
#2	n	-1	-0.969552	0.0937089	9.67	



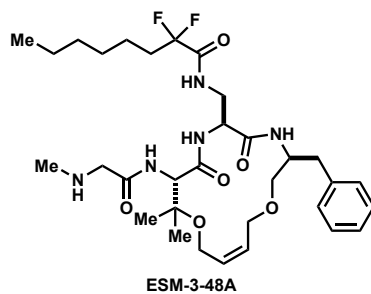


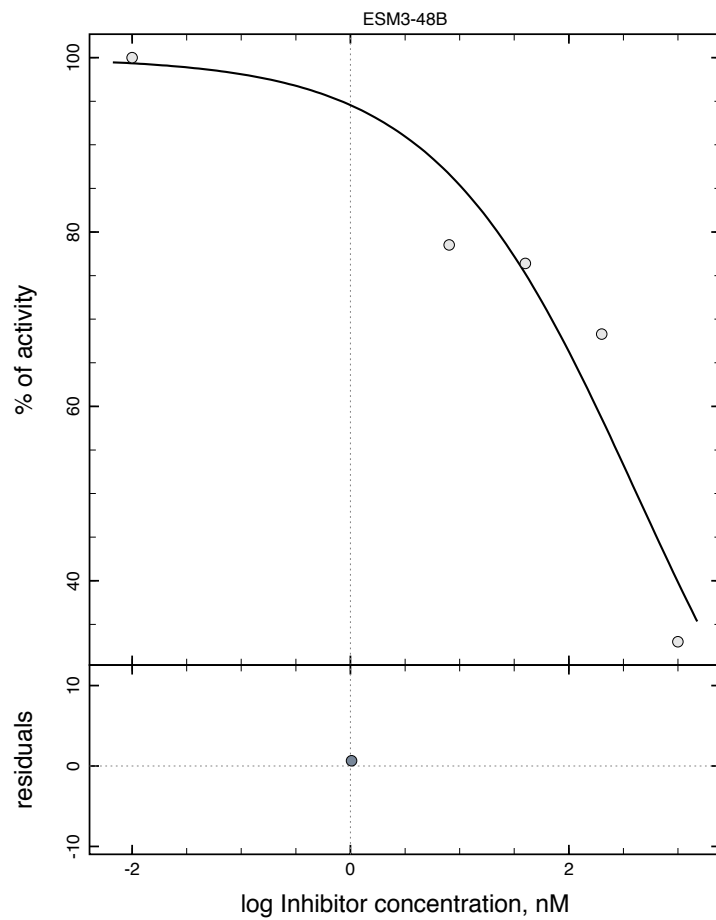
No.	Par#Set	Initial	Final	Std. Error	CV (%)	Note
#1	IC50	100	1085.49	62.0803	5.72	
#2	n	-1	-1.94134	0.445113	22.93	



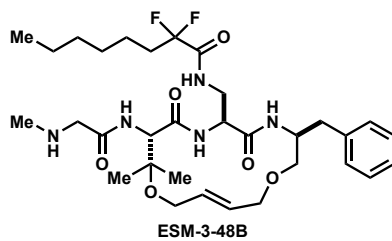


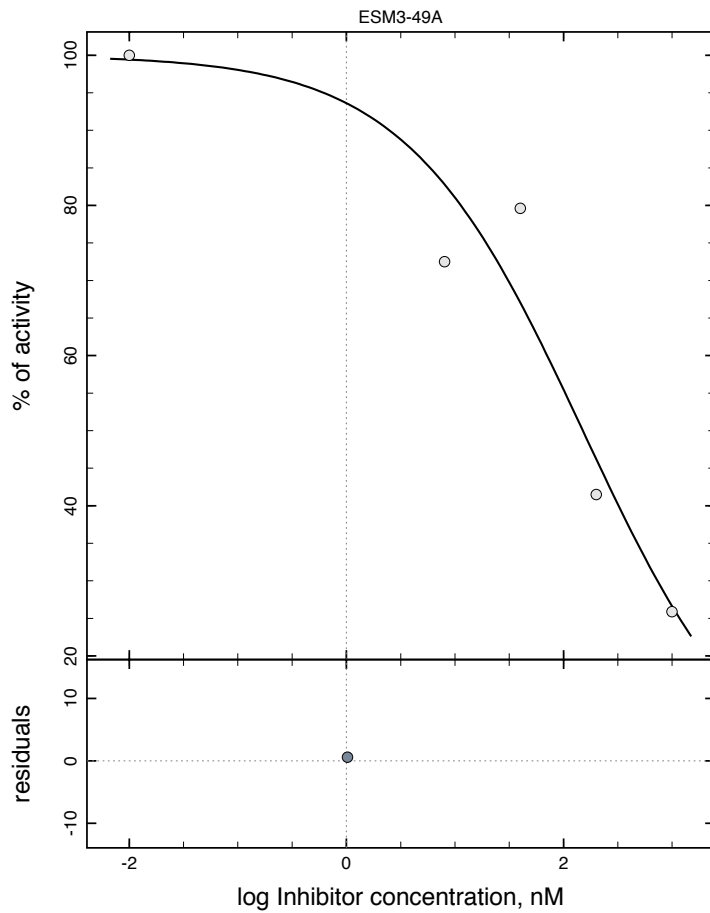
No.	Par#Set	Initial	Final	Std. Error	CV (%)	Note
#1	IC50	100	<b>207.643</b>	50.0409	24.10	
#2	n	-1	<b>-0.601842</b>	0.0988657	16.43	



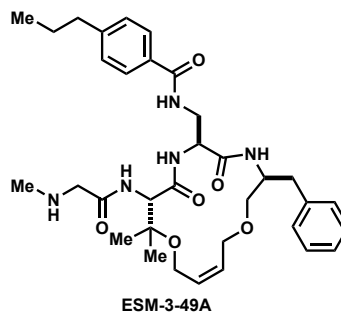


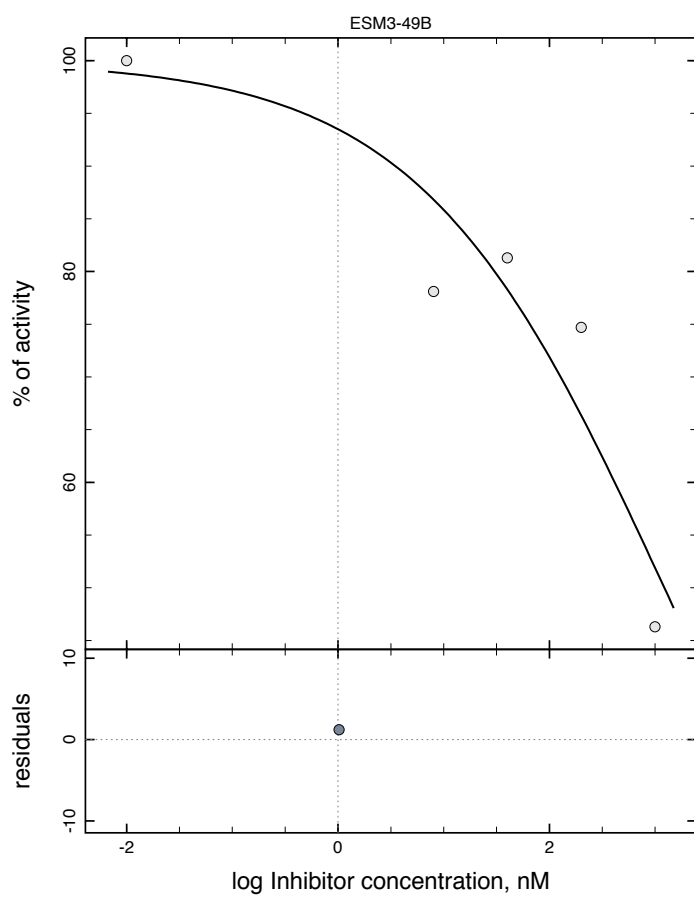
No.	Par#Set	Initial	Final	Std. Error	CV (%)	Note
#1	IC50	100	417.629	203.982	48.84	
#2	n	-1	-0.47283	0.135023	28.56	



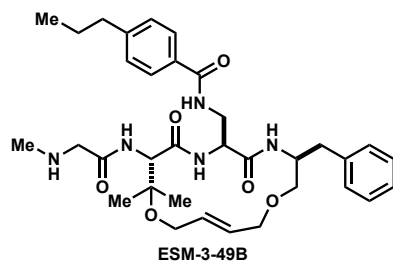


No.	Par#Set	Initial	Final	Std. Error	CV (%)	Note
#1	IC50	100	150.59	67.4746	44.81	
#2	n	-1	-0.535647	0.155039	28.94	

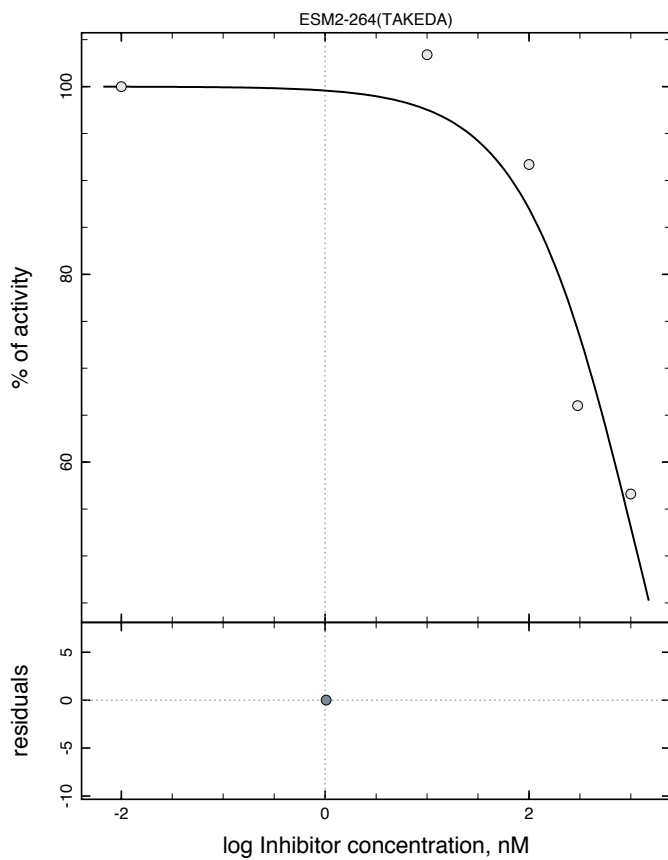




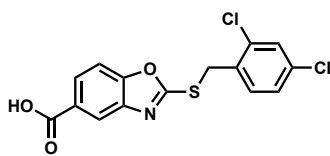
o.	Par#Set	Initial	Final	Std. Error	CV (%)	Note
	#1 IC50	100	1222.42	977.428	79.96	
	#2 n	-1	-0.375005	0.12741	33.98	



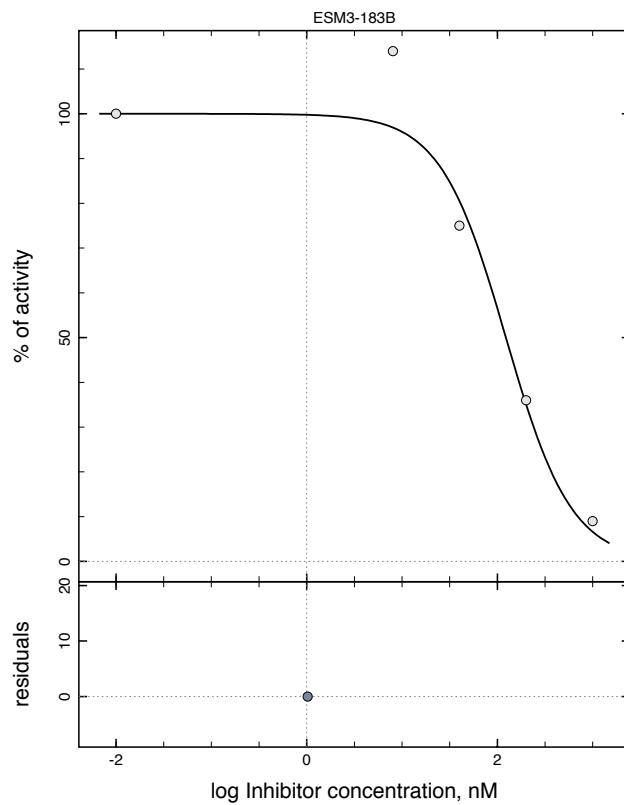




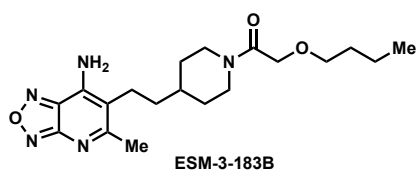
No.	Par# Set	Initial	Final	Std. Error	CV (%)	Note
#1	IC50	100	1171.47	426.507	36.41	
#2	n	-1	-0.772284	0.235131	30.45	



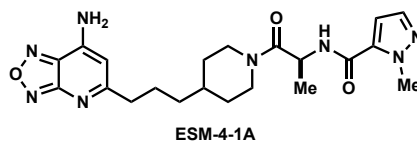
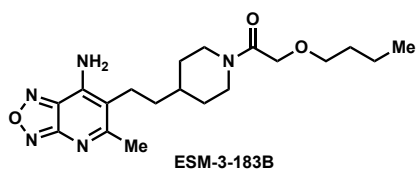
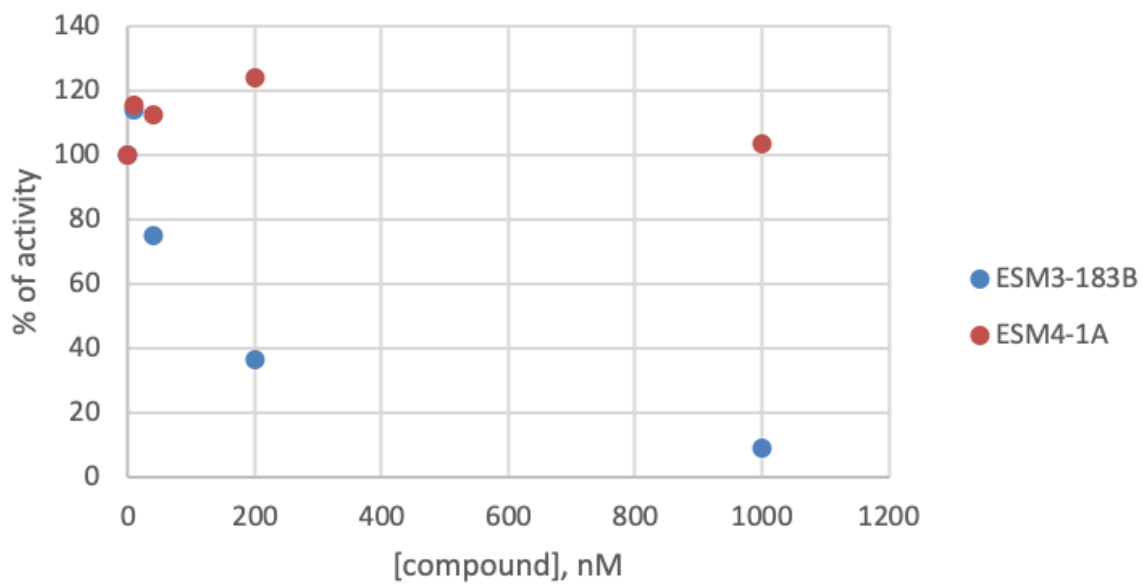
ESM-2-264  
(Takeda)

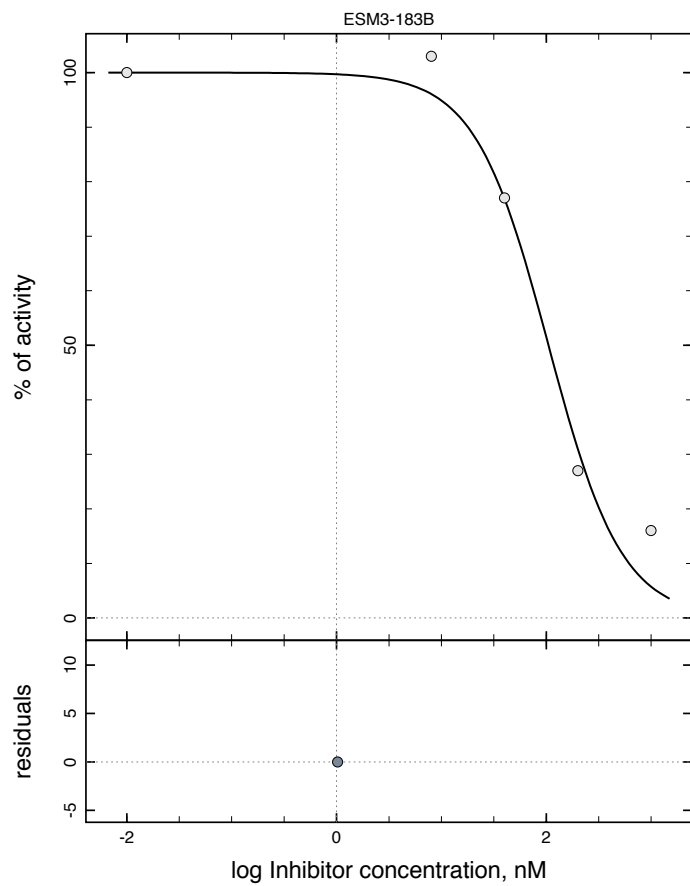


No.	Par#Set	Initial	Final	Std. Error	CV (%)	Note
#1	IC50	100	<b>122.892</b>	35.7309	29.08	
#2	n	-1	<b>-1.26434</b>	0.405875	32.10	

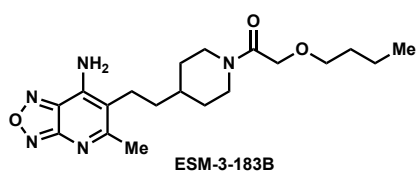


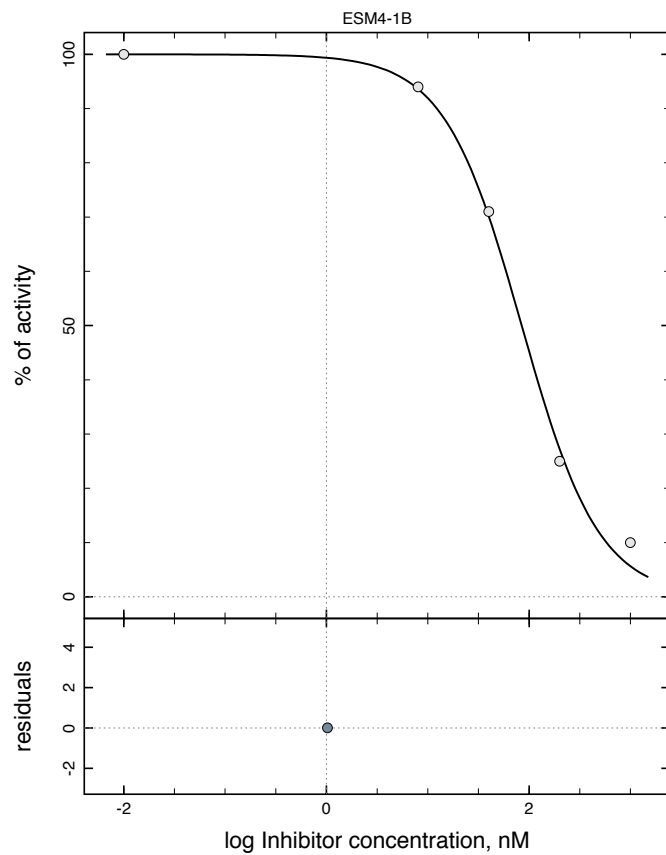
### GOAT in vitro assay



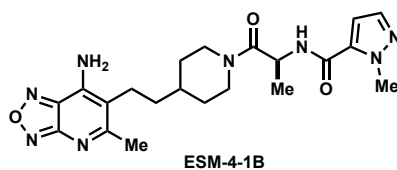


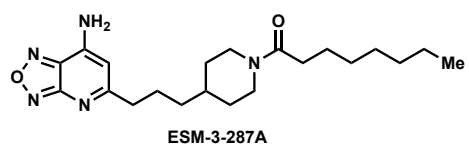
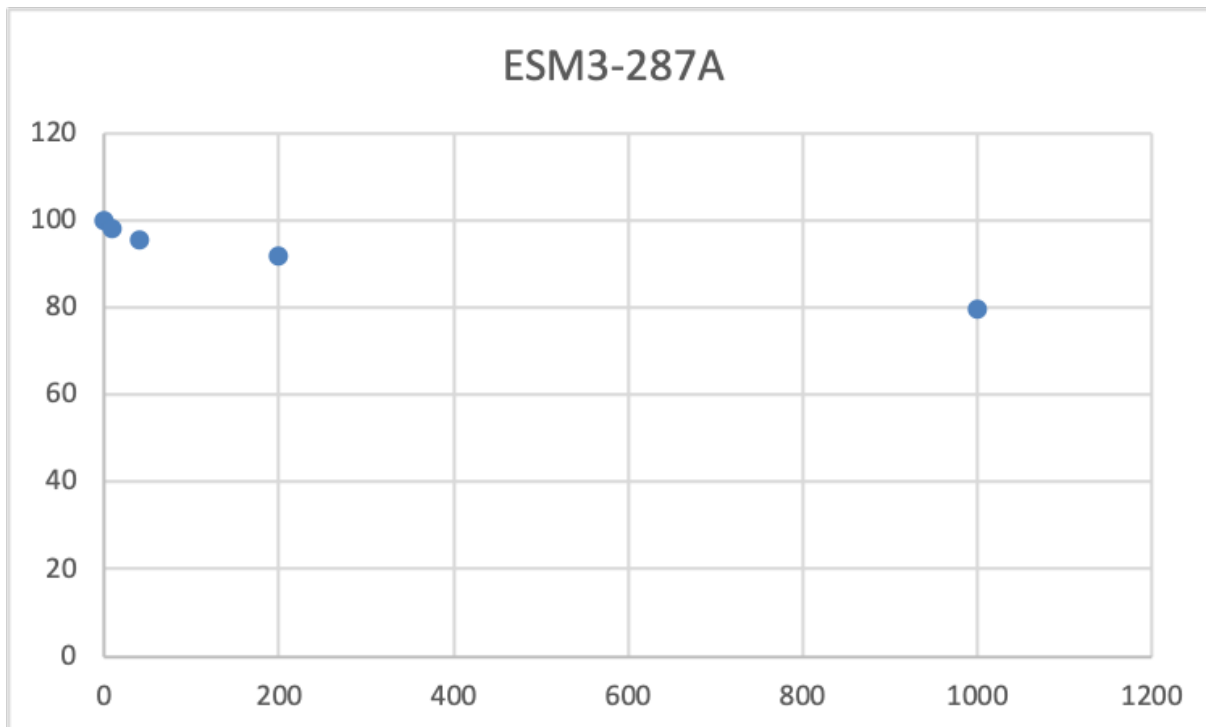
No.	Par#Set	Initial	Final	Std. Error	CV (%)	Note
#1	IC50	100	104.912	22.1911	21.15	
#2	n	-1	-1.24252	0.27863	22.42	

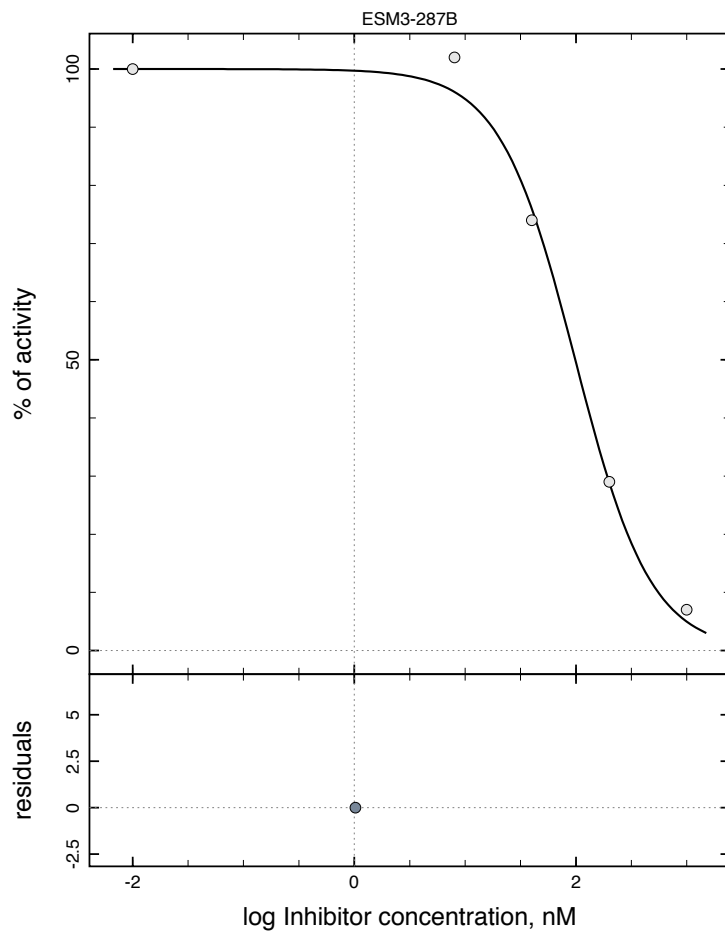




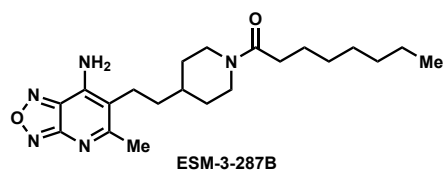
No.	Par# Set	Initial	Final	Std. Error	CV (%)	Note
#1	IC50	100	84.4614	7.13995	8.45	
#2	n	-1	-1.14028	0.0957654	8.40	

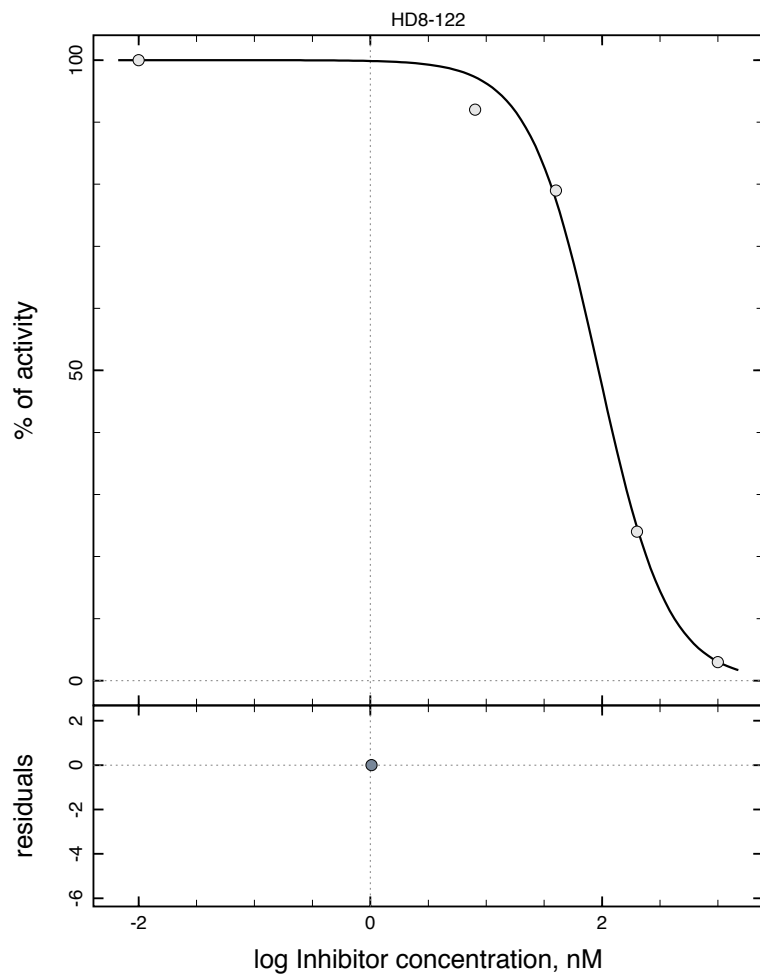




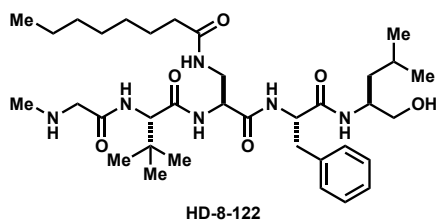


No.	Par#Set	Initial	Final	Std. Error	CV (%)	Note
#1	IC50	100	98.4819	10.3898	10.55	
#2	n	-1	-1.27414	0.14385	11.29	





No.	Par#Set	Initial	Final	Std. Error	CV (%)	Note
#1	IC50	100	93.1642	7.94482	8.53	
#2	n	-1	-1.45675	0.141839	9.74	





## INS-1 Cellular Inhibition Data

All data was collected and processed by Dr. David Strugatsky.

### A. Methods

#### ***Generation of Recombinant Retrovirus for mGOAT Expression:***

The mouse GOAT cDNA with C-terminal HA tag was amplified from pcDNA3.1-mouseGOAT-HA vector (gift from Brown and Goldstein lab) using the following primers: mGOAT\_attb1 5'-ggggacaagttgtacaaaaaagcaggctaccatggattggctccagctc-3' (forward primer; attb1 recombination sites in *italics*, 5' of mGOAT coding sequence in **bold**, Kozak sequence is underlined) and mGOAT\_attb2 (reverse primer; attb2 recombination site is in *italics*, 3' of mGOAT-HA coding sequence is in **bold**, stop codon is underlined) 5'-ggggaccactttgtacaagaaagctgggtctaagcgtaatctggaacatc -3'. The PCR product was cloned into donor vector pDONR221 (ThermoFisher) with BP clonase according to manufactory instructions. Positive clones were verified by DNA sequencing with M13F and M13R primers. The resulted entry plasmid pDONR221-mGOAT-HA was used for transfer of mGOAT-HA cDNA to destination vector pBabe-puro (Addgene catalog #51070) using LR clonase according to manufactory instructions. Positive clones were verified by DNA sequencing with pBABE-5 and pBABE-3 primers. The resulted plasmid pBABE-puro-mGOAT-HA was used to generate retrovirus. The retrovirus was packed in 293T PhoE (Phoenix-ECO ATTC® CRL-3214™) cells and used to infect INS-1 cells. The stable INS/GOAT cells were selecting on 1 µg/mL puromycin and GOAT expression was confirmed with immunoblot of membrane fraction isolated from antibiotic resistant culture using anti-HA antibody.

#### ***Generation of Lentivirus for Expression of Ghrelin:***

The cDNA for mouse preproghrelin was subcloned from pcDNA3.1-preproghrelin (gift from Brown and Goldstein lab) into pULTRA vector (Addgene catalog #24129) with *XbaI* and *BamHI* restriction enzymes. Use of these restriction sites for cloning will result in creation of bi-cistronic expression of ghrelin along with EGFP to facilitate identification of positive cells by fluorescence. The above restriction sites were engineered via PCR reaction using the following primers: ghrl\_pultra\_forw 5'-taccgagctctctagaat**gtcttcaggc**-3' (5' of preproghrelin coding sequence is in **bold**, *XbaI* site is in *italics*) and ghrl\_pultra\_rev 5'-agcggccgcggatccttacttgcagctggc-3' (3' of preproghrelin coding sequence is in **bold**, stop codon is underlined, *BamHI* site is in *italics*). The recombinant lentivirus encoding preproghrelin cDNA was packed in Lenti-X 293T cells (Takara catalog #632180) and envelope encoding plasmid pCMV-VSV-G (Addgene catalog #8454). The INS/GOAT cells were infected with recombinant lentivirus to generate INS/GOAT/GHRL cell line. After a few passages, the population of cells with puromycin resistance and ~90% fluorescence was saved for cell-based assay.

### **Cellular Assay:**

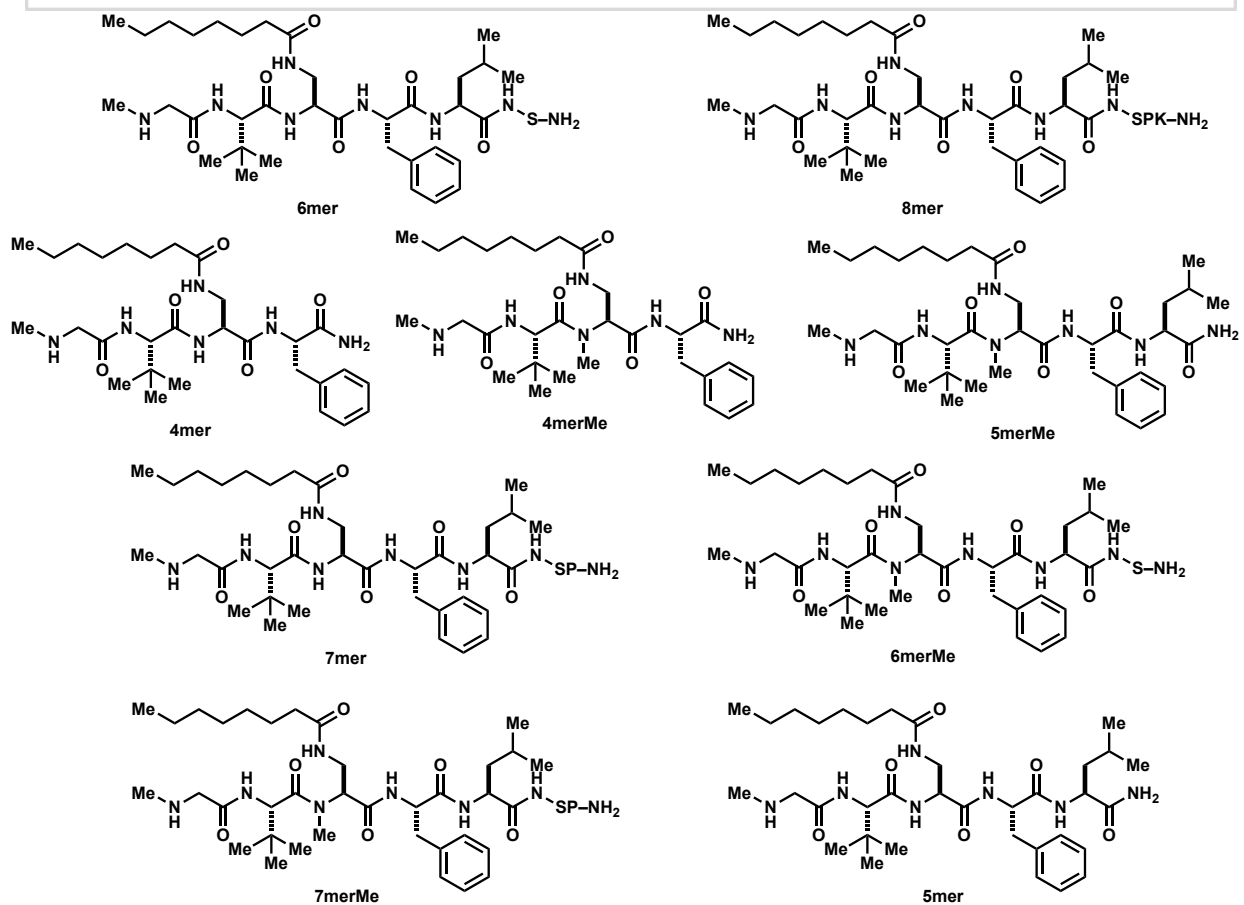
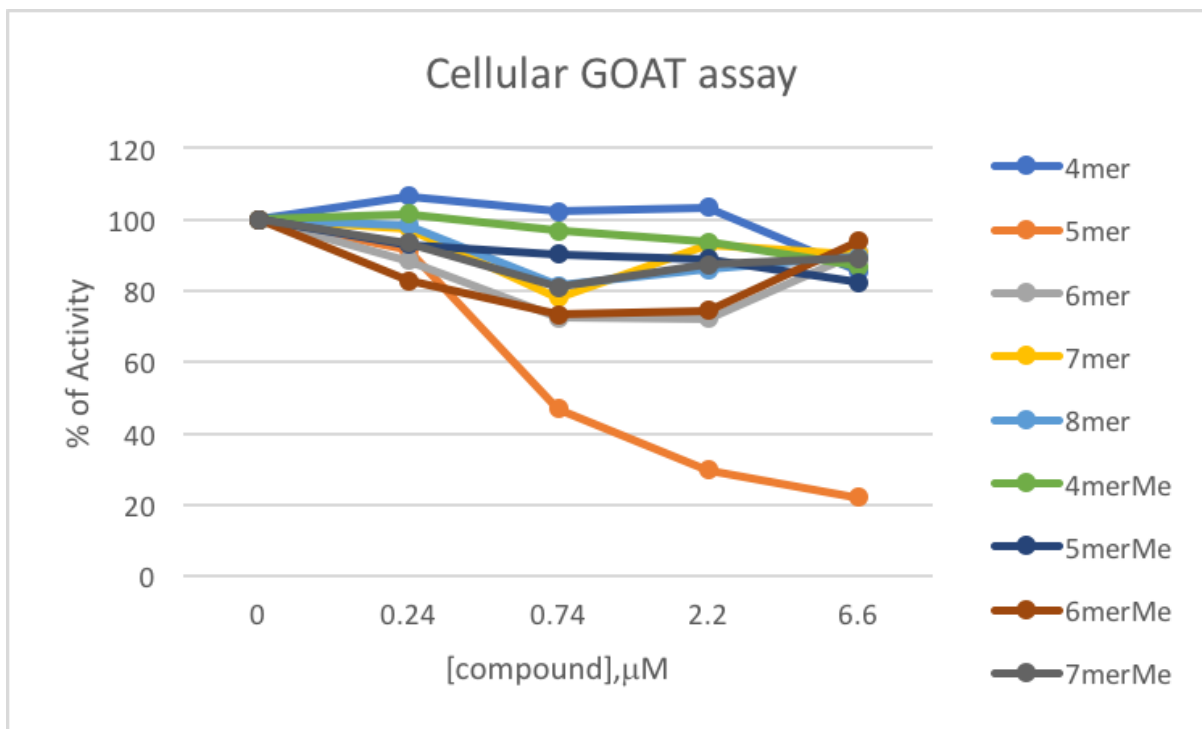
INS/GOAT/GHRL cell line was routinely cultured in RPMI medium supplemented with 10% FBS, 1% Pen/Strep, 10 mM HEPES pH 7.2 and 50  $\mu$ M 2-mercaptopyethanol.

Day 0: One 10 cm dish at full confluency was used to seed one 96-well plate.

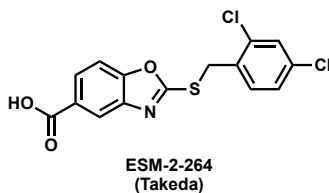
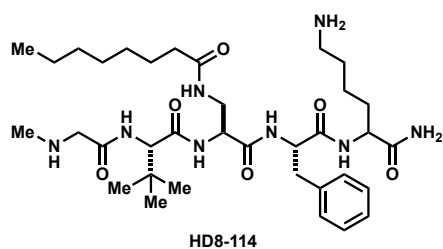
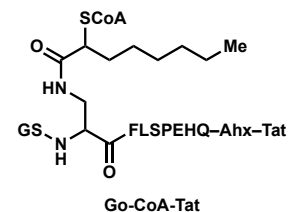
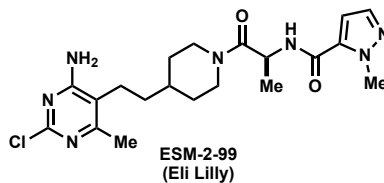
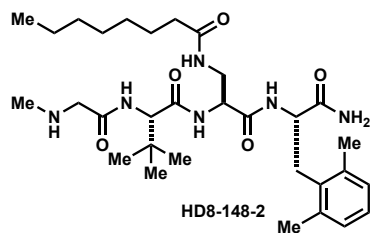
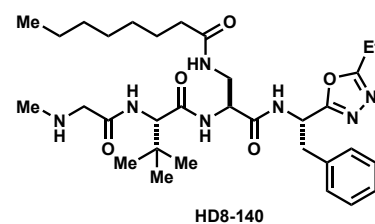
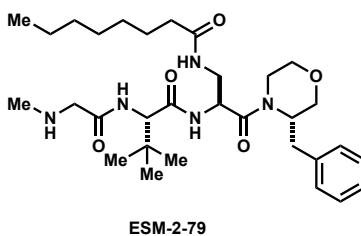
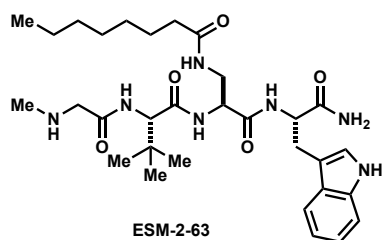
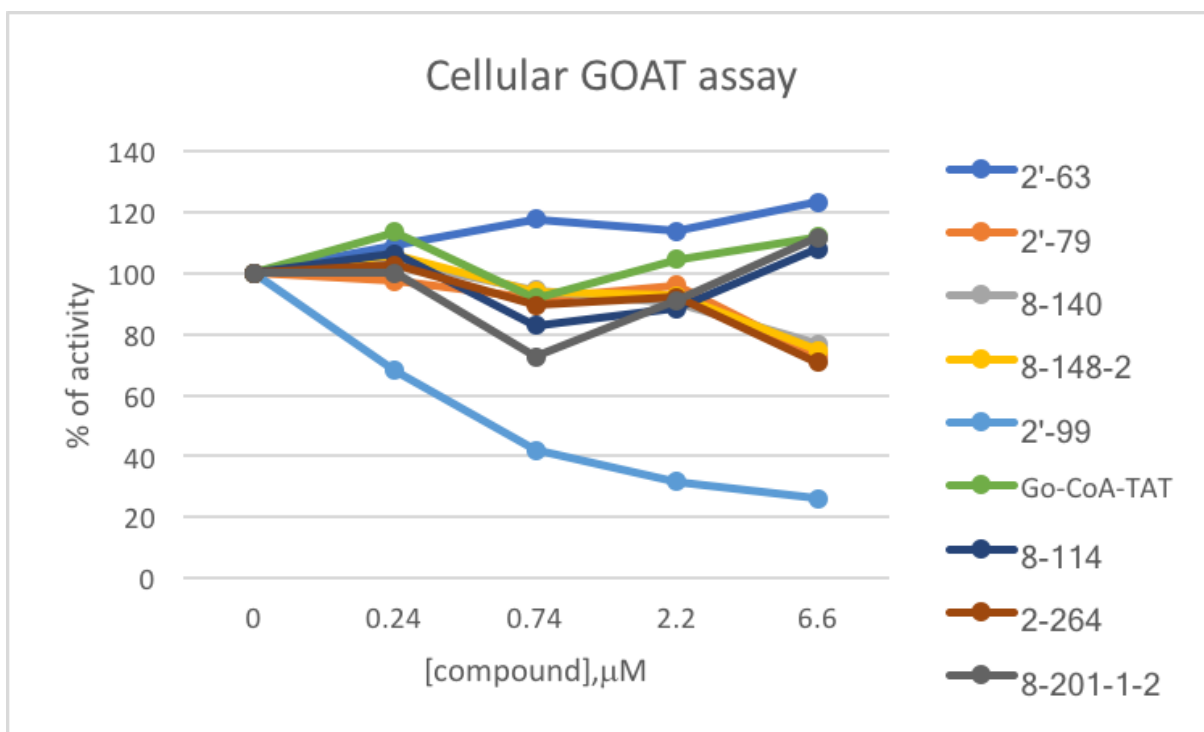
Day 1: Growth media was removed and cells were washed with PBS prior to adding fresh growth media as above but without 2-mercaptoethanol. The serial dilutions of tested compound at 50x concentration were prepared in vehicle containing growth media without 2-mercaptoethanol supplemented with 6% DMSO and were added to cells in duplicates.

Day 2: 10  $\mu$ L of growth media was removed from each and amount of secreted acyl-ghrelin was measured by ELISA (Cayman catalog #10006307).

## B. Cellular Assay Results







# Cellular GOAT assay

